

AD-A090 838

MOORE SCHOOL OF ELECTRICAL ENGINEERING PHILADELPHIA PA
SUPER-RESOLUTION IMAGERY BY FREQUENCY SWEEPING. (U)

F/G 17/9

AUG 80 N H FARHAT, C WERNER

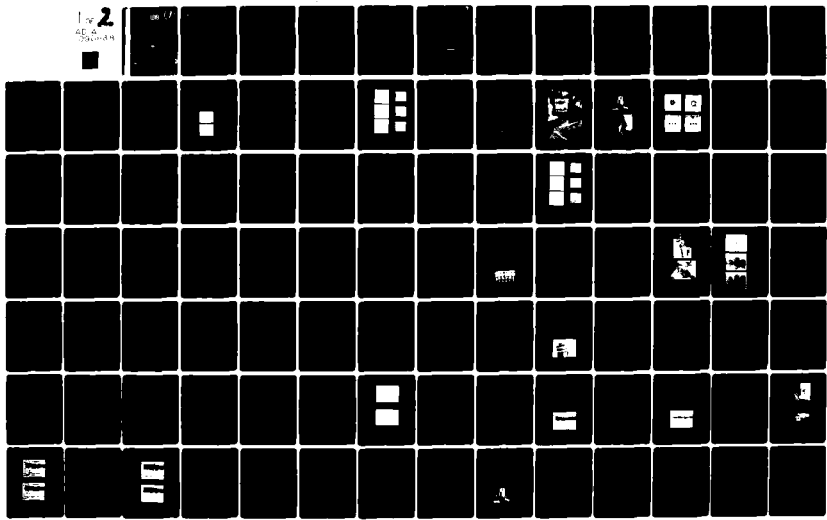
AFOSR-77-3256

UNCLASSIFIED

AFOSR-TR-80-1068

NL

Fig. 2
RE-
DUCED
COPY

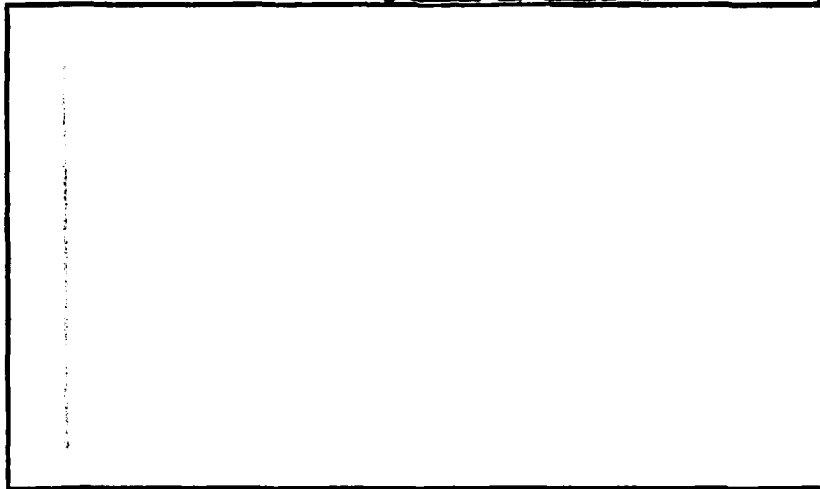


AFOSR-TR- 80 - 1068

LEVEL II

9

AD A090838



DDC FILE COPY

UNIVERSITY of PENNSYLVANIA
The Moore School of Electrical Engineering
PHILADELPHIA, PENNSYLVANIA 19104

DTIC
ELECTE
OCT 23 1980
S D D

Approved for public release;
distribution unlimited.

80 10 21 054

UNCLASSIFIED

(12) 1791

SECURITY CLASSIFICATION OF THIS PAGE (When Data Entered)

1. REPORT DOCUMENTATION PAGE		READ INSTRUCTIONS BEFORE COMPLETING FORM	
AFOSR-TR-80-1068		2. GOVT ACCESSION NO. AD-A090838	3. RECIPIENT'S CATALOG NUMBER 5-22277
4. TITLE (and Subtitle) Super-Resolution Imagery by Frequency Sweeping		5. TYPE OF REPORT & PERIOD COVERED 9 FINAL rept.	
6. AUTHOR(s) 10 N.H. Farhat C./Werner		8. CONTRACT OR GRANT NUMBER(s) 15 AFOSR-77-3256	
7. PERFORMING ORGANIZATION NAME AND ADDRESS University of Pennsylvania The Moore School of Electrical Engineering 200 S. 33rd St., Phila., Pa. 19104		10. PROGRAM ELEMENT, PROJECT, TASK AREA & WORK UNIT NUMBERS 16 61102F 2305/B1	
9. CONTROLLING OFFICE NAME AND ADDRESS United States Air Force Air Force Office of Scientific Research Bldg. 410, Bolling AFB, D.C. 20332		12. REPORT DATE 11 15 August 1980 N/A	
11. MONITORING AGENCY NAME & ADDRESS (if different from Controlling Office) Office of Research Administration 3451 Walnut St. Phila., Pa. 19104		13. NUMBER OF PAGES 76	
		15. SECURITY CLASS. (of this report) UNCLASSIFIED	
		15a. DECLASSIFICATION/DOWNGRADING SCHEDULE	

14. DISTRIBUTION STATEMENT (of this Report)

Approved for public release; distribution unlimited.

14. DISTRIBUTION STATEMENT (of the abstract entered in Block 20, if different from Report)

15. SUPPLEMENTARY NOTES

16. KEY WORDS (Continue on reverse side if necessary and identify by block number)

Microwave 3-D imaging, frequency diversity, holography, inverse scattering, aperture synthesis, Fourier domain projection, target derived reference, network analysis, radar cross-section, projection hologram, tomographic radar.

17. ABSTRACT (Continue on reverse side if necessary and identify by block number)

A longstanding problem in radar and electromagnetic scattering measurements is the reconstruction of object shape and detail, i.e. an image, from far field scatter data to be used in object identification and classification. During the period covered by this report we have been able to demonstrate in a feasibility study the first reconstruction of a 3-D image of a perfectly reflecting object from its wave-vector diversity (multifrequency and multi-aspect) scatter data making use of a new Weighted Fourier Domain Projection

UNCLASSIFIED

SECURITY CLASSIFICATION OF THIS PAGE (When Data Entered)

Theorem (WFDPT) and establish a relationship between holography with wavelength diversity and inverse scattering. Coherent wave vector diversity radar techniques are used to access a finite volume of the 3-D Fourier space (also known as reciprocal space or \bar{p} -space) of the scattering object. The WFDPT permits the use of hybrid (digital/optical) computing that enables the retrieval and display of 3-D image information in parallel slices or cross-sectional outlines. The major attributes of this approach as compared to totally digital computing are its potential for displaying a true 3-D image in real-time. Wave-vector diversity methods appear suitable for the imaging of two classes of practical objects namely non-dispersive perfectly reflecting objects of the type often encountered in radar (and sonar) and semitransparent weakly scattering objects such as certain ultrasound and light scattering objects encountered in biology and medicine. The method has several unique characteristics. It furnishes true super-resolution, i.e. resolution exceeding the classical Rayleigh Limit of the available recording aperture, in this case a highly thinned (widely dispersed) broad-band coherent receiver array. True super-resolution is achieved because of an inherent aperture synthesis due to frequency diversity (frequency scanning, stepping or comb illumination) and conversion of spectral degrees of freedom into spatial image detail. Accordingly, when applied to the imaging of a dispersive object, a *target signature* rather than a geometrical image should be expected. Such a target signature could still be useful in object identification and classification since it contains information pertaining to the material composition of the object intermixed with geometrical image detail. The use of frequency diversity was found to lead to a unipolar impulse response. This is very useful in suppressing coherent noise (speckle) which is known to be the major drawback of coherent imaging.

Preliminary work on 3-D image display has yielded encouraging results on 3-D display from a series of weighted projection holograms of various slices of a test object. The projection holograms were viewed in rapid succession using the virtual Fourier transform.

To identify optimal and practical approaches to wave-vector diversity data acquisition a unique microwave measurement system has been assembled, installed and tested in our anechoic chamber facility. The system was used also in the study of TDR (target derived reference) methods in which a reference for phase measurement can be furnished by the scattering object eliminating thus the need for costly local oscillator distribution networks and eliminating at the same time undesirable range phase ambiguities from the collected data. The measurement facility is computer aided furnishing thereby semi-automatic control of object positioning or orientation, frequency stepping, data acquisition and storage, and final data correction and analysis. A high resolution CRT display enables the display of *weighted projection holograms* computed from the \bar{p} -space data making use of the WFDPT. Preliminary results of this measurement system capabilities included in this report confirm its tremendous versatility. At this stage, the program strongly suggests the practical feasibility of a new generation of cost effective, real-time, super-resolving 3-D imaging radars that can because of their 3-D image slicing characteristic be appropriately referred to as *Tomographic Radars* (Tomos=slice in Greek).

Finally, a study of 3-D imaging using other forms of broadband radiation such as impulsive, random noise and particularly thermal emission for passive 3-D wavelength diversity imaging has been also initiated.

UNCLASSIFIED

The findings in this report are those of the authors and are not to be interpreted as the official position of the Air Force Office of Scientific Research or the U.S. Government.

TABLE OF CONTENTS

	<u>Page</u>
1. Introduction	1
2. Summary of Important Results	2
3. Conclusions	7
4. List of Publications	8
5. Appendices	19
I. The Frequency Displaced Target Derived Reference.	
II. Holography, Wavelength Diversity and Inverse Scattering.	
III. The Virtual Fourier Transform and its Application in Three Dimensional Display.	
IV. An Automated Frequency Response and Radar Cross-Section Measure- ment Facility for Microwave Imaging.	

LEVEL II

9

UNIVERSITY OF PENNSYLVANIA
PHILADELPHIA, PENNSYLVANIA 19104

FINAL REPORT

SUPER RESOLUTION IMAGERY
BY FREQUENCY SWEEPING

AIR FORCE OFFICE OF SCIENTIFIC RESEARCH/NE
BUILDING 410 BOLLING AIR FORCE BASE
WASHINGTON, D.C. 20332

AUGUST 15, 1980

GRANT NUMBER XXXXXXXXXX
AFOSR-77-3256

PREPARED BY

N.H. FARHAT AND C. WERNER

DTIC ELECTED
S **D**
OCT 25 1980
D

Accession For		
NTIS GRA&I	<input checked="" type="checkbox"/>	
DTIC TAB	<input type="checkbox"/>	
Unannounced	<input type="checkbox"/>	
Justification		
By		
Distribution/		
Availability Codes		
Dist Special		
A		

AIR FORCE OFFICE OF SCIENTIFIC RESEARCH (AFSC)
NOTICE OF TRANSMITTAL TO DDC
This technical report has been reviewed and is
approved for public release IAW AFR 190-12 (7b).
Distribution is unlimited.
A. D. BLOSE
Technical Information Officer

HIGH RESOLUTION FREQUENCY SWEPT IMAGING

1. Introduction

The aim of the research work outlined in this final report was the analysis and investigation of methods by which frequency or wavelength diversity techniques can be employed to impart to a highly thinned, and therefore cost-effective, longwave (microwave or ultrasound) imaging aperture resolution capabilities better than its monochromatic classical (Rayleigh) limit achieving thereby super-resolution by means of frequency synthesized apertures. This approach to longwave imaging gains practical significance when one considers the current highly developed state of the art of broadband microwave gear suitable for use in a new generation of cost-effective high resolution microwave imaging radars utilizing frequency diversity techniques.

It is well known that the development of longwave holographic imaging systems possessing resolution and image quality approaching those of optical systems is hampered by three factors: (a) prohibitive cost and size of longwave imaging apertures, (b) rapid deterioration of longitudinal resolution with range, (c) inability to view a 3-D image as with optical Fresnel holograms because of a wavelength scaling problem and (d) degradation of image quality by speckle or coherent noise because of the low numerical apertures attainable with present techniques. For example, a longwave imaging aperture operating at a wavelength of 3 cm should be about 3 km in size in order to achieve image resolution comparable to an ordinary photographic camera. In addition to inconvenient size, the cost of filling such a large aperture with suitable coherent sensors is clearly prohibitive. Furthermore, recall that in conventional longwave holography when optical image retrieval is utilized, it is necessary to store the longwave hologram data (fringe pattern) in an optical transparency suitable for processing on the optical bench using laser light. In order to avoid longitudinal distortion* of the reconstructed image, the size of the optical hologram replica must be $m (= \lambda_{\text{long}} / \lambda_{\text{laser}})$ times smaller than the longwave recording aperture. For the example cited earlier, this means an optical hologram replica of less than a millimeter in size. It is certainly not possible to view a virtual 3-D image through such a minute hologram even with optical aids since these tend to introduce their own longitudinal distortion. As a result, longwave holographers have long learned to forgo 3-D imagery and settled instead for 2-D imagery obtained by projecting the reconstructed real image on a screen. This permits lowering of the reduction factor m and consequently relaxing the resolution requirements of the photographic film which allows in turn the use of highly convenient Polaroid transparency film for preparation of the optical hologram replica. Because of the small size (measured in wavelength) of longwave apertures attainable in practice and the above methods of viewing the real image, speckle noise is always present leading to degradation in image quality.

* Longitudinal distortion causes for example the image of a sphere to appear elongated in the range direction like a very long ellipsoid.

In this report we summarize the main results of our investigation under this grant. Our findings show that frequency diversity techniques not only circumvent the limitations discussed above but provide a means of viewing true 3-D images of distant objects such as satellites and aircraft. It is worthwhile to point out that our studies of wave-vector diversity imaging (or frequency swept imaging) were motivated to some extent by evidence of super-resolved "imaging" capabilities in the dolphin and the bat which are known to use frequency swept (chirp) signals in their "sonar" to discern small objects in their environment.

2. Summary of Important Results

The main findings of the study, details of which are given in the appendices and our publications (see list of publications), are outlined next.

(a) Wave-vector diversity (multifrequency and multiaspect) techniques can be used to enhance the amount of object information collected by a broadband coherent aperture deployed in the far field of the scattering object. Thus the data collected by a highly thinned array of coherent receivers intercepting the wavefield scattered from a distant 3-D reflecting object, as the frequency of its illumination (and/or its direction of incidence) are changed (see Fig. 1-a for example), can be stored as a 3-D data manifold in \bar{p} -space (Fig. 2) from which an image of the object can be retrieved by means of a 3-D Fourier Transform. The size and shape of the 3-D data manifold, and therefore the resolution, depend on the relative positions of the object, the transmitter (illuminator), and the receiving array and on the spectral width of the illumination utilized.

(b) The data collected must be corrected for a quadratic phase factor F (caused by the unequal distances between the object and the receiving stations forming the widely dispersed imaging array) before it is stored in a 3-D manifold in \bar{p} -space and an undistorted image of the 3-D reflecting object reconstructed through the 3-D Fourier transform operation. A bothersome range-azimuth ambiguity is also avoided through elimination of this quadratic phase term.

The most promising methods for data acquisition and correction is that which utilizes a target derived reference (TDR) at the synchronous detectors of the various receivers to correct for the unequal phase shifts or propagation time delays from the object to each receiver. In this approach the data furnished by the various receivers of the recording array is free of the undesired factor F . Therefore no additional processing by a computer will be necessary before filing the data at the appropriate locations in \bar{p} -space. The TDR method has several advantages which include:

(i) Elimination of the need for a costly and unreliable central local oscillator distribution network.

(ii) Because TDR results in a recording configuration similar to that of a lensless Fourier Transform hologram, the resolution requirements from the recording device are greatly relaxed*.

*A. Macovski, "Hologram Information Capacity", J. Opt. Soc. Am., Vol. 60, Jan. 1970, pp. 21-29.

In longwave holography this fact is translated into a significant reduction of the number of receiving elements in the recording aperture. In addition the use of TDR allows us to place all the resolving power of the recording aperture on the target. This means that high resolution images of distant isolated targets should be feasible with array apertures consisting of tens of elements. The ability to synthesize a 2-D receiving aperture with a Wells array† consisting of two orthogonal linear arrays one of transmitters and the other of receivers provides further means of reducing the number of stations needed for data acquisition without sacrifice in resolution. A frequency swept Wells array of 10 transmitters and 10 receivers using a (2-4) GHz sweep should be able to easily furnish 10^4 3-D distinguishable resolution cells on the target which is more than sufficient for discerning the scattering centers on practical targets.

(iv) Greater immunity to phase fluctuations arising from turbulence and inhomogeneities in the propagation medium because both the reference and imaging signals arriving at each receiving element of the aperture travel roughly over the same path.

(v) TDR eliminates the range azimuth ambiguity and excessive bandwidth problems that arise in fast frequency swept imaging when the reference signal for the array aperture is distributed instead from the illumination source or a centrally located local oscillator phase locked to it.

Two TDR methods have been considered to some extent in our work to date. In one method which we term LFTDR (*Low Frequency Target Derived Reference*), the object is assumed to be illuminated simultaneously with a high frequency imaging signal and a low frequency signal that is a subharmonic of the illuminating frequency. The subharmonic reference frequency ω_r is chosen such that $k_r l \ll 1$, l being the maximum linear dimension of the object and $k_r = \omega_r/c$, c being the velocity of light. This places scattering from the object in the Rayleigh region where the object behaves as point scatterer with zero phase contribution. The far field phase of the reference signal at any receiver is therefore entirely due to propagation between a reference point formed at the object to the receiver. A method for measuring this reference signal phase and using it to correct the imaging signal phase due to propagation has been proposed by Porter* and analyzed for a one-dimensional object geometry. The reference signal phase and the imaging signal phase are measured separately at each receiving station with the aid of two receivers whose local oscillators (L.O)'s, one at the reference frequency and one at the imaging frequency, are phase-locked only to each other and not to a central local oscillator as would be the case were we to use a conventional receiver array. Phase locking of the two LO's can be accomplished by simply making the imaging L.O a harmonic of the

†C.N. Nilsen and D.N. Swingler, "Quasi-Real-Time Inertialless Microwave Holography", Proc. IEEE (Letters), Vol. 65, March 1975, pp. 491-492.

*R.P. Porter, "A Radar Imaging System Using the Object as Reference", Proc. IEEE (Letters), Vol. 59, Feb. 1971, pp. 307-308.

reference L.O. This would eliminate the difficulties encountered in the implementation of large or giant thinned coherent receiving arrays of the type required here, namely the distribution of a central local oscillator signal. A great reduction in cost and effort associated with installation of a central L.O. distribution network can thus be achieved. This cost reduction should be compared however with the cost of implementing a LFTDR. Because of the large difference between the high frequency imaging frequencies and the low frequency reference frequency required for the high resolution imaging of practical objects, the same microwave gear can not be used for both frequencies. This could increase system cost. In addition since the measured reference phase must be multiplied by a factor β equal to the ratio of the imaging to the reference frequency before being used as a reference phase in the imaging signal measurement, any errors in the reference phase measurement will also be amplified by this ratio. The precision of the reference phase measurement and phase error analysis are important and will have therefore to be examined further.

Another TDR methods which we call the *Frequency Displaced Target Derived Reference* (FDTDR) also shows promise. In this method, the analytical details of which are outlined in appendix I, the object is illuminated simultaneously during the sweep with two phase locked imaging frequencies ω_1 and $\omega_2 = \omega_1 + \Delta\omega$, $\Delta\omega$ being a small incremental frequency. This can be realized also by single side band modulation of the swept signal or by phase locking two sweep oscillators. Measurement of the differential phase between the signals scattered from the target at these frequencies yields $\frac{\Delta\omega}{c} (R_T + R_R)$, R_T being

the distance from the transmitter to the object and R_R being the distance from the object to the receiver. Multiplication of this phase by $\omega_1/\Delta\omega$ yields the phase factor F at frequency ω_1 which would be used to correct the phase measured at ω_1 . At first look this method would appear to still require a reference local oscillator. This however is not so since the procedure outlined above need not involve explicit phase measurements and multiplications. For example by mixing the two received signals at ω_1 and $\omega_1 + \Delta\omega$ in a square law detector at each receiver a beat signal at frequency $\Delta\omega$ is derived whose phase is equal to $\frac{\Delta\omega}{c} (R_R + R_T)$. The phase shift of

this signal due to the object is effectively zero because the wavelength at $\Delta\omega$ is much larger than the object extent making it behave effectively as a point scatterer. Harmonic mixing of the signal ω_1 received at each receiver with this beat signal should yield the corrected \bar{p} -space data at ω_1 . Because of the small difference $\Delta\omega$ between the two frequencies ω_1 and ω_2 utilized, the effect of phase errors due to system and atmospheric propagation could be more completely cancelled in this method than in the low frequency TDR methods. The small difference $\Delta\omega$ means also that unlike the LFTDR case the same microwave gear (antennas, transmission lines and other microwave circuit components) can be utilized in the handling of the reference and imaging signals. A variation of the TDR technique involving double side-band modulation is also possible and appears to be more simple to implement than the single side-band method.

(c) Because in addition to being dependent on geometry, the dimensions of the 3-D data in \bar{p} -space shown in Fig. 2 are dependent on the spectral range of the illumination, super-resolution (i.e. resolution beyond the classical limit of the available physical aperture) is achieved. This aperture synthesis by wave-vector or frequency diversity helps cut down array cost (since a thinned array can be used to frequency synthesize a large array with higher filling factor).

(d) *Fourier Domain Projection Theorems* (see appendixes II and III for details) enable the generation of two dimensional holograms from projections (or weighted projections) of the corrected \bar{p} -space 3-D data manifold of Fig. 2 permitting thereby optical image retrieval of the 3-D object in slices parallel to the projection plane one at a time. For example, Fig. 1-b shows the projection hologram for the \bar{p} -space data obtained in a computer simulation of the arrangement shown in Fig. 1-a. The central cross-sectional outline of the object (the two 1 m diameter reflecting spheres of Fig. 1-a) retrieved from this projection hologram by means of a 2-D Fourier transform carried out on the optical bench is shown in Fig. 1-c. A similar example is shown in Figs. 3 and 4. Figure 3 shows a second test object consisting of 3-D distribution of a set of 8 point scatterers with locations and spacings given in the Figure. Figure 4 shows the projection holograms corresponding to the three slices of the object containing the point scatterers and the image retrieved from each. The sweep width in this example, as in the previous example, was (2-4) GHz however the number of receivers in the recording array has been reduced from 50 to 16. These computer simulations demonstrate that a 3-D (lateral and longitudinal) resolution of the order of twenty centimeters* is easily achieved with a frequency sweep covering only (2-4) GHz using a broad-band array of 16 receivers and one transmitter. Wider-spectral windows should yield better resolution. It is worthwhile to note in this respect that commercial microwave sweepers and synthesizers are available with a spectral coverage of (.1-25) GHz indicating a potential for practical resolutions of the order of possibility few centimeters with cost-effective broad-band apertures consisting of tens of receivers operating with one central illuminator.

(e) The viewing or the display of a true 3-D image of the various slices or cross-sectional outlines should be possible by reconstruction of the various projection holograms in rapid succession while projecting the reconstructed real images of the corresponding slices on a rapidly moving projection screen. The screen would be displaced rapidly (together with the Fourier transforming lens) on the optical bench in the axial directions by small amounts proportional to the distances between the various slices. In another approach we have found that the 2-D *virtual Fourier transform* of a projection hologram can be carried out by simply viewing (with the unaided eye) a transparency containing an array of reduced replicas of the projection hologram arranged side-by-side with a point source. The image retrieved in this fashion would lie in the plane of the point source. This approach has the potential for 3-D display by viewing the virtual images retrieved from a series of projection holograms corresponding to different slices or cross-sectional outlines

*This means 10^3 distinguishable 3-D resolution cells in the $(2 \times 2 \times 2)\text{m}^3$ volume of the assumed object.

of the object passed in front of the eye in rapid succession while moving the reconstruction point source axially back and forth at a suitable rate of incremental axial displacements. A proposed electro-optical scheme that permits carrying out this procedure in real-time using a rapidly recyclable spatial light modulator (SLM) operating in a reflection mode is shown in Fig. 5. The computer, the high resolution CRT and the projection optics are used to project reduced noncoherent images of the various projection holograms in rapid succession on the SLM while the axial position of the reconstruction point sources is altered rapidly also under computer control. The point source need not be derived from a laser in order to yield an image but could also be a miniature "grain of wheat" light bulb. Details of this task are found in Appendix III.

(f) As seen in (e), unlike monochromatic longwave holographic imaging, there is no specific scaling requirements imposed on the projection holograms in order to avoid longitudinal distortion in the optical reconstruction circumventing thus the wavelength scaling problem.

(g) Because of the broad spectral extent of the illumination used and ability to display the reconstructed image in separate slices, speckle or coherent noise, which is known to plague coherent imaging systems, is suppressed making the system behave in as far as image noise is concerned like a noncoherent imaging system but at the same time enjoy the superior detection characteristics associated with synchronous detection techniques.

(h) The broad-band nature of the imaging process also helps suppress undesirable image detail that could arise from object resonances which could seriously degrade image quality in a monochromatic imaging system.

(i) The data collected at every receiver, represents after correction, essentially the frequency response of the scattering object measured from a different aspect angle. Assuming the scattering process is linear, this frequency response is related to the impulse response of the object by a Fourier transform (see ref. 5 in List of publications). This suggests that impulse illumination can be utilized instead of frequency swept illumination. When this is done, the 3-D data manifold in p -space may be generated by Fourier transforming the impulse response at each receiver, correcting the data for the Factor F mentioned in (b), and storing the result in the appropriate p -space locations for each receiver. The resulting p -space volume accessed in this fashion can then be employed as described earlier to yield 3-D image information. Impulse illumination is desirable in certain instances of rapid target motion but may be more difficult to implement than frequency swept illumination. Since the impulse response of a time invariant linear system can also be deduced from white noise excitation and correlation of the output response with the input as described elsewhere in more detail (see 5 in list of publications), it follows that the techniques described in this report for coherent broadband radiation should be equally applicable with minor signal processing modification to noise-like broadband

radiation including passive black-body radiation.

(j) Experimental verification for both the principle of frequency diversity imaging and the TDR concept were obtained with the aid of a semi-automated network analyzer configured and installed in a recently refurbished anechoic chamber within the scope of this program (see Figs. 6 and 7). This versatile system is capable of vector (amplitude and phase) measurements of wavefields scattered from test objects situated in the anechoic chamber over any frequency range lying in the (.1-18)GHz range for a variety of polarizations. A test object consisting of two parallel cylinders 25 cm apart each 5 cm in diameter and 50 cm long was mounted on a rotating styrofoam pedestal that is under computer control and illuminated as shown in Fig. 8. The distance from the center of the object to the illuminating parabolic antenna to the left and the receiving horn feeding the network analyzer was 2.5 m. The complex frequency response of this object was measured in the (5-14)GHz range and the data stored for 128 object orientation covering 360° . The stored data was corrected for range-phase with a synthetic TDR generated in the computer and the corrected data displayed and photographed yielding the frequency swept hologram shown in Fig. 9 (c). The image retrieved from this hologram via an optical Fourier transform carried out on the optical bench is shown in Fig. 9 (d). For reasons of comparison a computer simulation of this experiment assuring a (2-18)GHz sweep was performed. The resultant range-phase corrected hologram and the image retrieved from it optically are shown in Fig. 9 (a) and (b). Further detail on this phase of the program were reported in an MSc. thesis made part of this report in Appendix IV. This part of the program is being continued with the aim of further enhancing measurement accuracy and demonstrating imaging of a nonsimple 3-D test object such as a model aircraft utilizing polarization diversity to further enhance image quality.

3. Conclusions.

The primarily analytical and numerical study of frequency diversity imaging performed under this grant demonstrates conclusively the feasibility of a new generation of coherent broadband imaging radars capable of furnishing 3-D image detail of distant target with cost effective giant apertures and efficient digital/optical signal processing.

Future work in this area will focus more on the analysis and identification of optimal methods for data acquisition, processing and 3-D display. The ultimate aim is the generation of design criteria for a prototype system and its assessment in the 3-D imaging of low flying aircraft passing within range of our facilities on route for landing at the Philadelphia Airport.

List of Publications

1. N.H. Farhat, "Frequency Synthesized Imaging Apertures", Proc. 1976, International Optical Computing Conference, IEEE Cat. #76 CH 1100-7C, pp. 19-24.
2. N.H. Farhat, M.S. Chang, J.D. Blackwell and C.K. Chan, "Frequency Swept Imaging of a Strip", Proc. 1976, Ultrasonics Symposium, IEEE Cat. #76 CH 1120-5SU.
3. J.D. Blackwell and N.H. Farhat, "Image Enhancement in Longwave Holography by Electronic Differentiation", Optics Communications, Vol. 20, Jan. 1977, pp. 76-80.
4. C.K. Chan, N.H. Farhat, M.S. Chang and J.D. Blackwell, "New Results in Computer Simulated Frequency Swept Imaging", Proc. IEEE (Letters), Vol. 65, pp. 1214-1215, Aug. 1977.
5. N.H. Farhat, "Principles of Broad-Band Coherent Imaging", J. Opt. Soc. Am., Vol. 67, pp. 1015-1020, Aug. 1977.
6. N.H. Farhat, "Comment on Computer Simulation of Frequency Swept Imaging", Proc. IEEE, Vol. 65, pp. 1223-1226, Aug. 1977.
7. N.H. Farhat, "Comment on a New Imaging Principle", Proc. IEEE (Letters), Vol. 66, pp. 609-700, May 1978.
8. N.H. Farhat, "Microwave Holographic Imaging - Prospects For a Real-Time Camera", SPIE, Vol. 180, *Real-Time Signal Processing II*, (1979).
9. N.H. Farhat and C.K. Chan, "Three-Dimensional Imaging by Wave-Vector Diversity", *Acoustical Imaging*, Vol. 8, A. Metherell (ed.), Plenum Press, New York (1980), pp. 499-515.
10. C.K. Chan and N.H. Farhat, "Frequency Swept Imaging of Three Dimensional Perfectly Reflecting Objects", IEEE Trans. on Antennas and Propagation - Special Issue on Inverse Scattering. (Accepted for publication.)
11. C.K. Chan, "Analytical and Numerical Studies of Frequency Swept Imaging", University of Pennsylvania, Ph.D. Dissertation (1978).
12. N.H. Farhat, "Microwave Holography and Coherent Tomography", (Invited paper). Presented at 1980 IEEE/MTT's International Microwave Symposium, Electromagnetic Dosimetric Imaging. (To be published in special conference proceedings).

Related Publications

1. N.H. Farhat, "New Imaging Principle", Proc. IEEE (Letters), Vol. 64, pp. 379-380, March 1976.
2. N.H. Farhat, T. Dzekov and E. Ledet, "Computer Simulation of Frequency Swept Imaging", Proc. IEEE (Letters), Vol. 64, pp. 1453-1454, Jan. 1977.
3. G. Tricoles and N.H. Farhat, "Microwave Holography: Applications and Techniques", Invited paper, Proc. IEEE, Vol. 65, pp. 108-121, Jan. 1977.
4. M.A. Kujoory and N.H. Farhat, "Microwave Holographic Substraction for Imaging of Buried Objects", Proc. IEEE (Letters), Vol. 66, pp. 94-96, Jan. 1978.
5. M.A. Kujoory and N.H. Farhat, "Format Generation For Double Circular Scanners For Use in Longwave Holography", Acoustical Imaging and Holography, Vol. 1, No. 2, pp. 133-141 (1979).
6. N.H. Farhat and J. Bordogna, "An Electro-Optics and Microwave-Optics Program In Electrical Engineering", IEEE Trans. on Education - Special Issue on Optics Education (accepted for publication).
7. N.H. Farhat, "Holographically Steered Millimeter Wave Antennas", IEEE Trans. on Antennas and Propagation, Vol. AP-28, July 1980, pp. 476-480.

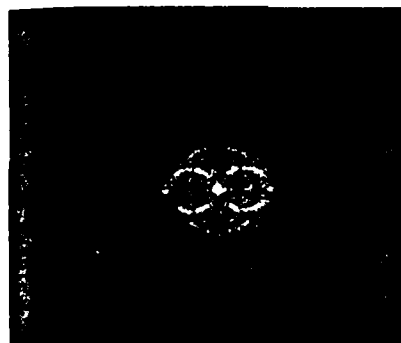
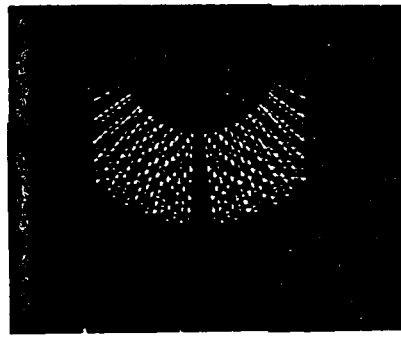
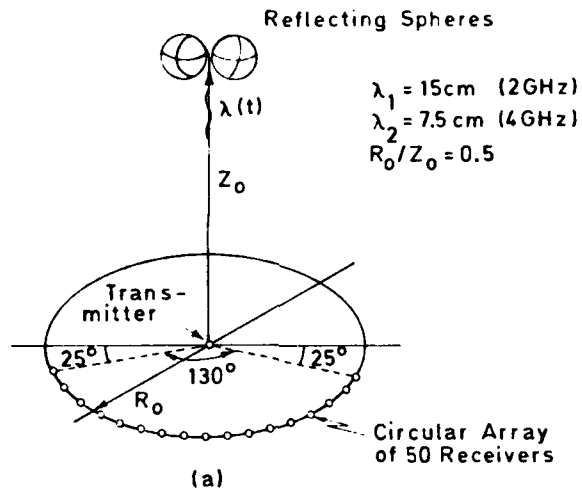


Fig. 1. Computer Simulation of Wave-vector Diversity Imaging, (a) Geometry, (b) Projection Hologram, (c) Retrieved Central Cross-sectional Image.

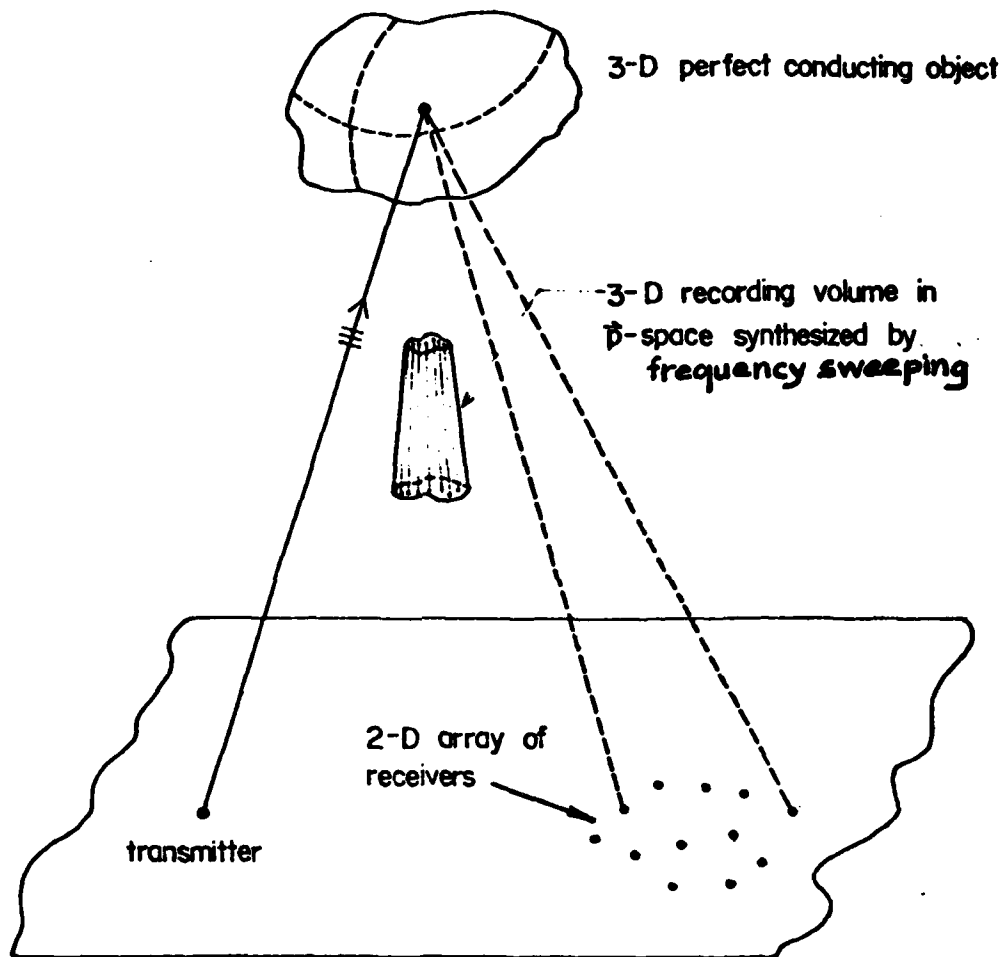


Fig.2 Three dimensional \bar{p} -space data generated by frequency sweeping and collected by a 2-D array of receivers.

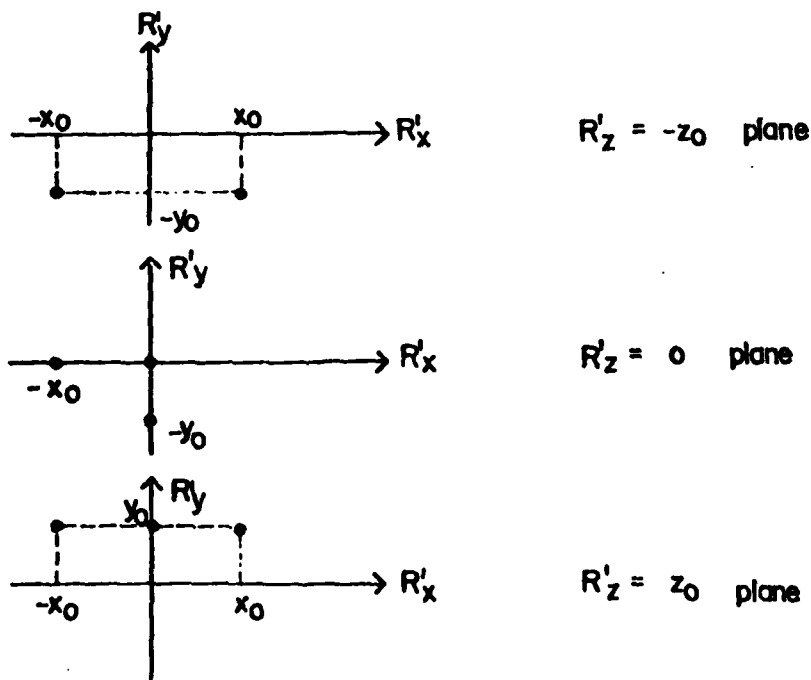
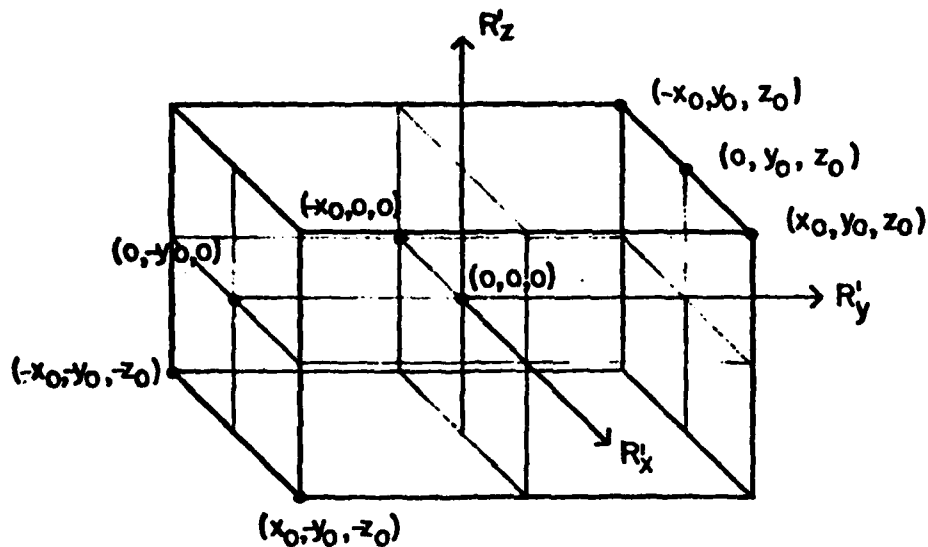


Fig. 3. 3-D object consisting of a set of eight point scatterers shown in isometric and R'_x - R'_y plane views at $R'_z = -z_0, 0, z_0$. $x_0 = y_0 = z_0 = 100^x \text{ cm}^y$.

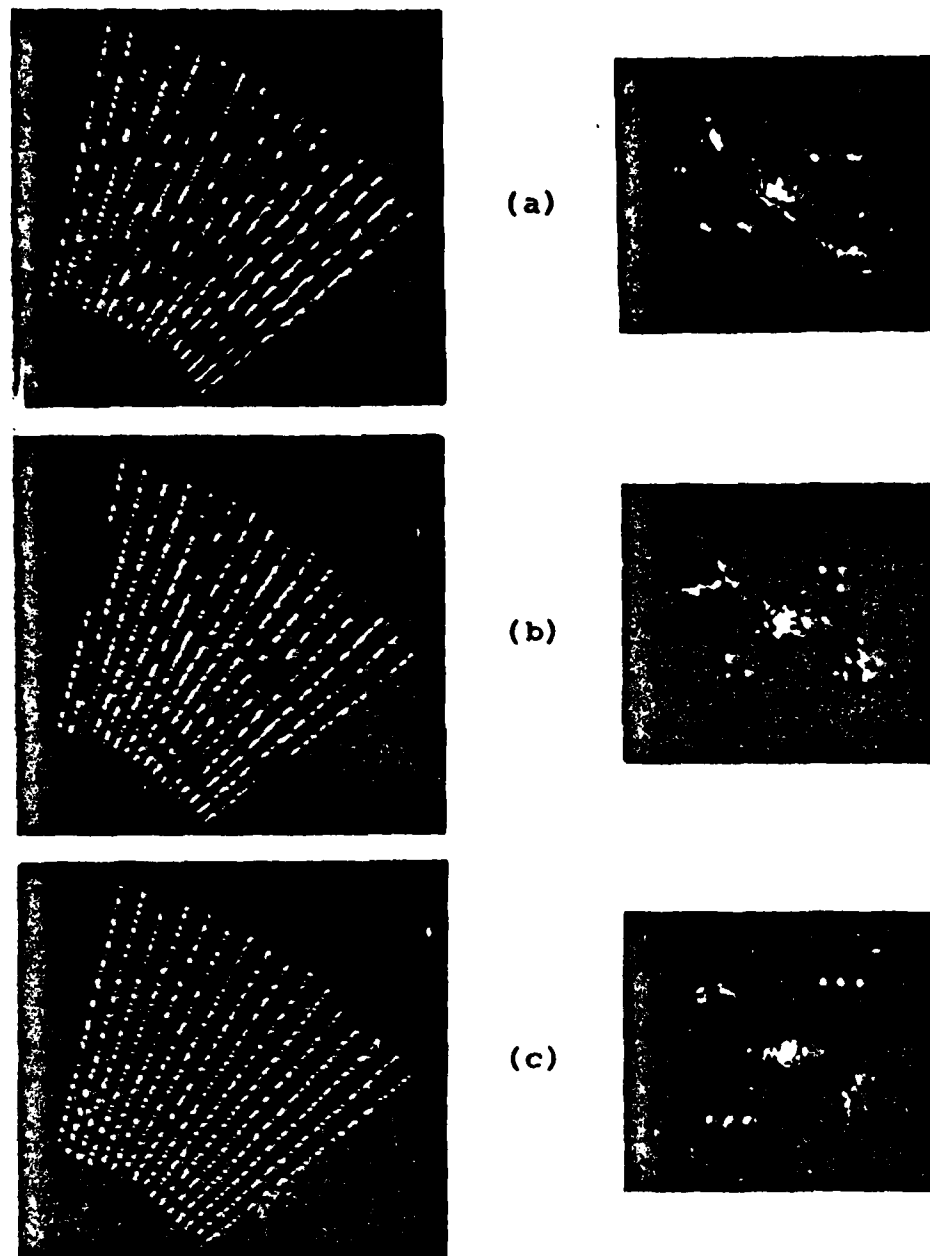


Fig. 4. Projection holograms and their optical reconstructions for the set of point scatterers in Fig.7.10 at different R'_z planes. (a) Hologram and reconstructed image of z scatterers at $R'_z = -z_0$ plane. (b) Hologram and image at $R'_z = 0$ plane. (c) Hologram and image at $R'_z = z_0$ plane. $x_0 = y_0 = z_0 = 100\text{cm}$.

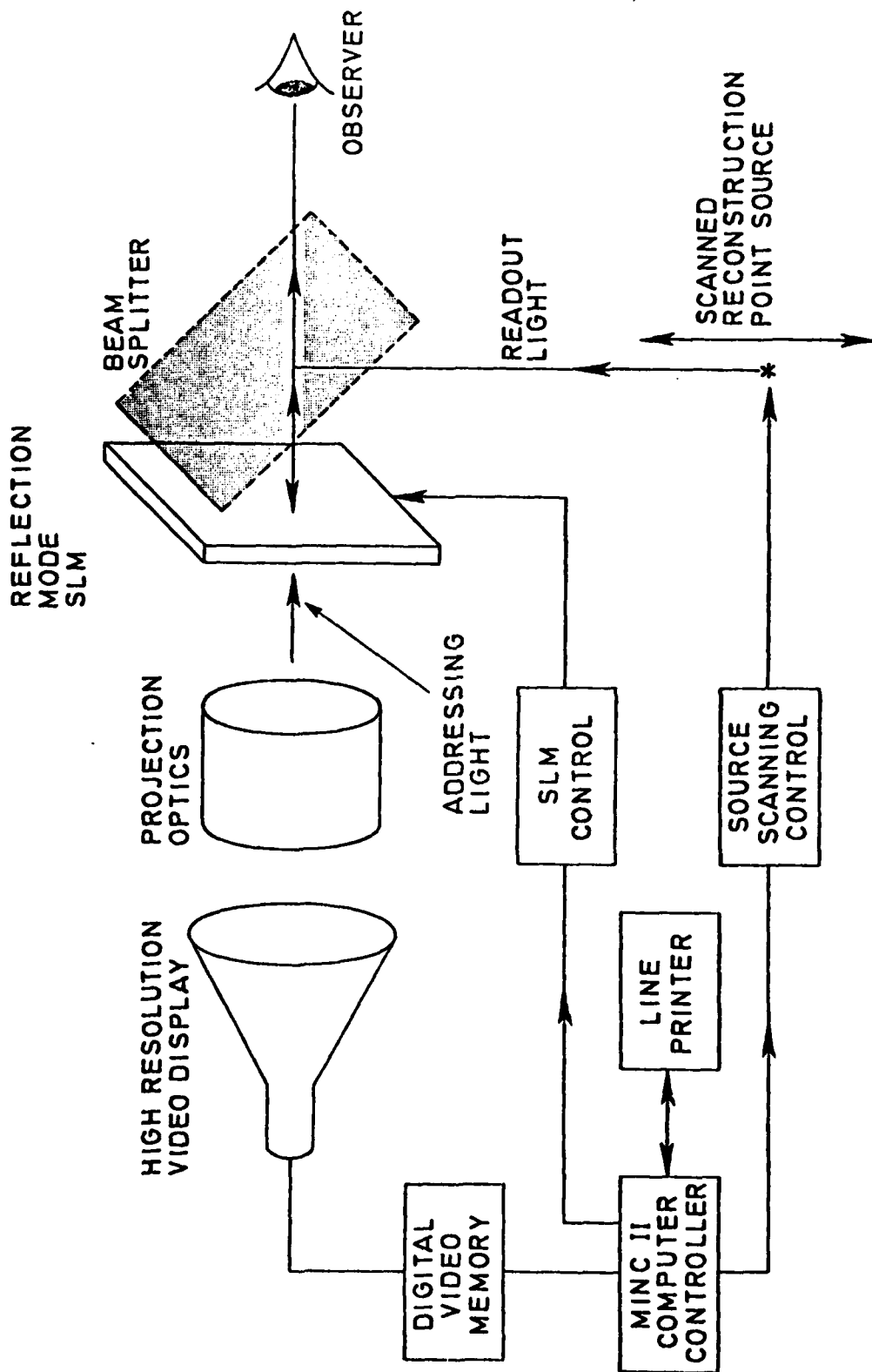


Fig. 5. True 3-D image reconstruction based on the virtual Fourier transform.

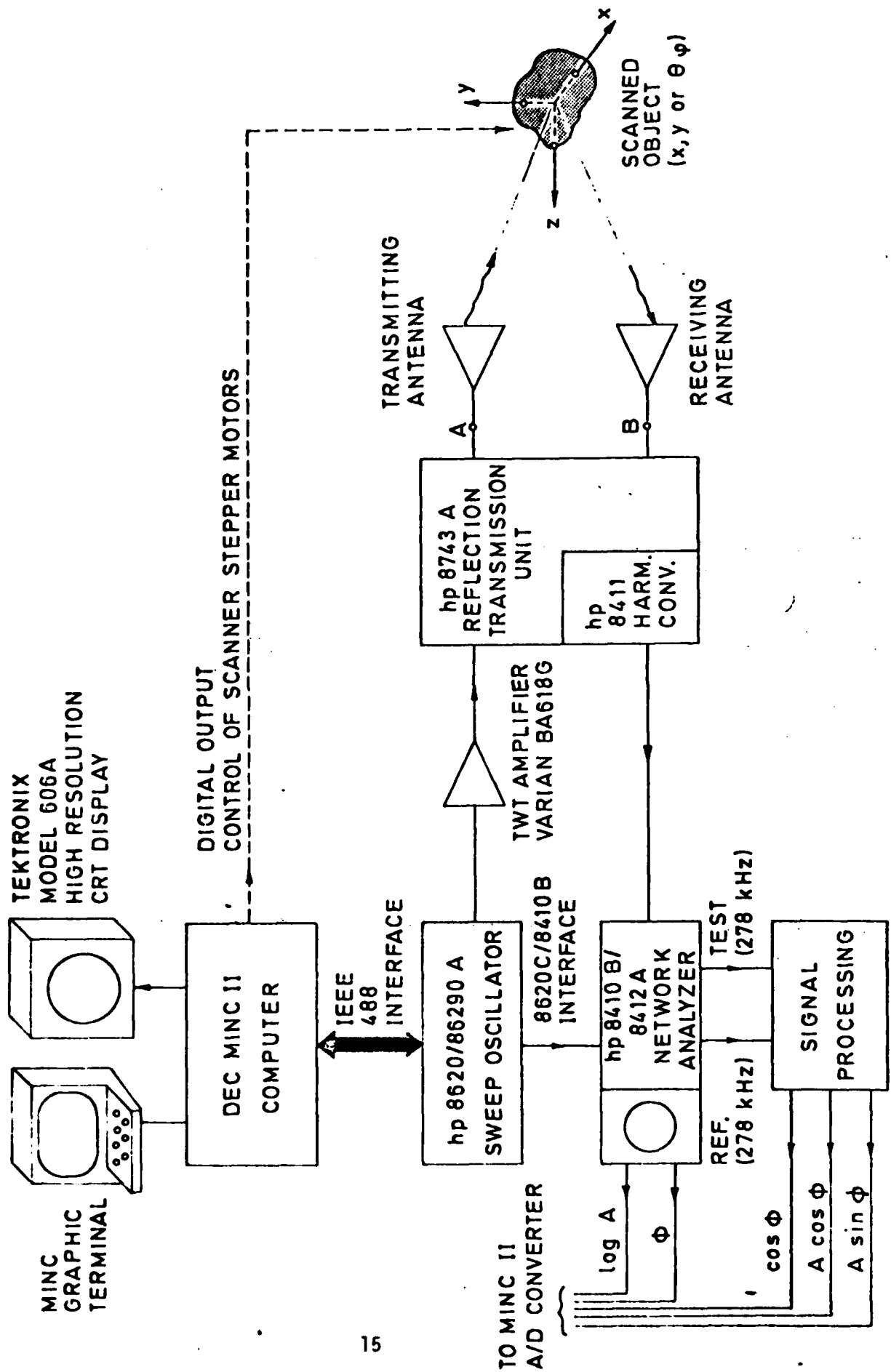


Fig. 6. Block Diagram of Automated Microwave Network Analyzer Showing Interface to MINC II Computer via IEEE 488 Standard Interface Bus.

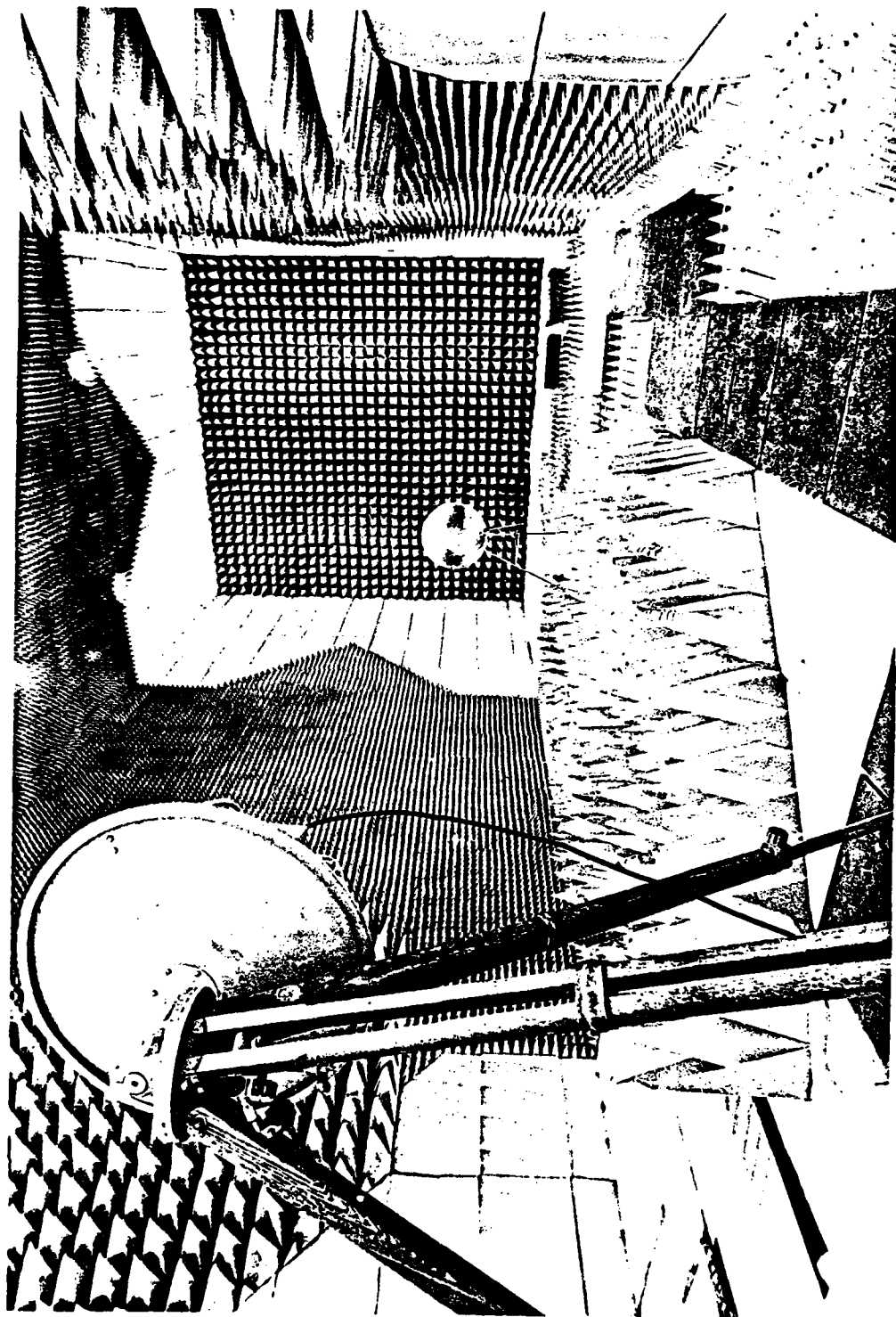
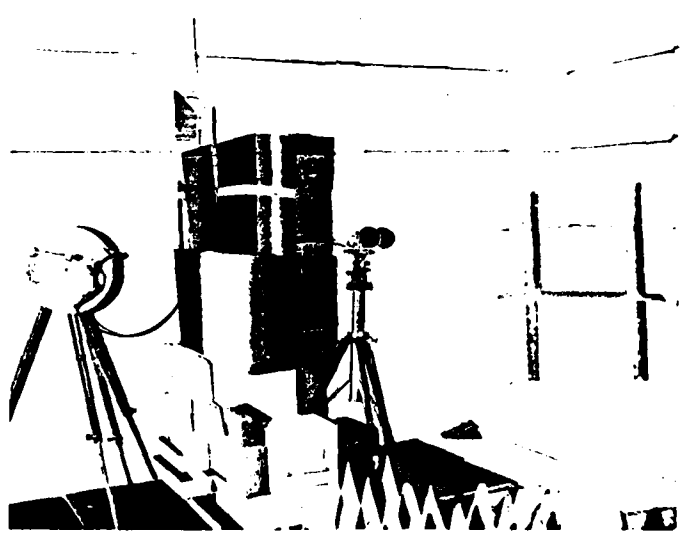
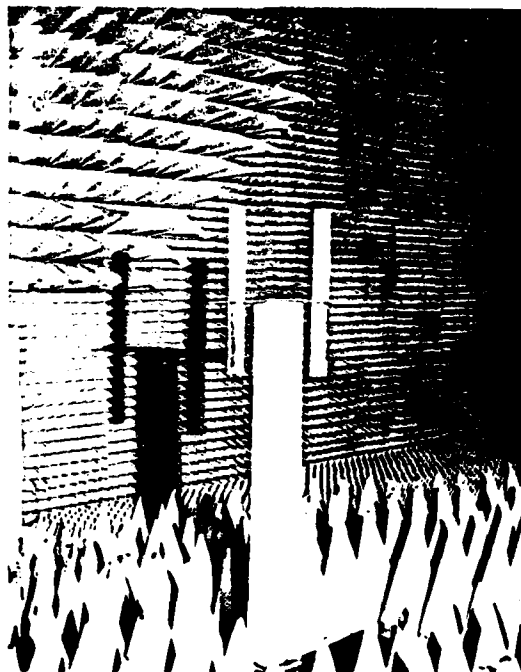


Fig. 7. View of Microwave Anechoic chamber showing illuminator antenna and a calibration sphere in background.

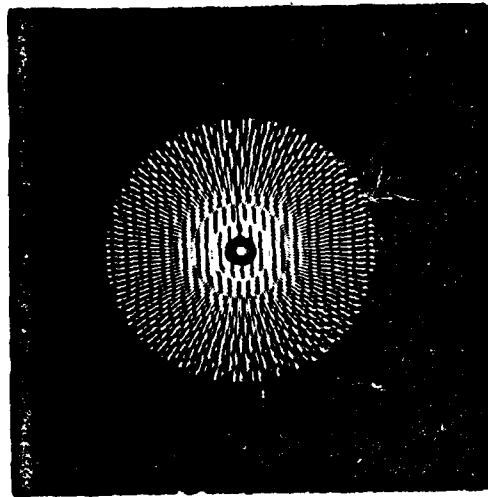


(a)

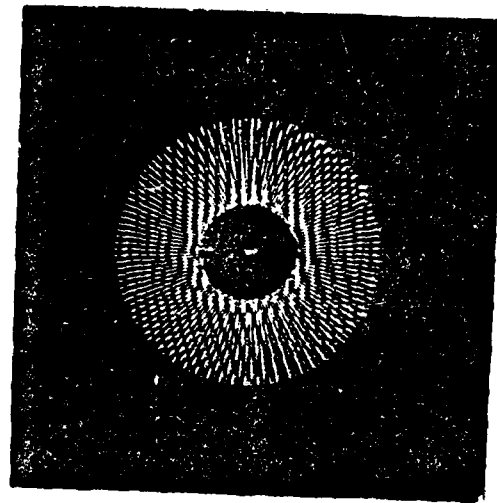


(b)

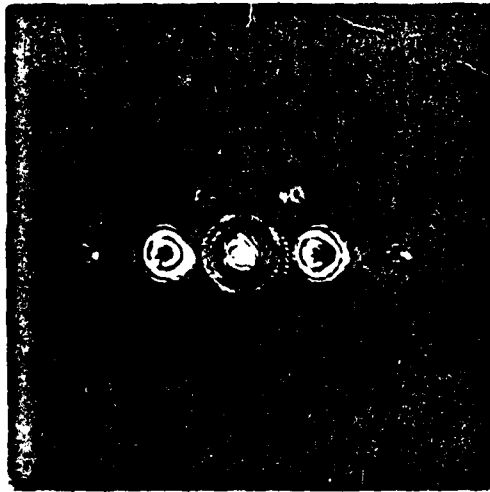
Fig. 8. Two views of dual-cylinder test object in Anechoic chamber. (a) View showing illuminator to the left and the receiving horn on the right separated by absorbing barrier. (b) View showing test object mounted on rotating styrofoam pedestal. Cylinders are 5 cm in diameter, 50 cm long, 25 cm apart.



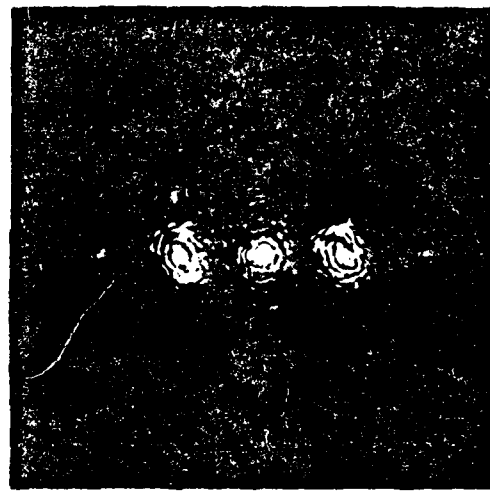
(a)



(c)



(b)



(d)

Fig. 9. Frequency swept holograms and retrieved images for a dual-cylinder test object. (a) Computed frequency swept hologram for a (2-18)GHz sweep and (b) retrieved image; (c) measured frequency swept hologram for a (5-14)GHz sweep and (d) retrieved image.

APPENDICES

APPENDIX I

The Frequency Displaced Target Derived Reference

A second TDR method which we refer to as a *Frequency Displaced Target Derived Reference* (FDTDR) method also shows promise. This method involves simultaneous illumination of the object with two phase locked imaging frequencies ω_1 and $\omega_2 = \omega_1 + \Delta\omega$ that differ by a small frequency increment $\Delta\omega$. Referring to eq. (9) of ref. 10 (see list of publications) we can write for the far field at a given receiver location R_R ,

$$\psi_1(k_1, R_R) = \frac{jk_1}{2\pi R_R} e^{-jk_1(R_T+R_R)} \int U(\vec{r}) e^{-j\vec{p}_1 \cdot \vec{r}} d\vec{r} \quad (1)$$

$$\psi_2(k_2, R_R) = \frac{j(k_1+\Delta k)}{2\pi R_R} e^{-jk_1(R_T+R_R)} e^{-j\Delta k(R_T+R_R)} \int U(\vec{r}) e^{-j\vec{p}_1 \cdot \vec{r} \left(1 + \frac{\Delta\omega}{\omega_1}\right)} d\vec{r} \quad (2)$$

where $k_{1,2} = \omega_{1,2}/c$ and $\Delta k = \Delta\omega/c$.

By making $\Delta\omega/\omega \ll 1$ the integral in (2) will approach that in (1). The only difference between the far fields ψ_1 and ψ_2 at the receivers is then the phase term $\Delta k(R_T + R_R)$. Measurement of this phase difference yields $(R_T + R_R)$ since Δk is known. This information can be used to correct the phase of either the ψ_1 or ψ_2 signals to obtain the required \vec{p} -space information.

$$\Gamma(\vec{p}) = \int U(\vec{r}) e^{j\vec{p} \cdot \vec{r}} d\vec{r} \quad (3)$$

Appendix II

HOLOGRAPHY, WAVE-LENGTH DIVERSITY AND INVERSE SCATTERING

ABSTRACT

The use of wavelength diversity to enhance the performance of thinned coherent imaging apertures is discussed. It is shown that wavelength diversity lensless Fourier transform recording arrangements that utilize a reference point source in the vicinity of the object can be used to access the three-dimensional Fourier space of non-dispersive perfectly reflecting or weakly scattering objects. Hybrid (opto-digital) computing applied to the acquired 3-D Fourier space data is shown to yield tomographic reconstruction of 3-D image detail either in parallel or meridional (central) slices. Because of an inherent ability of converting spectral degrees of freedom into spatial 3-D image detail true super-resolution is achieved together with suppression of coherent noise. The similarity of the key equations derived to those of inverse scattering theory is pointed out and the feasibility of using other forms of broadband radiation such as impulsive, noise and thermal is discussed. Finally, the potential of utilizing wavelength diversity imaging in microscopy and telescopy are discussed.

INTRODUCTION

A frequently encountered question in the science of image formation is how to make an available aperture collect more information about the scene or object being imaged in order to enhance its resolving power beyond the classical Rayleigh limit. This process is known as super-resolution and is relevant to all imaging systems whether holographic or conventional. There are five known methods for achieving super-resolution. These include: weighting or apodization of the aperture data^{1,2}; analytic continuation of the wavefield measured over the aperture^{3,4}; use of evanescent wave illumination⁵; maximum entropy method⁶; and use of the time channel⁷. Weighting and analytical continuation techniques are known to become rapidly ineffective as the signal to noise ratio of the data collected decreases. Maximum entropy techniques are known to be more robust as far as noise is concerned but involve usually extensive computation. Illumination with evanescent waves is practical in limited situations where full control of the recording arrangement exists as in microscopy for example.

This leaves the time channel approach in which one can collect in time more information about the object through the available recording aperture by altering the object aspect relative to the aperture by means of rotation or linear motion^{8,9} or by altering the parameters of the illumination such as directions of incidence, wavelength and/or polarization. These later operations are known to increase the degrees of freedom of the wavefields impinging on the recording aperture enhancing thereby their ability to convey information about the nature of the scattering object. Sophisticated imaging systems endeavour to convert the nonspatial degrees of freedom of the wavefield, e.g., angular, spectral and polarization to spatial image detail enhancing thereby the resolution capability beyond the classical Rayleigh limit of the available physical aperture. Obviously such procedures involve more signal processing than that performed by conventional imaging with lens systems or holography.

In this paper we consider generalizing the holographic concept to include wavelength diversity as a means of enhancing resolution. A quick examination of the basic equations of holography reveals that the lensless Fourier transform hologram recording arrangement is amenable to this generalization. This conclusion is used then as a starting point for a Fourier optics formulation of wavelength diversity imaging of 3-D (three dimensional) nondispersive objects. The results show that measurement of the multiaspect or multistatic frequency (or wavelength) response of the 3-D object permits accessing its 3-D Fourier space. The resulting formulas are identical to those obtained from a multistatic generalization of inverse scattering^{10,11,12} establishing thus a clear connection between holography and the inverse scattering imaging problem. The inclusion of wavelength diversity in holography is shown to have several important features: (a) the availability of the 3-D Fourier space data permits 3-D image retrieval tomographically in parallel or meridional (central) slices or cross-sectional outlines by the application of Fourier domain projection theorems, (b) suppression of coherent noise and speckle in the retrieved image, (c) removal of several longstanding constraints on longwave (microwave and acoustical) holography such as the impractically high cost of the apertures needed, the inability to view a true 3-D image as in optical holography because of a wavelength scaling problem, and minimization of the effects of resonances on the object.

WAVELENGTH DIVERSITY

We start by inquiring into the conditions under which the data from N holograms of the same nondispersive object recorded over the same aperture, each at a different wavelength, can be combined to yield a single image superior in quality to the image retrieved from any of the individual holograms.

One approach to answering the question posed above would be to determine the conditions under which the well known formulas¹³ for the focusing condition, magnification and image location in holography can be made independent of wavelength. This quickly leads to the conclusion that wavelength independence can be met if a reference point source centered on the object is used and proper scaling of the individual holograms by the ratio of recording to the reconstruction wavelength is performed before super-position^{15,24}. The former condition is that for recording a lensless Fourier transform hologram¹⁴ where the presence of the reference point source in the object plane leads to the recording of a Fraunhofer diffraction pattern of the object rather than its Fresnel diffraction pattern because of the elimination of a quadratic phase term in the object wavefield in the recorded hologram. This is known to result in a highly desirable reduction in the resolution required from the hologram recording medium and is therefore of practical importance especially in nonoptical holography. More detail of the processing involved in combining the data in multi wavelength hologram can be found elsewhere¹⁵.

Additional insight into the process of attaining super-resolution by wavelength diversity is obtained by considering the concept of wavelength or frequency synthesized aperture¹⁶⁻²⁰. The synthesis of a one dimensional aperture by wavelength diversity is based on the simple fact that the Fraunhofer or far field diffraction pattern of a nondispersive planar object changes its scale, i.e. it "breathes", but does not change its shape (functional dependence), as the wavelength is changed. A stationary array of broadband sensors capable of measuring the complex field variations deployed in this breathing diffraction pattern at suitably chosen locations would sense different parts of the diffraction pattern as the wavelength is altered collecting thereby more information on the nature of the diffraction pattern and therefore on the object that gave rise to it than if the wavelength was fixed (stationary diffraction pattern). Each stationary sensor in the array is thus able to collect as the wavelength is changed, and the breathing diffraction pattern sweeps over it, the same set of data or information collected by a movable sensor mechanically scanned over the appropriate part of the diffraction pattern when it is kept stationary by fixing the wavelength. Hence the term wavelength or frequency synthesized aperture.

The orientation and location of the wavelength synthesized aperture for any planar distribution of sensors deployed in the Fraunhofer diffraction pattern of a planar object and the retrieval of an image from the data collected has been treated earlier^{16,17}. It was clear, however, that extension of the wavelength diversity concept to the case of 3-D objects is necessary before its generality and practical use could be established.

For this purpose we considered²⁰ as shown in Fig. 1(a) an isolated planar object of finite extent with reflectivity $D(\bar{\rho}_0)$, where $\bar{\rho}_0$ is a two dimensional position vector in the object plane (x_0, y_0) . The object is illuminated by a coherent plane wave of unit-amplitude and of wave vector $\bar{k}_i = k \bar{I}_{k_i}$ produced for example by a distant source located at \bar{R}_T . The wavefield scattered by the object is monitored at a receiving point designated by position vector \bar{R}_R belonging to a recording aperture lying in the far field region of the object. The receiving point will henceforth be referred to as the receiver and the source point at the transmitter. The position vectors $\bar{\rho}_0$, \bar{R}_T and \bar{R}_R are measured from the origin of a cartesian coordinate system (x_0, y_0, z_0) centered in the object. The object is assumed to be nondispersive i.e., D is independent of k . However, when the object is dispersive such that $D(\bar{\rho}_0, k) = D_1(\bar{\rho}_0)D_2(k)$ and $D_2(k)$ is known, the analysis presented here can easily be modified to account for such object dispersion by correcting the data collected for $D_2(k)$ as k is changed.

Referring to Figure 1(a) and ignoring polarization effects, the field amplitude at \bar{R}_R caused by the object scattered wavefield may be expressed as,

$$\psi(k, \bar{R}_R) = \frac{jk}{2\pi} \int D(\bar{\rho}_0) e^{-j\bar{k}_i \cdot \bar{r}_T} \frac{e^{-jk r_R}}{r_R} d\bar{\rho}_0 \quad (1)$$

where $d\bar{\rho}_0$ is an abbreviation for $dx_0 dy_0$ and the integration is carried out over the extent of the object. Noting that $\bar{r}_T = \bar{\rho}_0 - \bar{R}_T$, $\bar{R}_T = -R_T \bar{I}_{k_i}$ and using the usual approximations valid here: $r_R \simeq R_R + \rho_0^2/2R_R - \bar{I}_R \cdot \bar{\rho}_0$ for the exponential in (1) and $r_R \simeq R_R$ for the denominator in (1) where $\bar{I}_R = \bar{R}_R/R_R$ and $\bar{I}_{k_i} = \bar{k}_i/k$ are unit vectors in the \bar{R}_R and \bar{k}_i directions respectively, one can write eq. (1) as,

$$\psi(k, \bar{R}_R) = \frac{jk}{2\pi R_R} e^{-jk(R_T + R_R)} \int D(\bar{\rho}_0) e^{-j\bar{p} \cdot \bar{\rho}_0} d\bar{\rho}_0, \quad (2)$$

where we have used the fact that the observation point is in the far field of the object so that $\exp(-jk \rho_0^2/2R_R)$ under the integral sign can be replaced by unity. In eq. (2), $\bar{p} = k(\bar{I}_{k_i} - \bar{I}_R) \triangleq p_x \bar{I}_x + p_y \bar{I}_y + p_z \bar{I}_z$ is a three dimensional vector whose length and orientation depend

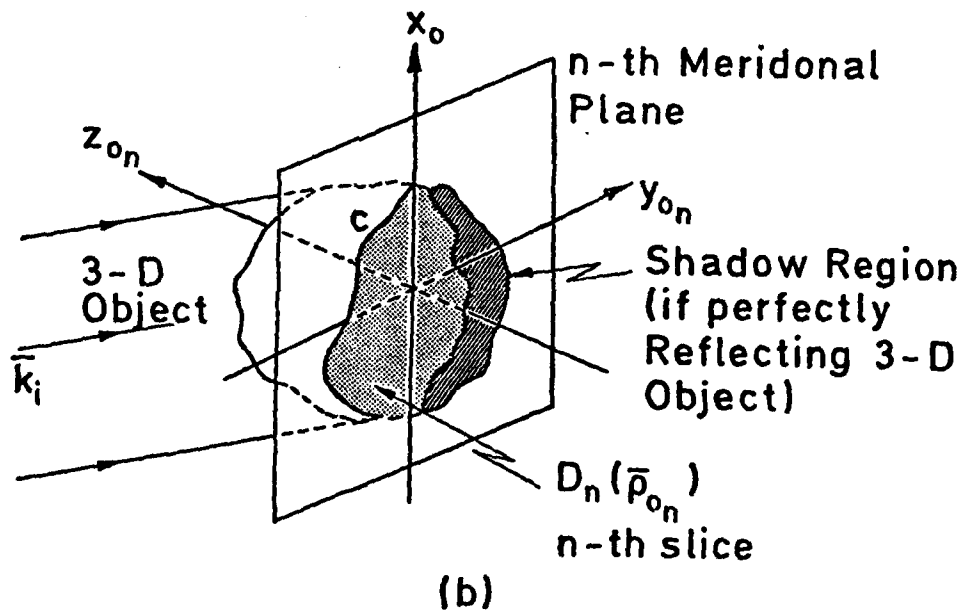
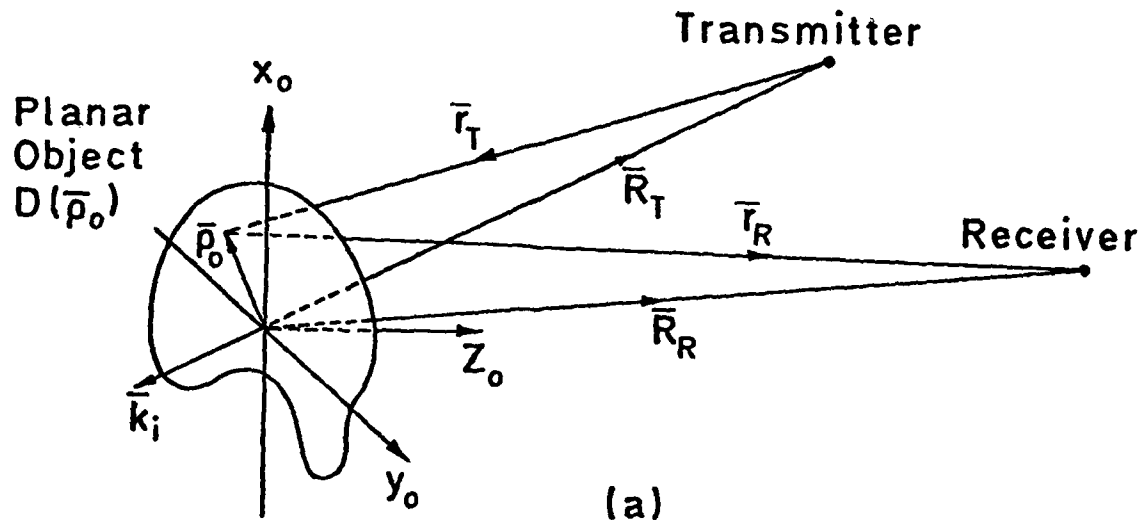


Fig. 1. Geometries for wavelength diversity imaging. (a) Two dimensional object, (b) Three dimensional object with the n -th meridional (central) slice and cross sectional outline c shown.

on the wavenumber k and the angular positions of the transmitter and the receiver. For each receiver and/or transmitter present, \bar{p} indicates the position vector for data storage. An array of receivers for example would yield therefore as k is changed (frequency diversity) or as \bar{k} ($=k\bar{1}_{k_i}$) is changed (wave-vector diversity) a 3-D data manifold.

The projection of this 3-D data manifold on the object plane yields $\psi(k, R_T)$ because $\bar{p} \cdot \bar{\rho}_0 = \bar{p}_t \cdot \bar{\rho}_0 = p_x x_0 + p_y y_0$ where $p_x = k(\bar{1}_{k_i} - \bar{1}_R)_x$ and $p_y = k(\bar{1}_{k_i} - \bar{1}_R)_y$ are the cartesian components of the projection \bar{p}_t of \bar{p} on the object plane. Accordingly eq. (2) can be expressed as,

$$\psi(k, R_R) = \frac{jk}{2\pi R_R} e^{-jk(R_T + R_R)} \int D(x_0, y_0) e^{-j(p_x x_0 + p_y y_0)} dx_0 dy_0 \quad (3)$$

Because of the finite extent of the object, the limits on the integral can be extended to infinity without altering the result. The integral in (3) is recognized then as the two dimensional Fourier transform $\tilde{D}(p_x, p_y)$ of $D(x_0, y_0)$. It is seen to be dependent on the object reflectivity function, the angular positions of the transmitter and the receiver and on the values assumed by the wavenumber k but is entirely independent of range. Information about D can thus be collected by varying these parameters. Note that the range information is contained solely in the factor $F = jk \exp[-jk(R_T + R_R)]/2\pi R_R$ preceding the integral. The field observed at \bar{R}_R has thus been separated into two terms one of which, the integral \tilde{D} , contains the lateral object information and the other F , contains the range information. The presence of F in eq. (3) hinders the imaging process since it complicates data acquisition and if not removed, gives rise to image distortion because R_R is generally not the same for all receivers. To retrieve an image of the object via a 2-D Fourier transform of eq. (3), the factor F must first be eliminated. Holographic recording of the complex field amplitude given in (3) using a reference point source located at the center of the object will result in the elimination of the factor F and the recording of a Fourier transform hologram. This operation yields \tilde{D} over a two dimensional region in the p_x, p_y plane.

The size of this region, which determines the resolution of the retrieved image depends on the angular positions of the transmitter and the receiver and on the values assumed by k , i.e. the extent of the spectral window used. The later dependence on k implies super-resolution imaging capability because of the frequency synthesized dimension of the 2-D data manifold generated. Because of the dependence of resolution on the relative positions of the object, the transmitter, and receiving aperture, the impulse response is clearly spatially variant. In fact a receiver point situated at \bar{R}_R for which \bar{p} is normal to the object

plane can not collect any lateral object information because for this condition ($\bar{p} \cdot \bar{\rho}_0 = 0$) the integrals in (2) and (3) yield a constant.

Such receiving point is located in the direction of specular reflection from the object where the diffraction pattern is stationary i.e. does not change with k . In this case the observed field is solely proportional to F containing thus range information only. Obviously this case can easily be avoided through the use of more than one receiver which is required anyway when 2-D or 3-D object resolution is sought^{20,21}.

The analysis presented above can be extended to three dimensional objects by viewing a 3-D object as a collection of thin meridional or central slices as depicted in Fig. 1(b) each of which representing a two dimensional object of the type analyzed above. With the n -th slice we associate a cartesian coordinate system $x_{o_n}, y_{o_n}, z_{o_n}$ that differ from other slices by rotation about the common x_{o_n} axis. Since the vectors \bar{p} , \bar{R}_T and \bar{R}_R are the same in all n -coordinate systems, eq. (3) holds. $\psi_n(k, \bar{R}_R)$ is then obtained from projection of the three dimensional data manifold collected for the 3-D object on the x_{o_n}, y_{o_n} plane associated with the n -th slice. An image for each slice can then be obtained as described before. An inherent assumption in this argument is that all slices are illuminated by the same plane wave. This is a reasonable approximation when the 3-D object is weakly scattering and the Born approximation is applicable or when the 3-D object is perfectly reflecting and does not give rise to multiple reflections between its parts. In the later case the two dimensional meridional slices $D_n(\bar{\rho}_{o_n})$ deteriorate into contours, such as C in Fig. 1(b) defined by the intersection of the meridional planes with the illuminated portion of the surface of the object. Accordingly we can write for the n -th meridional slice or contour,

$$\psi_n(k, \bar{R}_R) = F \int D_n(\bar{\rho}_{o_n}) e^{-j\bar{p} \cdot \bar{\rho}_{o_n}} d\bar{\rho}_{o_n} \quad (4)$$

We can regard $D_n(\bar{\rho}_{o_n})$ as the n -th meridional slice or contour of a three dimensional object of reflectivity $U(\bar{r})$ where \bar{r} is a three dimensional position vector in object space. This means that $D_n(\bar{\rho}_{o_n}) = U(\bar{r}) \delta(z_{o_n})$ where δ is the Dirac delta "function". Consequently eq. (4) becomes,

$$\begin{aligned}\psi_n(k, R_R) &= F \int U(\vec{r}) \delta(z_{o_n}) e^{-j\vec{p} \cdot \vec{\rho}_{o_n}} d\vec{\rho}_{o_n} \\ &= F \int U(\vec{r}) \delta(z_{o_n}) e^{-j\vec{p} \cdot \vec{r}} d\vec{r}\end{aligned}\quad (5)$$

where $d\vec{r}$ designated an element of volume in object space and where the last equation is obtained by virtue of the sifting property of the delta function.

Summing up the data from all slices or contours of the object we obtain,

$$\sum_n \psi_n = F \int U(\vec{r}) e^{-j\vec{p} \cdot \vec{r}} d\vec{r} = \psi(\vec{p}) \quad (6)$$

because

$$\sum_n U(\vec{r}) \delta(z_{o_n}) = U(\vec{r}).$$

Assuming that the Factor F in eq. (6) is eliminated as before, equation (6) reduces to

$$\psi(\vec{p}) = \int U(\vec{r}) e^{-j\vec{p} \cdot \vec{r}} d\vec{r} \quad (7)$$

which is the 3-D Fourier transform of the object reflectivity $U(\vec{r})$. Wavelength diversity permits therefore accessing the 3-D Fourier space of a nondispersive object providing thereby the basis for 3-D Lensless Fourier transform holography. An alternate formulation to that given above of super-resolved wave-vector diversity imaging of 3-D perfectly conducting objects is possible²² by extending the formulation of the inverse scattering imaging problem^{10,11} to the multistatic case, along lines that are similar but somewhat different than those given by Raz¹². The resulting scalarized formulas are identical to (7) establishing thus the connection between the holographic and the inverse scattering approaches to the imaging problem.

THREE DIMENSIONAL IMAGE RETRIEVAL

The above considerations of multiwavelength holography have lead us to determining a means by which the 3-D Fourier space of the object can be accessed employing synchronous detection. It is clear that once the 3-D Fourier space data is available, 3-D image detail can be retrieved by means of an inverse 3-D Fourier transform which can be carried out digitally. Alternately, holographic techniques

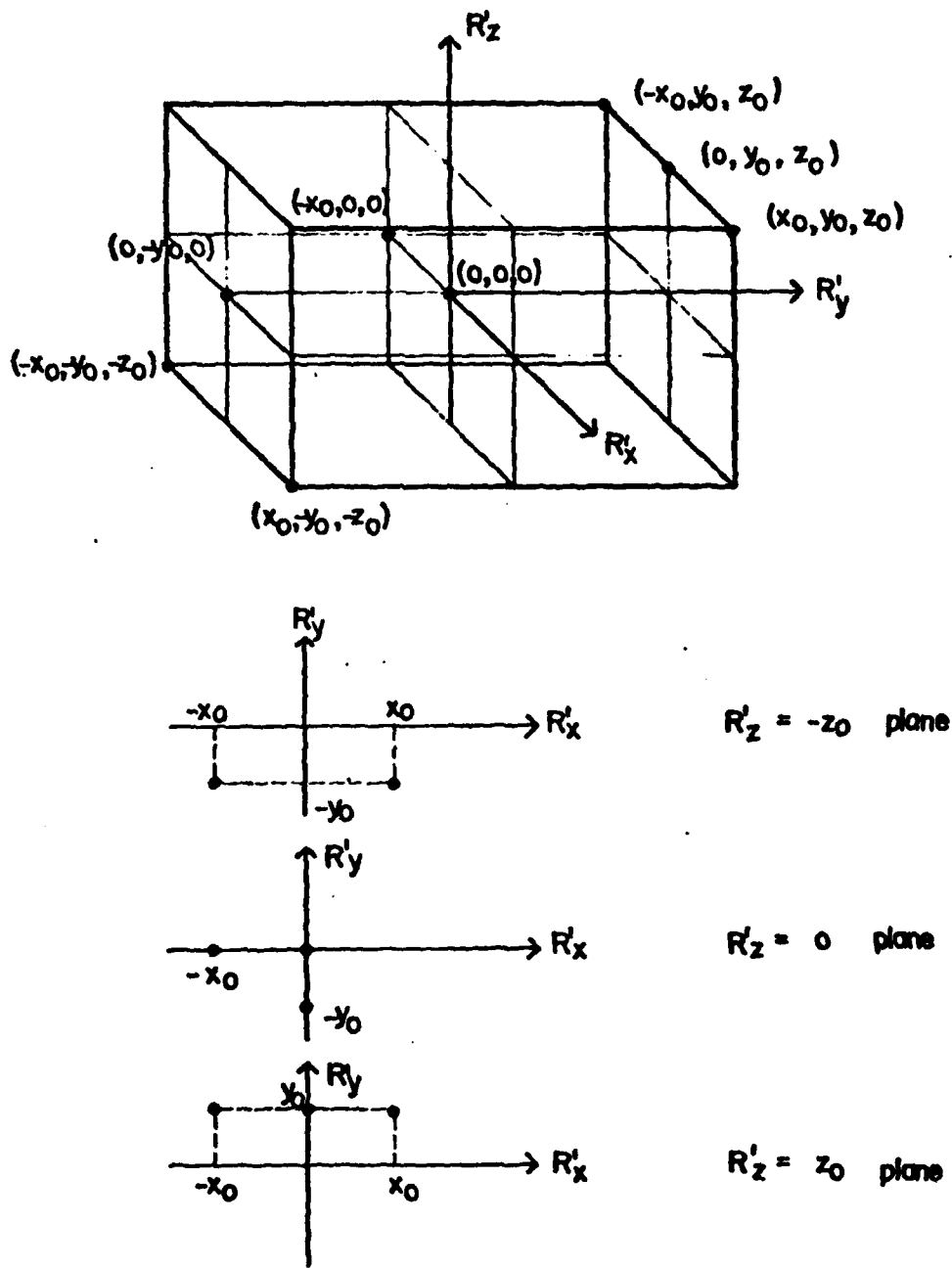


Fig. 2. 3-D object consisting of a set of eight point scatterers shown in isometric and R'_x - R'_y plane views at $R'_z = -z_0, 0, z_0$. $x_0 = y_0 = z_0 = 100$ cm.

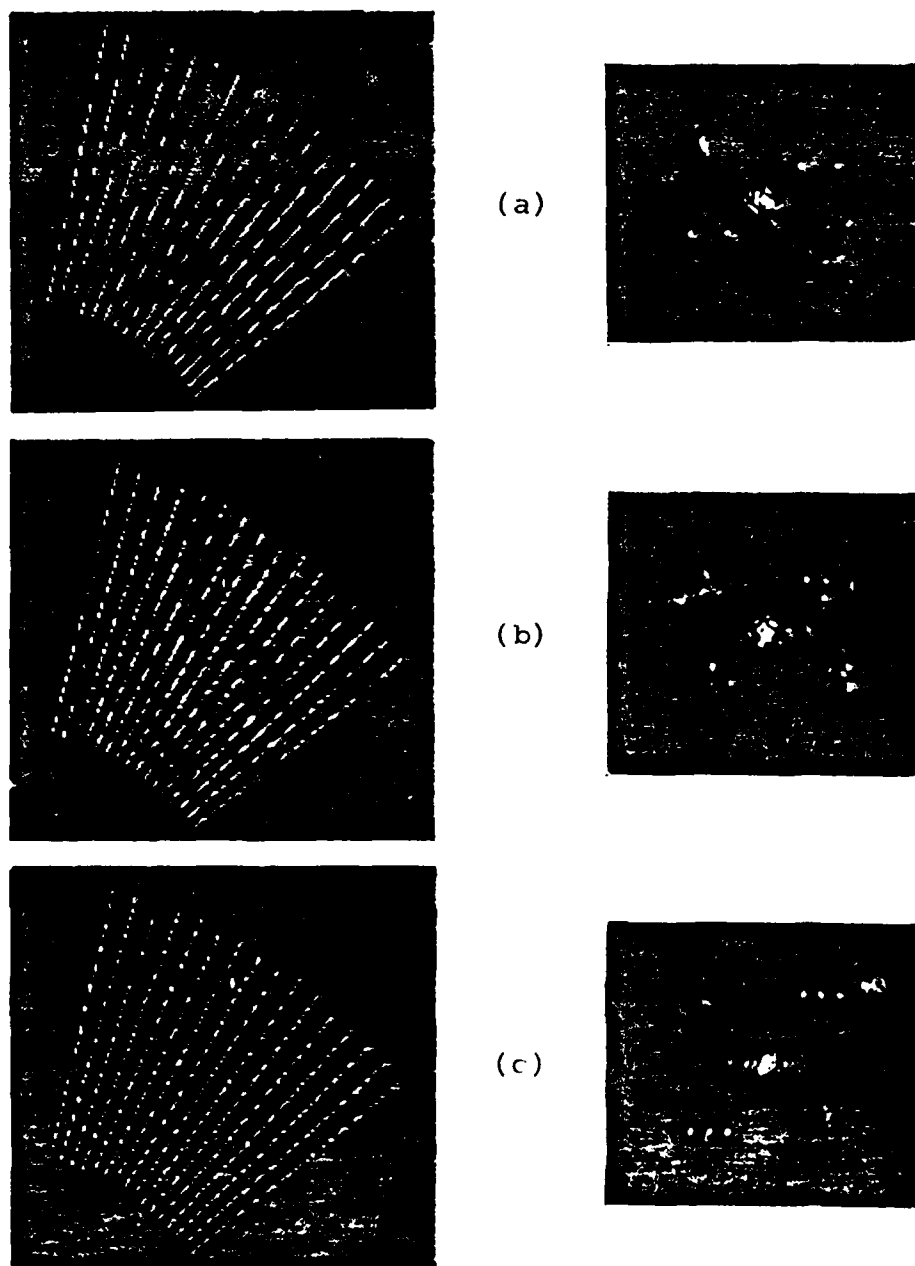


Fig. 3. Projection holograms and their optical reconstructions for the set of point scatterers in Fig. 2 at different R'_z planes. (a) Hologram and reconstructed image of scatterers at $R'_z = -z_0$ plane. (b) Hologram and image at $R'_z = 0$ plane. (c) Hologram and image at $R'_z = z_0$ plane. $x_0 = y_0 = z_0 = 100$ cm.

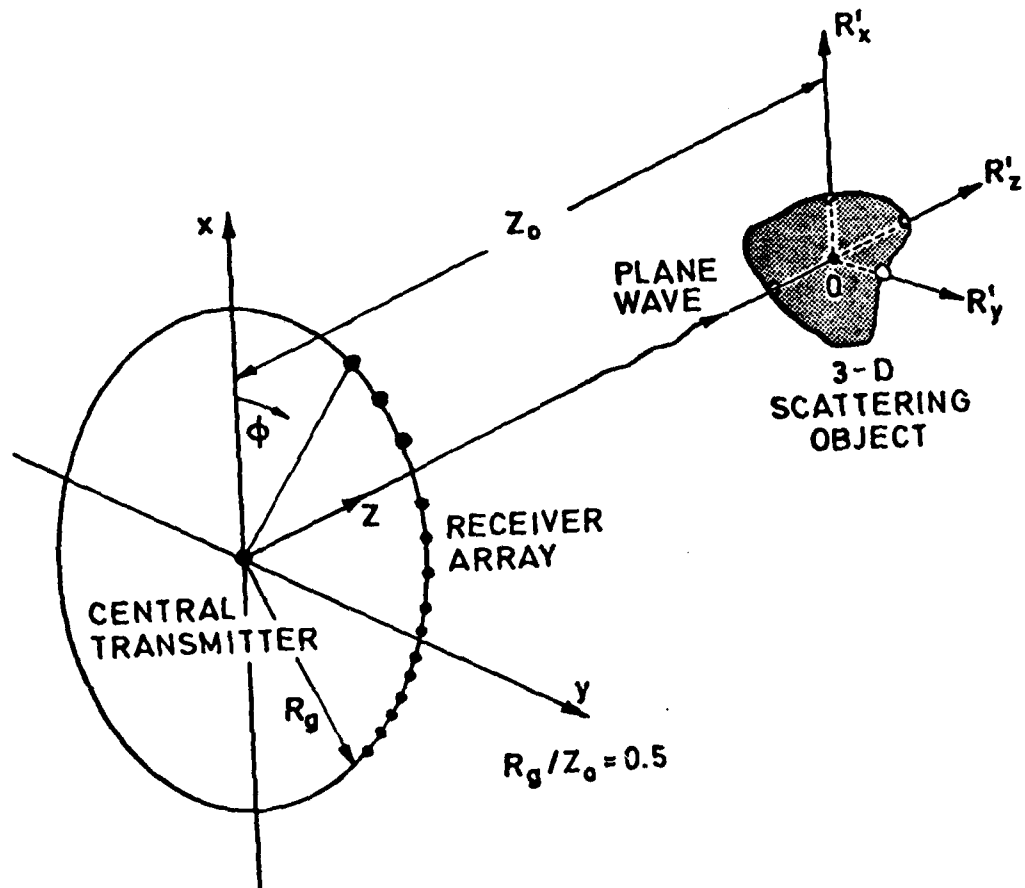


Fig. 4. Arrangement used in computer simulation of wavelength diversity imaging.

can be invoked again. Fourier domain projection theorems²³ that are dual to the spatial domain projection theorem^{25,26} can be applied to the Fourier space data to produce a series of projection holograms from which 2-D images of meridional or parallel slices of the object can be retrieved on the optical bench²⁰. This procedure does not involve any specific scaling of the size of the optical hologram transparency relative to the size of the original recording aperture by the ratio of the recording to the reconstruction wavelengths as in longwave holography where the scaling necessary for viewing a 3-D image free of longitudinal distortion usually leads to an impractically minute equivalent hologram transparency that cannot be readily viewed by an observer. The lateral and longitudinal resolutions in the retrieved image depend now on the dimensions of the volume in Fourier space accessed by wavelength diversity. This volume depends on the wavelength range and on the recording geometry. Thus the longitudinal resolution does not deteriorate now as rapidly with range as in conventional monochromatic imaging systems.

An example of computer simulations of frequency diversity holographic imaging of a 3-D object consisting of eight point scatterers distributed as shown in Fig. 2 is given in Fig. 3. Shown in Fig. 3 are three weighted Fourier domain projection holograms and the corresponding optically retrieved images for three equally spaced parallel slices of the object containing distinguishable 2-D distributions of scatterers. The simulated recording arrangement shown in Fig. 4 consisted of an array of 16 receivers equally distributed on an arc extending from $\phi = 40^\circ$ to $\phi = 77.5^\circ$ surrounding a central transmitter capable of providing plane wave illumination of the object. The results shown were obtained with microwave imaging in mind assuming a frequency sweep of (2-4)GHz. They clearly indicate a lateral and longitudinal resolution capability of the order of 25 cm. Wider sweep widths yield better resolution. For example a (1-18)GHz sweep would yield a 3-D resolution of the order of 1.5 cm.

DISCUSSION AND CONCLUSIONS

Seeking means by which the information content in a hologram can be increased for example by wavelength diversity we have arrived at a formulation of 3-D Lensless Fourier transform holography capable of furnishing 3-D image detail tomographically. This ability of producing 3-D images in slices from coherently detected wavefields enable us to regard the method also as coherent tomography. The Fourier space accessed in the above fashion by wavelength diversity can be viewed as a generalized 3-D hologram in which one dimension has been synthesized by wavelength diversity. Such a generalized hologram contains not only spatial amplitude and phase data as in conventional holography but also spectral information and hence can yield better

resolution than the classical Rayleigh limit of the available aperture operating at the shortest wavelength of the spectral window used. This super-resolving property is further enhanced through an inherent suppression of the effects of object resonances and coherent noise in the retrieved image, the latter being so because frequency diversity tends to make the impulse response of the system unipolar resembling that of a non-coherent imaging system that is free of speckle and coherent noise artifacts¹⁵. Further enhancement of information content and resolution can be achieved by polarization diversity where the p space can be multiply accessed for different nonredundant polarizations of the illumination and the receivers and the resulting polarization diversity images added either coherently or non-coherently in order to achieve a degree of noise averaging as discussed elsewhere¹⁵.

The removal of several longstanding constraints on conventional longwave (microwave and acoustic) holography attained through the use of wavelength diversity as described here leads to a new class of imaging systems capable of converting spectral degrees of freedom into 3-D spatial image detail furnishing thereby true super-resolution. Wavelength diversity is applicable to the imaging of two classes of objects: perfectly reflecting objects of the type encountered in radar and sonar and weakly scattering objects of low or known dispersion of the type encountered in biology and medicine. The practical application of the concepts presented here to optical wavefield is presently under consideration. The availability of tunable dye lasers and electronic imaging devices suggest interesting possibilities of three dimensional wavelength diversity microscopy. Here one can conceive of an arrangement in which a minute semitransparent object with homogeneous or known dispersion is transilluminated by a collimated coherent light beam from a tunable dye laser which can also be made to provide a coherent reference point source in the immediate vicinity of the object. The resulting reference and the object scattered wavefields are intercepted by the photocathode of an electronic imaging device of known spectral response such as a vidicon. Because of the minute size of the object, the photocathode can easily be situated in the far field of the object. Thus nearly a lensless Fourier transform hologram recording arrangement results. The spatial frequency content in the resulting hologram is therefore expected to be sufficiently low to be resolved by a high resolution electronic imaging device. By recording and digitally storing the resulting detected hologram fringe pattern as a function of dye laser wavelength one can gain access to the 3-D Fourier space of the object since \bar{k}_i and \bar{k}_R for the recording geometry are precisely known.

A similar recording arrangement can be envisioned in the active coherent imaging of a distant reflecting object (active telescope) where the object can be made to furnish a reference point source situated on its surface like a wavelength independent stationary glint point or an intentionally placed retroreflector. Because in such an arrangement the reference and the object wavefields travel over the same path, atmospheric effects are expected to be minimized. The generation of an

object derived reference geometry in longwave (microwave and acoustic) wavelength diversity imaging has been described elsewhere^{20,27}.

Finally it is worthwhile to note that since the scattering process is linear the multiaspect or multistatic frequency or wavelength response measurements referred to in this paper can be obtained also by measuring the multiaspect impulse response followed by Fourier transformation of the individual impulse responses measured¹⁹. This means that impulsive illumination can also be utilized. Because the impulse response of a linear system can be measured by using random noise excitation and cross-correlating the output with the input¹⁹, a possibility of using random noise (white light) illumination and cross-correlation detection techniques as a means for accessing the 3-D Fourier space of the object also emerges.

REFERENCES

1. Schelkunoff, S.A., Bell Syst. Tech. J., 22, 80, (1943).
2. Anderson, A.P. and J.C. Bennet, Proc. IEE (letters), 64, 376, (1976).
3. DiFrancia, G.T., J. Opt. Soc. Am., 45, 497, (1955).
4. DiFrancia, G.T., J. Opt. Soc. Am., 59, 799, (1969).
5. Nassenstein, H., Optics Communications, 2, 231, (1970).
6. Wernecke, S.J. and L. D'Addario, IEEE Trans. on Computers, C-26, 351, (1977).
7. Lukosz, W., J. Opt. Soc. Am., 56, 1463, (1966).
8. Leith, E.N., Advances in Holography, 2, N. Farhat (Ed.), (M. Decker, New York, 1976).
9. Lukosz, W., J. Opt. Soc. Am., 57, 932, (1967).
10. Bojarski, N.N., Final Report, contract B000-19-73-C-0316, Naval Air Syst. Command, (1974).
11. Lewis, R.M., IEEE Trans. on Ant. and Prop., AP-17, 308, (1969).
12. Raz, S.R., IEEE Trans. on Ant. and Prop., AP-24, 66, (1976).
13. Meier, R.W., J. Opt. Soc. Am., 55, 987, (1965).
14. Smith, H.M., Principles of Holography, (Wiley-Interscience, New York, (1969).
15. Farhat, N.H. and C.K. Chan, in Optica Hoy Y Mañana, J. Bescos et. al. (eds.), (Sociedad Espanola De Optica, Madrid, 1978), 399.
16. Farhat, N.H., Ultrasonics Symposium Proceedings, IEEE Cat. No. 75 CHO 944-4SU, (1975).
17. Farhat, N.H., Proc. International Optical Computing Conference, IEEE Cat. No. 76-CH 1100-7C, (1976).
18. Farhat, N.H., Proc. IEEE (letters), 64, 379, (1976).
19. Farhat, N.H., J. Opt. Soc. Am., 67, 1015, (1977).
20. Farhat, N.H. and C.K. Chan, in Acoustical Imaging, A. Metherell (ed.), (Plenum, New York, 1980), 499.

21. Waters, W.M., Proc. IEEE (letters), 66, 609, (1978).
22. Chan C.K., Analytical and numerical studies of frequency swept imagery, Ph.D. Dissertation, Univ. of Pennsylvania, Philadelphia, (1978).
23. Stroke, G.W. and M. Halioua, Trans. Amer. Crystallographic Assoc., 12, 27, (1976).
24. Farhat, N.H., Univ. of Pennsylvania Report No. F1 Annual Report, AFOSR Grant No. 77-3256, July (1978).
25. Bracewell, R.N. and S.J. Wernecke, J. Opt. Soc. Am., 65, 1342, (1975).
26. Bracewell, R.N., Australian Journal of Physicas, 9, 198, (1956).
27. Farhat, N.H., C.K. Chan and T.H. Chu, Proc. AP-S/URSI, Symposium, Quebec, Canada (1980).

APPENDIX III

THE VIRTUAL FOURIER TRANSFORM AND ITS APPLICATION IN THREE DIMENSIONAL DISPLAY

ABSTRACT

In contrast to the well known and widely used instantaneous Fourier transforming property of the convergent lens in coherent (laser) light, the "Virtual Fourier Transform" (VFT) capability of the divergent lens is less widely known or used despite many advantages. We will review the principle of the VFT and discuss its advantages in certain applications. In particular a method for viewing the virtual Fourier transform of a two dimensional function with the naked eye using an ordinary point source will be presented. A scheme for three-dimensional image display based on a "Fourier domain projection theorem" utilizing varifocal VFT is described and a discussion of the properties of the displayed image given.

INTRODUCTION

Several sophisticated three dimensional (3-D) imaging techniques such as x-ray tomography¹, electron microscopy², crystallography², wave-vector diversity imaging and inverse scattering³, involve measurements that give access to a finite volume in the 3-D Fourier space of a 3-D object function. A 3-D image of the original object can then be reconstructed by computing the inverse 3-D Fourier transform. The retrieved image normally represents the spatial distribution of a relevant parameter of the object such as absorption, reflectivity, scattering potential, etc.

Obviously, the required inverse transform can be performed digitally. Digital techniques however often preclude real-time operation particularly when the object being imaged is not simple but contains considerable resolvable intricate detail. More importantly, because of the inherent two dimensionality of CRT computer displays, direct true 3-D image display is not possible. Present day computer graphic displays are capable of displaying 3-D image detail either in separate cross-sections or slices, or in a computed perspective (isometric) view of the object, or in some instances stereoscopically where an illusion of a 3-D scene is created in the mind of the observer who is required usually to use special viewing glasses^{4,5}.

Hybrid (opto-digital) computing techniques offer an alternate approach to 3-D image retrieval from 3-D Fourier space data. They furnish as shown in this paper the ability to display true 3-D image detail. The approach is based on "Fourier Domain Projection Theorems"^{2,3} that are dual to "Spatial or Object Domain Projection Theorems" used in radio-astronomy^{6,7} and tomography¹. These theorems permit the reconstruction of 3-D image detail tomographically* i.e. in slices from 2-D projections of the 3-D Fourier space data^{2,3}. Although the required 2-D Fourier transform can be carried out digitally, the emphasis in this paper is on coherent optical techniques for performing the 2-D Fourier transform with particular attention to implementations that permit the execution of the necessary 2-D optical transforms of the various projection hologram sequentially in real-time. Specific attention is given to a technique that utilizes the virtual Fourier transform which permits the viewing of a virtual 3-D image in real-time.

FOURIER DOMAIN PROJECTION THEOREMS

There are two Fourier domain projection theorems. One leads to tomographic object reconstruction in parallel slices and is called the "weighted Fourier domain projection theorem"; the other leads to tomographic object reconstruction in meridional or central slices and can therefore be called the "meridional or central slice Fourier domain projection theorem".

We begin by considering a 3-D object function $f(\vec{r})$ with $\vec{r} = x\vec{i}_x + y\vec{i}_y + z\vec{i}_z$ being a position vector in object space. Let $F(\vec{w})$ be the 3-D Fourier transform of $f(\vec{r})$ defined by,

$$F(\vec{w}) = \int f(\vec{r}) e^{-j\vec{w} \cdot \vec{r}} d\vec{r} \quad (1)$$

where $d\vec{r} = dx dy dz$ and $\vec{w} = w_x\vec{i}_x + w_y\vec{i}_y + w_z\vec{i}_z$ is a position vector in the Fourier or spatial frequency domain.

Consider next the projection of $F(\vec{w})$ on the w_x, w_y plane defined by,

$$F_p(w_x, w_y) = \int_{w_z} F(\vec{w}) dw_z \quad (2)$$

and combining eq. (1) and (2),

$$F_p(w_x, w_y) = \int_{w_z} \left\{ \int \int \int f(x, y, z) e^{-j(w_x x + w_y y + w_z z)} dx dy dz \right\} dw_z \quad (3)$$

* From the Greek work Tomos meaning slice.

Integrating with respect to w_z first and assuming that the volume in \bar{w} space occupied by $F(\bar{w})$ is sufficiently large we obtain,

$$F_p(w_x, w_y) = \int_x \int_y \int_z f(x, y, z) \delta(z) e^{-j(w_x x + w_y y)} dx dy dz \quad (4)$$

$$= \int_x \int_y f(x, y, 0) e^{-j(w_x x + w_y y)} dx dy \quad (5)$$

The 2-D Fourier domain projection $F_p(w_x, w_y)$ and the central slice $f(x, y, 0)$ through the object form thus a Fourier transform pair. This may be symbolically expressed as,

$$F_p(w_x, w_y) \leftrightarrow f(x, y, 0) \quad (6)$$

Other parallel slices through the object at $z = z_n$, z_n being a constant describing the z coordinate of the n -th parallel slice, can in a similar manner be related to "weighted" Fourier domain projections of $F(\bar{w})$ defined by,

$$F_{p,n}(w_x, w_y) = \int_{w_z} F(\bar{w}) e^{jz_n w_z} dw_z \quad (7)$$

Making use of eq. (1) and again performing the integration with respect to w_z first we obtain,

$$F_{p,n}(w_x, w_y) \leftrightarrow f(x, y, z_n) \quad (8)$$

which indicates that the weighted projection $F_{p,n}(w_x, w_y)$ and the n -th parallel object slice $f(x, y, z_n)$ form a Fourier transform pair.

Equation (6) is seen to be a special case of eq. (8) when $z_n = 0$.

Given the 3-D Fourier space data manifold $F(\bar{w})$ one can digitally compute and display a set of "weighted projection holograms" $F_{p,n}(w_x, w_y)$.

A corresponding set of images of parallel slices or cross-sectional outlines of the 3-D object can then be retrieved via 2-D Fourier transform operations which can most conveniently be carried out optically from photographic transparency records of the weighted projection holograms displayed by the computer.

Returning to eqs. (1) and (2) one can also show that projections of $F(\bar{w})$ on arbitrarily oriented planes other than the w_x, w_y plane chosen for eq. (2), yields "meridional projection holograms" that are 2-D Fourier transforms of corresponding meridional (central) slices of the object. This is the "meridional Fourier domain projection theorem". It furnishes the basis for angular multiplexing of the resulting meridional projection holograms into a single composite hologram which can be used to form a 3-D image of the object in a manner similar to that in integral holography⁸ which is increasingly being referred to as Cross holography*.

THE VIRTUAL FOURIER TRANSFORM

In contrast to the well known spatial Fourier transforming property⁹ of the convergent lens widely used in coherent optical computing, the complementary virtual Fourier transform capability of a divergent lens¹⁰ is less widely known or used despite many attractive features. This is surprising since the power spectrum associated with the VFT is a phenomenon that is frequently observed in daily life when one happens to look at a distant point source such as a street light through a fine mesh screen or the fine fabric of transparent curtain material. The spectrum of the screen transmittance appears then as a virtual image in the plane of the point source.

The VFT concept of the divergent lens is easily derived from the Fourier transform expression of the convergent lens. Figure 1 illustrates the well known process of forming a real Fourier transform with a convergent lens. The object transparency, with complex transmittance $t(x_0, y_0)$, is placed at a distance d in front of a convergent lens of focal length F and illuminated with a normally incident collimated laser beam. The complex field amplitude of the wavefield in the back focal plane, the transform plane, is given by the well known formula

$$T(x,y) = \frac{j}{\lambda F} e^{-jk \frac{d}{2F} [(1 - \frac{d}{F})(x^2 + y^2)]} \times \iint_{-\infty}^{\infty} t(x_0, y_0) e^{jk \frac{d}{F} (x x_0 + y y_0)} dx_0 dy_0 \quad (1)$$

in which the integral is recognized as the two dimensional Fourier transform of the object transmittance. $T(x,y)$ becomes the exact Fourier transform of $t(x_0, y_0)$ when $d = F$ that is when the object transparency is placed in the Front focal plane of the lens. The power spectrum associated with the transform is real and can be projected on a screen placed in the back focal plane. It is also well known that a scaled version of the transform can be obtained in the back focal plane by placing the object transparency in the converging laser beam to the right of the lens⁹.

* Named after Lloyd Cross the originator of integral holography.

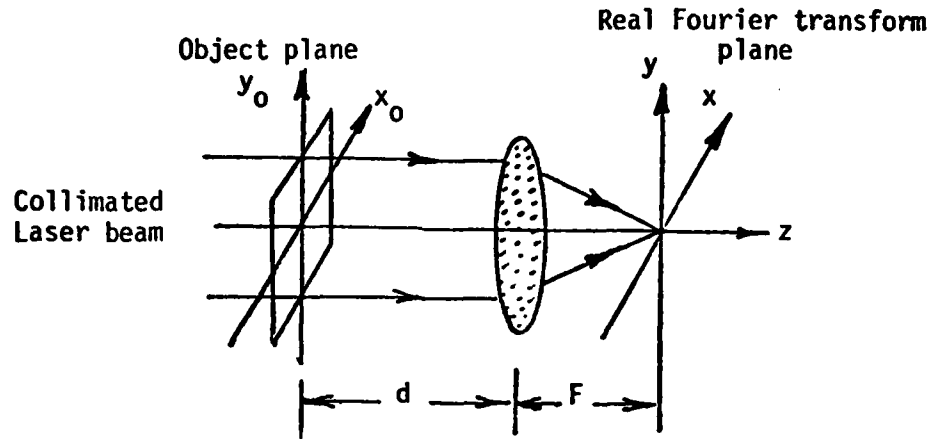


Fig. 1. Real Fourier transform formed with a convergent lens

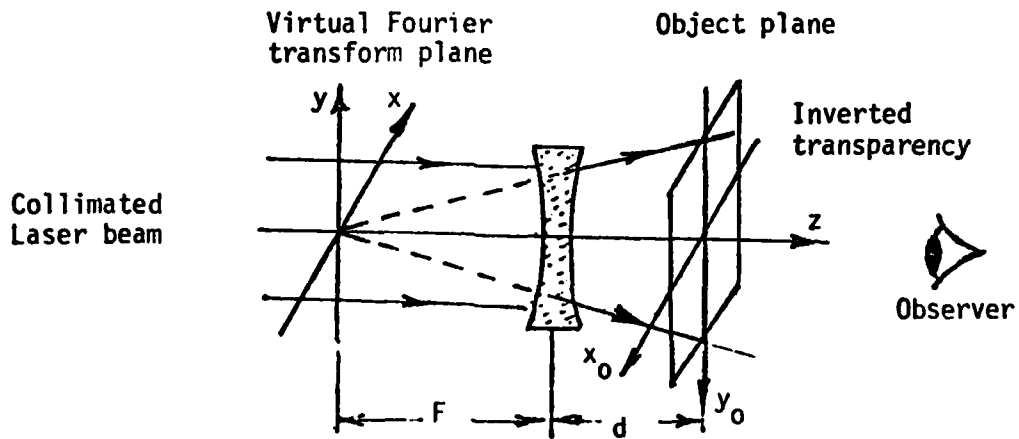


Fig. 2. Virtual Fourier transform formed with a divergent lens

Noting that eq. (1) does not change when we replace d by $-d$, F by $-F$, x_0 and y_0 by $-x_0$ and $-y_0$ respectively, we can arrive at the complementary VFT arrangement illustrated in Fig. 2. An inverted transparency $t(x_0, y_0)$ is placed now in the divergent coherent beam to the right of the divergent lens (of focal length $-F$) and a VFT given by eq. (1) is observed in the virtual focal plane of the lens. The same VFT can be seen by removing the divergent lens and replacing the laser beam with a point source placed at the origin of the VFT plane as depicted in Fig. 3. Thus a simple way of viewing the power spectrum associated with the VFT of a given diffracting screen (which is usually a Fourier transform hologram or a projection hologram of the type described above) is to hold the screen close to the eye and look through it at a distant bright point source. The point source used need not be derived from a laser. In fact it is preferable for safety purposes to use an LED or a spectrally filtered minute white light source such as a "grain-of-wheat" subminiature incandescent lamp or a miniature Christmas tree decorating lamp covered by a color or interference filter. This has the added advantage of furnishing a measure of control over the coherence properties of the wavefield impinging on the screen providing thereby a means for reducing coherent noise in the observed VFT and also, as will be discussed below, a means for coherent or noncoherent superposition of VFT's. As the distance of the point source from the diffracting screen is decreased in order to make it compatible with typical laboratory or optical bench dimensions, the size of the observed VFT decreased because of the change in the curvature of the wavefield illuminating the diffracting screen. To compensate for this effect it is necessary to reduce the size of the diffracting screen or transparency often to such a scale where viewing the VFT through the small available aperture becomes difficult. To overcome this limitation the displacement property of the Fourier transform can be utilized. A composite transparency containing an ordered or random array of reduced replicas of the transmittance function $t(x_0, y_0)$ arranged side by side as illustrated in Fig. 4 is prepared. When such a composite transparency is viewed with the point source, the VFT's formed by the individual elements will overlap in the virtual Fourier plane. The VFT's are identical except for linear phase dependence on x, y which depends in each VFT on the central position of each element in the composite transparency. This leads to a desirable noise averaging effect and the appearance of fine checkered texture in the image detail. All this leads to an enhancement of the quality of the observed power spectrum. Both coherent and noncoherent superposition of the overlapping VFT's is possible using this scheme by varying the coherence area of the wavefield illuminating the composite transparency. When the coherence area is roughly equal to the size of the individual elements of the composite transparency noncoherent superposition results, while a coherence area equal or greater than the size of the composite transparency would yield coherent superposition.

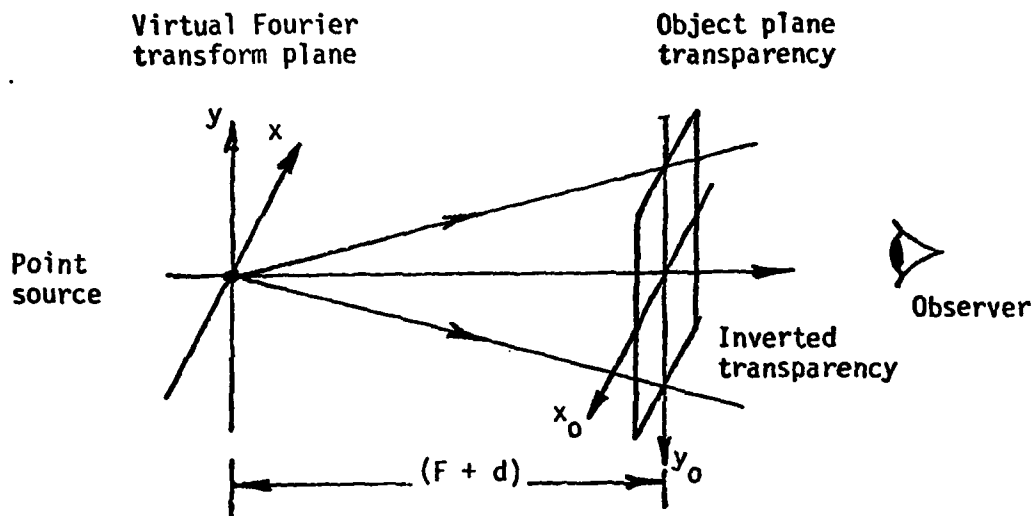


Fig. 3. Arrangement for viewing a virtual Fourier transform with a point source

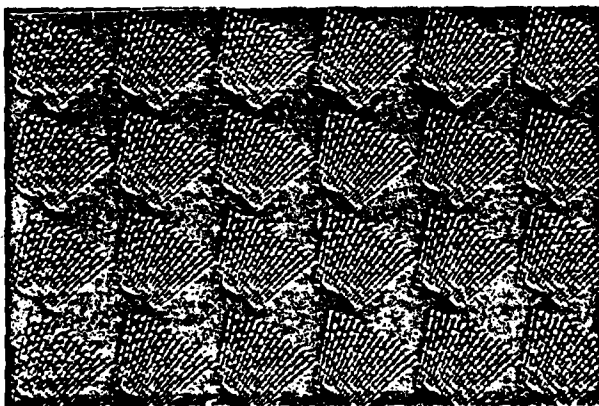


Fig. 4. A composite screen consisting of an ordered array of identical Fourier transform projection holograms.

THREE DIMENSIONAL DISPLAY

The VFT concept and the "weighted Fourier domain projection theorem" discussed above can be combined in an attractive scheme for the reconstruction and display of a 3-D image from a series of weighted projection holograms corresponding to different parallel slices through the object. The scheme is based on viewing a series of weighted projection holograms sequentially in the proper order of the occurrence of their corresponding slices in the original object while displacing the point source axially for one hologram to next by an axial increment proportional to the spacings between adjacent object slices. In this fashion the reconstructed virtual images of the various slices are seen in depth at different VFT planes that are determined by the positions of the axially incremented point source. Repeated rapid execution of this procedure by displacing the point source back and forth leads the observer to see a virtual 3-D image tomographically in parallel slices or sections as he looks through the series of projection holograms passed rapidly, as in a motion picture film, in front of his eyes.

More specifically the scheme is based on preparing a series of N weighted Fourier domain projection holograms from the 3-D Fourier domain data $F(\vec{w})$ of a given object $f(\vec{r})$ as described in the preceding sections. Each of the projection holograms would correspond to a different parallel slice through the object. A composite transparency similar to that shown in Fig. 4 is formed for each projection hologram. In fact Fig. 4 is an example of a computer generated composite hologram containing an array of identical weighted projection holograms corresponding to one slice of the test object shown in Fig. 5. The test object chosen consisted of eight point scatterers arranged as shown. The 3-D Fourier space of this test object was accessed in a computer simulation of wavelength diversity imaging as described in a companion paper in this volume*. The resulting computer generated Fourier space data manifold $F(\vec{w})$ was used to compute three weighted projection holograms corresponding to the three planes $R'_2 = 1m, 0, 1m$ of Fig. 5

containing the three different distributions of point scatterers. A composite array such as that of Fig. 4 was formed and displayed by the computer for each of the three projection holograms, each was photographed yielding a set of three projection hologram composite transparencies. Copies of these were then mounted on a rotating wheel as shown in Fig. 6 (a) and viewed with an axially scanned point source. Four sets of transparency copies of these three composite projection holograms were mounted in the order 1,2,3,2,1,2 ... on the periphery of a rotating wheel as shown in Fig. 6 (a). The wheel is driven by a computer controlled stepper motor. The axially scanned point source was produced by scanning a focused laser beam back and forth on a length of fine nylon thread with the aid of a deflecting mirror mounted on the shaft of a second computer controlled stepper motor as shown in Fig. 6 (b). The laser and optical bench arrangement for forming the scanned focused beam appear in the background of Fig. 6 (a). The computer controlled steppers enable precise positioning of the secondary point source on the scattering thread in synchronism with the hologram

*See paper entitled "Holography, Wavelength Diversity Inverse Scattering" in this volume.

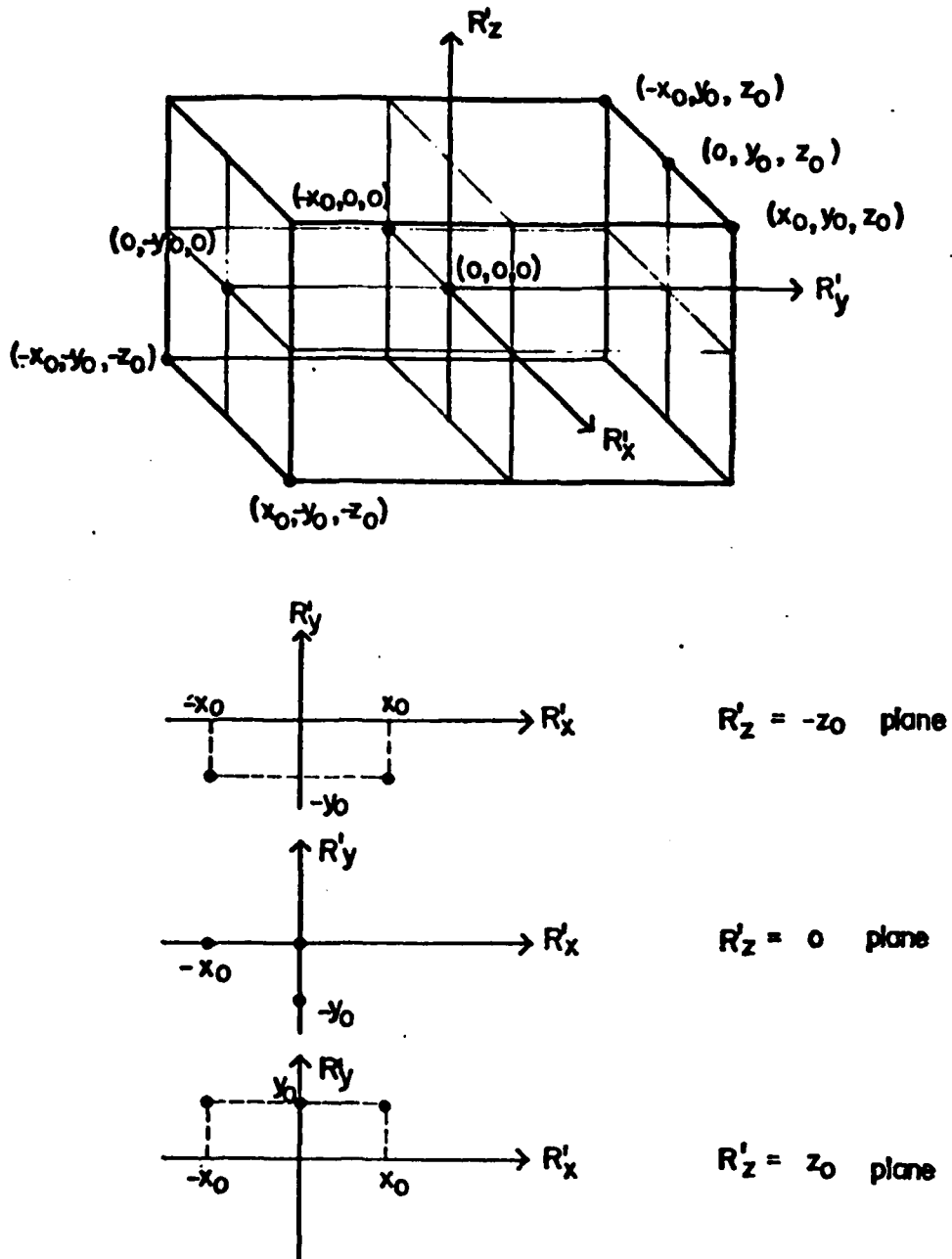
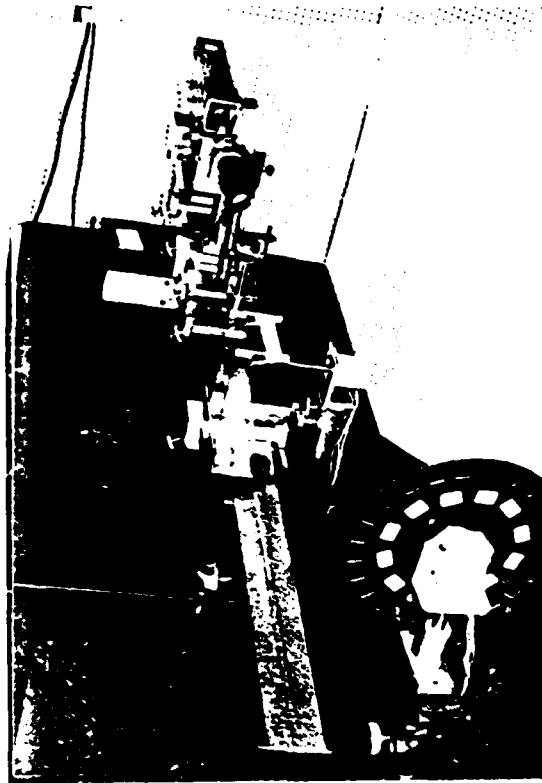
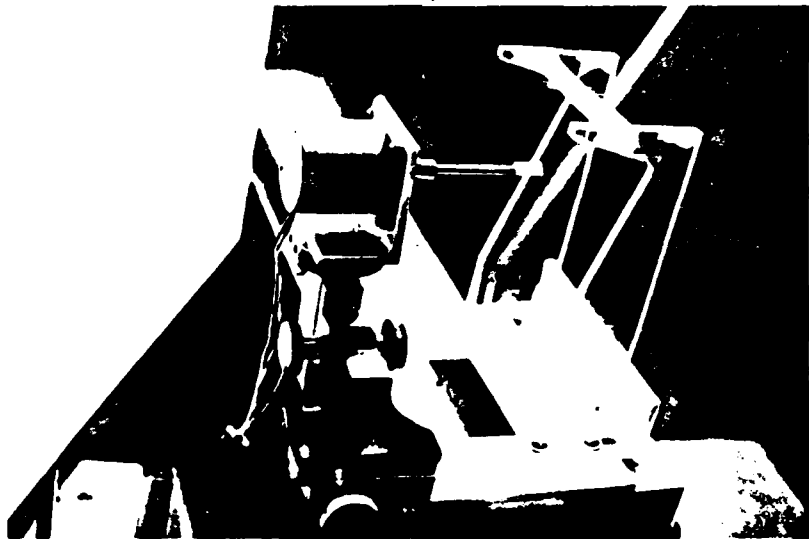


Fig. 5. A three-dimensional test object consisting of a set of eight point scatterers shown in isometric and R'_x - R'_y plane views at $R'_z = -z_0, 0, z_0$. $x_0 = y_0 = z_0 = 100$ cm.

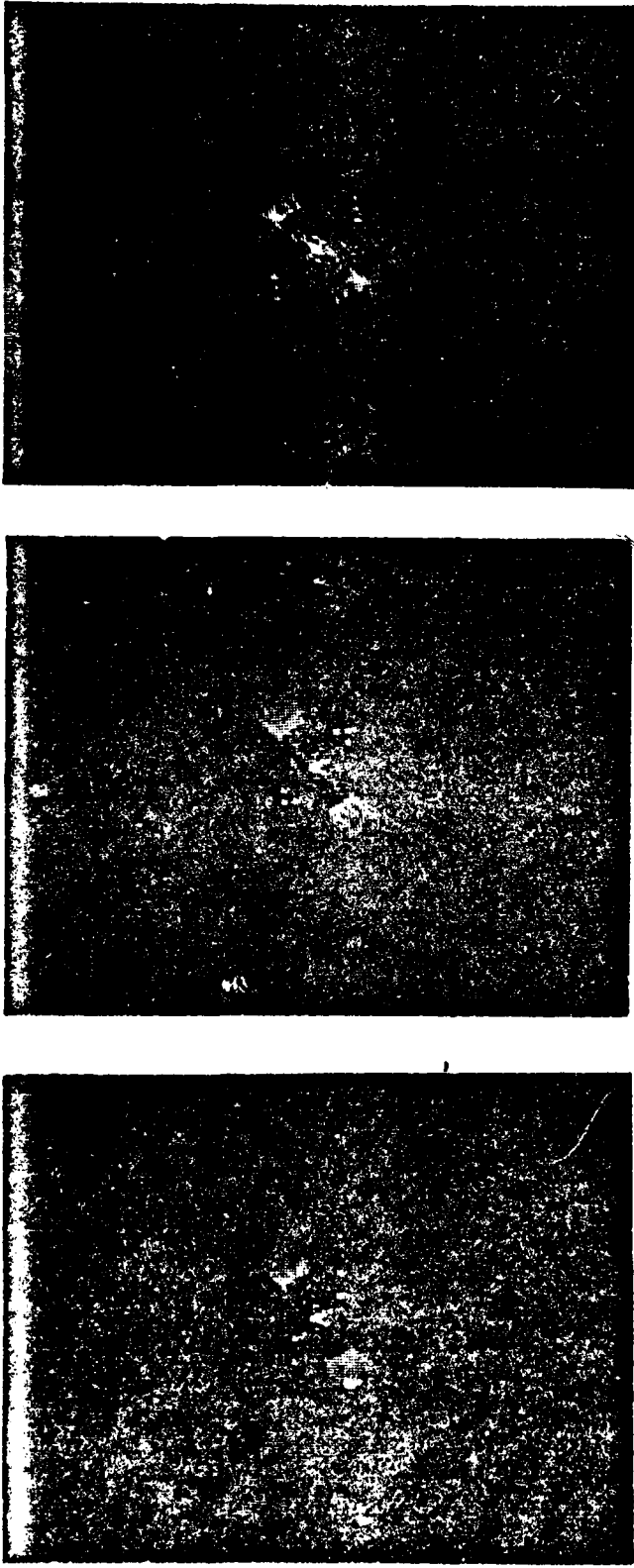


(a)



(b)

Fig. 6. Quasi real-time three-dimensional image reconstruction and tomographic display in successive slices from a series of projection holograms mounted on rotating wheel seen in foreground of (a); Detail of laser scanner used to produce linearly scanned point source is shown in (b).



(a)

(b)

(c)

Fig. 7. Photographs of three slices of the virtual 3-D image of the test object of Fig. 5 obtained by photographing the VFT's formed from corresponding Fourier domain projection holograms.

being viewed so that the VFTs are formed in their proper planes. A viewer looking at the axially displaced point source through each transparency mounted on the wheel as it passes in front of his eye will see a 3-D virtual image. Photographs of the three virtual images seen by an observer in this fashion are shown in Fig. 7. An opto-digital scheme for rapid real-time implementation of the procedure realized above is shown in Fig. 8. This scheme, presently under study, utilizes a rapid recyclable spatial light modulator (SLM) such as the Itek PROM in order to form VFT's of the projection holograms displayed by the computer in real-time.

CONCLUSIONS

We have presented the basic principles of tomographic 3-D image display based on Fourier domain projection theorems. One possible implementation of the principle using the virtual Fourier transform and a series Fourier domain projection holograms has been described. There are several advantages for using the VFT rather than the real Fourier transform (RFT), the most important of which is the ease with which the position of the VFT plane can be moved axially by simply moving the position of the reconstruction point source. The VFT approach was adopted in the present study because it is much easier to move a point source rapidly than to move the display screen needed in the RFT approach. Furthermore focusing in the VFT approach is carried out by the observer while in the RFT approach it must be performed by the system. Other attractive features of the VFT are:

- (a) Simplicity - enables direct viewing of the power spectrum of a transparency or a hologram with a variety of simple point sources.
- (b) The scale of the observed VFT can be easily altered by changing the distance between the projection hologram transparency and the reconstruction point source.
- (c) Lower speckle noise and therefore higher reconstructed image quality can be attained by using nonlaser point sources in the reconstruction such as LED or miniature spectrally filtered incandescent lamps. Further reduction in speckle noise occurs when an array of the projection hologram rather than a single hologram is used and when the hologram is slightly vibrated or is in motion because of a noise averaging effect.
- (d) Coherent and noncoherent superposition of VFT's is possible by altering the coherence area of the reconstruction wavefield.
- (e) Because of the Fourier transform nature of the projection holograms utilized, the resolution requirements from the storage medium (photographic film or the CRT/SLM system of Fig. 8) are much lower than would be needed in the recording of a Fresnel hologram of the object as a means of 3-D image display. The 3-D image detail contained in the single Fresnel hologram is now distributed over a series of lower resolution projection holograms which are used to form the 3-D image sequentially in time in individual slices.

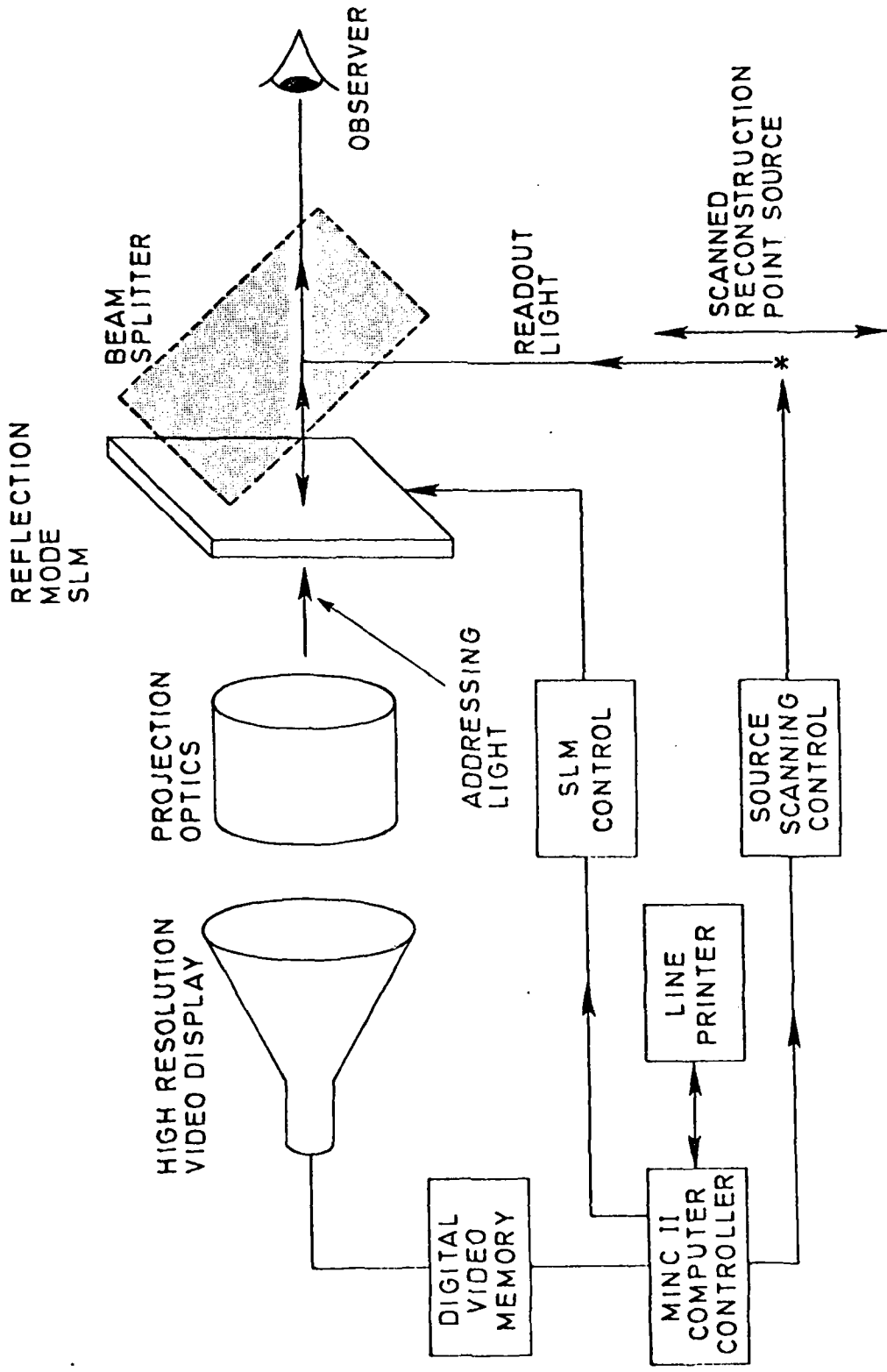


Fig. 8. Opto-digital scheme for the reconstruction and display of 3-D images using a recyclable spatial light modulator and a point source to view the VFT in real-time.

(f) Because 3-D image reconstruction is tomographic (in separate slices) there is no interference between the wavefields forming the various slices.

(g) Permits other forms of 3-D image display involving spatial or angular multiplexing in a fashion similar to integral holography.

REFERENCES

1. H.H. Barret and M.Y. Chiu, *Optica Hoy Y Manãna*, J. Bescos et.al., (eds.) 136, (Proc. of ICO-11, Sociedad Española De Optica, 1978).
2. N.H. Farhat and C.K. Chan, *Acoustical Imaging*, 8, 499, A. Methere1 (ed.), (Plenum Press, New York, 1980).
3. G.W. Stroke and M. Halioua, *Trans. Amer. Crystallographic Assoc.*, 12, 27, (1976).
4. T. Okoshi, *Three-Dimensional Imaging Techniques*, (Academic Press, New York, 1976).
5. T. Okoshi, *Proc. IEEE*, 68, 548, (1980).
6. R.N. Bracewell, *Australian Journal of Physics*, 9, 148, (1956).
7. R.N. Bracewell and S.J. Wernecke, *J. Opt. Soc. Am.*, 65, 1342, (1975).
8. D.L. Vickers, Lawrence Livermore Laboratory Report, No. UCID-17035, (February 1976).
9. J.W. Goodman, *Introduction to Fourier Optics*, 83, (McGraw Hill, New York, 1968).
10. J. Knapp and M.F. Becker, *App. Optics*, 17, 1669, (1976).

APPENDIX IV

AN AUTOMATED FREQUENCY RESPONSE AND
RADAR CROSS-SECTION MEASUREMENT FACILITY
FOR MICROWAVE IMAGING

UNIVERSITY OF PENNSYLVANIA

THE MOORE SCHOOL OF ELECTRICAL ENGINEERING

AN AUTOMATED FREQUENCY RESPONSE AND RADAR CROSS-SECTION
MEASUREMENT FACILITY FOR MICROWAVE IMAGING

CHARLES L. WERNER

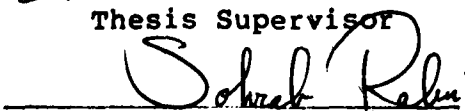
Presented to the faculty of the Moore School of Electrical
Engineering (Department of Electrical Engineering &
Science) in partial fulfillment of the requirements for the
degree of Master of Science in Engineering.

Philadelphia, Pennsylvania

May 1980



Thesis Supervisor



Graduate Group Chairman

UNIVERSITY OF PENNSYLVANIA

THE MOORE SCHOOL OF ELECTRICAL ENGINEERING

AN AUTOMATED FREQUENCY RESPONSE AND RADAR CROSS-SECTION
MEASUREMENT FACILITY FOR MICROWAVE IMAGING

ABSTRACT

This thesis investigates the development of a broadband microwave holographic imaging facility. Different methods for the correction of microwave target scatter data are discussed and implemented. A minicomputer automates all system functions including data acquisition, storage, calculation, and graphic display. The effects of range phase shift on holographic frequency diversity imaging is considered and techniques for the removal of this phase shift in a laboratory environment. The frequency dependent backscatter of several test targets is derived analytically and simulations done of the corresponding holograms. These holograms are compared to those measured experimentally. Finally both simulated and experimental holograms are optically reconstructed to yield target images using optical Fourier transforms and shown to be in excellent agreement.

Degree: Master of Science in Engineering for graduate work
in electrical Engineering and Science

Date: May 1980

Charles L. Werner

Author

ACKNOWLEDGEMENTS

I would like to extend my most sincere thanks to Dr. Nabil H. Farhat for making my studies at the University of Pennsylvania possible. His patience and wisdom were an inspiration for my research. I would also like to thank my parents for their love and understanding these many years. Finally I want to express appreciation to the Moore School for giving me the chance to study here.

TABLE OF CONTENTS

I.....	INTRODUCTION	1
II.....	SYSTEM OPERATION AND ERROR REMOVAL	
2.1.....	Microwave sweeper operation	4
2.2.....	Network analyzer-computer interface	6
2.3.....	Implementation of the data aquisition system	9
2.4.....	System error correction	13
III.....	RANGE PHASE ANALYSIS	
3.1.....	The effects of range phase on imaging	27
3.2.....	Practical considerations for range phase removal	38
IV.....	SYSTEM IMPLEMENTATION OF SWEPT FREQUENCY IMAGING	
4.1.....	System repeatability	41
4.2.....	Computer control of target rotation	43
4.3.....	Sphere simulation	45
4.4.....	Simulation of frequency swept imaging	53
4.5.....	Experimental results	60
V.....	CONCLUSION	72
	BIBLIOGRAPHY	74
	Appendix I...Error Correction Programs and Utilities	
	Appendix II..Microwave imaging programs-acquisition and display	

I INTRODUCTION

Frequency diversity imaging has been under study at the Electro-Optics and Microwave Optics laboratory of the Moore School Graduate Research Center.[1],[2],[3],[4] This study has established the theoretic feasibility of imaging objects by means of their multiaspect frequency response. For the purpose of experimentally studying frequency diversity imaging, an experimental measurement system has been assembled and installed in the Moore School anechoic chamber. In this thesis we will describe the automation of this measurement system and characterize its performance in the measurement of complex field amplitudes of scattered fields. A system block diagram fig.1.1, shows the major system components. The central element is the DEC MINC LSI 11/2 minicomputer. This computer performs several important functions. The MINC controls laboratory instrumentation via the IEEE-488 bus protocol standard. This allows the Hewlett-Packard 8620C microwave sweeper to be precisely tuned to any frequency in the 2.0 to 18.0 GHz range (fig.1.2). The computer collects data from the HP 8410B network analyzer through the four analog input channels available. These analog values are proportional to the amplitude in db and phase in the range $(-\pi)$ to $(+\pi)$ radians relative to the reference signal supplied to the network analyzer. The computer stores Experimental data on floppy discs. The available storage capacity is large, over 500,000 measurement pairs of complex field amplitude and

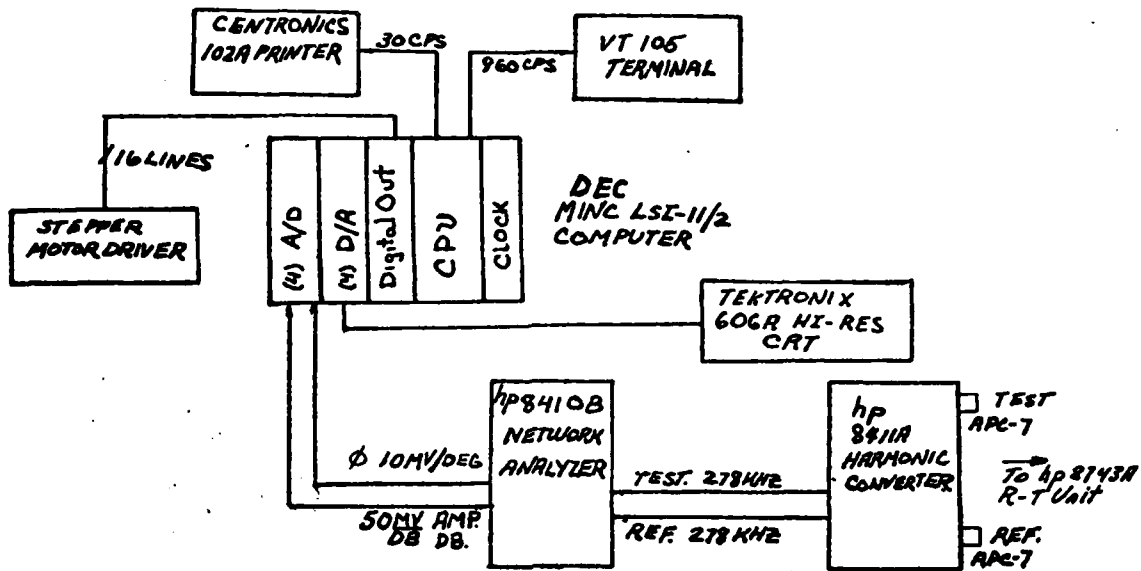


Fig. 1.1 System block diagram.



Fig. 1.2 HP 8620C microwave sweeper and HP 1410B network analyzer.

phase may be stored on a single disc. This data can be accessed for both processing and display on a Tektronix 606A high resolution CRT monitor. The disc system allows the MINC to operate under a sophisticated software system, DEC RT-11 V3.0B permitting programming in MINC BASIC, FORTRAN IV, and MACRO languages.

The processing capability of the system allows the removal of system response errors due to anechoic chamber clutter, antenna cross-coupling and receiver channel characteristics. The data may be processed for target range calculations and the removal of the phase shift due to the target range. In addition the collected data may be filtered to improve imaging and finally displayed on a high resolution Tektronix 606A X-Y CRT monitor using the MINC system D/A converter module.

The second part of this thesis will describe the simulation and actual operation of a holographic radar system verifying the theory of frequency diversity imaging. This is done using the system described in the first section. The scattering of various targets is derived and holograms using these results are generated for comparison with experimental data. Finally a system for the experimental measurement of the scattering for these targets is outlined and the results from this system compared to theory.

II SYSTEM OPERATION AND ERROR REMOVAL

This chapter will cover the operation of the microwave backscatter data acquisition system. This will include actual interfacing information and an analysis of the types of errors encountered when making microwave measurements. The error correction techniques developed are later used in the experimental verification of the frequency diversity imaging theory.[4]

2.1 Microwave sweeper operation

The first task in the development of an automated data acquisition system is the implementation of a data communications link between the intelligent controller and instrumentation. The IEEE-488 bus protocol is utilized in this application for the transfer of data to the Hewlett-Packard 8620C microwave sweeper from the MINC LSI 11/2 computer. This bus is a high speed 8 bit wide bidirectional data path with 5 additional lines dedicated to control. Data is transferred in ASCII format over the bus. For example the number 1 is transmitted as the ASCII code for the character '1'. Certain sequences of characters make the sweeper perform different functions or enter different modes of operation via its IEEE-488 interface.

In order to set the frequency of the sweeper a number must be sent to the IEEE-488 interface in the range 1-10000. Each sweeper frequency band has been split into 10000 frequency points. The frequency of operation is controlled

by an internal analog voltage that varies between 0.0 and 10.0 volts. A D/A converter on the 8620C IEEE-488 interface changes the data transmitted from the MINC into the frequency controlling voltage. The correspondence between voltage and output frequency is essentially linear. In order to obtain the interpolating function for frequency versus control voltage; a microwave frequency counter was used to measure the voltage-frequency characteristic function. Using the MINC-BASIC program CALAB.BAS a least squares fit for both linear and quadratic functions was made on the frequency vs voltage data. This type of program is used for determining the best polynomial fit to the frequency-voltage characteristic of the sweeper. Sample output and program listings are in appendix I along with an explanation of program operation. The results from this work indicate that the quadratic fit was statistically superior for all bands on the microwave sweeper. The FORTRAN subroutine SWEEP was written which utilizes the quadratic interpolation polynomial for each of the four bands of the 8620C. This subroutine automatically calculates the control voltage and band to generate any frequency in the 2-18 GHz range and transmits the appropriate commands over the IEEE-488 bus. The variance of the frequency setting using the quadratic fit for the three bands are as follows: .6 MHz in the 2.0-6.3 GHz band; 1.2 MHz in the 6.3-12.0 GHz band; and 1.6 MHz in the 12.0-18.0 GHz band. For higher accuracy the sweeper may be phase

locked to the reference in a locking frequency counter yielding very high accuracy as precise as the frequency reference itself. The EIP 371 locking counter may be used in this application to lock the HP 8620C sweep oscillator to the correct frequency once it is within 20 MHz of the desired frequency. The auxiliary output of the HP 8620C supplies a sample of the signal generated by the fundamental 2.0-6.3 GHz oscillator module within the sweeper to the locking counter. Sweeper output on higher bands is this fundamental multiplied by a factor of 2 or 3 for the 6.3-12.0 and 12.0-18.00 GHz bands respectively. For example the locking frequency for a 10.0 GHz sweeper output on band 2 would be 5.0 GHz. In operation, subroutine SWEEP will set the frequency of the sweeper within 2.0 MHz of the desired frequency and subroutine SLOCK will be called to calculate the locking frequency; lock the HP 8620C and return to the main calling routine when lock will have occurred. Lock time varies from .1 to 3 seconds and resolution is 100 KHZ. These subroutines are called whenever the sweeper must be set to a particular frequency or the sweeper must be placed in or be released from computer control.

2.2 Network analyzer-computer interface

The Hewlett-Packard 8410B network analyzer is the focus of the measurement capabilities of the microwave measurement system. It can make vector (amplitude and phase) measurements in the (.1-18.0)GHz range. The range of amplitude measurement is 80 db and phase may be measured

modulo (2π). The system reference signal is fed from a 20db directional coupler to the HP8411A harmonic converter sampling head of the network analyzer. This reference is compared to the backscatter from the illuminated target; both in amplitude and phase. The reference signal amplitude is kept constant by leveling the sweeper with a feedback signal derived from its amplified output by means of a crystal detector. This allows the sweeper-TWT (Traveling Wave Tube) system to yield nearly constant output in the (2.0-16.5) GHz range; see fig.2.1. TWT power output is on the order of 1 watt over these frequencies.

The complex field amplitude measurements are available as analog voltages from the back panel of the 8410B. The outputs are proportional to amplitude and phase: 25 MV/db and 10 MV/DEGREE. These values are digitized by the MINC using its built in analog to digital conversion channels. The MINC A/D converters digitize voltages lying in the range of -5.12 to +5.12 volts to the range of 0-4096 yielding 12 bit resolution. If the signal is corrupted by noise; the user has the option of employing signal averaging to cancel the effects of noise uncorrelated to the received signal.

A difficulty encountered when measuring phase angle modulo (2π) occurs when the phase is close to $(+\pi)$ or $(-\pi)$. At this point a small change in the signal phase may cause the phase to flip between these two equivalent extremes rapidly. If a data sample is taken close to $(+\pi)$ or $(-\pi)$ it may be in transition between them and therefore incorrect.

Since such points occur infrequently in a typical measurement they may be ignored. ;their presence does not seriously hinder any holographic imaging due to the inherent redundancy and therefore noise immunity of the holographic reconstruction process.[5] If it is desired that these points be identified and removed it is necessary to estimate the mean and variance of the samples taken at each frequency point. At frequencies where the phase is flipping between $(+\pi)$ and $(-\pi)$, the variance will be much larger than at other frequencies. The mean of the samples when this is occurring will be near zero. Hence to resolve the ambiguity problem it is necessary to decide if the variance exceeds a predetermined threshold when the mean in the neighborhood of zero. Two FORTRAN subroutines PHAMP and PHAMP2 which implement these algorithms are listed in appendix I.

Since such points occur infrequently in a typical measurement they may be ignored. ;their presence does not seriously hinder any holographic imaging due to the inherent redundancy and therefore noise immunity of the holographic reconstruction process.[5] If it is desired that these points be identified and removed it is necessary to estimate the mean and variance of the samples taken at each frequency point. At frequencies where the phase is flipping between $(+\pi)$ and $(-\pi)$, the variance will be much larger than at other frequencies. The mean of the samples when this is occurring will be near zero. Hence to resolve the ambiguity problem it is necessary to decide if the variance exceeds a predetermined threshold when the mean in the neighborhood of zero. Two FORTRAN subroutines PHAMP and PHAMP2 which implement these algorithms are listed in appendix I.

2.3 Implementation of the data acquisition system

In an experimental environment it is important to be aware of the various types of errors inherent in the equipment and the experimental procedure adopted. Conditions and equipment always vary from theoretical ideals. A clear understanding of the error removal process leads to the development of practical implementations of theoretical concepts and enhancement of measurement accuracy unattainable otherwise.

Errors in complex field amplitude measurement may be caused by several factors. These may be grouped into two categories. Errors caused by the instruments themselves fall into the first class. Such factors as measurement variations caused by electronic noise, ,inaccurate A/D and logarithmic conversions, and inaccuracy and instability in the microwave source make up this category. The second group of errors is caused by the test set, antennas , cables, connectors, amplifier, and room clutter. All these factors interact with each other in the microwave region and are the significant cause of error in microwave measurements. Little can be done about the first class of errors since they are inherent in the characteristics of the equipment used. The second group of errors can be removed through the use of automated measurement of system parameters in the frequency range of interest. These errors can be removed from any measurements of scattering objects by digital processing and the results stored for later recall. This

essentially provides an automated and improved version of the conventional two antenna radar cross-section measurement technique [6] ;in which a microwave bridge is balanced in the absence of the target and the degree of imbalance is measured when the target is introduced into the microwave field.

Let us look at the first class of errors more closely since these errors will set the ultimate performance limits on the system. The characteristics of the signal source are important in this regard. In this case the signal source is a Hewlett-Packard 8620C microwave sweeper. Since the sweeper is not phase locked frequency and stability problems exist. The carrier also has significant FM noise which appears as phase noise in the scattered signal. The phase shift of the scattered scattered signal as a function of frequency for small frequency variations is given by:

$$\Delta\theta = \Delta k \cdot R \quad (2.1)$$

where $k=(2\pi/\lambda)$ and R is the path length. For R greater than a few tens of meters ,the FM noise on the signal source causes measurable variations in the phase of the scattered signal. The stability of a synthesizer is required for the implementation of a holographic radar system when target ranges are in terms of kilometers.

Another limit on the ultimate accuracy of the system is the resolution of the A/D conversions and the accuracy of the network analyzer. Given the 2.2MV resolution of the MINC A/D converter and the network analyzer analog output of

50 MV/db, the system can resolve .048 db steps. This resolution limit restricts the minimum signal to system error ratio. If the error signal consisting of clutter, antenna coupling, system directivity and noise exceeds the scattered target signal the resolution of the target signal suffers. For example, if the system error signal and target scattered signal are of equal intensity, then a 1 db change in the scattered signal causes a .53 db change in the total received signal vector. When the system error is 13 db above the scattered signal it becomes impossible to resolve a 1 db change in the target signal given the resolution capabilities of the system. This difficulty is further compounded by errors in the network analyzer. These too are amplified when the clutter exceeds the target scatter signal. In fig.2.1 is a plot of the minimum system resolution in order to detect a 1 db change in the target return signal versus the system error signal to scattered signal level in db. In fig.2.2 is plotted the target signal resolution versus the noise to signal level in db. When the system error is 20 db below the target signal then the resolution of the target scatter signal is very close to the ultimate resolution, .048db. Clutter is the component of the received signal not scattered by the target but that signal that is the result of coupling between antennas and signal scattered by the anechoic chamber walls. As the clutter/signal ratio increases the target scatter signal resolution decreases exponentially. Clutter may be reduced

//

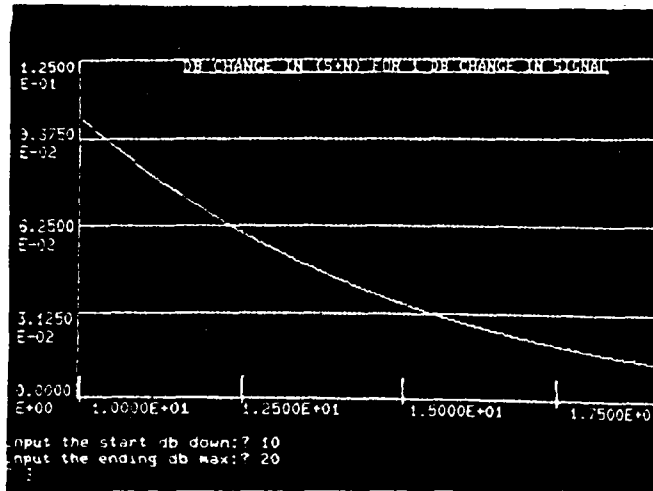


Fig. 2.1 The required resolution in db for a data acquisition system to detect a 1 db change in the desired signal vs. signal/error -signal ratio.

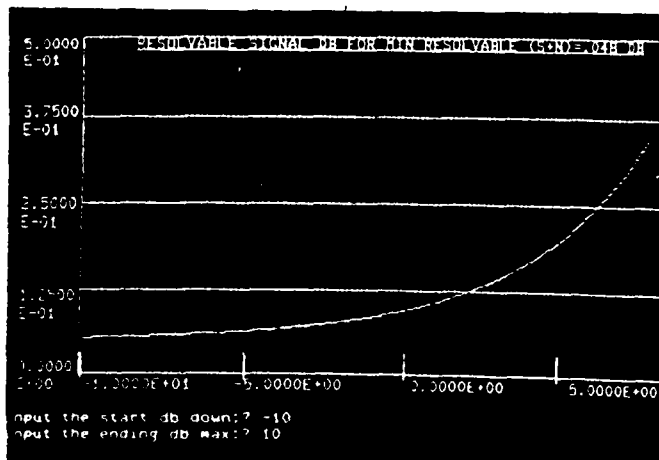


Fig. 2.2 Minimum change in desired signal level detectable versus signal/error signal level given .048 db system data acquisition resolution.

by improving the isolation between the transmitter and receiving antennas with the introduction of absorbing foam panels such as Emerson and Cummings' Ecosorb panels between the antennas.

2.4 System error correction

Turning next to the second class of errors; those directly measurable and therefore removable; define the following quantities which are functions of frequency :

$I(f)$ -- Isolation of reference to test channels

$T(f)$ -- Transfer characteristic of system

$A(f)$ -- Attenuator characteristic

$A_1(f)$ -- Antenna system characteristic

$S(f)$ -- Corrected backscatter for target

$C_1(f)$ -- Uncorrected antenna clutter and coupling

$C_2(f)$ -- Corrected antenna clutter and cross-coupling
(uncorrected for antenna system response)

$C(f)$ -- Corrected antenna clutter and coupling

$R_1(f)$ -- uncorrected reference target backscatter

$R_2(f)$ -- Corrected reference target data

(uncorrected for antenna system response)

$R(f)$ -- Corrected reference target data

Several possible techniques exist for the removal of system errors. The particular technique is dependent on the relative signal levels involved, the accuracy desired, ease of implementation, and computational speed. The first technique described here is similar to that used by Weir et al .[7]

The first step in the correction procedure measures the transfer function of an attenuator $A(f)$ as a function of frequency. The equipment setup for this procedure is shown in fig. 2.3. The two ports of the reflection-transmission unit connected through a precision HP 11605A flexible coaxial arm. The MINC then steps the sweeper to a number of frequency points and stores the system response (log amplitude and phase vs. frequency) in memory. When this completed the attenuator is placed in series with the arm and another set of measurements is made at the same frequency points as before. the system response characteristic is subtracted from the combined attenuator plus system response measurement made on the second sweep. An example of this procedure is shown in fig 2.4. Computer subroutine PAD performs this operation. It is listed in appendix I along with all other computer program listings and output pertaining to system response measurement and removal.

The next step in the calibration process is measurement of the reference to test channel isolation $I(f)$. This characteristic is dependent on the directivity of the network analyzer harmonic converter, and the reflection transmission unit. For the Hewlett-Packard 8411A harmonic converter the isolation is greater than 50 db. In this measurement the ports of the reflection-transmission unit are terminated in the cables used for the later target scatter measurement. These coaxial cables are terminated in

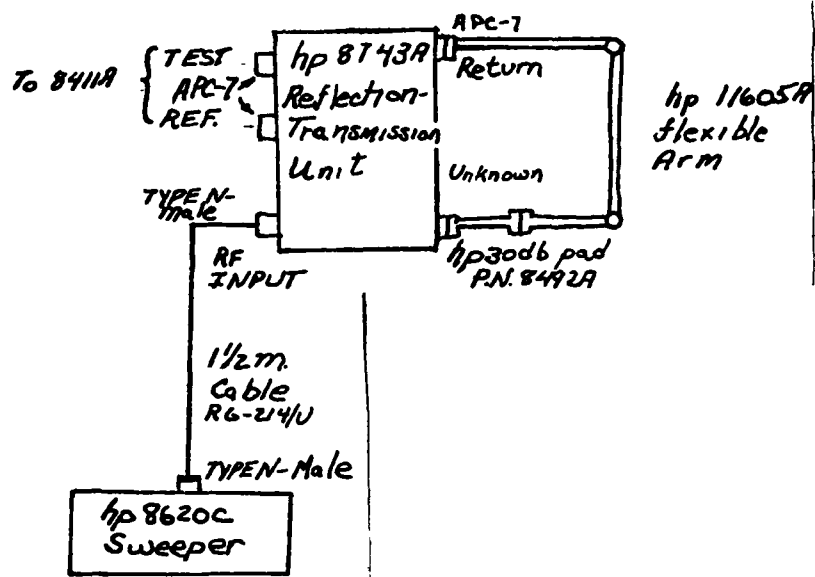


Fig. 2.3 Equipment setup for attenuator measurement.

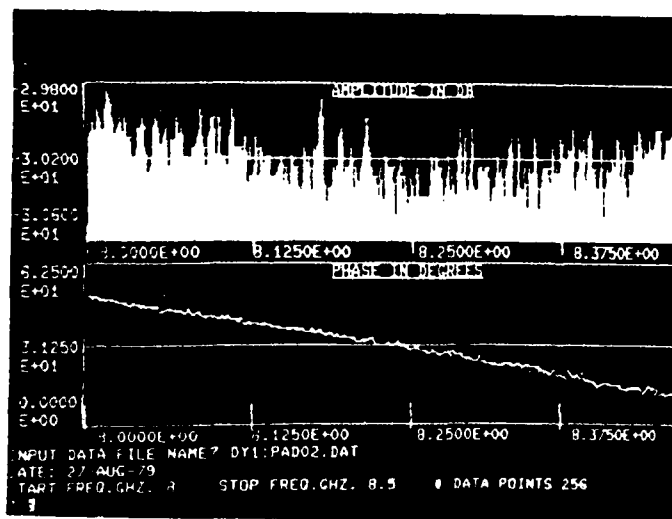


Fig. 2.4 30 db attenuator characteristic for 8.0-8.5 GHz.

50 ohm resistive loads as shown in fig.2.5. The results of a typical run are shown in fig.2.6. Computer subroutine IST automates this stage in the correction procedure. As can be seen the coupled signal is well in the noise of the system and would not affect later scatter data. If the isolation effect is ignored later calculation would be simplified greatly; but is included here to be consistent with the procedure outlined in the literature.[7]

The next stage in generating the data for correction of scatter data is measurement of the system transfer function $T(f)$. This consists of the characteristics of the traveling wave tube amplifier, system cables and connectors. This is done by connecting the cable from the transmitting antenna to the receiving antenna cable in fig.2.6 and placing the 30 db attenuator characterized previously in the line to avoid damage to the harmonic converter. The raw measurement $MT(f)$ is a combination of several factors:

$$MT(f) = T(f) * A(f) + I(f) \quad (2.2)$$

Solving for $T(f)$:

$$T(f) = (MT(f) - I(f)) / A(f) \quad (2.2a)$$

The equipment setup for this procedure is shown in fig 2.7 and typical uncorrected and corrected transfer function data in fig.2.8 and 2.9.

Measurement of the antenna cross-coupling and room clutter is the next step in the correction process. In this procedure shown in fig.2.7b, the target is removed from the anechoic chamber and the antennas pointed to the target

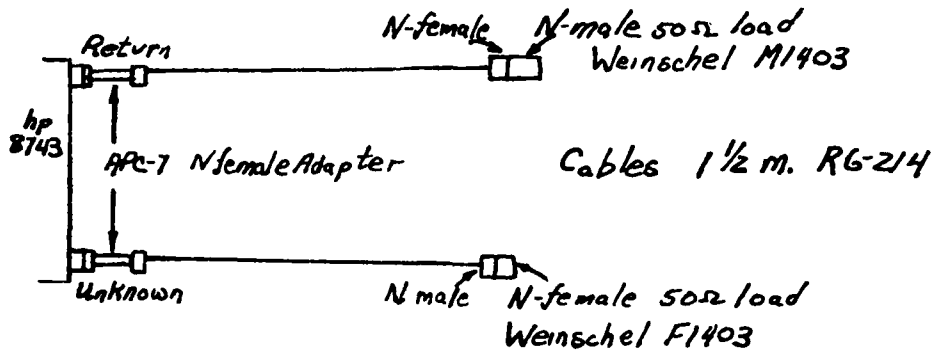


Fig. 2.5 System configuration for measuring isolation between reference and unknown ports.

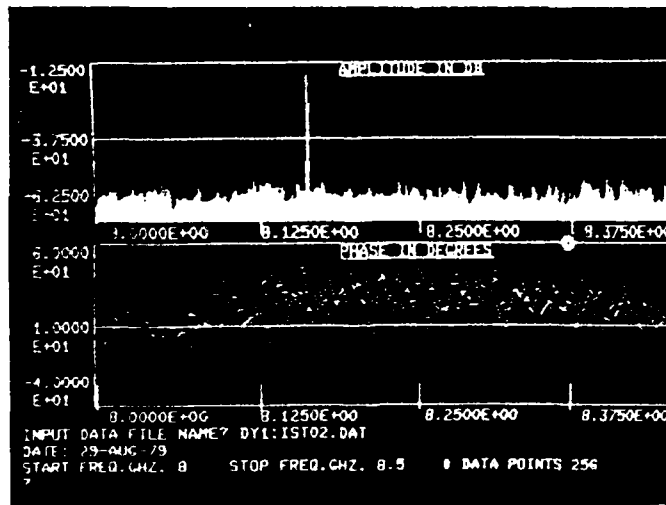


Fig. 2.6 Isolation between ports of reflection-transmission unit; 8.0-8.5 GHz.

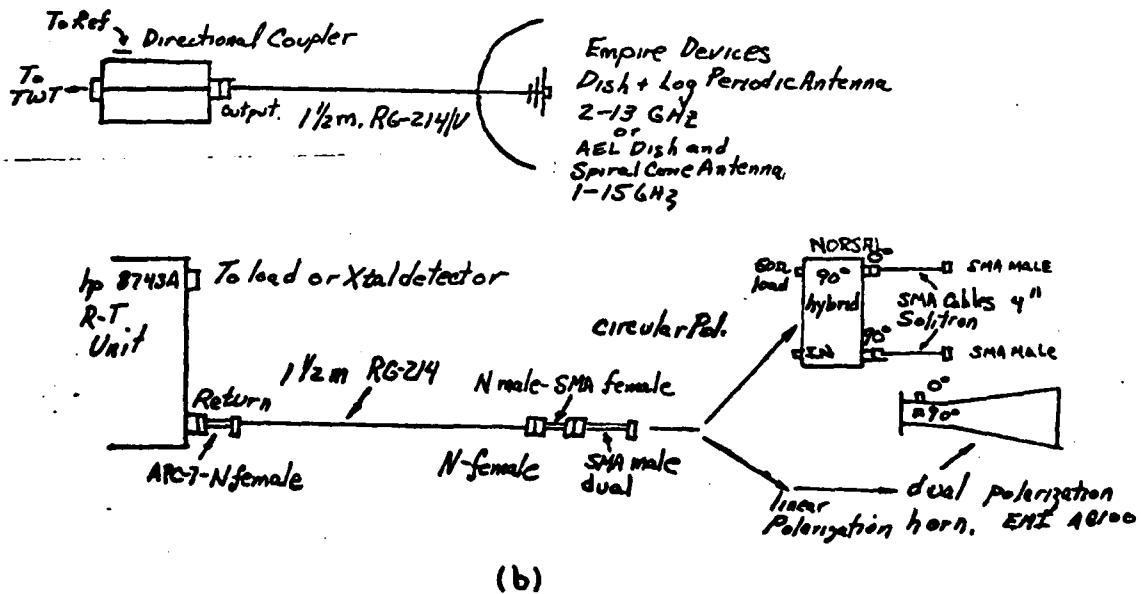
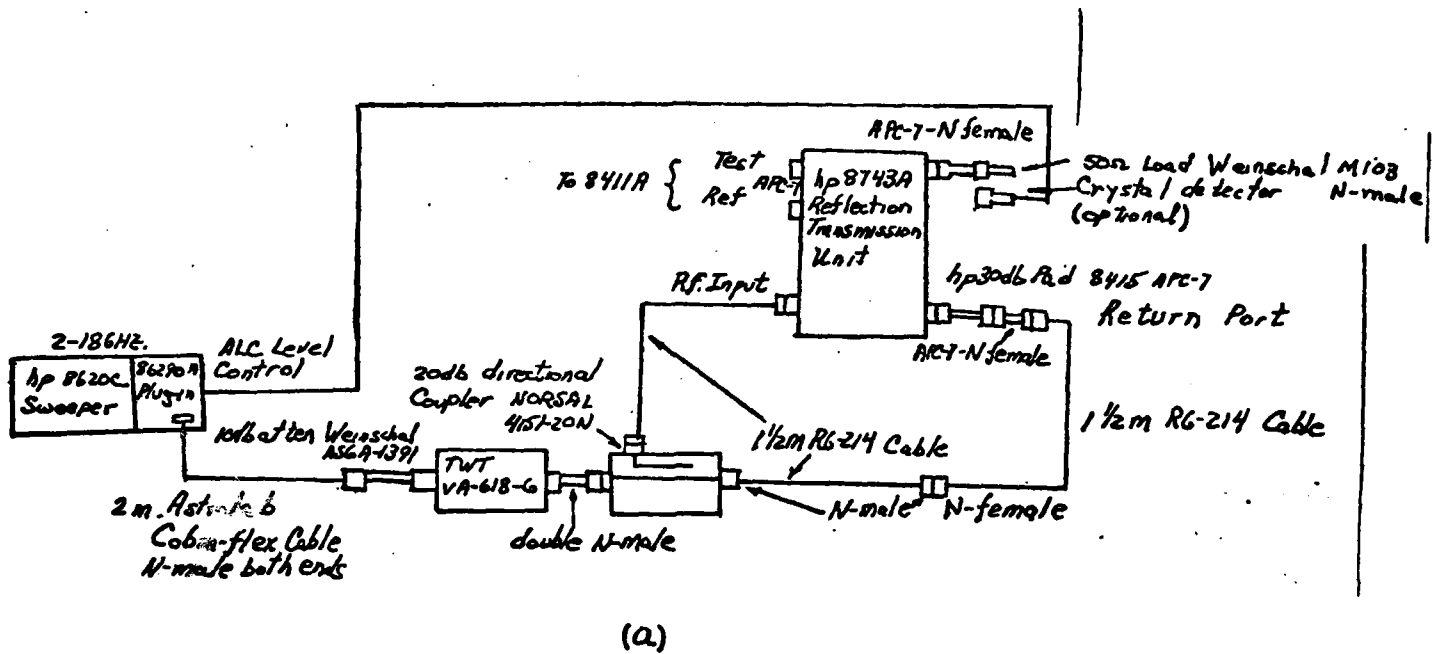
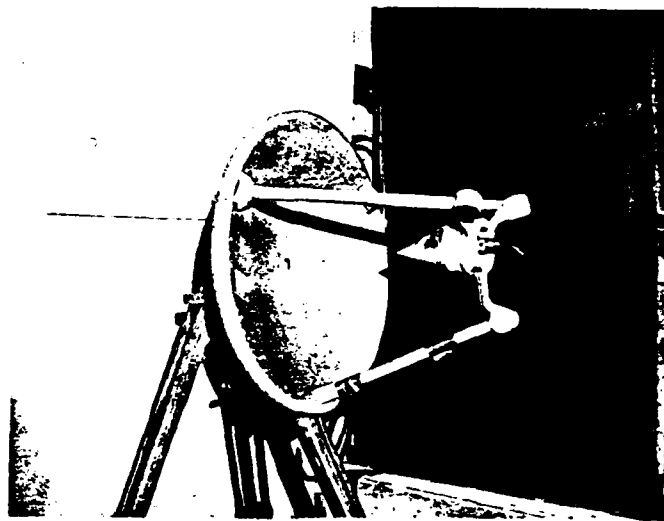
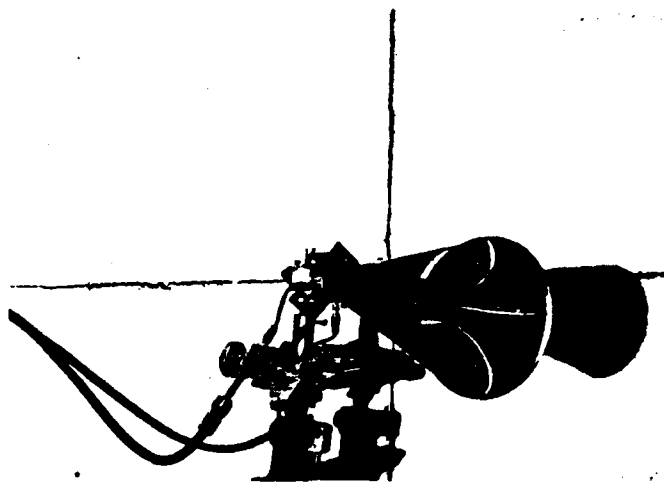


Fig. 2.7 a) System configuration for transfer characteristic measurement. b) Connection to antennas for scattering and clutter measurement. c) Transmitting antenna with spiral AEL antenna and parabolic dish. d) Receiving dual polarization horn ; EMI A6100 with Norsal 90 hybrid.



(c)



(d)

Fig. 2.7 (contd.) a) system configuration for transfer characteristic measurement. b) Connection to antennas for scattering and clutter measurement c) Transmitting antenna with spiral AEL antenna and parabolic dish. d) Receiving dual polarization horn; EMI A6100 with Norsal 90 hybrid.

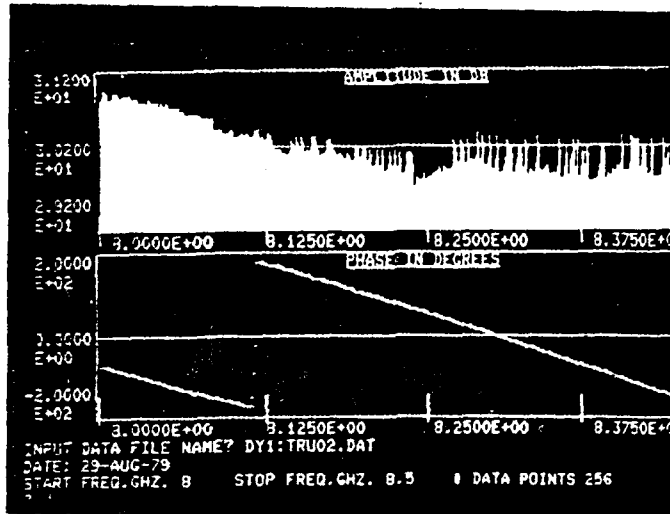


Fig. 2.8 Uncorrected transfer characteristic of system; 8.0-8.5 GHz.

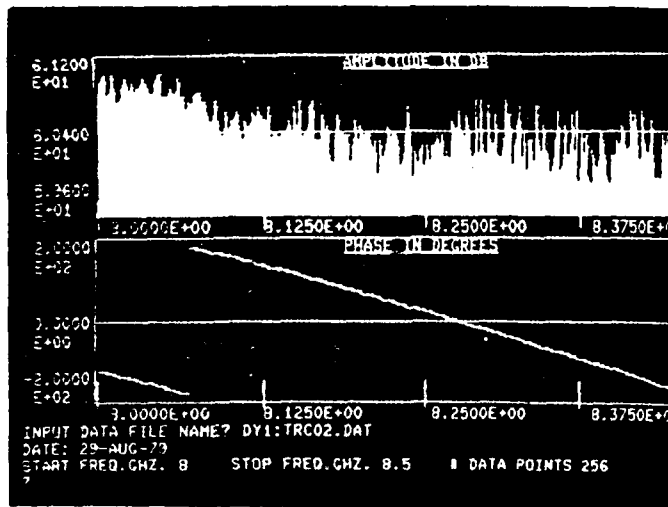


Fig. 2.9 Transfer characteristic corrected for attenuator response; 8.0-8.5 GHz.

location. A high gain parabolic dish antenna is used for illumination of the target since the narrow beam pattern of the antenna places most of the radiated power on the target area. A smaller dual polarization horn is used for receiving in order to sample a small area of the scattered field. The uncorrected clutter $C_1(f)$ is given by:

$$C_1(f) = C_2(f) * T(f) + I(f) \quad (2.3)$$

Solving for the corrected clutter and coupling:

$$C_2(f) = (C_1(f) - I(f)) / T(f) \quad (2.3a)$$

Subroutine ANTEN does the system clutter and coupling removal. Examples of the uncorrected and corrected clutter $C_1(f)$ and $C_2(f)$ are shown in figs. 2.10 and 2.11. The corrected clutter represents the actual signal reflected from the anechoic chamber walls and that signal coupled between the antennas with the system response removed.

These subroutines: PAD, IST, TRANS, and ANTEN, were combined into a program SYSRES. Data from each of these subroutines may be stored on disc for later recall or display. Theoretically if the system is not disturbed then the system response will remain constant. Then only the target data need be recorded in any run for a new corrected backscatter measurement.

The transfer function of the system and the range clutter- antenna cross coupling data are utilized the the next step of the error correction process. A reference object of known constant cross section is measured and the result stored. This data includes all the errors previously

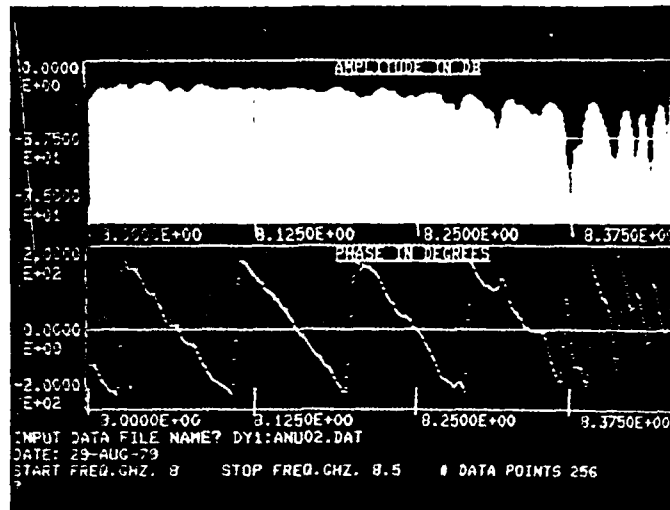


Fig. 2.10 Uncorrected system clutter; 8.0-8.5 GHz.

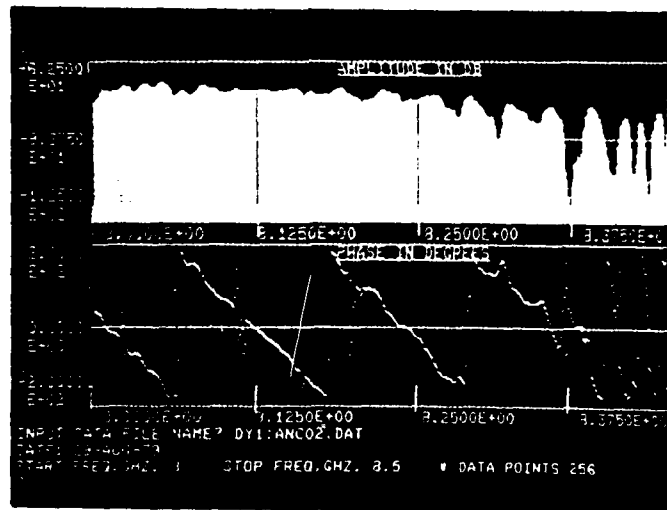


Fig. 2.11 System clutter corrected for transfer function; 8.0-8.5 GHz.

described but also takes into account the antenna system variations as a function of frequency:

$$R_1(f) = C_2(f) * T(f) + I(f) + R_2(f) * T(f) \quad (2.4)$$

Here $C_2(f)$ and $R_2(f)$ contain the antenna system response multiplying the actual values of corrected reference target and system clutter data.

$$R_2(f) = R(f) * A_1(f) \quad (2.5)$$

$$C_2(f) = C(f) * A_1(f) \quad (2.6)$$

This response $A_1(f)$ takes into account the varying amount of power received and transmitted as a function of frequency in the antenna system. If the reference target is chosen to have a constant cross section and linear phase over the frequency range of interest then $R(f)$ is of constant amplitude and linear phase. Solving for $R_2(f)$:

$$R_2(f) = (R_1(f) - I(f) - C_1(f)) / T(f) \quad (2.7)$$

This leaves $R_2(f)$ proportional to $A_1(f)$ shifted by a linear phase corresponding to the reference target range.

When the actual target is measured; it is corrected for system errors as was the reference target data and this result is divided the corrected reference target data to yield the final target scatter data.

$$S_2(f) = (S_1(f) - I(f) - C_1(f)) / T(f) \quad (2.8)$$

$$S(f) = S_2(f) / R_2(f) \quad (2.9)$$

This technique may be simplified considerably in the laboratory environment given the signal to noise ratio is greater than 10 db for the scattered signals. In this case only multiplicative errors remain and the additive errors

are masked by the high target scatter signal amplitude.

Hence:

$$\begin{aligned} I(f), C_1(f) &\rightarrow 0 \\ R_1(f) &= R_2(f) * T(f) \end{aligned} \quad (2.10)$$

and therefore:

$$S(f) = S_1(f) / R_1(f) \quad (2.11)$$

Weir and his group have reported that this technique has reduced equivalent range clutter to -45 db below 1 sq. meter.

There remains one source of error in the scattered signal measurement that cannot be removed by calculation. This error comes from multipath scattering from the object. The target scatters power in all directions. Some of this signal may be reflected off the walls or floor of the anechoic chamber. The signals reflected off the walls is over 48 db down from the incident wave amplitude in the 6.0-12.0 GHz range. However if the target is small in cross section; on the order of 100 sq. cm.; then it is possible for the walls (on the order of 100 000 sq. cm.) to contribute a significant component to the received signal.

In order to analyze the effect of the multipath scattering, let the directly received signal be written:

$$S_o(t) = A \cos(\omega t + \psi) \quad (2.12)$$

and the indirectly received signal:

$$S_i(t) = B \cos(\omega t + \psi + \theta) \quad (2.13)$$

Then the total received signal is given by:

$$S_r(t) = (A^2 + 2AB \cos \theta + B^2) \cos \left(\omega t + \psi + \tan^{-1} \left(\frac{-B \sin \theta}{A + B \cos \theta} \right) \right) \quad (2.14)$$

Since theta is a function of the indirect path length differences and frequency, it will lead to a periodic variation in the amplitude of the scattered signal. As an example; if the paths differ in length by 1 meter then the amplitude oscillations will occur every 300 MHz given all other factors remain constant.

A series of programs was written to test these various techniques of error removal. They differ in the only in the error removal technique employed; not in file storage or display formats nor in range calculation and removal to be described. These programs used together:

- 1) Measure and correct the reference target data with files of transfer function and clutter data generated by SYSRES.
- 2) Measure and correct the target data and finally take the corrected reference target data and remove the antenna system response from the target data.
- 3) Alternately for high SNR; calculate the correct scattered target signal directly using the reference target data.
- 4) Calculate and remove phase shift due to range from the target signal after error correction

These programs are briefly described and differ in the mentioned categories:

SPHERE-Reads transfer function and clutter data files generated by SYSRES; takes the reference or object data and corrects for errors in the

equipment.

SPHER2-Measures clutter and reference target data.

It then subtracts clutter and divides the target data by the reference target transfer function.

SPHER3-Measures reference target and object signals ignoring clutter, and divides the object data by the reference target complex field amplitude data.

In order to implement the complete error correction process program SPHERE would be run twice; once for the reference target and then again for the test object. This data would be stored for later retrieval. Program SPHER3 would read these files and process them such that the test object complex field data would be divided by the reference target data. For high SNR cases; program SPHER3 alone would be run: first measuring the reference target and then the test target and finally dividing them yielding the final result. Listings and a more complete description of program operation is given in the program appendix I.

III RANGE PHASE SHIFT ANALYSIS

This chapter contains an analysis of the effects on the phase shift due to target range on coherent imaging of a target. It includes a discussion of some of the available techniques for the removal of this phase shift and the required performance of these systems based on bandwidth and signal to noise ratio.

3.1 The effects of range phase on imaging

As previously described by Farhat and Chan ;[4]; the scattered field of the scattering target is given by:

$$\psi(k, R_r, R_t) = \frac{jk}{2\pi(R_r + R_t)} e^{-jk(\vec{R}_r + \vec{R}_t)} \int_{-\infty}^{\infty} U(\vec{r}) e^{-jk(\vec{R}_r + \vec{R}_t) \cdot \vec{r}} d\vec{r} \quad (3.1)$$

Where \vec{R}_r and \vec{R}_t are the vectors from the receiving and transmitting antennas to the target respectively and k is the wave vector of the illuminating wave. In this case the integration is over the extent of the object. The integral term is independent of the range of the target. While the term preceding the integral is target independent and contains range information. The argument of the complex exponential is a linear phase function of frequency.

In the single receiver-transmitter pair arrangement; shown in fig.3.1, the spatial frequency domain (\vec{p} space) data is collected in a plane perpendicular to the axis of rotation. In this case the multiplication of the range phase factor leads to the convolution of the transforms of the the range and target functions in the spatial domain. The real part of the range frequency domain function is a

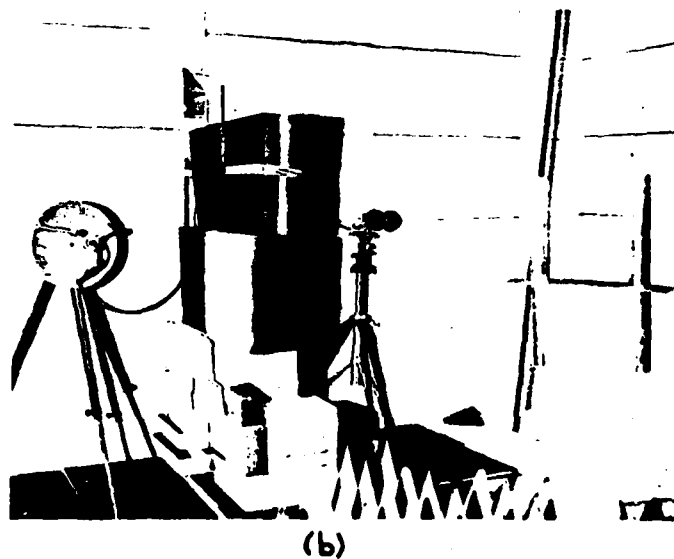
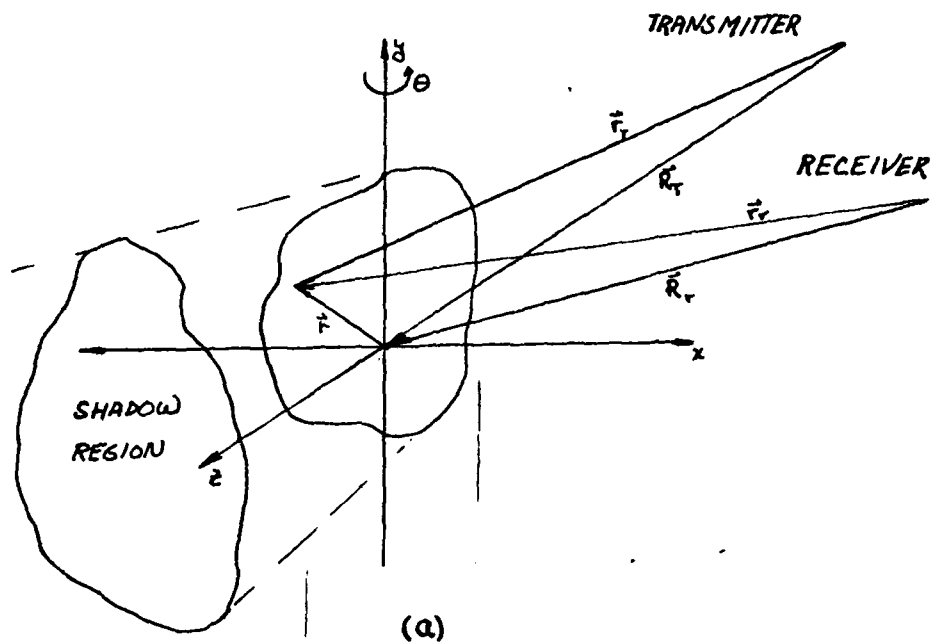


Fig. 2.12 a) Target and antenna placement relative to target considered in analysis. b) Experimental configuration in anechoic chamber; note target on rotating pedestal in forefront.

radially symmetric sinusoidal function:

$$R\{e^{-jk(R_T+R_r)}\} = \cos k(R_T+R_r) \quad (3.2)$$

This transforms to a circular ring of radius $(R_T + R_r)$. This indicates that each point of the reconstructed image is convolved with this circular ring pattern; seriously degrading the target image. In fact any error in the removal of phase will distort the image in this manner. The effect of removing the range phase factor is equivalent to the focusing of the system on the target.

There are several other reasons for the removal of the factor:

$$\frac{jk}{2\pi(R_T+R_r)} e^{-jk(R_T+R_r)} \quad (3.3)$$

from the received data. If the data is discrete then the considerations of aliasing and sufficient data sampling rate are introduced. When the sampling rate in the frequency domain is (f) then the maximum target range before aliasing will occur is $(c/4 * f)$. However if the phase factor is removed and the target is of smaller dimension L than the range, then the sampling rate in the frequency domain need only be sufficient to prevent aliasing over the dimensions of the object :

$$\Delta f \leq \frac{c}{4L} \quad (3.4)$$

This allows the entire resolution capability of the system to be placed on the target itself greatly reducing the data

volume.

Another reason for the removal of this phase factor term can be seen in systems involving multiple receiver-transmitter pairs. For each pair (\bar{R}_i) and (\bar{R}_j) is different and in order for the data to be coherent all phase centers must be equal for an image to be formed.

Several methods have been suggested for the removal of the range phase factor. [4] In all cases it is required that the range removal technique be accurate to within $(\lambda/5)$ for there not to be serious image degradation. It is important to investigate the constraints on the ranging system parameters necessary to attain the required accuracy.

From the scaling theorem in Fourier analysis; a signal cannot be both of narrow bandwidth and short duration. [8]

$$af(at) \rightarrow F\left(\frac{\omega}{a}\right) \quad (3.5)$$

We define the duration and the bandwidth of the signal in the following manner: []

$$(\Delta t)^2 = \frac{1}{E} \int_{-\infty}^{\infty} t^2 |f(t)|^2 dt \quad (a) \quad (\Delta \omega)^2 = \frac{1}{2\pi E} \int_{-\infty}^{\infty} \omega^2 |F(\omega)|^2 d\omega \quad (b) \quad (3.6a,b)$$

where:

$$E = \int_{-\infty}^{\infty} |f(t)|^2 dt = \frac{1}{2\pi} \int_{-\infty}^{\infty} |F(\omega)|^2 d\omega \quad (3.6c)$$

is the signal energy. Then if:

$$\lim_{|t| \rightarrow \infty} \sqrt{t} f(t) = 0 \quad (3.6d)$$

When applied to signals scattered by a target this may be translated to range uncertainty:

$$\Delta R \Delta f \geq \frac{c}{4\pi} \quad (3.7)$$

This represents a limit when the durations of the signal pairs are as previously defined. However it may be possible to improve the range resolution given that the signal to noise ratio is greater than 10 db.

Consider a sinusoid in narrow band gaussian noise:

$$r(t) = A \cos \omega t + n_c(t) \cos \omega t - n_s(t) \sin \omega t \quad (3.8)$$

$$n(t) = n_c(t) \cos \omega t - n_s(t) \sin \omega t$$

where $n(t)$ is the noise signal and $n_s(t)$ and $n_c(t)$ are the quadrature components of the noise signal. The amplitude and phase may be expressed as:[9]

$$|r(t)| = \sqrt{(A + n_c(t))^2 + n_s(t)^2} \quad (3.9a)$$

$$\text{Arg}(r(t)) = \tan^{-1} \left\{ \frac{n_s(t)}{A + n_c(t)} \right\} \quad (3.9b)$$

Since the noise is gaussian $n_c(t)$ and $n_s(t)$ are gaussian. Assuming that the SNR is high the phase may be approximated by:

$$\text{Arg}(r(t)) = \tan^{-1} \left\{ \frac{n_s(t)}{A} \right\} \approx \frac{n_s(t)}{A} \quad (3.10)$$

Also since the noise is white $n_s(t)$ may be related to the bandwidth of the receiving system.

$$\sigma_{n_s}^2 = 2N_b B \quad (3.11)$$

where $(\sigma_{n_s}^2)$ is the variance of the $n_s(t)$ quadrature phase component. The probability density of the phase may be written as:

$$f(\theta) = \frac{A}{\sqrt{2N_b B}} e^{-A^2 \theta^2 / 4N_b B} = N(0, \frac{\sigma_{n_s}^2}{A^2}) \quad (3.12)$$

This leads to an interesting result; the variance of the

phase is the inverse of the SNR:

$$\sigma_{\phi}^2 = \frac{\sigma_{n,3}^2}{A^2} = \frac{1}{\text{SNR}} \quad (3.13)$$

Translating this result to an uncertainty relationship the phase uncertainty may be expressed:

$$\Delta \omega \Delta t \geq \sqrt{\frac{8NB}{A}} \quad (3.14)$$

The uncertainty in phase is the product of the time and frequency uncertainties. This leads to an expression for the range resolution as a function of the SNR.

$$\Delta f \Delta R \geq \frac{c}{2\pi\sqrt{\text{SNR}}} \quad (3.15)$$

Wide band ranging systems measure range by calculating the propagation delay of the signal. In one such system a high speed code is transmitted. The received signal is correlated with the original coded signal in a delay locked loop. The value of the control signal in the loop is proportional to the target range. Obviously the resolution is only as good as the the period of one of the code bits(chips). Other wide band systems use other signals for ranging(chirps,walsh functions) to obtain high range resolution. [10], [11], [12]

The system implemented here at the Graduate Research center of the Moore school is a coherent amplitude-phase measurement facility. Ranging techniques that may be integrated into this system are therefore of special interest. The phase of a point scatterer is a linear function the frequency. This directly corresponds to the

phase factor preceding the scattering integral in eq (). If the target consists of multiple scattering centers; then each of these will be represented as a delta function in the in the reconstructed image. This suggests a technique using Fourier analysis to determine range. First place the reference target in the microwave field and measure the phase/amplitude response over as wide a frequency range as possible. Then inverse transform this one dimensional collection of data. This will transform to essentially a delta function occurring at the time corresponding to the propagation delay. This will occur when the target has a single scattering center such as a sphere. Even when the object is more complex the inverse transform will be centered around the transit time. In this Fourier technique for range determination the resolution (Δx) is inversely related to the frequency sweep width.

$$\Delta x = \frac{c}{2 \Delta f} \quad (3.16)$$

The factor of 1/2 results from the fact that the range is half the signal propagation path length.

A factor to be considered is that different scattering centers are visible from different receiver positions. It is imperative that all when several receivers are used simultaneously that all choose the same scattering center as the phase center for range removal. If the various phase centers do not coincide, the fringes of the hologram will be skewed. The data sets from each of the receivers must be brought into alignment using an adaptive

AD-A090 838

MOORE SCHOOL OF ELECTRICAL ENGINEERING PHILADELPHIA PA
SUPER-RESOLUTION IMAGERY BY FREQUENCY SWEEPING. (U)

F/6 17/9

AUG 80 N H FARHAT, C WERNER

AFOSR-77-3256

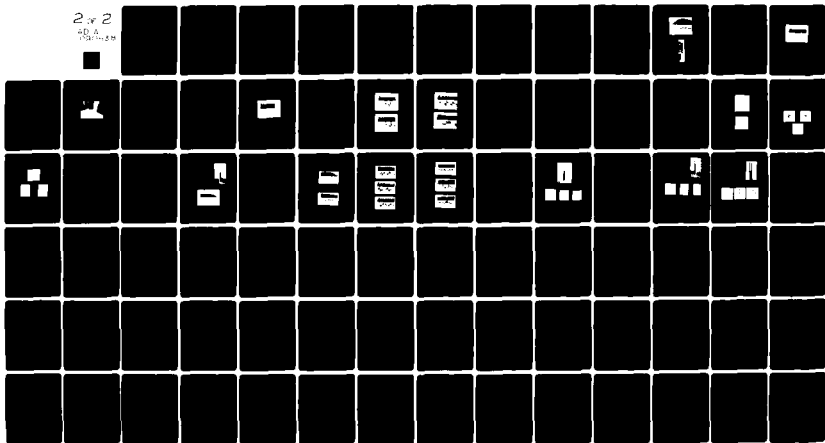
UNCLASSIFIED

AFOSR-TR-80-1068

NL

2 of 2

10/1/80



END
DATE
FILMED
12-80
DTIC

Information is lost in the hologram if the phase centers for the scan lines are separated.

When this process is automated the sweep is done by measuring the response at discrete frequency points. The amplitude and phase are stored at N frequency points in the sweep range. The range at which aliasing will occur is given by:

$$R_{\text{alias}} = \frac{c}{4 \Delta f} \quad (3.17)$$

This system exhibits processing gain ; a quality of all systems which spread a baseband signal into a wide spectrum. For this system the processing gain is a function of the number of measurements and the sweep width.

$$G_{\text{gain}} = \frac{\Delta f}{f_{\text{stepsize}}} = n \quad (3.18)$$

$$G_{\text{gain db}} = 10 \log_{10} n$$

As an example, for 256 measurement points, this would give 24 db of processing gain.

A set of subroutines was written to test this range removal technique. In one of them , RANGE, the range of the strongest scattering center is calculated and in the other ,RANCOR, the phase factor is calculated and removed from the target data. These subroutines are used in programs SPHERE, SPHER2 ,and, SPHER3.

The time domain equivalent of this technique is fitting a linear trend to the phase signal from the network analyzer. Since the phase signal is modulo (2π) ; this means

estimating the frequency of a ramp waveform; either using a least squares approximation or implementing the equivalent of a phase locked loop. The slope of the ramp waveform is proportional to the range of the target. The accuracy to which the range may be determined depends on the sweep width, the target structure and the noise in the system. If the sweep is wide, then there will be more data with which to estimate the slope. Noise in the data will obviously interfere with the estimation process as will as any phase shifts due to the target structure.

Another type of system for generating a reference signal utilizes a Target Derived Reference. This system has been extensively studied at the Electro-Optics and Microwave Optics laboratory. [13] A brief review of the ideas developed to date in this regard are given below. The complex exponential in the integral term of scattered signal remains constant when the target is small relative to the illuminating signal wavelength.

$$\psi(\vec{p}) = \int_{\infty}^{\infty} U(\vec{r}) e^{-j\vec{p} \cdot \vec{r}} d\vec{r} \approx e^{-j\vec{p} \cdot \vec{r}} \int_{\infty}^{\infty} U(\vec{r}) d\vec{r} \quad (3.19)$$

This is true if (L_{∞}) is sufficiently small such that $(\vec{p} \cdot \vec{r} \ll 1)$. In this case the integral value approaches a constant multiplied by a linear phase; i.e. a point scatterer. It will only occur when the target dimensions are less than a tenth wavelength of the illuminating signal, placing it in the Rayleigh scattering region. The TDR signal is mixed harmonically with a phase locked scattered

estimating the frequency of a ramp waveform; either using a least squares approximation or implementing the equivalent of a phase locked loop. The slope of the ramp waveform is proportional to the range of the target. The accuracy to which the range may be determined depends on the sweep width, the target structure and the noise in the system. If the sweep is wide, then there will be more data with which to estimate the slope. Noise in the data will obviously interfere with the estimation process as will as any phase shifts due to the target structure.

Another type of system for generating a reference signal utilizes a Target Derived Reference. This system has been extensively studied at the Electro-Optics and Microwave Optics laboratory. [13] A brief review of the ideas developed to date in this regard are given below. The complex exponential in the integral term of scattered signal remains constant when the target is small relative to the illuminating signal wavelength.

$$\psi(\vec{p}) = \int_{-\infty}^{\infty} U(\vec{r}) e^{-j\vec{p}\cdot\vec{r}} d\vec{r} \approx e^{-j\vec{p}\cdot\vec{r}} \int_{-\infty}^{\infty} U(\vec{r}) d\vec{r} \quad (3.19)$$

This is true if $(L_{\infty i})$ is sufficiently small such that $(\vec{p}\cdot\vec{r} \ll 1)$. In this case the integral value approaches a constant multiplied by a linear phase; i.e. a point scatterer. It will only occur when the target dimensions are less than a tenth wavelength of the illuminating signal, placing it in the Rayleigh scattering region. The TDR signal is mixed harmonically with a phase locked scattered

signal at the imaging frequency. here the two signal sources are phase locked by a phase synchronizer. The high frequency sweeper acts as the slave signal source. These two signals simultaneously illuminate the target. Harmonic mixing of the suitably limited TDR and imaging signals will yield the desired phase corrected data.

Another technique which is useful for ranging is the frequency displaced reference method. Here the carrier is displaced (Δf). It is important that the object not contribute to the phase shift; hence the displacement must satisfy the following condition:

$$\Delta f \ll \frac{2c}{L} \quad (3.20)$$

In this case the target structure will not contribute to the net phase shift. The range to the target phase center is given by:

$$R = \frac{\Delta \phi c}{\Delta f 2\pi} \quad (3.21)$$

c - speed of light

Where ($\Delta \phi$) is the change in phase for the carrier and displace carrier signals respectively. If the frequency shift is small then the phase shift will not be large. The resolution of the system then is directly related to the SNR in the receiver channel since the accuracy to which the phase may be measured is a function of the channel noise. If the displacement is large then the phase shift is increased and the SNR requirements on the signal for a specific resolution is decreased. This relationship may be expressed:

$$R_{\text{resolution}} = \frac{r_{\text{oc}} c}{\Delta f 2\pi} = \frac{\sqrt{2N_s B} c}{4\pi A \Delta f} \quad 3.22$$

The factor of 2 comes about due to the phase uncertainty existing in both the carrier and displaced carrier signals.

An alternate method for implementation of the displaced frequency ranging system is a swept frequency chirp system.

The ranging signal frequency is given by :

$$f(t) = f_0 (1 + \alpha t) \quad \text{where } \alpha = \frac{f_1 - f_0}{T} \quad 3.23$$

T- Sweep period

f_0 - Initial frequency for sweep

f_1 - final frequency

The scattered signal from the target is given by:

$$f_s(t) = f_0 + \frac{d\phi}{dt} - \frac{f_0 \alpha}{c} (R_T + R_r) \quad (3.24)$$

where $(d\phi/dt)$ is the change in frequency due to the target structure. The range of the target may then be simply calculated using a frequency counter and sweep time T and sweep width $(f_1 - f_0)$. This method could be used in an analog imaging system.

Other Target Derived Reference systems simulate the low frequency reference carrier by measuring the change in phase of the imaging frequency over a narrow band. Over this small band the phase shift is assumed to be linear. In one system a series measurements is made for each frequency point. The first displaced down by a small amount, (Δf) ; the second at f ; and the final measurement at $(f + \Delta f)$. Phase and amplitude are measured at each frequency and processed to obtain the target range. In a similar system the three

signals are transmitted simultaneously by amplitude modulation of the carrier. These systems are presently under intense investigation by other workers at the Electro-Optics and Microwave Optics Laboratory of the Moore School.

3.2 Practical considerations for range phase removal

Several factors influence which of these systems would be of value in a long range imaging radar system versus a controlled laboratory environment. The distribution of the reference signal for complex field amplitude measurement makes implementation of system requiring a central reference difficult to implement. Techniques are being considered in the E.O. laboratory for reference distribution using fiber optic that might remove this limitation. Reference distribution is accomplished in the lab readily since the distances are small.

Typical transmitter-receiver pattern arrangements might be the Wells array [14], an orthogonal pattern of receivers and transmitters, a circular array of receivers with central transmitter or a random array. Each combination of receiver and transmitter contributes another line in the frequency domain 3D data volume. For this reason it is advantageous that all combinations of the receivers and transmitters are utilized for data collection. Reference signal distribution difficulty therefore leaves the TDR systems as the only practical alternatives for long range imaging systems. The AM TDR system eliminates

reference distribution by transmitting the reference signal along with the imaging signal and automatically corrects for the target range. TDR systems have the additional advantage that they have immunity to turbulence and inhomogeneities in the propagation medium since both the reference and imaging signals follow the same path.

There are several considerations for determining the best TDR system. Narrow band systems yield only a weighted average of the range to the phase center of the object while wide band system can resolve individual scatters on the target body. A wide band system could adaptively choose one of the scattering centers for the phase reference of the system. A narrow band system could not do this, and any error would introduce image distortion. The narrow band systems have the advantage of automatically correcting the target data for the range phase factor.

For the laboratory imaging experiments a TDR system would not yield the correct phase factor since in this arrangement the object rotates about an axis and the correct phase factor would be a constant, representing the phase shift to the axis of rotation, not the target. The TDR system looks only at the range to the strongest specular reflector on the target surface.

If movement of the target is utilized for aperture synthesis then only one receiver-transmitter pair is required for 3-D imaging and the adaptive system is not required.

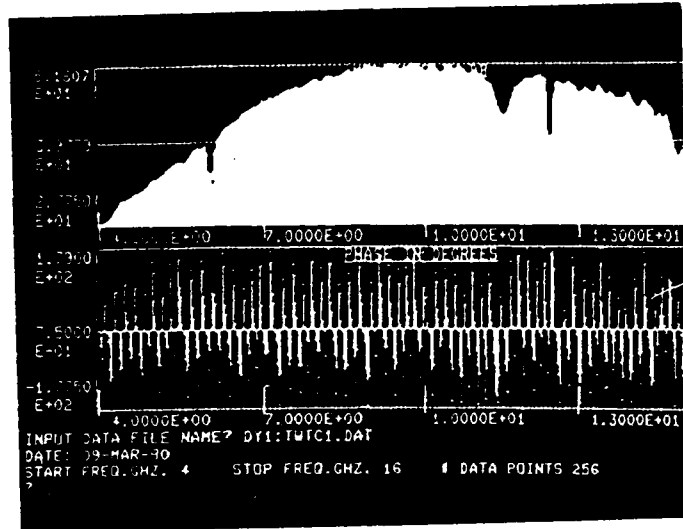
Knowledge of the placement of the data in the 3-D frequency domain volume is necessary for the reconstruction of the hologram. The azimuth and elevation angle of the target can be obtained from a conventional radar located at a central location where the data processing and reconstruction is taking place.

IV SYSTEM IMPLEMENTATION OF SWEEP FREQUENCY IMAGING

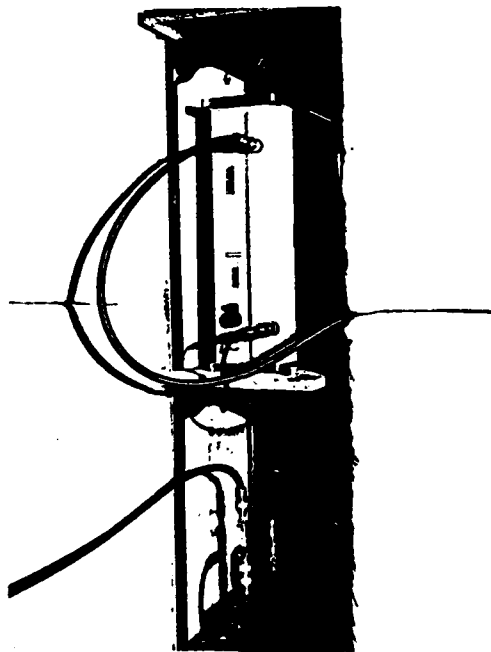
This section of the thesis will describe the research that was done in order to obtain a clear understanding of system performance. Following this will be a section of the thesis devoted to the experimental verification of the swept frequency imaging theory.[] The theory is applied in the simulation of the experiments performed.

4.1 System repeatability

An important parameter of system performance is the repeatability of an experimental measurement. The frequency range over which this possible for the equipment used indicates the bandwidth for which imaging is possible. There are several feedback loops in the system which allow it to track variations in the transmitted signal level. The traveling wave tube amplifier characteristic is shown in fig.4.1. This plot is on a logarithmic scale, indicating that the TWT amplifier gain drops off exponentially below 7.0 GHz and above 15.0 GHz. This measurement was done by first measuring the system response (cables, connectors, attenuator) less the TWT amplifier and then subtracting this response from the TWT amplifier plus system data. A sample of the amplifier output is sampled using a 20 db directional coupler and this is fed to the RF input of the HP 8743A reflection-transmission (R-T) unit. A crystal detector at the 'unknown' port of the R-T unit rectifies a portion of this signal. The detector output is brought to the external signal leveling input of the HP 8620C sweeper.



(a)



(b)

Fig. 4.1 a) Traveling Wave Tube amplifier gain characteristic in db; 4.0-16.0 GHz. b) Varian VA 618G TWT amplifier (bottom) and HP 8743A reflection-transmission unit (top).

The leveling circuit of the sweeper can level the output over a 20 db range. In addition the AGC in the HP 8410B network analyzer can track the reference signal amplitude over a 40 db dynamic range. System performance may be seen in fig.4.2 for a cylindrical target 7 meters distant from the receiving and transmitting antennas. Two consecutive measurements of the target were made and the results divided. The ideal response would be 0 db flat amplitude and 0 degree phase difference over the entire frequency sweep. With few exceptions due to phase noise at the (+/-) transition point, the system has the desired repeatability in the 5.5 to 16.0 GHz range. Below 4.5 GHz there are phase errors due to insufficient reference power whereas above 15 GHz errors come about due to the low amplitude of the received signal. Noise may be cancelled by taking multiple measurements and finding the mean. These results indicate the useful data can be recorded in the 5.5-16.0 GHz range

4.2 Computer control of target rotation

When implementing a frequency diversity system with just one pair of receiving and transmitting antennas, the target must then be rotated in the electromagnetic field and the scattering measured for different rotation angles. The target used in the experimental system rotates on a stepper motor driven pedestal. The column of the pedestal is 1 1/2 meters in length and is made of styrofoam material with minimal cross section. A stepper motor controls table rotation precisely. In order for the pedestal to rotate one

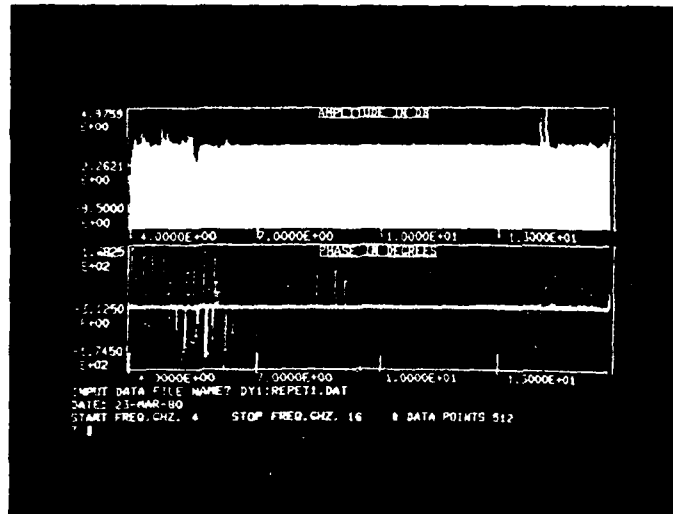


Fig. 4.2 System repeatability for two consecutive scattering measurements of a 80 cm long cylinder 7 cm in diameter; 4.0-16.0 GHz.

revolution the motor must be stepped 10 000 times. The motor is under direct computer control using the digital output port the MINC. A FORTRAN subroutine STEP2 was written for control of the stepper motor. It calculates the number of steps required for a specified angular rotation and moves the table clockwise or counter clockwise based on the direction parameters passed in the subroutine call. The stepper and pedestal are shown in fig.4.3.

4.3 Sphere Simulation

For the calibration of a radar system a reference target is required. The most commonly used reference target is the conducting sphere since its high degree of symmetry does not favor any particular polarization for the incident illumination. Both the bistatic and monostatic scattering of a metallic sphere was simulated.

The general solution for the plane wave electro-magnetic scattering of the sphere was first done by Mie in 1908. [15], [16] In the far field approximation, the scattered field is given by:

$$E_s(A, r, \theta, \phi) = E \frac{e^{ik_r r}}{k_r r} \left[\cos \phi S_1(\theta) \hat{e} - \sin \phi S_2(\theta) \hat{\phi} \right] \quad (4.1)$$

where

$$S_1(\theta) = \sum_{n=1}^{\infty} (-1)^{n+1} \left[A_n \frac{P'_n(\cos \theta)}{\sin \theta} + i B_n \frac{d}{d\theta} \left\{ P'_n(\cos \theta) \right\} \right] \quad (4.2)$$

and

$$S_2(\theta) = \sum_{n=1}^{\infty} (-1)^{n+1} \left[A_n \frac{d}{d\theta} \left\{ \frac{P'_n(\cos \theta)}{\sin \theta} \right\} + i B_n \frac{P'_n(\cos \theta)}{\sin \theta} \right]$$

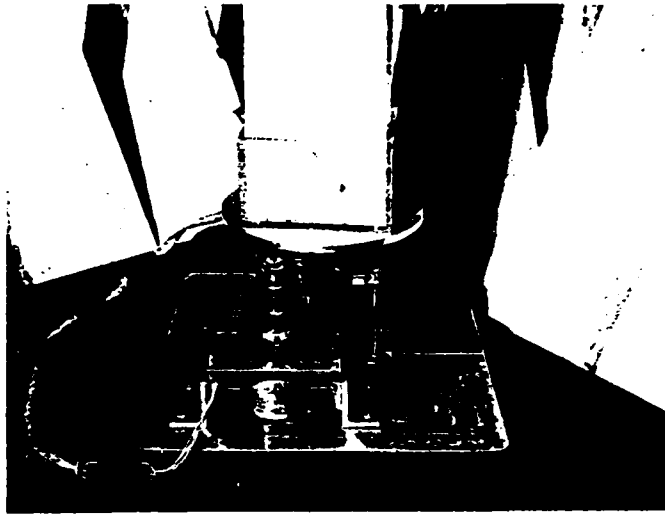


Fig. 4.3 Stepper motor and rotating pedestal.

$S_1(\theta)$ and $S_2(\theta)$ are called the complex far field amplitudes for the $(\hat{\theta})$ and $(\hat{\phi})$ polarizations respectively. The quantity in the square brackets of eq. 4.1 is called the scattering function.

$$F(\theta, \phi) = \cos \phi S_1(\theta) \hat{\theta} - \sin \phi S_2(\theta) \hat{\phi} \quad (4.4)$$

The scattering cross section in any arbitrary polarization $(\hat{\eta})$ for an incident wave polarized in the $(\hat{\tau})$ direction may be written:

$$\sigma_n(\theta, \phi) = \frac{4\pi}{k^2} |F(\theta, \phi)|^2 |\hat{\tau} \cdot \hat{\eta}|^2 \quad (4.5)$$

Where $(\hat{\eta})$ is the polarization of the incident wave and $(\hat{\tau})$ is the polarization vector of the receiving system. For the perfectly conducting sphere the coefficients A_n and B_n are:

$$A_n = -(-i)^n \frac{2n+1}{n(n+1)} \frac{J_n(k_0 a)}{h_n'(k_0 a)} \quad (4.6a)$$

$$B_n = (-i)^n \frac{2n+1}{n(n+1)} \frac{[k_0 a J_n(k_0 a)]'}{[k_0 a h_n'(k_0 a)]'} \quad (4.6b)$$

$j_n(k_0 a)$ - Spherical Bessel function

$h_n'(k_0 a)$ - Spherical Hankel function

$P_n^1(x)$ - Associated Legendre function

k_0 - Wave number of incident wave

a - Sphere radius

The prime on the expression for B_n denotes differentiation with respect to $(k_0 a)$.

Polynomial approximations exist for the Mie series exact solution. [15] Different polynomials are used for the three frequency regions for scattering. These are: low

frequency or Rayleigh region $(k,a) < .4$; the resonance region $.4 < (k,a) < 20$; and finally the high frequency or physical optics region $(k,a) > 20$. Two programs BISCAT and SPSCAT implement both bistatic and monostatic cases in the three frequency regions. Fig.4.4 shows the monostatic scattering of the sphere as calculated. This is exactly the same answer for the scattering of the sphere as the exact solution. The horizontal axis is in terms of the dimensionless quantity (k,a) . Figure 4.5 a,b,c and d show the bistatic scattering of the metallic sphere of bistatic angles of $30^\circ, 60^\circ, 90^\circ$, and 120° degrees. Note that the approximation are only valid in the range:

$$\delta < \theta' < \pi - \delta \quad (4.7)$$

where

$$\delta = O\left(\frac{1}{k,a}\right)$$

which leads to the discontinuities for small (k,a) at large bistatic angles. BASIC programs BIDISP and SDISP generate the graphs for the sphere simulations. These programs are in appendix II.

An important result from these simulations is that at high frequencies the scattered signal is of constant amplitude and linear phase irrespective of the bistatic scattering angle. The only exception to this is the forward scattering case when (θ) equals (π) , where the cross section grows without bound as k increases. This indicates that the only portion of the sphere that is scattering for large (k,a) is the front face closest to both the receiver and transmitter; and therefore a ray optics approximation

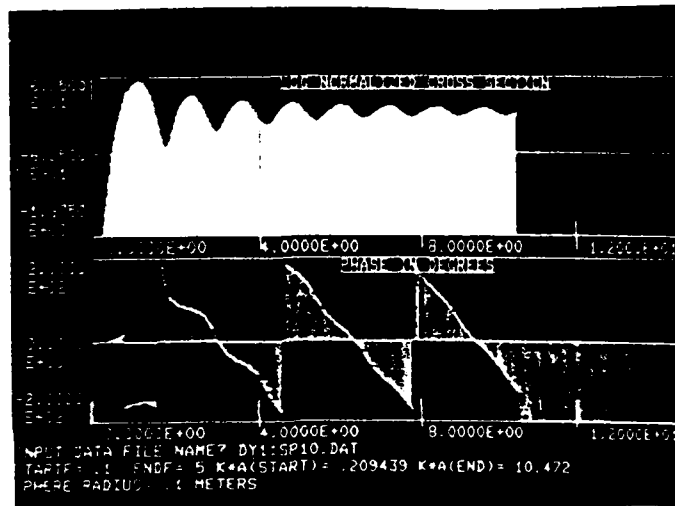
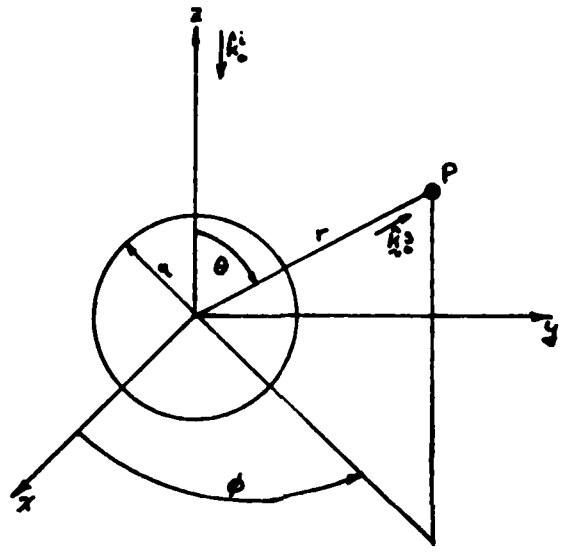
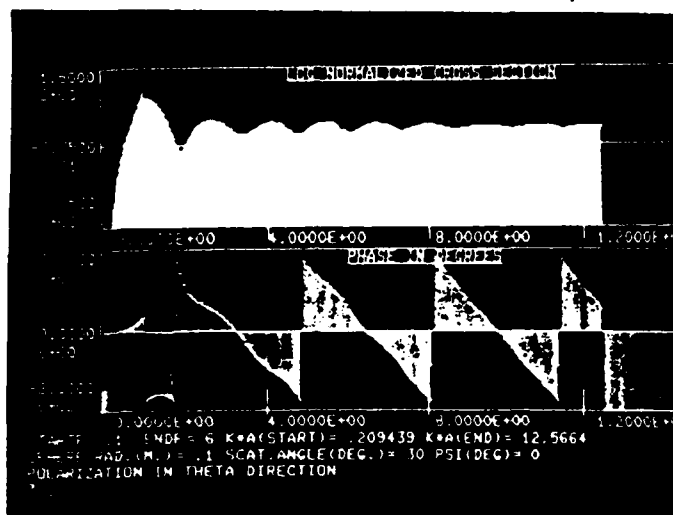


Fig. 4.4 Monostatic scattering for the perfectly conducting sphere. $(k a)$ varies from .2 to 10.5 which corresponds to the scattering of a 20 cm. diameter sphere in the frequency range of .1 to 5.0 GHz. Log normalized cross section: $\log(\quad)$.

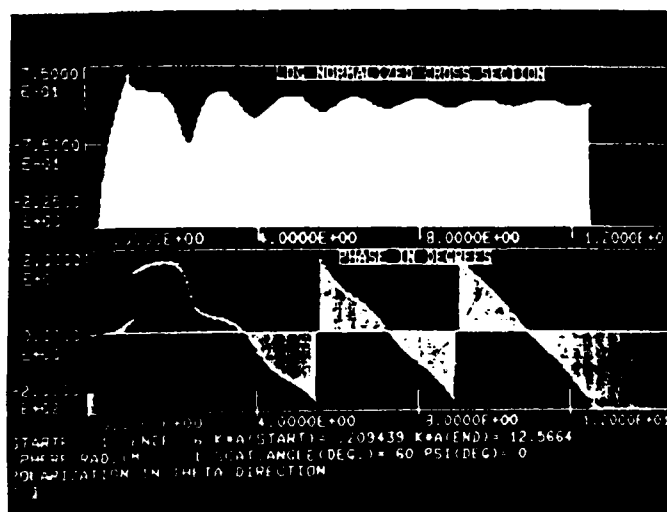


(a)

Fig. 4.5 Bistatic scattering of a 20 cm. diameter conducting sphere in the frequency range .1 to 6.0 GHz; $.2 < (k \cdot a) < 12.6$; polarization of the receiver equal to scattered wave polarization. a) Geometry for scattering expression. b) Bistatic angle 30° . c) Bistatic angle 60° . d) Bistatic angle 89° . e) Bistatic angle 120° .

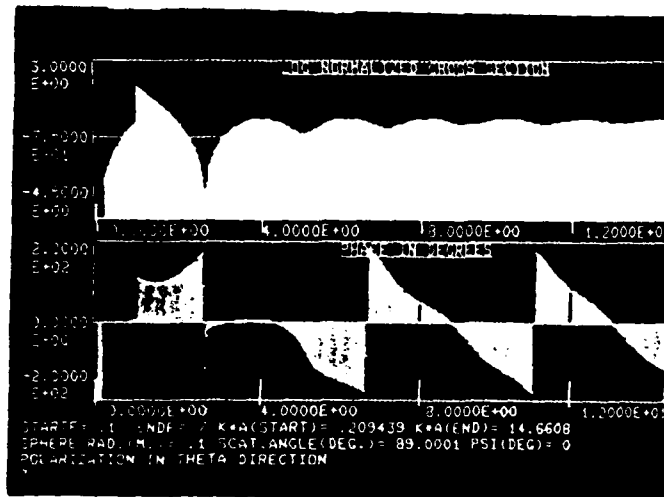


(b)

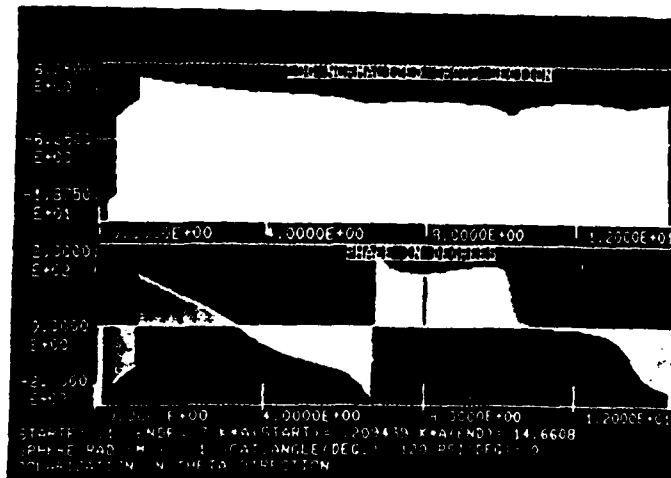


(c)

Fig. 4.5 (contd.) Bistatic scattering of a 20 cm. diameter conducting sphere in the frequency range .1 to 6.0 GHz; $.2 < (k_0 a) < 12.6$; polarization of the receiver equal to the scattered wave polarization. a) Geometry for scattering expression. b) Bistatic angle 30° . c) Bistatic angle 60° . d) Bistatic angle 89° . e) Bistatic angle 120° .



(d)



(e)

Fig. 4.5 (contd.) Bistatic scattering of a 20 cm. diameter conducting sphere in the frequency range .1 to 6.0 GHz; $.2 < (k_0 a) < 12.6$; polarization of the receiver equal to the scattered wave polarization. a) Geometry for scattering expression. b) Bistatic angle 30° . c) Bistatic angle 60° . d) Bistatic angle 89° . e) Bistatic angle 120° .

may be applied to find the scattered field.

$$S_i(\theta) = S_s(\theta) = -\frac{1}{2} k_0 a e^{-i2k_0 a \cos \theta/2} \quad (4.8)$$

for the bistatic case. In the monostatic case this reduces to:

$$F(\theta) = -\frac{1}{2} k_0 a e^{-i2k_0 a} \quad (4.9)$$

For targets with features larger than a few wavelengths in size resonance effects become minimal.

Another possible reference target is the long cylinder ($l \gg a$). The scattering of the cylinder in the high frequency region when it is oriented vertically yields an answer similar to that of the sphere. For $(ka) > 5$ where a is the cylinder radius, resonance effects disappear and the copolarized scattered field is given by: [15]

$$E_s = E_i \left(\sqrt{\frac{2 \cos \theta/2}{2r}} \right) \exp \{ i k_0 2a \cos \theta/2 \} \quad (4.10)$$

$$r = (R_T + R_r)$$

The equation for the scattering of the cylinder is used for the computer simulations of frequency swept holography.

4.4 Simulation of frequency swept imaging

A series of frequency swept hologram simulations were done of targets that would later be imaged experimentally. The basic arrangement consists of separate receiving and transmitting antennas which measure the scattering of a target that rotates about an axis. The center of rotation is chosen as the phase center of the imaging system. For this configuration the frequency domain data lies in a plane

perpendicular to the axis of rotation. Therefore the transforms of the holograms will be slices in this plane. The first object hologram simulated was comprised of two cylinders equidistant from the rotational axis. This target is shown in fig.4.6. Approximations for the various distances were derived:

$$r_1 \approx r - \frac{a}{2} \sin(\frac{\phi}{2} - \theta) \quad (4.11a) \quad r_2 \approx r + \frac{a}{2} \sin(\frac{\phi}{2} - \theta) \quad (4.11b)$$

$$x_1 \approx r + \frac{a}{2} \sin(\frac{\phi}{2} + \theta) \quad (4.11c) \quad x_2 \approx r - \frac{a}{2} \sin(\frac{\phi}{2} + \theta) \quad (4.11d)$$

the waves striking cylinders C1 and C2 are given by:

$$E_{c1} = E_0 e^{-i k_0 (\vec{x}_1)} \quad (4.12a)$$

$$E_{c2} = E_0 e^{-i k_0 (\vec{x}_2)} \quad (4.12b)$$

The scattered waves from the two cylinders including the cylinder response then follows:

$$E_{sc1} = E_{c1} \frac{\sqrt{a \cos \frac{\phi}{2}}}{Z(Rr)} e^{-i k_0 (r_1 - 2a \cos \frac{\phi}{2})} \quad (4.13a)$$

$$E_{sc2} = E_{c2} \frac{\sqrt{a \cos \frac{\phi}{2}}}{Z(Rr)} e^{-i k_0 (r_2 - 2a \cos \frac{\phi}{2})} \quad (4.13b)$$

This is further simplified by combining terms :

$$E_s = 2 E_0 e^{i k_0 (2a \cos \frac{\phi}{2})} \frac{\sqrt{a \cos \frac{\phi}{2}}}{Z(Rr)} \left\{ \cos k_0 l \cos \frac{\phi}{2} \sin \theta \right\} \quad (4.14 b)$$

Finally take the real part of this function for display:

$$R(E_s) = C \cdot \cos(2 k_0 a \cos \frac{\phi}{2}) \cos(k_0 l \cos \frac{\phi}{2} \sin \theta) \quad (4.14b)$$

This was done for a two cylinder target with cylinders 5 cm.

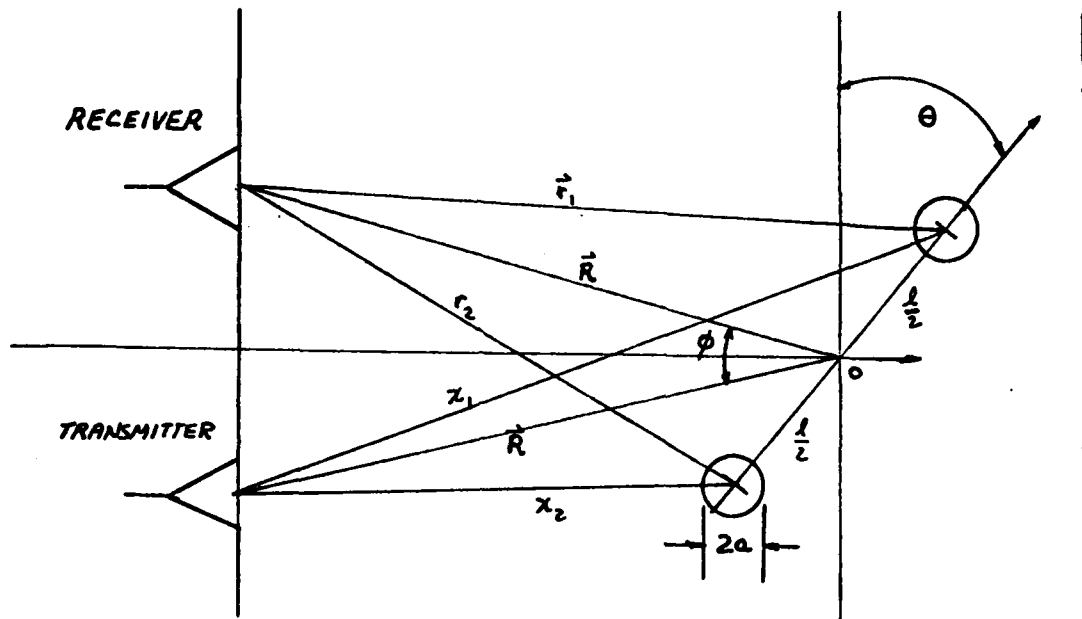
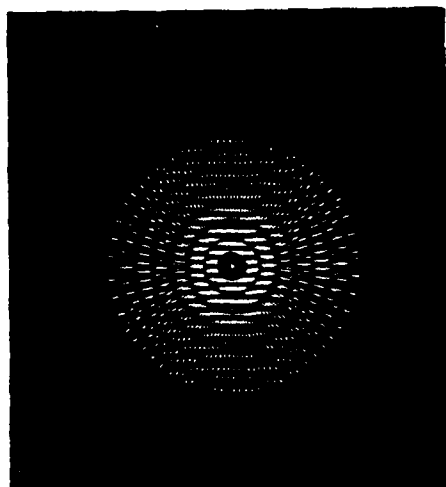


Fig. 4.6 Bistatic scattering of two cylinder target.

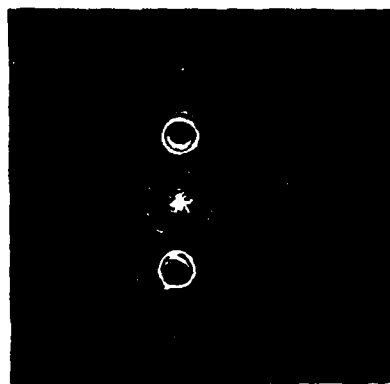
in radius ,separated by 25 cm. using program CYLIN. The results were displayed by program CDISP on a Tektronix 606A CRT display. CDISP gives the option of varying the gray scale compression of the hologram either logarithmically or by constant multiplication. These programs are listed in appendix II. The resultant hologram and the reconstructions obtained through Fourier transformation on the optical bench appear in figs.4.7 a,b The hologram simulated a sweep from 2.0 to 18.0 GHz in 64 frequency steps. The target in the simulation rotated 360 degrees in 128 steps.

Another target simulated which did not have the symmetry of the first target was comprised of two cylinders both mounted to one side of the rotational axis, as shown in fig.4.8. Two simulations were done of this target with varying diameter cylinders. In the first case 7 cm radius cylinders were used. The hologram for this case and the Fourier transform reconstructions are shown in figs.4.8 b,c,d. For the second simulation the target was two cylinders 3.5 cm in radius. In both cases the cylinders were located 10 cm from the center of rotation and the simulation was for a 2.0 to 18.0 GHz sweep. The hologram and the transformed images are shown in figs.4.9 a,b,c. The two cylinder off axis target was simulated by first calculating the copolarized scattered field for a single cylinder:

$$\vec{E}_s = 2\vec{E}_i e^{ikza} e^{-ikl\sin\theta} \quad (4.15)$$



(a)



(b)

Fig. 4.7 a) Simulation Hologram of two cylinder target; 10 cm. diameter, 25 cm. apart. Frequency range: 2.0-18.0 GHz; 128 lines, 64 points/line. b) Optical Fourier transform of hologram.

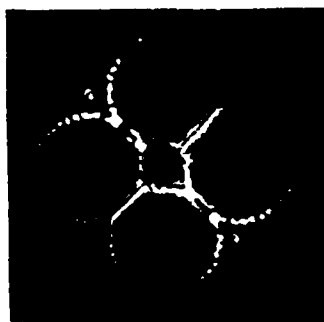
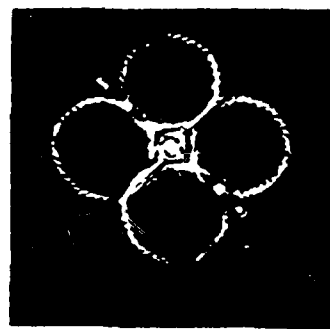
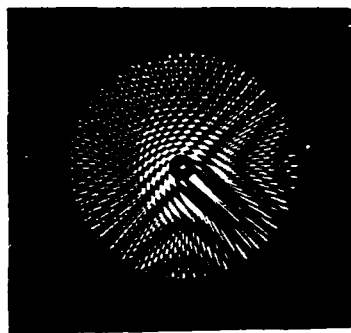
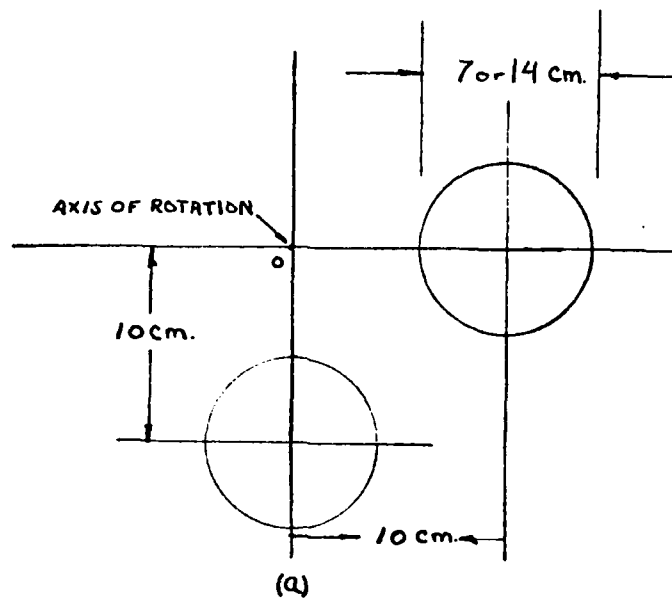
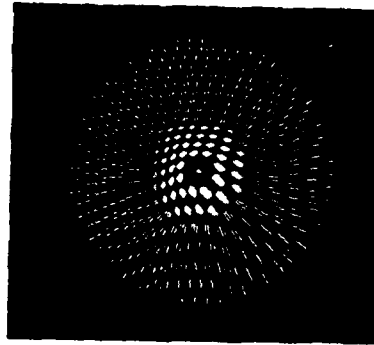
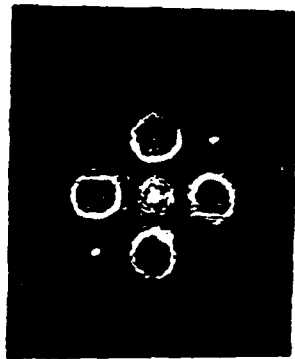


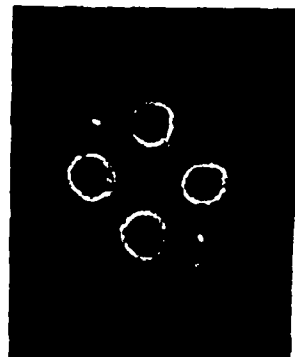
Fig. 4.8 a) Geometry of two cylinder off-axis target. b) Hologram simulation two cylinder off-axis target; 2.0-18.0 GHz; 64 points/line; 128 lines. c) Transform with zero order term. d) Transform with zero order removed.



(a)



(b)



(c)

Fig. 4.9 a) Hologram simulation of off-axis two cylinder target with cylinders 7 cm. in diameter; 2.0-18.0 GHz b) Optical Fourier transform with zero order. c) Transform with zero order term removed.

taking the real part:

$$R\{E_s\} = 2E_0 \left\{ \cos k_z z a \cos k_z l \sin \theta + \sin z a k_z \sin k_z l \sin \theta \right\} \quad (4.15a)$$

$$= 2E_0 \cos(k_z z a - k_z l \sin \theta)$$

For the two cylinder off axis target, one cylinder is at $(\theta)=0$ and the other at $(\theta)=90^\circ$, therefore the scattered field is given by:

$$R\{E_s\} = C \cdot \left\{ \cos(k_z z a - k_z l \sin \theta) + \cos(k_z z a - k_z l \cos \theta) \right\} \quad (4.16)$$

In general for an arbitrary set of circular scatterers of radius a and distance l from the origin; the scattered field may be written:

$$R\{E_s\} = \sum_n \cos \{ k_z z a_n - k_z l_n \sin(\theta + \theta_n) \} \quad (4.17)$$

This gives the capability to simulate the scattering of any target given that it can be decomposed into N spherical scattering centers.

4.6 Experimental results

An experimental system for the implementation of swept frequency imaging was setup in the anechoic chamber at the Graduate Research Center in the Moore School. The frequency range for these experiments was from 6.3 to 16.0 GHz in 64 discrete steps. The targets were rotated 360 degrees in 128 steps. These holograms were then identical in form to the simulations previously done.

The system for error correction and range phase shift removal was that used for high signal to noise ratio signals. The reference target was a cylinder positioned so

that its front face was located on the axis of rotation as in fig.4.10. A plot of system response is shown in fig.4.11. This data represents the combined characteristics of the antennas, amplifier, cables and clutter. In addition it contains the linear phase shift that is the range phase factor. As an example for the two cylinder target shown in 4.12 the raw data, magnitude and phase is shown in fig.4.13. Figure 4.14 shows how this data has been corrected for range phase and system response. This data was generated using the Fortran program SPHER3.

The experimental properties of the two cylinder target were studied extensively. Both the scattering as a function of frequency for a specific orientation of the target and the scattering as a function of angular rotation at specific frequencies was obtained. In figs. 4.15 a,b,c are shown the corrected frequency response of the target for orientations of 45° , 90° and 135° degrees.

Another computer program ANTPAT was written to obtain the radiation pattern of an arbitrary target or antenna. In the two cylinder case the pattern was measured at 5.0, 10.0 and 15.0 GHz. Note that when the cylinders are collinear all that is seen is the front surface specular reflection of the one cylinder hence the pattern of a point scatterer in the vicinity of 0° degrees. These patterns are shown in figs.4.16 a,b,c. At high frequencies the lobe spacing is much closer than at low frequencies, consistent with the theoretical result for the pattern. To see this examine the

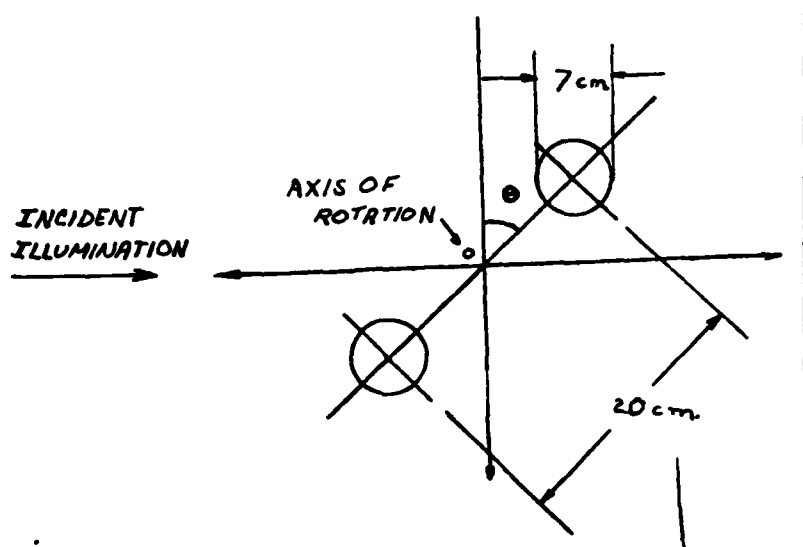


Fig. 4.12 Two cylinder target geometry.

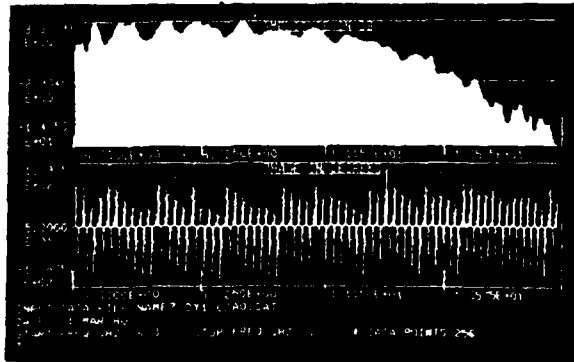


Fig. 4.13 Uncorrected scatter data for symmetrical two cylinder target ; $(\theta) = 0^\circ$, 6.3-16.0 GHz.

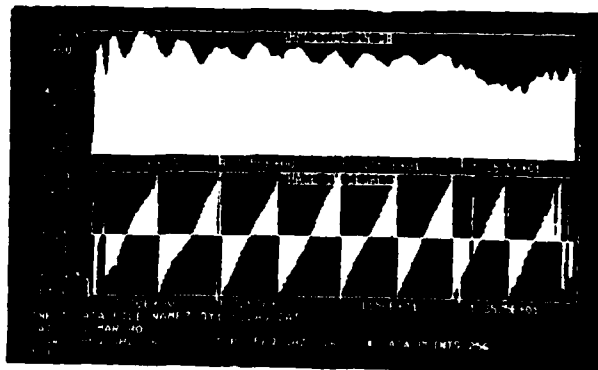
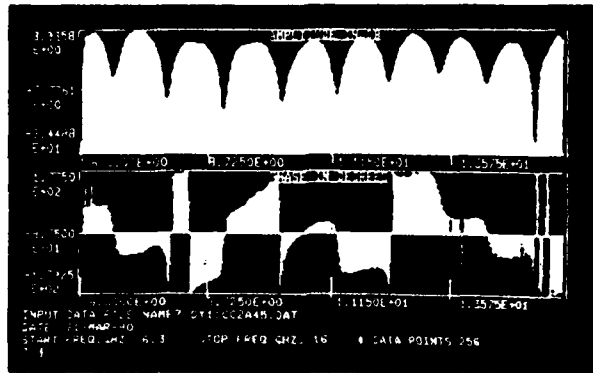
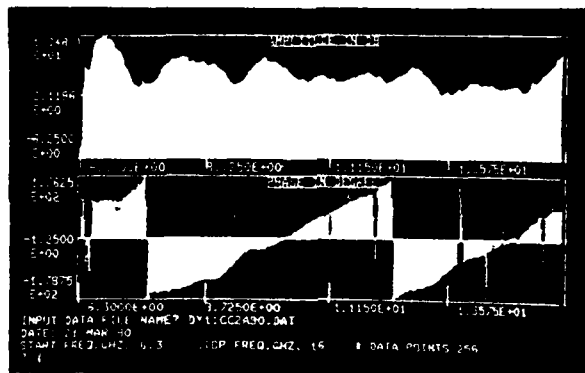


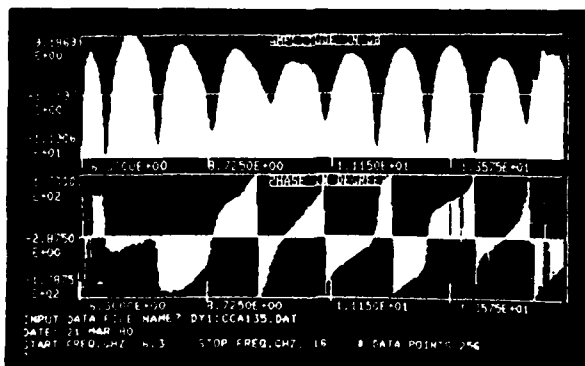
Fig. 4.14 Corrected two cylinder target data using system response of Fig. 4.11.



(a)

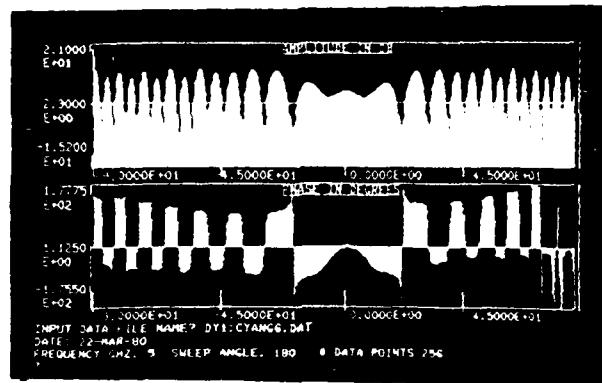


(b)

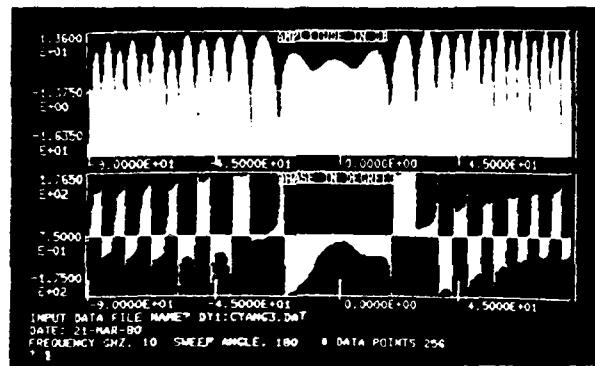


(c)

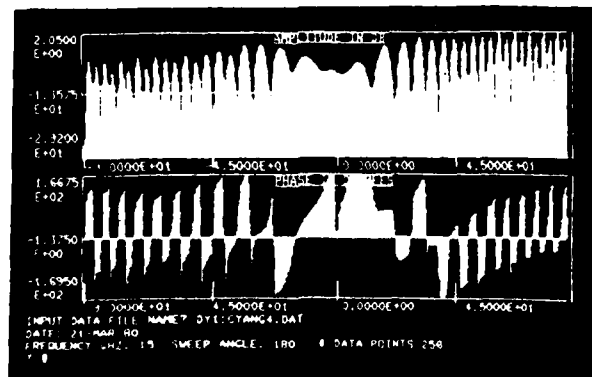
Fig. 4.15 a) Corrected two cylinder symmetrical target response; 6.3-16.0 GHz, $(\theta) = 45^\circ$. b) $(\theta) = 90^\circ$. c) $(\theta) = 135^\circ$.



(a)



(b)



(c)

Fig. 4.16 Scattering pattern of two cylinder target of Fig. 4.12 at different frequencies as a function target rotation angle. a) 5.0 GHz. b) 10.0 GHz. c) 15.0 GHz.

expression for the monostatic scattering of the symmetrical two cylinder target:

$$E_s = C \cdot \{ e^{i k_0 z a} \cdot \cos k_0 l \cdot \sin \theta \} \quad (4.18)$$

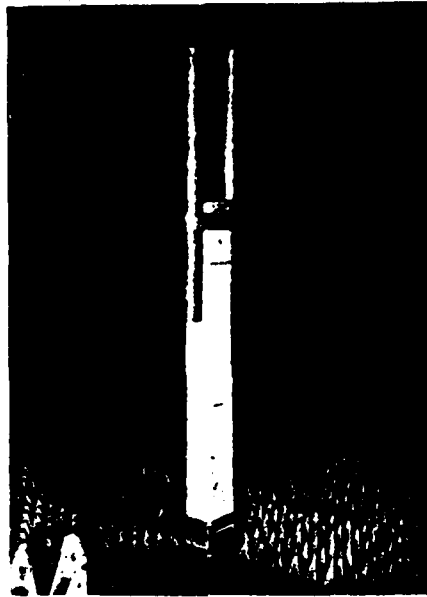
The expression for the scattering of the target at a given frequency as a function of angular rotation may be written:

$$E_s(k_0 = k) = C \cdot \cos k_0 l \sin \theta \quad C\text{-constant} \quad (4.19)$$

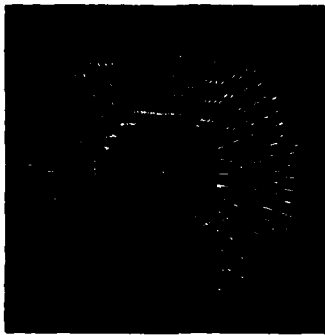
As for the swept frequency response; $l \sin(\theta)$ remains constant, and hence the swept frequency response is sinusoidal with period dependent on (k) and l .

The final test for the system was the generation of actual holograms. The first target measured was the two cylinder target shown in fig.4.17a. The cylinders are of aluminum, 80 cm. in length and 7 cm. in diameter. The real part of the corrected swept frequency data in the range 6.3 to 16.0 GHz was stored and displayed on the CRT. The targets were rotated 360 degrees in 128 steps yielding a total of 8192 points in the hologram (64 points/line * 128 lines). The center of the hologram is at 0 Hz with radial distance directly proportional to frequency. An example is shown in fig.4.17b and the reconstructions in figs.4.17c and d. These Fourier transforms were done optically. [17]

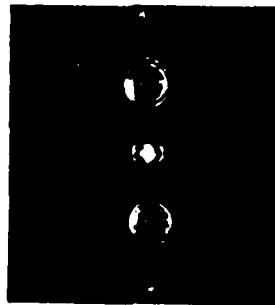
This procedure was followed for other targets not having the symmetry of the first object used. The target type was the same as the simulations done previously. The



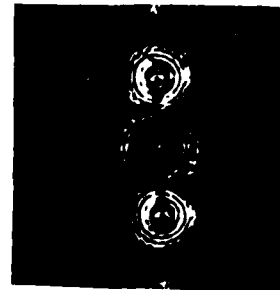
(a)



(b)



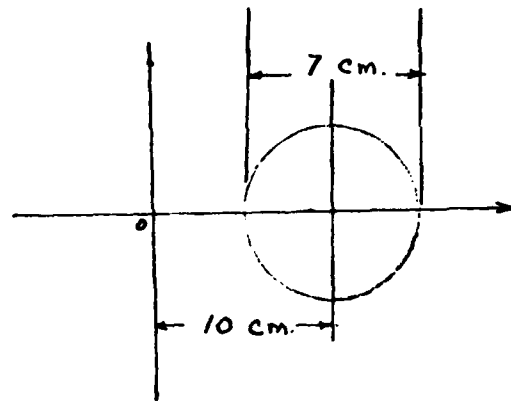
(c)



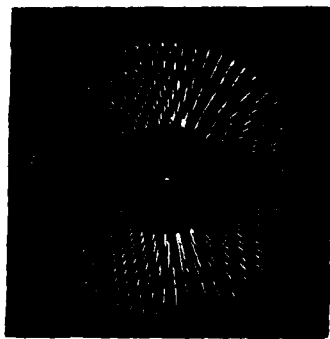
(d)

Fig. 4.17 a) Two cylinder target in anechoic chamber on rotating pedestal. b) Hologram of target measured between 5.3 and 16 GHz corrected for range and system response; 128 lines, 64 points/line. c) Optical Fourier transform of hologram. d) Optical Fourier transform without zero order term.

first of these was a single cylinder mounted off axis as shown in fig.4.18a. This cylinder was the same as the others used and the frequency range and angular sweep were identical to that of the two cylinder target. The hologram and reconstructions are shown in figs.4.18 b,c,d. The final target was the two off axis cylinder target pictured in fig.4.19a. The frequency diversity hologram and transforms are in figs.4.19 b,c,d.



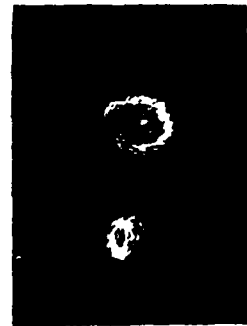
(a)



(b)

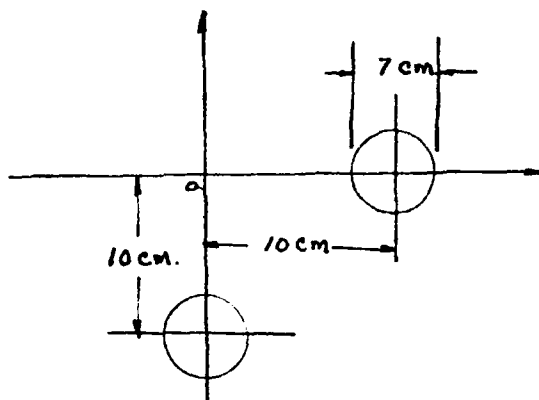


(c)

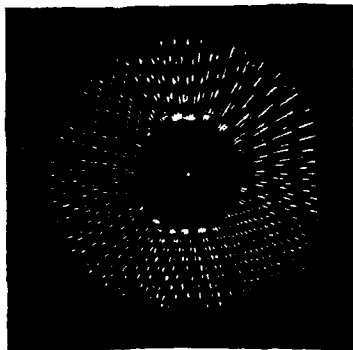
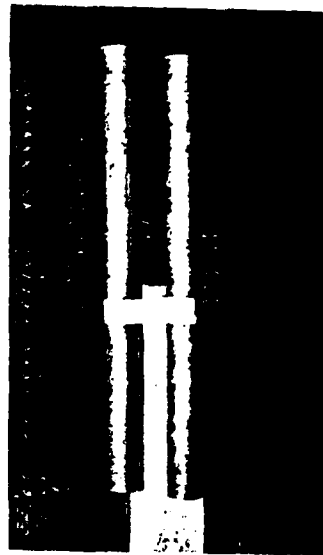


(d)

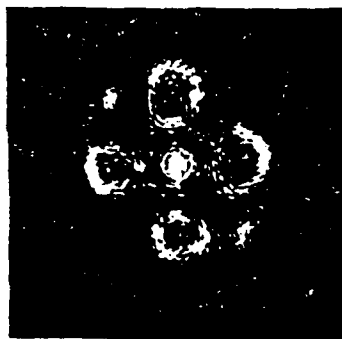
Fig. 4.18 a) Single cylinder off-axis target and position in anechoic chamber. b) Experimental hologram of target; 6.3-16 GHz; 128 lines, 64 points/line; corrected for range and system response. c) Optical Fourier transform of hologram. d) Optical Fourier transform without zero order term.



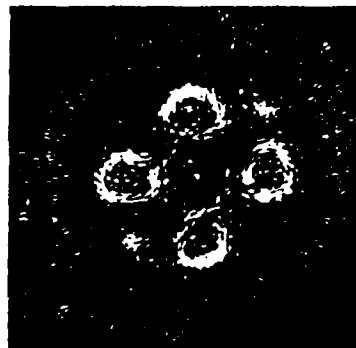
(a)



(b)



(c)



(d)

Fig. 4.19 a) Two cylinder off-axis target geometry and position in anechoic chamber. corrected for range and system response. c) Optical Fourier transform of hologram. d) Optical Fourier transform without zero order term.

V Conclusion

This thesis has described an automated swept frequency measuring system. This system may be used for radar cross section measurement, antenna pattern measurement and swept frequency holography. The system has a useful range of 5.0-17.0 GHz in which amplitude and phase of the scattered microwaves from targets in the anechoic chamber of the Graduate Research Center may be recorded and stored. A DEC MINC LSI-11/2 completely automates the data acquisition process. A complete error correction algorithm was implemented using the data storage and processing capabilities of the minicomputer.

The effect of range phase shift on swept frequency holograms was investigated and various techniques for its removal were investigated. It is believed that a TDR system for range phase removal is required for implementation of a practical radar system. This system must have extremely high resolution for coherent imaging. The relationship between TDR system bandwidth, receiver channel bandwidth and resolution was derived:

$$\text{Resolution} = \frac{\sigma_0 c}{\Delta f 2\pi} = \frac{\sqrt{2N_0} B c}{4\pi A \Delta f} \quad 322$$

where (Δf) is the imaging bandwidth, (R) the range uncertainty, B the receiver channel bandwidth and N_0 the noise power spectral density.

Simulations were performed for the scattering of various radar targets which include the conducting sphere,

V Conclusion

This thesis has described an automated swept frequency measuring system. This system may be used for radar cross section measurement, antenna pattern measurement and swept frequency holography. The system has a useful range of 5.0-17.0 GHz in which amplitude and phase of the scattered microwaves from targets in the anechoic chamber of the Graduate Research Center may be recorded and stored. A DEC MINC LSI-11/2 completely automates the data acquisition process. A complete error correction algorithm was implemented using the data storage and processing capabilities of the minicomputer.

The effect of range phase shift on swept frequency holograms was investigated and various techniques for its removal were investigated. It is believed that a TDR system for range phase removal is required for implementation of a practical radar system. This system must have extremely high resolution for coherent imaging. The relationship between TDR system bandwidth, receiver channel bandwidth and resolution was derived:

$$\text{Resolution} = \frac{\sigma_0 c}{\Delta f 2\pi} = \frac{\sqrt{2N_0 B} c}{4\pi R \Delta f} \quad 322$$

where (Δf) is the imaging bandwidth, (R) the range uncertainty, B the receiver channel bandwidth and N_0 the noise power spectral density.

Simulations were performed for the scattering of various radar targets which include the conducting sphere,

infinite cylinder and combinations of these. The holograms recorded from these analytical results reconstruct the targets extremely well and set a goal for practical system performance. An expression was derived for the scattering of N spherical/cylindrical cylinders in a plane passing through their centers:

$$R\{E_s\} = \sum_n \cos\{-kz a_n - k l_n \sin(\theta + \theta_n)\} \quad (4.17)$$

where l is the distance from the axis of rotation (θ_n) the angle relative to some reference for the target angular position and a the target radius.

Finally experimental swept frequency holograms were generated using a rotating pedestal under computer control to scan the target in one dimension. The experiments done indicate the feasibility of implementing a practical holographic radar system. The holograms obtained for various targets agree well with theory even though the error correction and range phase shift removal techniques used were robust in nature. It is believed that better images are possible given that the error correction techniques previously outlined are implemented.

Further work can be done in testing the TDR techniques for their suitability for an imaging system. The system may also be expanded to include scanning in the () direction to give true 3-D imaging capability. This may be implemented by adding a stepper motor controlled azimuthal scanner to the top of the rotating column.

infinite cylinder and combinations of these. The holograms recorded from these analytical results reconstruct the targets extremely well and set a goal for practical system performance. An expression was derived for the scattering of N spherical/cylindrical cylinders in a plane passing through their centers:

$$R\{E_s\} = \sum_n \cos\{kz a_n - k l_n \sin(\theta + \theta_n)\} \quad (4.17)$$

where l is the distance from the axis of rotation (θ_n) the angle relative to some reference for the target angular position and a the target radius.

Finally experimental swept frequency holograms were generated using a rotating pedestal under computer control to scan the target in one dimension. The experiments done indicate the feasibility of implementing a practical holographic radar system. The holograms obtained for various targets agree well with theory even though the error correction and range phase shift removal techniques used were robust in nature. It is believed that better images are possible given that the error correction techniques previously outlined are implemented.

Further work can be done in testing the TDR techniques for their suitability for an imaging system. The system may also be expanded to include scanning in the () direction to give true 3-D imaging capability. This may be implemented by adding a stepper motor controlled azimuthal scanner to the top of the rotating column.

BIBLIOGRAPHY

- [1] N.H. Farhat, 'Frequency Synthesized Imaging Apertures', Proceedings of the 1976 International Optical Computing Conference, IEEE Cat. No. 76 CH 1100-7c, 1976
- [2] N.H. Farhat, 'Principles of Broadband Coherent Imaging', J. Opt. Soc of Am., Vol.67, pp. 1015-1021, Aug. 1977.
- [3] N.H. Farhat, 'Microwave Holographic Imaging-Prospects for a Real time Camera', Proc. SPIE Technical Symposium, Vol. 180, Real-Time Signal Processing II, 1979.
- [4] N.H. Farhat and C.K. Chan, "Three Dimensional Imaging by Wave Vector Diversity", Presented at 8 Symposium on Acoustical Imaging; Key Biscayne, Fla. May 29-June 2 1978.
- [5] Robert J. Collier, C.B. Burckhardt and L.H. Lin, Optical Holography. New York: Academic Press, 1971.
- [6] J.S. Hollis, T.J. Lyon and L. Clayton, Microwave Antenna Measurements. Atlanta, Georgia: Scientific Atlanta, 1970
- [7] William B. Weir, LLOYD A. Robinson, Don Parker, "Broadband Automated Radar Cross Section Measurements", IEEE Transactions on Antennas and Propagation. Vol. 12 pp. 780-784, Nov. 1974.
- [8] Athanasios Papoulis, Signal Analysis. New York: McGraw-Hill, 1977.
- [9] John B. Thomas, An Introduction to Statistical Communication Theory. New York: John Wiley & Sons, 1969.
- [10] Advisory Group for Aerospace Research and Development: "Spread Spectrum Communications", U.S. Department of Commerce. AD-766-914, July 1973.
- [11] Henning F. Harmuth, Sequency Theory, Foundations and Applications. New York: Academic Press, 1977.
- [12] Athanasios Papoulis, Systems and Transforms with Applications in Optics. New York: McGraw-Hill, 1968.
- [13] CHI Keung Chan, "Analytical and Numerical Studies of

BIBLIOGRAPHY

- [1] N.H. Farhat, 'Frequency Synthesized Imaging Apertures', Proceedings of the 1976 International Optical Computing Conference, IEEE Cat. No. 76 CH 1100-7c, 1976
- [2] N.H. Farhat, 'Principles of Broadband Coherent Imaging', J. Opt. Soc of Am., Vol.67, pp. 1015-1021, Aug. 1977.
- [3] N.H. Farhat, 'Microwave Holographic Imaging-Prospects for a Real time Camera', Proc. SPIE Technical Symposium, Vol. 180, Real-Time Signal Processing II, 1979.
- [4] N.H. Farhat and C.K. Chan, "Three Dimensional Imaging by Wave Vector Diversity", Presented at 8 Symposium on Acoustical Imaging; Key Biscayne, Fla. May 29-June 2 1978.
- [5] Robert J. Collier, C.B. Burckhardt and L.H. Lin, Optical Holography. New York: Academic Press, 1971.
- [6] J.S. Hollis, T.J. Lyon and L. Clayton, Microwave Antenna Measurements. Atlanta, Georgia: Scientific Atlanta, 1970
- [7] William B. Weir, Lloyd A. Robinson, Don Parker, "Broadband Automated Radar Cross Section Measurements", IEEE Transactions on Antennas and Propagation. Vol. 12 pp. 780-784, Nov. 1974.
- [8] Athanasios Papoulis, Signal Analysis. New York: McGraw-Hill, 1977.
- [9] John B. Thomas, An Introduction to Statistical Communication Theory. New York: John Wiley & Sons, 1969.
- [10] Advisory Group for Aerospace Research and Development: "Spread Spectrum Communications", U.S. Department of Commerce. AD-766-914, July 1973.
- [11] Henning F. Harmuth, Sequency Theory, Foundations and Applications. New York: Academic Press, 1977.
- [12] Athanasios Papoulis, Systems and Transforms with Applications in Optics. New York: McGraw-Hill, 1968.
- [13] Chi Keung Chan, "Analytical and Numerical Studies of

Frequency Swept Imaging", Phd. Thesis. Department of Electrical Engineering; University of Pennsylvania, 1978.

- [14] W.H. Wells, "Acoustical Imaging with Linear Transducer Arrays", Acoustical Holography, Vol. 2, A.F. Melherall and L.Larmaore, (Eds.) New York: Plenum, 1970.
- [15] G.T. Ruck, Radar Cross Section Handbook. New York: Plenum, 1970.
- [16] G. Mie, "Beitrage zur Optik truber Median speziell Kolloidaler Metallosungen", Ann. Phys. 25:377 1908.
- [17] J.W. Goodman, Introduction to Fourier Optics. New York: McGraw-Hill, 1968.

APPENDIX I

```

620 PRINT B2, B1, B0
630 PRINT \ PRINT
640 INPUT A$ \ IF A$='N' THEN GO TO 1020
650 PRINT 'THIS IS A TEST OF THE PREDICTION CAPABILITIES OF THE INTERPOLAT
670 PRINT 'FUNCTIONS. INPUT THE VOLTAGE IN MILLIVOLTS. TO TERMINATE ENTER
680 PRINT 'NUMBER GREATER THAN 10000.'
690 SEND('M', A)
700 PRINT \ PRINT
710 INPUT A \ IF A>9999 THEN GO TO 820
720 A$='V'+STR$(A)+'E'+CHR$(13)+CHR$(10)
730 SEND(A$, A)
740 F=80-B1*A-82*A^2
750 F=MAA+C
760 PRINT \ PRINT 'QUADRATIC FIT: ', F
770 PRINT 'LINEAR FIT: ', TAB(14), F
800 GO TO 710
810 PRINT \ PRINT
820 PRINT \ PRINT 'THIS PART OF THE PROGRAM WILL GENERATE THE ENTERED FRE
830 PRINT 'THE RANGE IS FROM 2.005-17.970 GHZ. ENTER 0 TO TERMINATE.'
840 PRINT 'WIT RETURN FOR QUADRATIC FIT.'
850 INPUT 'INPUT FREQUENCY IN GHZ.'
850 PRINT
870 INPUT F \ IF F=0 THEN GO TO 1020
880 V=(F-C)/M
890 V1=(-B1+SOR(B1^2-4*B2*(80-F)))/(2*B2)
900 IF INT(10*V1)-10=INT(V1)>5 THEN V1=V1+1
910 IF INT(10*V1)-10=INT(V1)>5 THEN V1=V1+1
920 V1=INT(V1)
930 PRINT
940 V=INT(V)
950 A$='V'+STR$(V)+'E'+CHR$(13)+CHR$(10)
960 SEND(A$, A) \ PRINT 'FREQUENCY GENERATED FROM LINEAR FIT'
970 A$='V'+STR$(V1)+'E'+CHR$(13)+CHR$(10)
980 INPUT Z$
990 SEND(A$, A)
1000 PRINT 'FREQUENCY GENERATED FROM QUADRATIC FIT' \ PRINT
1010 GO TO 850
1020 CLOSE #1
1030 S=0 \ S1=0
1040 FOR I=1 TO 25
1050 S=S+(B11)-(M+A(I)+C))^2
1060 S1=S1*(B11)-(80-B1*A(I)+82*A(I)^2))^2
1070 NEXT I
1080 S=S/25 \ S1=S1/25
1090 PRINT \ PRINT 'STANDARD DEVIATION FOR THE LINEAR FIT: ', SOR(S), ' GHZ
1100 PRINT \ PRINT 'STANDARD DEVIATION FOR THE QUADRATIC FIT: ', SOR(S1), '
1110 END

```

```

10 DIM A(25), B(25)
20 PRINT 'THIS PROGRAM WILL CALIBRATE THE MICROWAVE SHEEPER' \ PRINT
30 PRINT 'ENTER NEW DATA (Y OR N)'
40 INPUT D$
50 IF D$='Y' THEN GO TO 120
60 PRINT 'WHAT FILE NAME?' \ INPUT Z$
70 OPEN Z$ FOR INPUT AS FILE #1
80 INPUT #1, A(1), B(1)
100 NEXT L
110 GO TO 240
120 SEND('M', A)
130 PRINT 'WHAT FILE NAME?' \ INPUT Z$
140 OPEN Z$ FOR OUTPUT AS FILE #1
150 FOR I=1 TO 25
160 A(I)=500+375*(I-1)
170 C$='V'+STR$(A(I))+'E'+CHR$(13)+CHR$(10)
180 PRINT 'COMMAND: ', C$
190 SEND(C$, A)
200 PRINT 'INPUT THE COUNTER FREQUENCY'
210 INPUT B(I)
220 PRINT #1, A(I) \ PRINT #1, B(I)
230 NEXT I
240 V1=0 \ V2=0 \ C=0 \ N1=0 \ N2=0
250 FOR I=1 TO 25
260 N1=N1+A(I) \ N2=N2+B(I) \ V1=V1+A(I)^2 \ V2=V2+B(I)^2 \ C=C+A(I)*B(I)
270 NEXT I
280 FOR J=1 TO 25 \ PRINT A(J), B(J) \ NEXT J
290 PRINT 'CONTINUE FOR GRAPH (RETURN)' \ INPUT Z$
300 DISPLAY+CLEAR
310 GRAPH('LINES, BRANDS', 25, A(1), B(1))
320 LABEL('UNDERLINE', '*** SHEEPER CALIBRATION ***', 1)
330 PRINT 'CONTINUE (RETURN)' \ INPUT Z$
340 DISPLAY+CLEAR
350 N1=N1/25 \ N2=N2/25 \ C=C/25 \ V1=V1/25 \ V2=V2/25
360 PRINT 'MUX', 'MUJ', 'VARY', 'VARY', 'COVAY'
370 PRINT N1, N2, V1, V2, C
380 M=(C-N1*N2)/(V1-N1^2)
390 PRINT \ PRINT
400 PRINT 'SLOPE='; M
410 PRINT
420 C=N2-M*N1
430 PRINT 'INTERCEPT='; C
440 N=25
450 Z1=0 \ Z2=0 \ Z3=0 \ Z4=0 \ V1=0 \ V2=0 \ V3=0
460 FOR I=1 TO 25
470 Z1=Z1+A(I) \ Z2=Z2+A(I)^2 \ Z3=Z3+A(I)^3 \ Z4=Z4+A(I)^4
480 V1=V1+B(I) \ V2=V2+B(I)*B(I) \ V3=V3+B(I)^2*B(I)
490 NEXT I
500 PRINT 'Z1', 'Z2', 'Z3', 'Z4'
510 PRINT Z1, Z2, Z3, Z4
520 PRINT \ PRINT
530 PRINT 'V1', 'V2', 'V3'
540 PRINT V1, V2, V3
550 PRINT \ PRINT
560 D=M*(Z2*Z4-Z3^2)-Z1*(Z1*Z4-Z2*Z3)+Z2*(Z1*Z3-Z2^2)
570 B0=V1*(Z2*Z4-Z3^2)-V2*(Z1*Z4-Z2*Z3)+V3*(Z1*Z3-Z2^2)
580 B1=M*(V2*Z4-V3*Z3)-V1*(Z1*Z4-Z2*Z3)+Z2*(Z1*V3-Z2*V2)
590 B2=M*(Z2*V3-V3*V2)-Z1*(Z1*V3-Z2*V2)+V1*(Z1*Z3-Z2^2)
600 B0=B0/D \ B1=B1/D \ B2=B2/D
610 PRINT 'B2', 'B1', 'B0'

```

0001 FORTTRAN IV V02 1-1 THU 09-AUG-79 00:36:32 PAGE 001

PROGRAM SYSRES
VERSION 1 2
THIS PROGRAM WILL GENERATE THE SYSTEM RESPONSE USING THE
SUBROUTINES FOR PAD, ISOLATION, TRANSFER FUNCTION AND
ANTENNA RESPONSE GENERATION AND REMOVAL. THE END RESULT IS A
FILE WITH NORMALIZED INTEGERS WITH THE SYSTEM RESPONSE FILES
AND GENERATED AT EACH STEP YIELDING A MODULAR PROCEDURE IN
THIS PROCESS. HENCE A COMPONENT OF THE SYSTEM COULD BE
CHANGED WITH OUT HAVING TO START FROM THE BEGINNING. FOR
EXAMPLE A DIFFERENT ANTENNA COULD BE SUBSTITUTED AND THE
SYSTEM RESPONSE COULD BE MEASURED WITHOUT HAVING TO START
FROM THE BEGINNING WITH THE MEASUREMENT OF THE PAD
CHARACTERISTICS.

COMMON/PADA/IAMPAD, IPHA, IFLAG, FSTART, FEND, STEP, NPOINT, NSAMP
COMMON/ISTA/IAMP2, IPH2, IFLAG2, NSAMP2
COMMON/TRANS/IAMP3, IPH3, IFLAG3, NSAMP3, IAMP4, IPH4
COMMON/ANTA/IAMP5, IPH5, IFLAG4, NSAMP4, IAMP6, IPH6

INTEGER IAMPAD(S12), IPHA(S12), IAMP2(S12), IPH2(S12), IAMP3(S12)
INTEGER IPH3(S12), IAMP4(S12), IPH4(S12), IPH5(S12), IAMP5(S12)
INTEGER IPH6(S12), IAMP6(S12)

BYTE A
TYPE 900
TYPE 801
ACCEPT *, IUNIT
TYPE 907
ACCEPT *, IFLAG
IF (IFLAG) 10, 10, 20
ACCEPT *, NSAMP
CALL PAD

ACCEPT 700, A
IF (A EQ 'N') GO TO 200
WRITE(IUNIT, 902)
WRITE(IUNIT, 903)
DO 100 K=1, NPOINT
AMPLIT=FLOAT(IAMPAD(K))* .05
PHASE=FLOAT(IPHA(K))* .25
FREQ=FLOAT(IAMP(K-1))*STEP
WRITE(IUNIT, 800)K, FREQ, AMPLIT, PHASE
CONTINUE
TYPE 909
ACCEPT *, IFLAG2
IF (IFLAG2) 210, 210, 220

FORTTRAN IV V02 1-1 THU 09-AUG-79 00:36:32 PAGE 002
0035 210 TYPE 908
0036 ACCEPT *, NSAMP2
0037 220 CALL IST
0038 TYPE 901

0039 ACCEPT 700, A
0040 IF (A EQ 'N') GO TO 300
0041 WRITE(IUNIT, 904)
0042 WRITE(IUNIT, 802)FSTART, FEND, STEP, NPOINT
0043 WRITE(IUNIT, 903)
0044 DO 250 K=1, NPOINT
0045 AMPLIT=FLOAT(IAMP2(K))* .05
0046 PHASE=FLOAT(IPH2(K))* .25
0047 FREQ=START+FLOAT(K-1)*STEP
0048 WRITE(IUNIT, 800)K, FREQ, AMPLIT, PHASE
0049 CONTINUE
0050 TYPE 910
0051 ACCEPT *, IFLAG3
0052 IF (IFLAG3) 310, 310, 320
0053 TYPE 908
0054 ACCEPT *, NSAMP3
0055 CALL TRANS
0056 TYPE 901
0057 ACCEPT 700, A
0058 IF (A EQ 'N') GO TO 400
0059 WRITE(IUNIT, 912)
0060 WRITE(IUNIT, 802)FSTART, FEND, STEP, NPOINT
0061 WRITE(IUNIT, 903)
0062 DO 330 K=1, NPOINT
0063 AMPLIT=FLOAT(IAMP3(K))* .05
0064 PHASE=FLOAT(IPH3(K))* .25
0065 FREQ=START+FLOAT(K-1)*STEP
0066 WRITE(IUNIT, 800)K, FREQ, AMPLIT, PHASE
0067 CONTINUE
0068 TYPE 905
0069 WRITE(IUNIT, 902)FSTART, FEND, STEP, NPOINT
0070 WRITE(IUNIT, 903)
0071 DO 350 K=1, NPOINT
0072 AMPLIT=FLOAT(IAMP4(K))* .05
0073 PHASE=FLOAT(IPH4(K))* .25
0074 FREQ=START+FLOAT(K-1)*STEP
0075 WRITE(IUNIT, 800)K, FREQ, AMPLIT, PHASE
0076 CONTINUE
0077 TYPE 911
0078 ACCEPT *, IFLAG4
0079 IF (IFLAG4) 410, 410, 420
0080 TYPE 908
0081 ACCEPT *, NSAMP4
0082 CALL ANTEN
0083 TYPE 901
0084 ACCEPT 700, A
0085 IF (A EQ 'N') GO TO 500
0086 WRITE(IUNIT, 913)
0087 WRITE(IUNIT, 802)FSTART, FEND, STEP, NPOINT
0088 WRITE(IUNIT, 903)
0089 V02 1-1 THU 09-AUG-79 00:36:32
0090 DO 430 K=1, NPOINT
0091 AMPLIT=FLOAT(IAMP5(K))* .05
0092 PHASE=FLOAT(IPH5(K))* .25
0093 FREQ=START+FLOAT(K-1)*STEP
0094 WRITE(IUNIT, 800)K, FREQ, AMPLIT, PHASE
0095 CONTINUE
0096 TYPE 906
0097 WRITE(IUNIT, 906)
0098 WRITE(IUNIT, 802)FSTART, FEND, STEP, NPOINT
0099 WRITE(IUNIT, 903)
0100 DO 450 K=1, NPOINT
0101 AMPLIT=FLOAT(IAMP6(K))* .05
0102

0039
0040
0041
0042
0043
0044
0045
0046
0047
0048
0049
0050
0051
0052
0053
0054
0055
0056
0057
0058
0059
0060
0061
0062
0063
0064
0065
0066
0067
0068
0069
0070
0071
0072
0073
0074
0075
0076
0077
0078
0079
0080
0081
0082
0083
0084
0085
0086
0087
0088
0089
0090
0091
0092
0093
0094
0095
0096
0097
0098
0099
0100
0101
0102

```

0103 PHASE=FLOAT(IPH6(K)),.25
0104 FREQ=FSTART+FLOAT(K-1)*STEP
0105 WRITE(UNIT,800)K,FREQ,AMPLIT,PHASE
0106 CONTINUE
0107 RETURN
C
C
C
0108 900 ***** FORMAT STATEMENTS *****
0109 901 FORMAT(/IX,'***** WELCOME TO THE SYSTEM RESPONSE
0110 902 IGENERATION SYSTEM *****')
0111 903 FORMAT(/IX,'LIST RESPONSE DATA (Y OR N)?')
0112 904 FORMAT(/IX,75(' ')/12X,'POINT #,5X,'FREQUENCY,7X,
0113 905 1-AMPLITUDE DB ,5X,'PHASE DEGREES/1X,75(' ')/1)
0114 906 FORMAT(/IX,'***** ISOLATION OF NETWORK ANALYZER *****
0115 907 1SYSTEM *****')
0116 908 FORMAT(/IX,'***** CORRECTED TRANSFER FUNCTION OF
0117 909 1SYSTEM *****')
0118 910 FORMAT(/IX,'***** CORRECTED ANTENNA SYSTEM CLUTTER
0119 911 1*****')
0120 912 FORMAT(/IX,'ENTER PAD RESPONSE FILE FLAG (0=>NEW 1=>OLD)')
0121 913 FORMAT(/IX,'ENTER NUMBER OF SAMPLES PER FREQUENCY POINT. ')
0122 914 FORMAT(/IX,'ENTER ISOLATION CHARACTERISTIC FILE FLAG
0123 915 1 (0=>NEW 1=>OLD)')
0124 916 FORMAT(/IX,'ENTER TRANSFER FUNCTION FILE FLAG (0=>NEW 1=>OLD)')
0125 917 FORMAT(/IX,'ENTER ANTENNA SYSTEM RESPONSE FILE FLAG (0=>NEW
0126 918 1-1=>OLD)')
0127 919 FORMAT(/IX,'***** UNCORRECTED TRANSFER FUNCTION OF
0128 920 1SYSTEM *****')
0129 921 FORMAT(/IX,'***** UNCORRECTED ANTENNA SYSTEM RESPONSE
0130 922 1*****')
0131 923 FORMAT(A1)
0132 924 FORMAT(10X,17.5X,1P015,7.3X,1P015,7)
0133 925 FORMAT(/IX,'ENTER LOGICAL UNIT FOR OUTPUT (7=>IT, 2=>LP.)')
0134 926 FORMAT(/IX,'STARTING FREQUENCY GHZ. ',1P015,7/15X,
0135 927 1-ENDING FREQUENCY IN GHZ. ',1P015,7/15X,'FREQUENCY STEP GHZ.
0136 928 2-1P015,7/15X,'NUMBER OF STEPS. ',17)
0137 929 STOP
0138 930 END

```

```

FORTRAN IV STORAGE MAP FOR PROGRAM UNIT SYSRES
LOCAL VARIABLES. PSECT @DATA, SIZE = 000070 ( 28. WORDS)
NAME TYPE OFFSET NAME TYPE OFFSET
A L=1 000032 AMPLIT R=4 000040 FREQ R=4 000050
IUNIT I=2 000034 K I=2 000036 PHASE R=4 000044
COMMON BLOCK /PADA /, SIZE = 004022 ( 1033. WORDS)
NAME TYPE OFFSET NAME TYPE OFFSET
IAPPAD I=2 000000 IPHA I=2 002000 IFLAG I=2 004000
FSTART R=4 004002 FEND R=4 004006 STEP R=4 004012

```

```

NSAMP I=2 004016 NSAMP I=2 004020
COMMON BLOCK /ISTA /, SIZE = 004004 ( 1026. WORDS)
NAME TYPE OFFSET NAME TYPE OFFSET NAME TYPE OFFSET
IAMP2 I=2 000000 IPH2 I=2 002000 IFLAG2 I=2 004000
NSAMP2 I=2 004002
COMMON BLOCK /TRANSA/, SIZE = 010004 ( 2050. WORDS)
NAME TYPE OFFSET NAME TYPE OFFSET NAME TYPE OFFSET
IAMP3 I=2 000000 IPH3 I=2 002000 IFLAG3 I=2 004000
NSAMP3 I=2 004002 IAMP4 I=2 004004 IPH4 I=2 006004
COMMON BLOCK /ANTA /, SIZE = 010004 ( 2050. WORDS)
NAME TYPE OFFSET NAME TYPE OFFSET NAME TYPE OFFSET
IAMP5 I=2 000000 IPH5 I=2 002000 IFLAG4 I=2 004000
NSAMP4 I=2 004002 IAMP6 I=2 004004 IPH6 I=2 006004

```

```

LOCAL AND COMMON ARRAYS:
NAME TYPE SECTION OFFSET -----SIZE----- DIMENSIONS
IAPPAD I=2 PADA 000000 002000 ( 512 ) (512)
IAMP2 I=2 ISTA 000000 002000 ( 512 ) (512)
IAMP3 I=2 TRANSA 000000 002000 ( 512 ) (512)
IAMP4 I=2 TRANSA 004004 002000 ( 512 ) (512)
IAMP5 I=2 ANTA 000000 002000 ( 512 ) (512)
IAMP6 I=2 ANTA 004004 002000 ( 512 ) (512)
IPHA I=2 PADA 002000 002000 ( 512 ) (512)
IPH2 I=2 ISTA 002000 002000 ( 512 ) (512)
IPH3 I=2 TRANSA 002000 002000 ( 512 ) (512)
IPH4 I=2 TRANSA 006004 002000 ( 512 ) (512)
IPH5 I=2 ANTA 002000 002000 ( 512 ) (512)
IPH6 I=2 ANTA 006004 002000 ( 512 ) (512)

```

```

SUBROUTINES, FUNCTIONS, STATEMENT AND PROCESSOR-DEFINED FUNCTIONIS
NAME TYPE NAME TYPE NAME TYPE NAME TYPE NAME TYPE
ANTEN R=4 FLOAT R=4 IST I=2 PAD R=4 TRANS R=4
FORTRAN IV V02 1-1 THU 09-AUG-79 00.46.59
0001 SUBROUTINE PAD
C
C VERSION 1 0

```

THIS ROUTINE WILL GENERATE THE CHARACTERISTIC OF THE PAD USED IN THE DETERMINATION OF THE SYSTEM RESPONSE IN THE FREQUENCY DIVERSITY IMAGING SYSTEM. IT INVOLVES PLACING THE FLEETLE ARM WITH THE REFLECTION TRANSMISSION UNIT WITH THE ARM CONNECTED FROM THE UNKNOWN TO THE TRANSMISSION RETURN PORTS WITH A 6 DB PAD IN SERIES WITH THE ARM. THE PRECISION AFC-7

TO N ADAPTER IN SERIES. THE R-T UNIT OBTAINS RF DIRECTLY FROM THE MICROWAVE SWEOPER. DATA IS OBTAINED IN THE FREQUENCY REGION SPECIFIED AND IN THE INCREMENT SPECIFIED. AT THIS POINT THE PAD WAVE CHARACTERISTIC IS DESIRED IS PLACED INTO THE CIRCUIT AND THE SAME FREQUENCY POINTS ARE MEASURED. THEN THE MAGNITUDE AND PHASE OF THE TWO MEASUREMENTS ARE SUBTRACTED AND THE RESULTANT VALUES ARE THE CHARACTERISTIC THE ONLY THE PAD

IN THE EVENT THAT THE FILE CONTAINING THE PAD RESPONSE ALREADY EXISTS THEN THE PROGRAM WILL FILL THE ARRAY PAD WITH THE PAD RESPONSE

IAMPAD: ARRAY WITH AMPLITUDE OF PAD RESPONSE IN INTEGER FORM
 IPHA: ARRAY WITH PHASE STORED IN INTEGER FORMAT RECEIVED
 IFLAG: 0=GENERATE NEW DATA
 I=READ OLD DATA
 FSTART: STARTING FREQUENCY FOR FREQ RESPONSE
 FEND: ENDING FREQUENCY FOR FREQ RESPONSE
 STEP: FREQUENCY STEP SIZE
 NPOINT: NUMBER OF POINTS IN THE SWEEP
 NSAMP: NUMBER OF SAMPLES TAKEN AT EACH FREQ POINT THEN AVERAGED

THE CONVERSION FROM INTEGER TO REAL AMPLITUDE IS

AMPLITUDE=(IAMPAD(I)-2048)*.05

PHASE=(IPHA-2048)*.25

COMMON DECLARATION

COMMON/PADA/IAMPAD,IPHA,IFLAG,FSTART,FEND,STEP,NPOINT,NSAMP
 INTEGER IAMPAD(512),IPHA(512)

IF (IFLAG) 100,100,500 'NEW OR OLD DATA?'
 TYPE 900 'PRINT FIRST INSTRUCTIONS'

CREATE SEQUENTIAL ACCESS ASCII FILE USING SIMPLE LIST NOT FORTRAN CARriage CONTROL THE FILE WILL EXPAND AS NECESSARY THE RECORD SIZE IS 6 CHARACTERS. THE UNIT NUMBER IS LOGICAL UNIT 12 THE NAME WILL BE ASSIGN USING THE ASSIGN SUBROUTINE IN THE LIBRARY. THIS IS A NEW FILE ON THE DISC AND

FORTRAN IV V02 1-1 THU 09-AUG-79 00 46:59 PAGE 002
 WILL BE SAVED WHEN THE FILE IS CLOSED

USE ASSIGN SUBROUTINE TO GET NAME FOR FILE

CALL ASSIGN(12,1,'NEW','NC',1,1)

SECTION TO OBTAIN CHARACTERISTICS OF ARM AND A DB PAD. NOT THE ACTUAL PAD TO BE MEASURED

TYPE 901 'NUMBER OF POINTS IN SYSTEM RESPONSE'
 ACCEPT #,NPOINT
 TYPE 902 'STARTING FREQUENCY IN GHZ'
 ACCEPT #,FSTART

0011 TYPE 903 'CALL SWEEP(1,FSTART,1,4)'
 0012 ACCEPT #,FEND
 0013 TYPE 904
 0014 PAUSE
 0015 STEP#=(FEND-FSTART)/FLOAT(NPOINT)
 0016 DO 200 K=1,NPOINT
 0017 FREQ=FSTART+FLOAT(K-1)*STEP
 0018 CALL SWEEP(1,FREQ,1,4)
 0019 CALL PHAMP2(1A,IP,NSAMP)
 0020 IAMPAD(I)=IA-2048
 0021 IPHA(I)=IP-2048
 0022 CONTINUE
 0023 CALL SWEEP(1,FSTART,1,4)
 0024 TYPE 905
 0025 PAUSE
 0026 DO 300 I=1,NPOINT
 0027 FREQ=FSTART+FLOAT(K-1)*STEP
 0028 CALL SWEEP(1,FREQ,1,4)
 0029 CALL PHAMP2(1A,IP,NSAMP)
 0030 IA=IA-2048
 0031 IP=IP-2048
 0032 IAMPAD(I)=IA-IAMPAD(K)
 0033 IPHA(I)=IP-IPHA(K)
 0034 IF (IPHA(I) GT 720) IPHA(K)=IPHA(K)-1440
 0035 IF (IPHA(I) LT -720) IPHA(K)=IPHA(K)+1440
 0036 CONTINUE
 0037 CALL SWEEP(10,FREQ,1,4) 'RESET IEEE BUS'
 0038 WRITE(12,*) FSTART
 0039 WRITE(12,*) FEND
 0040 WRITE(12,*) NPOINT
 0041 DO 400 K=1,NPOINT
 0042 WRITE(12,*) IAMPAD(K)
 0043 WRITE(12,*) IPHA(K)
 0044 CONTINUE
 0045 CALL CLOSE(12)
 0046 GO TO 700

FORTRAN IV V02 1-1 THU 09-AUG-79 00 46:59 PAGE 003
 THIS SECTION WILL READ AN OLD PAD RESPONSE

TYPE 906
 CALL ASSIGN(12,1,'OLD','NC',1)

READ(12,*) FSTART
 READ(12,*) FEND
 READ(12,*) NPOINT

STEP=(FEND-FSTART)/FLOAT(NPOINT)
 DO 500 I=1,NPOINT

READ(12,*) IAMPAD(K)
 READ(12,*) IPHA(K)
 CONTINUE

CALL CLOSE(12)
 RETURN

FORMAT(//,'#') 'ENTER THE PAD RESPONSE FILE NAME'
 FORMAT(//,'#') 'ENTER NUMBER OF POINTS IN PAD RESPONSE'
 FORMAT(//,'#') 'ENTER START FREQUENCY IN GIGHERTZ'
 0064 902 FORMAT(//,'#') 'ENTER ENDING FREQUENCY IN GIGHERTZ'
 0065 903 FORMAT(//,'#') 'CONNECT THE FLEXIBLE ARM PLUS 6 DB PAD IN'

1' SERIES', ' AND CONNECT FROM THE UNKNOWN TO THE RETURN',
 2' PART ON THE NETWORK ANALYZER')
 FORMAT('11', 'CONNECT THE DESIRED PAD IN SERIES WITH THE',
 1' & DB PAD')
 FORMAT('9', 'ENTER THE OLD PAD RESPONSE FILE NAME'
 END

FORTRAN IV STORAGE MAP FOR PROGRAM UNIT PAD
 LOCAL VARIABLES. PSECT DATA. SIZE = 000044 (18 WORDS)
 NAME TYPE OFFSET NAME TYPE OFFSET NAME TYPE OFFSET
 FREQ R=4 000024 IA I=2 000030 IP I=2 000032
 K I=2 000022

COMMON BLOCK /PADA /, SIZE = 004022 (1033 WORDS)

NAME TYPE OFFSET NAME TYPE OFFSET NAME TYPE OFFSET
 IAMPAD I=2 000000 IPHA I=2 002000 IFLAG I=2 004000
 FSTART R=4 004002 FEND R=4 004006 STEP R=4 004012
 NPOINT I=2 004016 NSAMP I=2 004020

LOCAL AND COMMON ARRAYS

NAME TYPE SECTION OFFSET -----SIZE----- DIMENSIONS
 IAMPAD I=2 PADA 000000 002000 (512) (512)
 IPHA I=2 PADA 002000 002000 (512) (512)

SUBROUTINES, FUNCTIONS, STATEMENT AND PROCESSOR-DEFINED FUNCTIONS.

NAME TYPE NAME TYPE NAME TYPE NAME TYPE NAME TYPE
 ASSIGN R=4 CLOSE R=4 FLOAT R=4 PHAMP2 R=4 SWEEP R=4

FORTRAN IV V02 I-1 THU 09-AUG-79 00 57.36 PAGE 001
 SUBROUTINE IST
 VERSION 1.3

THIS SUBROUTINE WILL MEASURE THE ISOLATION BETWEEN THE TWO
 CHANNELS OF THE NETWORK ANALYZER. THE FREQUENCY RANGE AND
 THE NUMBER OF STEPS WILL BE PASSED THROUGH COMMON BLOCK
 PADA. THE OUTPUT WILL BE THROUGH COMMON BLOCK ISTA. THE
 CARLES TO BE USED IN THE ACTUAL MEASUREMENT OF THE IFA-1103
 SYSTEM ARE TERMINATED IN THEIR CHARACTERISTIC IMPEDANCE AND
 THE MAGNITUDE AND PHASE OF THE LEAKAGE SIGNAL ARE MEASURED
 AT THE SAME DATA OF THE N/A FRONT PANEL AS THE SYSTEM
 MEASUREMENTS

IAMP2 ARRAY WITH AMPLITUDE OF LEAKED SIGNAL
 IPHA ARRAY WITH PHASE OF LEAKED SIGNAL
 IFLAG2 FLAG FOR OLD OR NEW DATA 0->GENERATE NEW DATA
 1-> READ OLD DATA
 NSAMP2 NUMBER OF SAMPLE POINTS TAKEN AT EACH FREQUENCY

COMMON/PADA/IAMPAD,IPHA,IFLAG,FSTART,FEND,STEP,NPOINT,NSAMP
 COMMON/ISTA/IAMP2,IPHA2,IFLAG2,NSAMP2

INTEGER IAMPAD(512),IPHA(512),IAMP2(512),IPHA2(512)

IF(IFLAG2) 100,100,500

TYPE 900

PAUSE

CALL SWEEP(1,FSTART,1,4)

DO 200 K=1,NPOINT

FREQ=FSTART+FLOAT(K-1)*STEP

CALL SWEEP(1,FREQ,1,4)

CALL PHAMP2(1A,IP,NSAMP2)

IAMP2(K)=IA-2048

IPHA2(K)=IP-2048

CONTINUE

CALL SWEEP(10,FSTART,1,4)

TYPE 901

CALL ASSION(12,-1,'NEW','NC',1,1)

WRITE(12,*) FSTART

WRITE(12,*) FEND

WRITE(12,*) NPOINT

DO 300 K=1,NPOINT

WRITE(12,*) IAMP2(K)

WRITE(12,*) IPHA2(K)

CONTINUE

CALL CLOSE(12)

GO TO 700

TYPE 902

TYPE 903

CALL ASSION(12,-1,'OLD','NC',1,1)

READ(12,*) FSTART

READ(12,*) FEND

FORTRAN IV V02 I-1 THU 09-AUG-79 00 57.36

READ(12,*) NPOINT

STEP=(FEND-FSTART)/FLOAT(NPOINT)

DO 600 K=1,NPOINT

READ(12,*) IAMP2(K)

READ(12,*) IPHA2(K)

CONTINUE

0001 SUBROUTINE TRANS
 VERSION 1 3
 THIS SUBROUTINE WILL FIND THE TRANSFER FUNCTION OF THE CABLES AND THE NETWORK ANALYZER SYSTEM THE ISOLATION AND PAD CHARACTERISTICS ARE PASSED THROUGH COMMON TO THIS ROUTINE AT THAT POINT THE CABLES FROM THE TRANSMITTING AND RECEIVING ANTENNAS ARE CONNECTED TOGETHER THROUGH A PAD WHOSE RESPONSE IS ALREADY KNOWN THE TRANSFER CHARACTERISTIC IS THEN CALCULATED AND STORED

IAMP3 ARRAY CONTAINING UNCORRECTED TRANSFER CHARACTERISTIC AMPLITUDE
 IPH3 ARRAY CONTAINING UNCORRECTED TRANSFER CHARACTERISTIC PHASE
 IAMP4 ARRAY CONTAINING CORRECTED AMP TRANS CHAR
 IPH4 ARRAY CONTAINING CORRECTED TRANS PHASE CHAR
 NSAMP3 NUMBER OF SAMPLES AT EACH FREQUENCY POINT
 IFLAG3 FLAG FOR OLD OR NEW DATA 0=>NEW 1=>OLD DATA

T/R=(C+*G)/R
 T: RECEIVER CHANNEL SIGNAL
 R: REFERENCE CHANNEL SIGNAL
 C: NETWORK ANALYZER REFERENCE-TO-RECEIVER CHANNEL ISOLATION
 P: PAD CHARACTERISTIC
 O: FREQUENCY CHARACTERISTICS(TRANSFER FUNCTION) OF THE RECEIVER CHANNEL AND ITS CABLE

CORRECT THIS FOR THE REFERENCE TO RECEIVER CHANNEL ISOLATION AND THE PAD FREQUENCY CHARACTERISTICS
 C/R => M1 MEASUREMENT OF REFERENCE TO RECEIVER ISOLATION OVER REFERENCE
 (C+P+G) => M2 MEASUREMENT OF TRANSFER FUNCTION PLUS PAD AND ISOLATION

G/R=(M2-H1)/P SUBTRACT PAD AND ISOLATION RESPONSES AND STONE
 COMMON/PADA/IAMPAD, IPHA, IFLAG, FSTART, FEND, STEP, NPOINT, NSAMP
 COMMON/ISTA/IAMP2, IPH2, IFLAG2, NSAMP2
 COMMON/TRANSA/IAMP3, IPH3, IFLAG3, NSAMP3, IAMP4, IPH4
 INTEGER IAMPAD(512), IPHA(512), IAMP2(512), IAMP3(512), IPH3(512), IAMP4(512), IPH4(512)

IF (IFLAG3) 100, 100, 500
 TYPE 900
 TYPE 901

FORTRAN IV V02 1-1 THU 09-AUG-79 01.03.11 PAGE 002
 CALL SWEEP(1, FSTART, 1, 4)
 DEG=3.1415926/180.

0039 CALL CLOSE(12)
 0040 RETURN
 C

0041 900 FORMAT(//1X, 'SUBROUTINE 1ST MEASURES AMPLITUDE AND PHASE FROM 1/1X, THE NETWORK ANALYZER IN ORDER TO OBTAIN ITS DIRECTIVITY. 2/1X, 'CONNECT THE ANTENNA SYSTEM CABLES TERMINATED IN THEIR CHARACTERISTIC IMPEDENCE. '//)
 0042 901 FORMAT(' ', 'ENTER THE NEW FILE NAME FOR THE ISOLATION DATA ')
 0043 902 FORMAT(//1X, 'SUBROUTINE 1ST READS MAGNITUDE AND PHASE DATA 1/1X, 'FROM THE SPECIFIED DATA FILE '//)
 0044 903 FORMAT(//1X, 'ENTER THE OLD FILE NAME FOR THE ISOLATION DATA. ')
 0045 END

FORTRAN IV STORAGE MAP FOR PROGRAM UNIT 1ST
 LOCAL VARIABLES, PSECT 9DATA, SIZE = 000036 (15 WORDS)

NAME	TYPE	OFFSET	NAME	TYPE	OFFSET	NAME	TYPE	OFFSET
FREQ	R*4	000020	IA	I*2	000024	IP	I*2	000028
K	I*2	000016						

COMMON BLOCK /PADA /, SIZE = 004022 (1033 WORDS)

NAME	TYPE	OFFSET	NAME	TYPE	OFFSET
IAMPAD	I*2	000000	IPHA	I*2	002000
FSTART	R*4	004002	FEND	R*4	004006
NPOINT	I*2	004016	NSAMP	I*2	004020

COMMON BLOCK /ISTA /, SIZE = 004004 (1026 WORDS)

NAME	TYPE	OFFSET	NAME	TYPE	OFFSET
IAMP2	I*2	000000	IPH2	I*2	002000
NSAMP2	I*2	004002	IFLAG2	I*2	004006

LOCAL AND COMMON ARRAYS.

NAME	TYPE	SECTION	OFFSET	NAME	TYPE	SECTION	OFFSET	NAME	TYPE	SECTION	OFFSET
IAMPAD	I*2	PADA	000000	IPHA	I*2	IPHA	002000	IFLAG	I*2	IFLAG	004000
FSTART	R*4	ISTA	000000	FEND	R*4	ISTA	002000	STEP	R*4	ISTA	004012
NPOINT	I*2	PADA	002000	NSAMP	I*2	PADA	004002				
		ISTA	000000			ISTA	002000				

SUBROUTINES, FUNCTIONS, STATEMENT AND PROCESSOR-DEFINED FUNCTIONIS.

NAME	TYPE	NAME	TYPE	NAME	TYPE	NAME	TYPE
ASSIGN	R*4	CLOSE	R*4	IFLAG	R*4	PHAMP2	R*4
				PHAMP2	R*4	SWEEP	R*4

0002 COMMON/PADA/IAMPAD, IPHA, IFLAG, FSTART, FEND, STEP, NPOINT, NSAMP
 0003 COMMON/ISTA/IAMP2, IPH2, IFLAG2, NSAMP2
 0004 COMMON/TRANSA/IAMP3, IPH3, IFLAG3, NSAMP3, IAMP4, IPH4
 0005 INTEGER IAMPAD(512), IPHA(512), IAMP2(512), IAMP3(512), IPH3(512), IAMP4(512), IPH4(512)

0006 IF (IFLAG3) 100, 100, 500
 0007 TYPE 900
 0008 TYPE 901

FORTRAN IV V02 1-1 THU 09-AUG-79 01.03.11 PAGE 002
 CALL SWEEP(1, FSTART, 1, 4)
 DEG=3.1415926/180.

```

0047 ATEMPX=ATRNK-AISTX
0048 ATEMPY=ATRNY-AISTY
C
C CONVERT BACK TO DEGREES AND DB
C
0049 ATEMP=SORT(ATEMPX**2+ATEMPY**2)
0050 TPHASE=ATAN2(ATEMPY,ATEMPX)
C
C DIVIDE BY PAD RESPONSE TO REMOVE IT FROM TRANSFER FUNCTION
C
0051 ADSTEM=10.*ALOG10(ATEMP)
0052 APAD=.05*FLOAT(IAMPAD(K))
0053 ATRANS=ADSTEM/APAD
0054 IAMP4(K)=IFIX(20.*TRANS)
0055 PTRANS=IPHASE-(.25*FLOAT(IPH4(K))*DEG)
0056 IF (PTRANS .GT. PI) PTRANS=PTRANS-2.*PI
0057 IF (PTRANS .LT. -PI) PTRANS=PTRANS+2.*PI
0058 IPH4(K)=IFIX(4.*(PTRANS/DEG))
0060 WRITE(12,*) IAMP4(K)
0061 WRITE(12,*) IPH4(K)
0062 CONTINUE
0063 CALL CLOSE(12)
0064 GO TO 700
0065 TYPE 900
0066 CALL ASSIGN(12,-1,'OLD','NC',1)
0067 READ(12,*) FSTART
0068 READ(12,*) FEND
0069 DO 600 K=1,NPOINT
0070 READ(12,*) NPOINT
0071 READ(12,*) IAMP3(K)
0072 READ(12,*) IPH3(K)
0073 CONTINUE
0074 CALL CLOSE(12)
0075 TYPE 904
0076 CALL ASSIGN(12,-1,'OLD','NC',1)
0077 READ(12,*) FSTART
0078 READ(12,*) FEND
0079 DO 650 K=1,NPOINT
0080 READ(12,*) NPOINT
0081 DO 650 K=1,NPOINT
0082 READ(12,*) IAMP4(K)
0083 READ(12,*) IPH4(K)
0084 CONTINUE
0085 CALL CLOSE(12)
0086 RETURN
0087 900
0088 904
FORTRAN IV
0088 901 THU 09-AUG-79 01 03 11 PAGE 004
FORMAT(/1X,'CORRECT THE INPUT AND OUTPUT CABLES THROUGH A',
1,'PRECISION PAD',)
0089 902 FORMAT(/1X,'ENTER THE NAME OF THE NEW FILE TO OBTAIN THE',
1,'$','UNCORRECTED TRANSFER FUNCTION DATA:',)
0090 903 FORMAT(/1X,'ENTER THE NAME OF THE NEW FILE TO OBTAIN THE',
1,'$','CORRECTED TRANSFER FUNCTION DATA:',)
0091 904 FORMAT(/1X,'ENTER THE NAME OF THE OLD FILE CONTAINING THE',
1,'$','CORRECTED TRANSFER FUNCTION DATA:',)
0092 905 FORMAT(/1X,'ENTER THE NAME OF THE OLD FILE CONTAINING THE',
1,'$','UNCORRECTED TRANSFER FUNCTION DATA:',)
0093 STOP
0094
FORTRAN IV STORAGE MAP FOR PROGRAM UNIT TRANS

```

```

0012 DO 200 K=1,NPOINT
0013 FREQ=FSTART+FLOAT(K-1)*STEP
0014 CALL SLEEP(1,FREQ,1,4)
0015 CALL PHIMP2(IA,IP,NSAMP3)
0016 IAMP3(K)=(IA-2048)
0017 IPH3(K)=(IP-2048)
C
C 0018 200 CONTINUE
0019 CALL SLEEP(10,FSTART,1,4)
0020 TYPE 902
0021 CALL ASSIGN(12,-1,'NEW','NC',1,1)
C
C STORE THE UNCORRECTED DATA
C
0022 WRITE(12,*) FSTART
0023 WRITE(12,*) FEND
0024 WRITE(12,*) NPOINT
0025 DO 300 K=1,NPOINT
0026 WRITE(12,*) IAMP3(K)
0027 WRITE(12,*) IPH3(K)
0028 CONTINUE
0029 CALL CLOSE(12)
C
C 300
C
C OPEN FILE WITH CORRECTED DATA
C
0030 TYPE 903
0031 CALL ASSIGN(12,-1,'NEW','NC',1,1)
0032 WRITE(12,*) FSTART
0033 WRITE(12,*) FEND
0034 WRITE(12,*) NPOINT
C
C 0035
0036 K=1,NPOINT
C
C GENERATE CORRECTED DATA AND STORE
C
0037 PI=3.1415924
0038 DO 400 K=1,NPOINT
0039 CONVERT TO DEGREES AND DB
0040 PIST= 25*FLOAT(IPH2(K))*DEG
ADBST= .05*FLOAT(IAMP2(K))
PTRAN= 25*FLOAT(IPH3(K))*DEG
ALBTRN=.05*FLOAT(IAMP3(K))
C
C CONVERT TO MATTS
C
0041 AIST=10.*(ADBST/10)
0042 ATRN=10.*(ALBTRN/10)
C
C FIND REAL AND IMAGINARY PARTS
C
FORTRAN IV
0043 V02 1-1 THU 09-AUG-79 01 03 11 PAGE 005
0043 ATRNX=ATRN*COS(PTRAN)
0044 ATRNY=ATRN*SIN(PTRAN)
0045 AISTX=AIST*COS(PIST)
0046 AISTY=AIST*SIN(PIST)
C
C SUBTRACT ISOLATION FROM TRANSFER+ISOLATION
C

```


WRITE(12,*) NPOINT
WRITE(12,*) IAMP5(K)
WRITE(12,*) IPH5(K)
CONTINUE
CALL CLOSE(12)

***** THIS SECTION WILL CALCULATE THE SYSTEM CLUTTER *****

PI=3.1415926
DEG=PI/180.
TYPE 902
CALL ASSIGN(12,-1,'NEW','NC',1.)
WRITE(12,*) FSTART
WRITE(12,*) FEND
DO 400 K=1,NPOINT
PIST= 25*FLOAT(IPH2(K))*DEG
PANT= 25*FLOAT(IPH5(K))*DEG
ADBIST= 05*FLOAT(IAMP2(K))
ADABANT= 05*FLOAT(IAMP5(K))
AIST=10.**(ADBIST/10.)
AANT=10.**(ADABANT/10.)
AISTX=AIST*COS(PIST)
AANTX=AANT*COS(PANT)
AANTY=AANT*SIN(PANT)

SUBTRACT ISOLATION FROM ANTENNA RESPONSE

ATEMPX=AANTX-AISTX
ATEMPY=AANTY-AISTY

CONVERT BACK TO PHASOR FORM

PTEMP=ATAN2(ATEMPY,ATEMPX)
ATEMP=SQRT(ATEMPX**2+ATEMPY**2)
AIBITEM=10.*ALOG10(ATEMP)
PRES=ADBTM-(.05*FLOAT(IAMP4(K)))
PRES=PTEMP-(.25*FLOAT(IPH4(K))*DEG)
IF (PRES.LT.-PI)PRES=PRES+2.*PI
IF (PRES.GT.PI)PRES=PRES-2.*PI
IPH6(K)=IFIX(4.*PRES/DEG)
IAMP6(K)=IFIX(20.*PRES)
WRITE(12,*)IAMP6(K)
WRITE(12,*)IPH6(K)
CONTINUE

FORTRAN IV V02 I-1 THU 09-AUG-79 01:12:37
SUBROUTINE ANTEN
VERSION 1 4

***** THIS SUBROUTINE WILL MEASURE THE ANTENNA AND ROOM CHARACTERISTICS EXPLICITLY. FIRST A MEASUREMENT INCLUDING THE SYSTEM CHARACTERISTICS IS TAKEN AND STORED AT EACH FREQUENCY. IN ADDITION THE ROOM CLUTTER AND ANTENNA CHARACTERISTICS ARE CALCULATED WHEN THE CABLE RESPONSE AND ISOLATION CHARACTERISTIC OF THE NETWORK ANALYZER ARE REMOVED. *****

G/R: THE TRANSFER CHARACTERISTIC OF THE N/A FROM SUBROUTINE TRANS

T/R=(C+O*X)/R

WHERE X:

O RECEIVED SIGNAL FORM CROSS COUPLING AND CLUTTER
R TRANSFER FUNCTION OF N/A + CABLE
T/R REFERENCE CHANNEL SIGNAL
M1 RECEIVED MEASUREMENT => M3
ISOLATION MEASUREMENT

X/R=(M3-M1)/(O/R)

ALL MEASUREMENTS ARE RELATIVE TO THE REFERENCE CHANNEL SIGNAL IE. TRANSMITTED SIGNAL

COMMON/PAD4/IAMP4D, IPH4, IFLAG, FSTART, FEND, STEP, NPOINT, NSAMP
COMMON/ISTA/IAMP2, IPH2, IFLAG2, NSAMP2
COMMON/TRINSA/IAMP3, IPH3, IFLAG3, NSAMP3, IAMP4, IPH4
COMMON/ANTA/IAMP5, IPH5, IFLAG4, NSAMP4, IAMP6, IPH6

INTEGER IAMP4D(512), IPH4(512), IAMP2(512), IPH2(512), IAMP5(512)
INTEGER IPH3(512), IAMP4(512), IPH4(512), IAMP5(512), IPH5(512)
INTEGER IAMP6(512), IPH6(512)

IF (IFLAG4) 100,100,500
TYPE 900
CALL SWEEP(1,FSTART,1,4)
PAUSE

DO 200 K=1,NPOINT
FREQ=FSTART+FLCAT(K-1)*STEP
CALL SWEEP(1,FREQ,1,4)
CALL PHAMP2(IA,IP,NSAMP4)
IAMP5(K)=IA-2048
IPH5(K)=IP-2048
CONTINUE

CALL SWEEP(10,FSTART,1,4)
TYPE 901

FORTRAN IV V02 I-1 THU 09-AUG-79 01:12:37
CALL ASSIGN(12,-1,'NEW','NC',1.)
WRITE(12,*) FSTART
READ(12,*) FEND
DO 600 K=1,NPOINT

0001

0002

0003

0004

0005

0006

0007

0008

0009

0010

0011

0012

0013

0014

0015

0016

0017

0018

0019

0020

0021

0022

0023

0024

0025

0026

0027

0028

0029

0030

0031

0032

0033

0034

0035

0036

0037

0038

0039

0040

0041

0042

0043

0044

0045

0046

0047

0048

0049

0050

0051

0052

0053

0054

0055

0056

0058

0060

0061

0062

0063

0064

0065

0066

0067

0068

0069

0070

0071

0072

FORTRAN IV

V02 I-1 THU 09-AUG-79 01:12:37

CALL CLOSE (12)

GO TO 700

TYPE 904

CALL ASSIGN(12,-1,'OLD','NC',1.)

READ(12,*) FSTART

READ(12,*) FEND

READ(12,*) NPOINT

DO 600 K=1,NPOINT

```

0073 READ(12,*) IAMP5(K)
0074 READ(12,*) IPH5(K)
0075 CONTINUE
0076 CALL CLOSE(12)
0077 TYPE 903
0078 CALL ASSIGN(12,*,1,'OLD','NC',1)
0079 READ(12,*) FSTART
0080 READ(12,*) FEND
0081 DO 50 K=1,NPOINT
0082 READ(12,*) IAMP6(K)
0083 READ(12,*) IPH6(K)
0084 CONTINUE
0085 CALL CLOSE(12)
0086 RETURN
0087 C
0088 C
0089 C
0090 C
0091 C
0092 C
0093 C
0094 C

```

```

FORMAT(/IX'SUBROUTINE ANTEN DETERMINES THE ANTENNA
1.'CHARACTERISTICS AND'/IX.'ANTENNA CROSS COUPLING.
2.'/IX.'CONFIGURE THE SYSTEM IN ITS FINAL FORM')
1 NAME ' '
0090 FORMAT(/' ', 'ENTER THE ANTENNA CLUTTER DATA FILE NAME. ')
0091 FORMAT(/' ', 'ENTER THE ANTENNA CLUTTER OLD FILE
1 NAME ' ')
0092 FORMAT(/' ', 'ENTER THE ANTENNA SYSTEM RESPONSE OLD FILE
1 NAME ' ')
0093 STOP
0094 END

```

```

FORTRAN IV STORAGE MAP FOR PROGRAM UNIT ANTEN
LOCAL VARIABLES. PSECT $DATA, SIZE = 000216 ( 71. WORDS)
NAME TYPE OFFSET NAME TYPE OFFSET NAME TYPE OFFSET
AANT R*4 000110 AANTX R*4 000124 AANTY R*4 000130
ADANT R*4 000100 ADBIST R*4 000074 ADBTEM R*4 000154
AIST R*4 000104 AISTX R*4 000114 AISTY R*4 000120
ARES R*4 000160 ATEMP R*4 000150 ATEMPX R*4 000154
ATEMPY R*4 000140 DEG R*4 000060 FREQ R*4 000044
IA I*2 000050 IP I*2 000052 K I*2 000042
PANT R*4 000070 PI R*4 000054 PIST R*4 000064
PRES R*4 000164 PTEMP R*4 000144
COMMON BLOCK /PADA /, SIZE = 004022 ( 1033. WORDS)
NAME TYPE OFFSET NAME TYPE OFFSET NAME TYPE OFFSET
IAMPAD I*2 PADA 000000 002000 ( 512 ) ( 512 )
IAMP2 I*2 ISTA 000000 002000 ( 512 ) ( 512 )
IAMP3 I*2 TRANSA 000000 002000 ( 512 ) ( 512 )
IAMP4 I*2 TRANSA 004004 002000 ( 512 ) ( 512 )
IAMP5 I*2 ANTA 000000 002000 ( 512 ) ( 512 )
IAMP6 I*2 ANTA 004004 002000 ( 512 ) ( 512 )
IPHA I*2 PADA 002000 002000 ( 512 ) ( 512 )
IPH2 I*2 ISTA 002000 002000 ( 512 ) ( 512 )
IPH3 I*2 TRANSA 002000 002000 ( 512 ) ( 512 )
IPHA I*2 TRANSA 004004 002000 ( 512 ) ( 512 )
IPH5 I*2 ANTA 002000 002000 ( 512 ) ( 512 )
IPH6 I*2 ANTA 004004 002000 ( 512 ) ( 512 )

```

```

FORTRAN IV STORAGE MAP FOR PROGRAM UNIT ANTEN
SUBROUTINES, FUNCTIONS, STATEMENT AND PROCESSED-DEFINED FUNCTIONIS
NAME TYPE NAME TYPE NAME TYPE NAME TYPE NAME TYPE
ALOO10 R*4 ASSION R*4 ATAN2 R*4 CLOSE R*4 COS R*4
FLOAT R*4 IFIX I*2 PHAMP2 R*4 SIN R*4 SORT R*4
SHEEP R*4

```

```

FORTRAN IV STORAGE MAP FOR PROGRAM UNIT ANTEN
LOCAL VARIABLES. PSECT $DATA, SIZE = 000216 ( 71. WORDS)
NAME TYPE OFFSET NAME TYPE OFFSET NAME TYPE OFFSET
AANT R*4 000110 AANTX R*4 000124 AANTY R*4 000130
ADANT R*4 000100 ADBIST R*4 000074 ADBTEM R*4 000154
AIST R*4 000104 AISTX R*4 000114 AISTY R*4 000120
ARES R*4 000160 ATEMP R*4 000150 ATEMPX R*4 000154
ATEMPY R*4 000140 DEG R*4 000060 FREQ R*4 000044
IA I*2 000050 IP I*2 000052 K I*2 000042
PANT R*4 000070 PI R*4 000054 PIST R*4 000064
PRES R*4 000164 PTEMP R*4 000144
COMMON BLOCK /PADA /, SIZE = 004022 ( 1033. WORDS)
NAME TYPE OFFSET NAME TYPE OFFSET NAME TYPE OFFSET
IAMPAD I*2 PADA 000000 002000 ( 512 ) ( 512 )
IAMP2 I*2 ISTA 000000 002000 ( 512 ) ( 512 )
IAMP3 I*2 TRANSA 000000 002000 ( 512 ) ( 512 )
IAMP4 I*2 TRANSA 004004 002000 ( 512 ) ( 512 )
IAMP5 I*2 ANTA 000000 002000 ( 512 ) ( 512 )
IAMP6 I*2 ANTA 004004 002000 ( 512 ) ( 512 )
IPHA I*2 PADA 002000 002000 ( 512 ) ( 512 )
IPH2 I*2 ISTA 002000 002000 ( 512 ) ( 512 )
IPH3 I*2 TRANSA 002000 002000 ( 512 ) ( 512 )
IPHA I*2 TRANSA 004004 002000 ( 512 ) ( 512 )
IPH5 I*2 ANTA 002000 002000 ( 512 ) ( 512 )
IPH6 I*2 ANTA 004004 002000 ( 512 ) ( 512 )

```

FORTRAN IV V02 1-1 PAGE 001

0001 PROGRAM SPHERE

0002 VERSION 1.2

0003 THIS PROGRAM WILL TAKE EXPERIMENTAL DATA FOR THE SPHERE AND CORRECT IT FOR THE SYSTEM RESPONSE. IT WILL PRINT BOTH THE CORRECTED AND UNCORRECTED DATA AND FINALLY DISPLAY IT ON THE HIGH RESOLUTION CRT.

0004 ALSO IT DESIRED IT WILL GENERATE IF DESIRED ANALYTICAL DATA FOR THE SPHERE AND STORE IT IN A FILE. IT WILL ALSO PRINT THIS DATA IF DESIRED TO A FILE AND ALSO DISPLAY IT ON THE HIGH RESOLUTION CRT MONITOR.

0005 COMMON/RANGE/1/DIST,IRFLAG,IUNIT

0006 COMMON/OBJ/OBJA,OBJP,NSAMPZ

0007 COMMON/SYST/TRANA,TRAMP,CLUTA,CLUTP,FSTART,FEND,NPOINT

0008 INTEGER OBJA(512),OBJP(512),TRANA(512)

0009 INTEGER TRAMP(512),CLUTA(512),CLUTP(512),NPOINT,NSAMPZ

0010 BYTE A

0011 TYPE 900

0012 TYPE 912

0013 ACCEPT *,IUNIT

0014 THIS SECTION WILL GENERATE CORRECTED SPHERE DATA FROM EXPERIMENTAL DATA

0015 TYPE 902

0016 CALL SYSIMP

0017 STEP=(FEND-FSTART)/FLOAT(NPOINT)

0018 CALL SPHEAT

0019 TYPE 903

0020 ACCEPT 1000,A

0021 IF (A EQ 'N') GO TO 220

0022 WRITE(IUNIT,904)

0023 WRITE(IUNIT,905)

0024 WRITE(IUNIT,906)

0025 DO 210 I=1,NPOINT

0026 AMPLIT=FLOAT(OBJA(K))* .05

0027 PHASE=FLOAT(OBJP(K))* .25

0028 FREQ=1/STEP

0029 WRITE(IUNIT,907)K,FREQ,AMPLIT,PHASE

0030 CONTINUE

0031 CALL CORREC

0032 HERE LIST THE CORRECTED SPHERE DATA

0033 TYPE 915

0034 ACCEPT 1000,A

0035 FORTRAN IV V02 1-1 PAGE 002

0036 IF (A EQ 'N') GO TO 280

0037 WRITE(IUNIT,909)

0038 WRITE(IUNIT,905)FSTART,FEND,STEP,NPOINT

0039 WRITE(IUNIT,906)

0040 INDI=K

0041 AMPLIT=FLOAT(OBJA(K))* .05

0042 PHASE=FLOAT(OBJP(K))* .25

0043 FREQ=1/STEP

0044 WRITE(IUNIT,907)K,FREQ,AMPLIT,PHASE

0045 CONTINUE

0046 CONTINUE

0047 THIS SECTION WILL STORE THE CORRECTED DATA FOR SYSTEM RESPONSE

0048 TYPE 902

0049 ACCEPT 1000,A

0050 IF (A EQ 'N') GO TO 400

0051 TYPE 801

0052 CALL ASSIGN(20,-1,'NEW','NC',)

0053 WRITE(20,*)FSTART

0054 WRITE(20,*)FEND

0055 WRITE(20,*)NPOINT

0056 DO 310 K=1,NPOINT

0057 WRITE(20,*)OBJA(K)

0058 WRITE(20,*)OBJP(K)

0059 CONTINUE

0060 CALL CLOSE(20)

0061 THIS SECTION WILL CORRECT FOR RANGE

0062 TYPE 914

0063 ACCEPT *,IRFLAG

0064 CALL RANGE

0065 TYPE 913,DIST

0066 CALL RANCOR

0067 TYPE 916

0068 ACCEPT 1000,A

0069 IF (A EQ 'N') GO TO 470

0070 WRITE(IUNIT,913)DIST

0071 WRITE(IUNIT,911)

0072 WRITE(IUNIT,905)FSTART,FEND,STEP,NPOINT

0073 WRITE(IUNIT,906)

0074 DO 410 K=1,NPOINT

0075 INDI=K

0076 AMPLIT=FLOAT(OBJA(K))* .05

0077 PHASE=FLOAT(OBJP(K))* .25

0078 FREQ=1/STEP

0079 WRITE(IUNIT,907)K,FREQ,AMPLIT,PHASE

0080 CONTINUE

0081 THIS SECTION WILL STORE THE RANGE CORRECTED DATA

0082 FORTRAN IV V02 1-1

0083 TYPE 901

0084 ACCEPT 1000,A

0085 IF (A EQ 'N') GO TO 500

0086 TYPE 800

0087 CALL ASSIGN(20,-1,'NEW','NC',)

0088 WRITE(20,*)FSTART

THIS SUBROUTINE WILL READ IN THE SYSTEM RESPONSE FILES
 AND PLACE THEM IN A COMMON BLOCK TO BE PASSED TO OTHER
 ROUTINES.

COMMON/SYSTA/TRANA, TRAMP, CLUTA, CLUTP, FSTART, FEND, NPOINT
 INTEGER TRANA(S12), TRAMP(S12), CLUTA(S12), CLUTP(S12), NPOINT
 TYPE 900
 TYPE 901
 CALL ASSIGN(12,-1,'OLD','NC',1)
 READ(12,*) FSTART
 READ(12,*) FEND
 READ(12,*) NPOINT
 DO 100 K=1,NPOINT
 READ(12,*) TRANA(K)
 READ(12,*) TRAMP(K)
 CONTINUE
 CALL CLOSE(12)
 TYPE 902
 CALL ASSIGN(12,-1,'OLD','NC',1)
 READ(12,*) FSTART
 READ(12,*) FEND
 READ(12,*) NPOINT
 DO 200 K=1,NPOINT
 READ(12,*) CLUTA(K)
 READ(12,*) CLUTP(K)
 CONTINUE
 CALL CLOSE(12)
 RETURN
 FORMAT(//IX,'**** SUBROUTINE SYSINP READS THE SYSTEM RESPONSE
 1 FILES ****')
 0027 901 FORMAT(//9,'ENTER THE TRANSFER FUNCTION FILE NAME. ')
 0028 902 FORMAT(//9,'ENTER THE ANTENNA SYSTEM FUNCTION FILE NAME. ')
 0029 END

FORTRAN IV STORAGE MAP FOR PROGRAM UNIT SYSINP
 LOCAL VARIABLES, PSECT \$DATA, SIZE = 000020 (8 WORDS)
 NAME TYPE OFFSET NAME TYPE OFFSET NAME TYPE OFFSET
 K I*2 000012

COMMON BLOCK /SYSTA /, SIZE = 010012 (2053 WORDS)
 NAME TYPE OFFSET NAME TYPE OFFSET NAME TYPE OFFSET
 TRANA I*2 000000 TRAMP I*2 002000 CLUTA I*2 004000
 CLUTP I*2 006000 FSTART R*4 010000 FEND R*4 010004
 NPOINT I*2 010010

LOCAL AND COMMON ARRAYS:
 NAME TYPE SECTION OFFSET ----SIZE----- DIMENSIONS

WRITE(20,*)NPOINT
 DO 460 K=1,NPOINT
 WRITE(20,*)OBJA(K)
 WRITE(20,*)OBJP(K)
 CONTINUE
 CALL CLOSE(20)

THIS SECTION WILL DISPLAY THE DATA
 CONTINUE
 FORMAT STATEMENTS
 FORMAT(//,'ENTER THE FILE NAME FOR THE RANGE
 1 CORRECTED DATA. ')
 0094 901 FORMAT(//,'ENTER THE FILE NAME FOR THE CORRECTED DATA. ')
 0095 902 FORMAT(//,'DO YOU WANT TO STORE THE CORRECTED DATA (Y OR N)
 1 ')
 0096 900 FORMAT(//,'**** PROGRAM SPHERE ****')
 0097 901 FORMAT(//,'DO YOU WANT TO STORE THE RANGE CORRECTED
 1 DATA (Y OR N) ? ')
 0098 902 FORMAT(//,' THIS SECTION WILL GENERATE CORRECTED SPHERE DATA
 1 FROM ** EXPERIMENTAL DATA ')
 0099 903 FORMAT(//,'PRINT THE UNCORRECTED DATA (Y OR N): ')
 0100 904 FORMAT(//IX,'***** UNCORRECTED SPHERE DATA *****')
 0101 905 1 ENDING FREQUENCY IN GHZ ',IP015 7/15X,'FREQUENCY STEP OHZ.
 2,IP015 7/15X,'NUMBER OF STEPS ',I7)
 0102 906 1 AMPLITUDE DB ',5X,'PHASE REGRES',1X,75(' ')/)
 0103 907 FORMAT(10X,17.5X,IP015 7.3X,IP015 7.3X,IP015 7)
 0104 908 FORMAT(//IX,'***** CORRECTED EXPERIMENTAL SPHERE
 1 DATA *****')
 0109 911 FORMAT(//IX,'***** EXPERIMENTAL SPHERE DATA CORRECTED
 1 FOR RANGE *****')
 0106 912 FORMAT(//9,'ENTER LOGICAL UNIT NUMBER FOR OUTPUT (7=>
 1 TERMINAL) ')
 0107 913 FORMAT(//IX,' CALCULATED RANGE TO THE TARGET= ',IP015 7,
 1 ' METERS ')
 0109 914 FORMAT(//IX,' ENTER THE RANGE CALCULATION FLAG',I2,DIRECT
 1 MEASUREMENT',I2,>FOURIER ANALYSIS',I2,'INPUT FLAG. ')
 0109 915 FORMAT(//IX,'PRINT SPHERE DATA CORRECTED FOR SYSTEM RESPONSE
 1 (Y OR N): ')
 0110 916 FORMAT(//IX,'PRINT SPHERE DATA CORRECTED FOR RANGE (Y OR N): ')
 0111 1000 FORMAT(A1)
 0112 STOP '***** END OF PROGRAM *****'

FORTRAN IV STORAGE MAP FOR PROGRAM UNIT SPHERE
 LOCAL VARIABLES, PSECT \$DATA, SIZE = 000066 (27 WORDS)
 NAME TYPE OFFSET NAME TYPE OFFSET NAME TYPE OFFSET
 A L*1 000026 AMPLIT R*4 000036 FREQ R*4 000046
 I*01 I*2 000052 K I*2 000034 PHASE R*4 000042
 STEP R*4 000030

FORTRAN IV V02 1-1 PAGE 004
 0113 END

FORTRAN IV STORAGE MAP FOR PROGRAM UNIT SPHERE
 LOCAL VARIABLES, PSECT \$DATA, SIZE = 000066 (27 WORDS)
 NAME TYPE OFFSET NAME TYPE OFFSET NAME TYPE OFFSET
 A L*1 000026 AMPLIT R*4 000036 FREQ R*4 000046
 I*01 I*2 000052 K I*2 000034 PHASE R*4 000042
 STEP R*4 000030

FORTRAN IV STORAGE MAP FOR PROGRAM UNIT SPHDAT
 LOCAL VARIABLES: PSECT @DATA, SIZE = 000022 (9 WORDS)

THIS SUBROUTINE WILL CALL OBJDAT AND OBTAIN ONE LINE OF DATA FOR THE SPHERE IF NEW DATA IS SPECIFIED OTHERWISE AN OLD DATA FILE WILL BE READ. IN THE CASE OF NEW DATA THIS ROUTINE WILL WRITE THE NEW FILE WITH THE DESIRED NAME

COMMON/OBJ/OBJA, OBJP, NSAMP2
 COMMON/SYSTA/TRANA, TRAMP, CLUTA, CLUTP, FSTART, FEND, IPOINT

INTEGER OBJA(S12), OBJP(S12)
 INTEGER TRANA(S12), TRAMP(S12), CLUTA(S12), CLUTP(S12), IPOINT
 BYTE A

COMMON BLOCK /OBJ /, SIZE = 004002 (1025 WORDS)

COMMON BLOCK /SYSTA /, SIZE = 010012 (2053 WORDS)

NAME	TYPE	OFFSET	NAME	TYPE	OFFSET	NAME	TYPE	OFFSET
A	L*1	000012	K	I*2	000014			
OBJA	I*2	000000	OBJP	I*2	002000	NSAMP2	I*2	004000
TRANA	I*2	000000	TRAMP	I*2	002000	CLUTA	I*2	004000
CLUTP	I*2	006000	FSTART	R*4	010000	FEND	R*4	010004
IPOINT	I*2	010010						

LOCAL AND COMMON ARRAYS:

NAME	TYPE	SECTION	OFFSET	-----SIZE-----	DIMENSIONS
CLUTA	I*2	SYSTA	004000	002000 (512)	(512)
CLUTP	I*2	SYSTA	006000	002000 (512)	(512)
OBJA	I*2	OBJ	000000	002000 (512)	(512)
OBJP	I*2	OBJ	002000	002000 (512)	(512)
TRANA	I*2	SYSTA	000000	002000 (512)	(512)
TRAMP	I*2	SYSTA	002000	002000 (512)	(512)

SUBROUTINES, FUNCTIONS, STATEMENT AND PROCESSOR-DEFINED FUNCTIONS.

NAME	TYPE	NAME	TYPE	NAME	TYPE	NAME	TYPE
ASSIGN	R*4	CLOSE	R*4	OBJDAT	R*4		

SUBROUTINE SPHDAT

THIS SUBROUTINE WILL CALL OBJDAT AND OBTAIN ONE LINE OF DATA FOR THE SPHERE IF NEW DATA IS SPECIFIED OTHERWISE AN OLD DATA FILE WILL BE READ. IN THE CASE OF NEW DATA THIS ROUTINE WILL WRITE THE NEW FILE WITH THE DESIRED NAME

COMMON/OBJ/OBJA, OBJP, NSAMP2
 COMMON/SYSTA/TRANA, TRAMP, CLUTA, CLUTP, FSTART, FEND, IPOINT

INTEGER OBJA(S12), OBJP(S12)
 INTEGER TRANA(S12), TRAMP(S12), CLUTA(S12), CLUTP(S12), IPOINT
 BYTE A

COMMON/OBJ/OBJA, OBJP, NSAMP2
 COMMON/SYSTA/TRANA, TRAMP, CLUTA, CLUTP, FSTART, FEND, IPOINT

INTEGER OBJA(S12), OBJP(S12)
 INTEGER TRANA(S12), TRAMP(S12), CLUTA(S12), CLUTP(S12), IPOINT
 BYTE A

TYPE 900
 TYPE 901
 ACCEPT 700, A
 IF (A EQ 'N') GO TO 300
 TYPE 905
 ACCEPT *, NSAMP2
 TYPE 902
 PAUSE
 CALL OBJDAT
 TYPE 903
 CALL ASSIGN(12, -1, 'NEW', 'NC', 1, 1)
 WRITE(12, *) FSTART
 WRITE(12, *) FEND
 WRITE(12, *) IPOINT
 DO 200 K=1, IPOINT
 WRITE(12, *) OBJA(K)
 WRITE(12, *) OBJP(K)
 CONTINUE
 CALL CLOSE(12)
 GO TO 500

TYPE 904
 CALL ASSIGN(12, -1, 'OLD', 'NC', 1, 1)
 READ(12, *) FSTART
 READ(12, *) FEND
 READ(12, *) IPOINT
 DO 400 K=1, IPOINT
 READ(12, *) OBJA(K)
 READ(12, *) OBJP(K)
 CONTINUE
 CALL CLOSE(12)
 RETURN

FORMAT(A1)
 FORMAT(//IX, '**** SUBROUTINE SPHDAT OBTAINS SWEPT FREQUENCY
 DATA ****')
 FORMAT(//IX, 'TAKE NEW DATA (Y OR N) ?')
 FORMAT(//IX, 'SET UP THE SPHERE, HIT RETURN TO CONTINUE')

V02.1-1 THU 09-AUG-79 01:43:34 PAGE 002
 FORMAT(//IX, 'ENTER NEW SPHERE DATA FILE NAME: ')
 FORMAT(//IX, 'ENTER OLD SPHERE DATA FILE NAME: ')
 FORMAT(//IX, 'ENTER NUMBER OF MEASUREMENTS AT EACH FREQUENCY

0001
 0002
 0003
 0004
 0005
 0006
 0007
 0008
 0009
 0010
 0011
 0012
 0013
 0014
 0015
 0016
 0017
 0018
 0019
 0020
 0021
 0022
 0023
 0024
 0025
 0026
 0027
 0028
 0029
 0030
 0031
 0032
 0033
 0034
 0035
 0036
 0037
 0038
 0039
 0040
 0041
 0042
 0043
 0044
 0045

THIS SUBROUTINE WILL OBTAIN DATA FOR AN OBJECT OVER THE FREQ RANGE SET WITH THE NUMBER OF POINTS SPECIFIED.

```
COMMON/OBJ/OBJA,OBJP,NSAMP2
COMMON/SYSTA/TRANA,TRANP,CLUTA,CLUTP,FSTART,FEND,NPOINT
INTEGER OBJA(512),OBJP(512),NPOINT
INTEGER TRANA(512),TRANP(512),CLUTA(512),CLUTP(512)
STEP=(FEND-FSTART)/FLOAT(NPOINT)
CALL SWEEP(1,FSTART,1.4)
DO 100 K=1,NPOINT
  FREQ=FSTART+FLOAT(K-1)*STEP
  CALL SWEEP(1,FREQ,1.4)
  CALL PHAMP2(1A,IP,NSAMP2)
  OBJA(K)=1A-2048
  OBJP(K)=IP-2048
CONTINUE
CALL SWEEP(1,FSTART,1.4)
RETURN
END
```

FORTTRAN IV STORAGE MAP FOR PROGRAM UNIT OBJDAT
LOCAL VARIABLES: PSECT 9DATA, SIZE = 000026 (11. WORDS)

NAME	TYPE	OFFSET	NAME	TYPE	OFFSET	NAME	TYPE	OFFSET
FREQ	R=4	000014	1A	I=2	000020	IP	I=2	000022
K	I=2	000012	STEP	R=4	000006			
COMMON BLOCK /OBJ /, SIZE = 004002 (1025 WORDS)								
NAME	TYPE	OFFSET	NAME	TYPE	OFFSET	NAME	TYPE	OFFSET
OBJA	I=2	000000	OBJP	I=2	002000	NSAMP2	I=2	004000
COMMON BLOCK /SYSTA /, SIZE = 010012 (2053 WORDS)								
NAME	TYPE	OFFSET	NAME	TYPE	OFFSET	NAME	TYPE	OFFSET
TRANA	I=2	000000	TRANP	I=2	002000	CLUTA	I=2	004000
CLUTP	I=2	006000	FSTART	R=4	010000	FEND	R=4	010004
NPOINT	I=2	010010						

LOCAL AND COMMON ARRAYS:

NAME	TYPE	SECTION	OFFSET	SIZE	DIMENSIONS
CLUTA	I=2	SYSTA	004000	002000 (512)	(512)
CLUTP	I=2	SYSTA	006000	002000 (512)	(512)
OBJA	I=2	OBJ	000000	002000 (512)	(512)

THIS SUBROUTINE WILL TAKE THE DATA THAT WAS TAKEN FROM SPHADAT AND CORRECT IT WITH THE DATA FROM SUBROUTINE SYSPIN, WHICH IS THE SYSTEM RESPONSE.

```
VERSION 1.1 7-OCT-79
COMMON/OBJ/OBJA,OBJP,NSAMP2
COMMON/SYSTA/TRANA,TRANP,CLUTA,CLUTP,FSTART,FEND,NPOINT
INTEGER OBJA(512),OBJP(512),TRANA(512),TRANP(512)
INTEGER CLUTA(512),CLUTP(512),NPOINT,NSAMP2
SUBTRACT ANTENNA CLUTTER FROM OBJECT DATA THIS CLUTTER DATA MUST NOT!!! BE CORRECTED FOR THE SYSTEM TRANSFER FUNCTION
THE NEXT STEP IS TO DIVIDE BY THE TRANSFER CHARACTERISTIC OF THE SYSTEM IN ARRAYS TRANA(AMPLITUDE) AND TRANP(PHASE).
```

```
P1=3 1415926
DED=P1/180
DO 100 K=1,NPOINT
```

```
CDRAMP=FLOAT(CLUTA(K))* 05
CLPH=FLOAT(CLUTP(K))* 25*DEG
TDAMP=FLOAT(TRANA(K))* 05
TRPH=FLOAT(TRANP(K))* 25*DEG
ODRAMP=FLOAT(OBJA(K))* 05
OBJPH=FLOAT(OBJP(K))* 25*DEG
```

```
CDRAMP=>CLUTTER IN DBM
CLPH=>CLUTTER PHASE IN RADIAN
TDAMP=>TRANSFER CHARACTERISTIC IN DBM
TRPH=>PHASE OF TRANSFER CHARACTERISTIC IN RADIAN
ODRAMP=>OBJECT AMPLITUDE IN DBM
OBJPH=>PHASE OF OBJECT DATA IN RADIAN
OBJAMP=>OBJECT AMPLITUDE IN MILLIWATTS
CLAMP=>CLUTTER AMPLITUDE IN MILLIWATTS
```

```
CLAMP=10.**((CDRAMP/10)
OBJAMP=10.**((OBJAMP/10)
```

```
CLCOS=>REAL PART OF CLUTTER
CLCSIN=>IMAGINARY PART OF CLUTTER
OBJCOS=>REAL PART OF OBJECT DATA
OBJSIN=>IMAGINARY PART OF OBJECT DATA
```

```
OBJCOS=OBJAMP*COS(OBJPH)
OBJSIN=OBJAMP*SIN(OBJPH)
CLCOS=CLAMP*COS(CLPH)
```

```

0020 C CLSIN=CLAMP*SIN(CLPH)
C *****
C TEMCOS=REAL PART OF OBJECT-CLUTTER
C TEMSIN=IMAGINARY PART OF OBJECT-CLUTTER
C ATEMP= MAGNITUDE OF OBJECT-CLUTTER
C PTEMP=PHASE OF OBJECT-CLUTTER
C ADRES= MAGNITUDE OF RESULT (ATEMP/TRAMP) DIVIDE BY TRANSFER
C CHARACTERISTIC IN DBM
C PRES=PHASE OF RESULT ((OBJECT-CLUTTER)/TRANSFER)
C *****
C ***** SUBTRACT CLUTTER FROM OBJECT DATA *****
C TEMCOS=OBJCOS-CLCOS
C TEMSIN=OBJSIN-CLSIN
C ***** CONVERT BACK TO PHASOR FORM *****
C PTEMP=ATAN2(TEMSIN,TEMCOS)
C *****
C ATEMP=SQRT(TEMSIN**2+TEMCOS**2)
C ***** DIVIDE BY TRANSFER CHARACTERISTIC *****
C ADITEM=10.*ALOG10(ATEMP)
C ADPEP=ADITEM-TDBAMP
C IF(PRES GT.PI)PRES=PI-PRES
C IF(PRES LT.-PI)PRES=PI-PRES
C ***** REPLACE DATA INTO INTEGER ARRAY *****
0022 C OBJA(K)=IFIX(20.*ADRES)
0023 C OBJP(K)=IFIX((PRES/DEG)*4.)
0024 C CONTINUE
0025 C RETURN
0026 C END

```

FORTRAN IV STORAGE MAP FOR PROGRAM UNIT CORREC
LOCAL VARIABLES: PSECT \$DATA, SIZE = 000162 (57. WORDS)

NAME	TYPE	OFFSET	NAME	TYPE	OFFSET
ADRES	R=4	000134	ADITEM	R=4	000130
ADPEP	R=4	000030	CLAMP	R=4	000060
CLSIN	R=4	000034	CLSIN	R=4	000104
CLPH	R=4	000026	OBJJOS	R=4	000070
PI	R=4	000054	OBJSIN	R=4	000074
PTEMP	R=4	000016	PRES	R=4	000140
TEMCOS	R=4	000040	TEMSIN	R=4	000114
TDBAMP	R=4	000044			

```

0001 C SUBROUTINE RANGE
C VERSION 1.1
C THIS SUBROUTINE WILL CALCULATE THE DISTANCE TO THE OBJECT
C AND RETURN THAT VALUE. DEPENDING ON THE FLAG PASSED IT WILL
C QUERY WHAT TECHNIQUE TO BE USED IN THE RANGE CALCULATION
C *****
C COMMON /RANGE1/DIST,IRFLAG,LUNIT
C COMMON /OBJ/OBJA,OBJP,NSAMP2
C COMMON /SYSTA/TRANA,TRANP,CLUTA,CLUTP,FSTART,FENCL,NPOINT
C *****
C INTEGER OBJA(S12),OBJP(S12),TRANA(S12),TRANP(S12)
C INTEGER CLUTA(S12),CLUTP(S12),NPOINT,NSAMP2,IRFLAG
C REAL PWR(S12),C,PI
C DATA C/2.99792458*10**8,PI/3.1415926/
C ***** THIS SECTION FOR DIRECT RANGE INPUT *****
0009 C IF (IRFLAG.NE.1) GO TO 200
C ***** THIS SECTION FOR FOURIER TRANSFORM METHOD FOR RANGE *****
0011 C TYPE 900
0012 C ACCEPT *.DIST
0013 C GO TO 1000
0014 C IF (IRFLAG.NE.2) GO TO 1000
C ***** THIS SECTION FOR FOURIER TRANSFORM METHOD FOR RANGE *****
0016 C AMULT=ALOG(FLOAT(NPOINT))/ALOG(12.)
0017 C IF (ABS(AMULT-IFIX(AMULT))-001) 300,300,400
0018 C N=2.*IFIX(AMULT*.01)
0019 C GO TO 500
0020 C N=2.*IFIX(AMULT*.1)
0021 C TYPE *. THE NUMBER OF POINTS IN TRANSFORM: ',N
C ***** ZERO OUT CLUTA AND CLUTP ARRAYS FOR LATER USE *****
0022 C DO 510 K=1,512
0023 C CLUTAIK)=0
0024 C CLUTP(F)=0
0025 C CONTINUE
C ***** FIND SCALE FACTOR *****
0026 C AMX=0
0027 C DO 550 K=1,NPOINT
0028 C AMP=10.*(FLOAT(OBJA(K)).OS)/10.)
0029 C AMY=AMY+AMP
0030 C CONTINUE
0031 C AMX=6.*(AMX/FLOAT(NPOINT))
0032 C SCALE=32676./AMX
0033 C TYPE *,SCALE FACTOR: ',SCALE
0034 C DO 600 K=1,NPOINT
0035 C *****

```

```

0038 AM=SCALE*10 ** (AMDB/10.)
0039 AM=AMCOS(PHASE)
0040 AMI=AM*SIGN(PHASE)
0041 IF (ABS(AM)) GE 32676) AMR=SIGN(32676.,AMR)
0043 IF (ABS(AMI)) GE 32676) AMI=SIGN(32676.,AMI)
C
C ***** REUSE CLUTA AND CLUTP ARRAYS FOR FOURIER TRANSFORM *****
C
0045 CLUTA(K)=IFIX(AMR)
0046 CLUTP(I)=IFIX(AMI)
0047 CONTINUE
0049 CALL FFT(ERROR,N,CLUTA,CLUTP,1,ISCALE)
0049 CALL POWSP(N,CLUTA,CLUTP,PHR)
0050 ALIAS=C/(4 ** ((FEND-FSTART)/FLOAT(N))*.1.E9)
0051 RESC=(((FEND-FSTART)**2)*.1.E9)
0052 WRITE(IUNIT,901)ALIAS,RES
C
C ***** FIND MAXIMUM ENERGY POINT AND RANGE *****
0053 AMPHAX=0
0054 DO 800 K=1, (N/2)
0055 IF (AMPHAX-PMR(K)) 750,750,800
0056 AMPHAX=PMR(K)
0057 PMR=0
0058 CONTINUE
0059 DIST=AMPHAX*RES
0060 RETURN
0061 900 FORMAT('//////ENTER THE DISTANCE TO THE OBJECT IN METERS. ')
0062 901 FORMAT('////// ALIASING RANGE (METERS): ',IPO15,7
0063 '////// RESOLUTION (METERS): ',IPO15,7)
END

```

```

FORTRAN IV STORAGE MAP FOR PROGRAM UNIT RANGE
LOCAL VARIABLES. PSECT 9DATA, SIZE = 004196 ( 1079 WORDS)
NAME TYPE OFFSET NAME TYPE OFFSET NAME TYPE OFFSET
ALIAS R+4 004104 AM R+4 004064 AMDB R+4 004060
AMI R+4 004074 AMP R+4 004044 AMPHAX R+4 004114
AMP R+4 004070 AMULT R+4 004030 AMI R+4 004040
C R+4 004090 IERROR I+2 004100 ISCALE I+2 004102
Y I+2 004036 YMAX I+2 004120 N I+2 004034
PHASE R+4 004054 PI R+4 004004 RES R+4 004110
SCALE R+4 004050
COMMON BLOCK /RANGE1/, SIZE = 000010 ( 4 WORDS)
NAME TYPE OFFSET NAME TYPE OFFSET NAME TYPE OFFSET
DIST R+4 000000 IIRFLAG I+2 000004 IUNIT I+2 000006
COMMON BLOCK /OBJ /, SIZE = 004002 ( 1025 WORDS)
NAME TYPE OFFSET NAME TYPE OFFSET NAME TYPE OFFSET

```

```

FORTRAN IV V02.1-1 SUN 07-OCT-79 00:10:47 PAGE 001
SUBROUTINE RANCOR
VERSION 1.3 7-OCT-79
THIS SUBROUTINE WILL CORRECT THE OBJECT DATE FOR RAISE
COMMON/RANGE)/DIST,IRFLAG,IUNIT
COMMON/OBJ/OBJA,OBJP,NSAMP2
COMMON/SYSTA/TRANA,TRAMP,CLUTA,CLUTP,FSTART,FEND,NPOINT
INTEGER IIRFLAG,OBJA(S12),OBJP(S12),NSAMP2,TRANA(S12)
INTEGER TRAMP(S12),CLUTA(S12),CLUTP(S12),NPOINT
REAL*4 DIST,FSTART,FEND,PATH,KSTART,KFREQ,PI,C,KDELTA
DATA PI/3.1415926/,C/2.997925E+08/
C
C PATH=2.*DIST
KSTART=2.*PI*(FSTART+1.E+09)/C
FDELTA=(FEND-FSTART)/FLOAT(NPOINT)
PDELTA=2.*PI*(FDELTA+1.E+09)/C
KFREQ=KSTART
TMOP1=2.*PI
RAD=PI/180
DEG=180./PI
DO 100 I=1,NPOINT
PHASE=(PATH+KFREQ)
PHADAT=FLOAT(OBJP(K))*25.*RAD
PHEN=PHADAT-PHASE
PHEN=MOD(PHEN,2*PI)
IF (PHEN GT. PI) PHEN=PHEN-TMOP1
IF (PHEN LT. -PI) PHEN=PHEN+TMOP1
OBJP(K)=IFIX(PHEN/DEG+4.)
KFREQ=KFREQ+KDELTA
CONTINUE
RETURN
END

```

```

FORTRAN IV STORAGE MAP FOR PROGRAM UNIT RANCOR
LOCAL VARIABLES. PSECT 9DATA, SIZE = 000104 ( 34 WORDS)
NAME TYPE OFFSET NAME TYPE OFFSET NAME TYPE OFFSET
C R+4 000006 DEG R+4 000050 FDELTA R+4 000034
K I+2 000034 KDELTA R+4 000030 KFREQ R+4 000024
KSTART R+4 000020 PATH R+4 000014 PHADAT R+4 000032
PHASE R+4 000056 PHEN R+4 000044 PI R+4 000002
RAD R+4 000044 TMOP1 R+4 000040
COMMON BLOCK /RANGE1/, SIZE = 000010 ( 4 WORDS)
NAME TYPE OFFSET NAME TYPE OFFSET NAME TYPE OFFSET

```



```

0038          TYPE 903
0039          ACCEPT 1000,A
0040          IF (A EQ 'N') GO TO 220
0041          WRITE(IUNIT,904)
0042          WRITE(IUNIT,905)FSTART,FEND,STEP,NPOINT
0043          WRITE(IUNIT,906)
0044          DO 210 K=1,NPOINT
0045             AMPLIT=FLOAT(OBJA(K))* .05
0046             PHASE=FLOAT(OBJP(K))* .25
0047             FREQ=FSTART+FLOAT(K-1)*STEP
0048             WRITE(IUNIT,907)K,FREQ,AMPLIT,PHASE
0049             CONTINUE
0050             CALL CORREC
0051             C
0052             C
0053             C
0054             C
0055             C
0056             C
0057             C
0058             C
0059             C
0060             C
0061             C
0062             C
0063             C
0064             C
0065             C
0066             C
0067             C
0068             C
0069             C
0070             C
0071             C
0072             C
0073             C
0074             C
0075             C
0076             C
0077             C
0078             C
0079             C
0080             C
0081             C
0082             C
0083             C
0084             C
0085             C
0086             C
0087             C
0088             C
0089             C
0090             C
0091             C
0092             C

```

```

0093             C
0094             C
0095             C
0096             C
0097             C
0098             C
0099             C
0100             C
0101             C
0102             C
0103             C
0104             C
0105             C
0106             C
0107             C
0108             C
0109             C
0110             C
0111             C
0112             C
0113             C
0114             C
0115             C
0116             C
0117             C
0118             C
0119             C
0120             C
0121             C
0122             C
0123             C
0124             C
0125             C
0126             C
0127             C
0128             C
0129             C
0130             C
0131             C
0132             C
0133             C
0134             C
0135             C
0136             C
0137             C
0138             C
0139             C
0140             C
0141             C
0142             C
0143             C
0144             C
0145             C
0146             C
0147             C
0148             C
0149             C
0150             C
0151             C
0152             C
0153             C
0154             C
0155             C
0156             C
0157             C
0158             C
0159             C
0160             C
0161             C
0162             C
0163             C
0164             C
0165             C
0166             C
0167             C
0168             C
0169             C
0170             C
0171             C
0172             C
0173             C
0174             C
0175             C
0176             C
0177             C
0178             C
0179             C
0180             C
0181             C
0182             C
0183             C
0184             C
0185             C
0186             C
0187             C
0188             C
0189             C
0190             C
0191             C
0192             C
0193             C
0194             C
0195             C
0196             C
0197             C
0198             C
0199             C
0200             C
0201             C
0202             C
0203             C
0204             C
0205             C
0206             C
0207             C
0208             C
0209             C
0210             C
0211             C
0212             C
0213             C
0214             C
0215             C
0216             C
0217             C
0218             C
0219             C
0220             C
0221             C
0222             C
0223             C
0224             C
0225             C
0226             C
0227             C
0228             C
0229             C
0230             C
0231             C
0232             C
0233             C
0234             C
0235             C
0236             C
0237             C
0238             C
0239             C
0240             C
0241             C
0242             C
0243             C
0244             C
0245             C
0246             C
0247             C
0248             C
0249             C
0250             C
0251             C
0252             C
0253             C
0254             C
0255             C
0256             C
0257             C
0258             C
0259             C
0260             C
0261             C
0262             C
0263             C
0264             C
0265             C
0266             C
0267             C
0268             C
0269             C
0270             C
0271             C
0272             C
0273             C
0274             C
0275             C
0276             C
0277             C
0278             C
0279             C
0280             C
0281             C
0282             C
0283             C
0284             C
0285             C
0286             C
0287             C
0288             C
0289             C
0290             C
0291             C
0292             C
0293             C
0294             C
0295             C
0296             C
0297             C
0298             C
0299             C
0300             C
0301             C
0302             C
0303             C
0304             C
0305             C
0306             C
0307             C
0308             C
0309             C
0310             C
0311             C
0312             C
0313             C
0314             C
0315             C
0316             C
0317             C
0318             C
0319             C
0320             C
0321             C
0322             C
0323             C
0324             C
0325             C
0326             C
0327             C
0328             C
0329             C
0330             C
0331             C
0332             C
0333             C
0334             C
0335             C
0336             C
0337             C
0338             C
0339             C
0340             C
0341             C
0342             C
0343             C
0344             C
0345             C
0346             C
0347             C
0348             C
0349             C
0350             C
0351             C
0352             C
0353             C
0354             C
0355             C
0356             C
0357             C
0358             C
0359             C
0360             C
0361             C
0362             C
0363             C
0364             C
0365             C
0366             C
0367             C
0368             C
0369             C
0370             C
0371             C
0372             C
0373             C
0374             C
0375             C
0376             C
0377             C
0378             C
0379             C
0380             C
0381             C
0382             C
0383             C
0384             C
0385             C
0386             C
0387             C
0388             C
0389             C
0390             C
0391             C
0392             C
0393             C
0394             C
0395             C
0396             C
0397             C
0398             C
0399             C
0400             C
0401             C
0402             C
0403             C
0404             C
0405             C
0406             C
0407             C
0408             C
0409             C
0410             C
0411             C
0412             C
0413             C
0414             C
0415             C
0416             C
0417             C
0418             C
0419             C
0420             C
0421             C
0422             C
0423             C
0424             C
0425             C
0426             C
0427             C
0428             C
0429             C
0430             C
0431             C
0432             C
0433             C
0434             C
0435             C
0436             C
0437             C
0438             C
0439             C
0440             C
0441             C
0442             C
0443             C
0444             C
0445             C
0446             C
0447             C
0448             C
0449             C
0450             C
0451             C
0452             C
0453             C
0454             C
0455             C
0456             C
0457             C
0458             C
0459             C
0460             C
0461             C
0462             C
0463             C
0464             C
0465             C
0466             C
0467             C
0468             C
0469             C
0470             C
0471             C
0472             C
0473             C
0474             C
0475             C
0476             C
0477             C
0478             C
0479             C
0480             C
0481             C
0482             C
0483             C
0484             C
0485             C
0486             C
0487             C
0488             C
0489             C
0490             C
0491             C
0492             C
0493             C
0494             C
0495             C
0496             C
0497             C
0498             C
0499             C
0500             C
0501             C
0502             C
0503             C
0504             C
0505             C
0506             C
0507             C
0508             C
0509             C
0510             C
0511             C
0512             C
0513             C
0514             C
0515             C
0516             C
0517             C
0518             C
0519             C
0520             C
0521             C
0522             C
0523             C
0524             C
0525             C
0526             C
0527             C
0528             C
0529             C
0530             C
0531             C
0532             C
0533             C
0534             C
0535             C
0536             C
0537             C
0538             C
0539             C
0540             C
0541             C
0542             C
0543             C
0544             C
0545             C
0546             C
0547             C
0548             C
0549             C
0550             C
0551             C
0552             C
0553             C
0554             C
0555             C
0556             C
0557             C
0558             C
0559             C
0560             C
0561             C
0562             C
0563             C
0564             C
0565             C
0566             C
0567             C
0568             C
0569             C
0570             C
0571             C
0572             C
0573             C
0574             C
0575             C
0576             C
0577             C
0578             C
0579             C
0580             C
0581             C
0582             C
0583             C
0584             C
0585             C
0586             C
0587             C
0588             C
0589             C
0590             C
0591             C
0592             C
0593             C
0594             C
0595             C
0596             C
0597             C
0598             C
0599             C
0600             C
0601             C
0602             C
0603             C
0604             C
0605             C
0606             C
0607             C
0608             C
0609             C
0610             C
0611             C
0612             C
0613             C
0614             C
0615             C
0616             C
0617             C
0618             C
0619             C
0620             C
0621             C
0622             C
0623             C
0624             C
0625             C
0626             C
0627             C
0628             C
0629             C
0630             C
0631             C
0632             C
0633             C
0634             C
0635             C
0636             C
0637             C
0638             C
0639             C
0640             C
0641             C
0642             C
0643             C
0644             C
0645             C
0646             C
0647             C
0648             C
0649             C
0650             C
0651             C
0652             C
0653             C
0654             C
0655             C
0656             C
0657             C
0658             C
0659             C
0660             C
0661             C
0662             C
0663             C
0664             C
0665             C
0666             C
0667             C
0668             C
0669             C
0670             C
0671             C
0672             C
0673             C
0674             C
0675             C
0676             C
0677             C
0678             C
0679             C
0680             C
0681             C
0682             C
0683             C
0684             C
0685             C
0686             C
0687             C
0688             C
0689             C
0690             C
0691             C
0692             C
0693             C
0694             C
0695             C
0696             C
0697             C
0698             C
0699             C
0700             C
0701             C
0702             C
0703             C
0704             C
0705             C
0706             C
0707             C
0708             C
0709             C
0710             C
0711             C
0712             C
0713             C
0714             C
0715             C
0716             C
0717             C
0718             C
0719             C
0720             C
0721             C
0722             C
0723             C
0724             C
0725             C
0726             C
0727             C
0728             C
0729             C
0730             C
0731             C
0732             C
0733             C
0734             C
0735             C
0736             C
0737             C
0738             C
0739             C
0740             C
0741             C
0742             C
0743             C
0744             C
0745             C
0746             C
0747             C
0748             C
0749             C
0750             C
0751             C
0752             C
0753             C
0754             C
0755             C
0756             C
0757             C
0758             C
0759             C
0760             C
0761             C
0762             C
0763             C
0764             C
0765             C
0766             C
0767             C
0768             C
0769             C
0770             C
0771             C
0772             C
0773             C
0774             C
0775             C
0776             C
0777             C
0778             C
0779             C
0780             C
0781             C
0782             C
0783             C
0784             C
0785             C
0786             C
0787             C
0788             C
0789             C
0790             C
0791             C
0792             C
0793             C
0794             C
0795             C
0796             C
0797             C
0798             C
0799             C
0800             C
0801             C
0802             C
0803             C
0804             C
0805             C
0806             C
0807             C
0808             C
0809             C
0810             C
0811             C
0812             C
0813             C
0814             C
0815             C
0816             C
0817             C
0818             C
0819             C
0820             C
0821             C
0822             C
0823             C
0824             C
0825             C
0826             C
0827             C
0828             C
0829             C
0830             C
0831             C
0832             C
0833             C
0834             C
0835             C
0836             C
0837             C
0838             C
0839             C
0840             C
0841             C
0842             C
0843             C
0844             C
0845             C
0846             C
0847             C
0848             C
0849             C
0850             C
0851             C
0852             C
0853             C
0854             C
0855             C
0856             C
0857             C
0858             C
0859             C
0860             C
0861             C
0862             C
0863             C
0864             C
0865             C
0866             C
0867             C
0868             C
0869             C
0870             C
0871             C
0872             C
0873             C
0874             C
0875             C
0876             C
0877             C
0878             C
0879             C
0880             C
0881             C
0882             C
0883             C
0884             C
0885             C
0886             C
0887             C
0888             C
0889             C
0890             C
0891             C
0892             C
0893             C
0894             C
0895             C
0896             C
0897             C
0898             C
0899             C
0900             C
0901             C
0902             C
0903             C
0904             C
0905             C
0906             C
0907             C
0908             C
0909             C
0910             C
0911             C
0912             C
0913             C
0914             C
0915             C
0916             C
0917             C
0918             C
0919             C
0920             C
0921             C
0922             C
0923             C
0924             C
0925             C
0926             C
0927             C
0928             C
0929             C
0930             C
0931             C
0932             C
0933             C
0934             C
0935             C
0936             C
0937             C
0938             C
0939             C
0940             C
0941             C
0942             C
0943             C
0944             C
0945             C
0946             C
0947             C
0948             C
0949             C
0950             C
0951             C
0952             C
0953             C
0954             C
0955             C
0956             C
0957             C
0958             C
0959             C
0960             C
0961             C
0962             C
0963             C
0964             C
0965             C
0966             C
0967             C
0968             C
0969             C
0970             C
0971             C
0972             C
0973             C
0974             C
0975             C
0976             C
0977             C
0978             C
0979             C
0980             C
0981             C
0982             C
0983             C
0984             C
0985             C
0986             C
0987             C
0988             C
0989             C
0990             C
0991             C
0992             C
0993             C
0994             C
0995             C
0996             C
0997             C
0998             C
0999             C
1000             C

```

```

PAGE 001
PROGRAM SPHER2
VERSION 1.0 30-NOV-79
THIS PROGRAM WILL TAKE EXPERIMENTAL DATA FOR THE SPHERE
AND CORRECT IT FOR THE SYSTEM RESPONSE. IT WILL PRINT
BOTH THE CORRECTED AND UNCORRECTED DATA AND FINALLY DISPLAY
IT ON THE HIGH RESOLUTION CRT
ALSO IT DESIRED IT WILL GENERATE IF DESIRED ANALYTICAL
DATA FOR THE SPHERE AND STORE IT IN A FILE. IT WILL ALSO
PRINT THIS DATA IF DESIRED TO A FILE AND ALSO DISPLAY IT ON
THE HIGH RESOLUTION CRT MONITOR.
COMMON/PANEL/DIST,IRFLAG,IUNIT
COMMON/OBJ/OBJA,OBJP,NSAMP2
COMMON/SYSTA/TRANA,TRAMP,CLUTA,CLUTP,FSTART,FEND,NPOINT
INTEGER OBJA(512),OBJP(512),TRANA(512)
INTEGER TRAMP(512),CLUTA(512),CLUTP(512),NPOINT,NSAMP2
BYTE A
TYPE 900
TYPE 912
ACCEPT *,IUNIT
THIS SECTION WILL GENERATE CORRECTED SPHERE DATA FROM
EXPERIMENTAL DATA
TYPE 902
CALL SFS1
STEP=(FEND-FSTART)/FLOAT(NPOINT)
TYPE *,PRINT THE SYSTEM RESPONSE DATA (Y OR N)
ACCEPT 1000,A
IF (A EQ 'N') GO TO 100
WRITE(IUNIT,917)
WRITE(IUNIT,905)FSTART,FEND,STEP,NPOINT
DO 20 K=1,NPOINT
AMPLIT=FLOAT(TRANA(K))* .05
PHASE=FLOAT(TRAMP(K))* .25
FREQ=FSTART+FLOAT(K-1)*STEP
WRITE(IUNIT,907)K,FREQ,AMPLIT,PHASE
CONTINUE
WRITE(IUNIT,918)
WRITE(IUNIT,905)FSTART,FEND,STEP,NPOINT
WRITE(IUNIT,906)
DO 30 K=1,NPOINT
AMPLIT=FLOAT(CLUTA(K))* .05
FREQ=FSTART+FLOAT(K-1)*STEP
PHASE=FLOAT(CLUTP(K))* .25
WRITE(IUNIT,907)K,FREQ,AMPLIT,PHASE
CONTINUE
WRITE(IUNIT,919)
CONTINUE
CALL SPHAD
CALL SHEEP(10,....)

```

THIS SECTION WILL STORE THE CORRECTED DATA FOR SYSTEM RESPONSE

THIS SECTION WILL CORRECT FOR RANGE

```

0133 916 I(Y OR N)
0134 917 FORMAT(//)SPRINT SPHERE DATA CORRECTED FOR RANGE (Y OR N)
***** TRANSFER CHARACTERISTIC OF SYSTEM *****
0135 918 FORMAT(//)SPRINT SPHERE DATA CORRECTED FOR RANGE (Y OR N)
***** TRANSFER CHARACTERISTIC OF SYSTEM *****
0136 1000 FORMAT(A)
0137 STOP ***** END OF PROGRAM *****
0138 END

```

LOCAL VARIABLES, PSECT \$DATA, SIZE = 000102 (33. WORDS)

NAME	TYPE	OFFSET	NAME	TYPE	OFFSET	NAME	TYPE	OFFSET
A	L+1	000036	AMPLIT	R+4	000046	FREQ	R+4	000056
IND1	I+2	000062	K	I+2	000044	PHASE	R+4	000052
STEP	R+4	000040						

COMMON BLOCK /RANGE1/, SIZE = 000010 (4. WORDS)

NAME	TYPE	OFFSET	NAME	TYPE	OFFSET	NAME	TYPE	OFFSET
DIST	R+4	000000	IRFLAG	I+2	000004	LUNIT	I+2	000006

COMMON BLOCK /OBJ /, SIZE = 004002 (1025. WORDS)

NAME	TYPE	OFFSET	NAME	TYPE	OFFSET	NAME	TYPE	OFFSET
OBJA	I+2	000000	OBJP	I+2	002000	NSAMP2	I+2	004000

COMMON BLOCK /SYSTA /, SIZE = 010012 (2053. WORDS)

NAME	TYPE	OFFSET	NAME	TYPE	OFFSET	NAME	TYPE	OFFSET
TRANA	I+2	000000	TRAMP	I+2	002000	CLUTA	I+2	004000
CLUTP	I+2	006000	FSTART	R+4	010000	FEND	R+4	010004
NPPOINT	I+2	010010						

LOCAL AND COMMON ARRAYS

NAME	TYPE	SECTION	OFFSET	SIZE	DIMENSIONS
CLUTA	I+2	SYSTA	004000	(512)	(512)
CLUTP	I+2	SYSTA	006000	(512)	(512)
OBJA	I+2	OBJ	000000	(512)	(512)
OBJP	I+2	OBJ	002000	(512)	(512)
TRANA	I+2	SYSTA	000000	(512)	(512)
TRAMP	I+2	SYSTA	002000	(512)	(512)

SUBROUTINES, FUNCTIONS, STATEMENT AND PROCESSOR-DEFINED FUNCTIONS

NAME	TYPE	NAME	TYPE	NAME	TYPE	NAME	TYPE
ASSION	R+4	CLOSE	R+4	CORREC	R+4	FLOAT	R+4
RANGE	R+4	SPHDAT	R+4	SWEAP	R+4	SYS1	R+4

```

0103 WRITE(LUNIT,906)
0104 DO 410 Y=1,NPOINT
0105 I=IND1*Y
0106 PHASE=FLOAT(OBJA(K))*0.5
0107 FREQ=FLOAT(OBJP(K))*2.5
0108 FREQ=START+FLOAT(IND1-1)*STEP
0109 WRITE(LUNIT,907)K,FREQ,AMPLIT,PHASE
0110 CONTINUE
0111
0112
0113
0114

```

THIS SECTION WILL STORE THE RANGE CORRECTED DATA

```

0111 TYPE 901
0112 ACCEPT 1000,A
0113 IF (A EQ 'N') GO TO 500
0114 TYPE 900
0115 CALL ASSION(20,-1,'NEW','NC',)
0116 WRITE(20,9)FSTART
0117 WRITE(20,9)FEND
0118 DO 460 Y=1,NPOINT
0119 WRITE(20,9)OBJA(K)
0120 WRITE(20,9)OBJP(K)
0121 CONTINUE
0122 CALL CLOSE(20)

```

THIS SECTION WILL DISPLAY THE DATA

```

0115 500 CONTINUE
0116 600 FORMAT(//)ENTER THE FILE NAME FOR THE RANGE
0117 801 /CORRECTED DATA. /
0118 802 FORMAT(//)DO YOU WANT TO STORE THE CORRECTED DATA (Y OR N)
0119 900 FORMAT(//)***** PROGRAM SPHERE *****
0120 901 /DATA (Y OR N) /
0121 902 FORMAT(//)THIS SECTION WILL GENERATE CORRECTED SPHERE DATA
0122 903 /EXPIMENTAL DATA /
0123 904 FORMAT(//)***** UNCORRECTED SPHERE DATA *****
0124 905 /STARTING FREQUENCY GHZ. /,IPG15 7/15X,
/ENDING FREQUENCY IN GHZ. /,IPG15 7/15X, /FREQUENCY STEP GHZ.
/1PG15 7/15X, /NUMBER OF STEPS. /,I7)
0125 906 /FORMAT(//)1X,75(//)12X, /POINT #,5X, /FREQUENCY, /7X,
/AMPLITUDE DB. /,5X, /PHASE DEGREES//1X,75(//)X//
0126 907 /FORMAT(//)10X,17.5X,IPG15 7.3X,IPG15 7)
0127 909 /FORMAT(//)***** CORRECTED EXPERIMENTAL SPHERE
/DATA *****
0128 911 /FORMAT(//)***** EXPERIMENTAL SPHERE DATA CORRECTED
/FOR RANGE *****
0129 912 /FORMAT(//)$. /ENTER LOGICAL UNIT NUMBER FOR OUTPUT (7->
/TERMINAL) /
0130 913 /FORMAT(//)$. /CALCULATED RANGE TO THE TARGET= /,IPG15. 7,
/ METERS)
0131 914 /FORMAT(//)$. /ENTER THE RANGE CALCULATION FLAG// 1=>DIRECT
/ MEASUREMENT// 2=>FOURIER ANALYSIS // 9=INPUT FLAG. /
0132 915 /FORMAT(//)SPRINT SPHERE DATA CORRECTED FOR SYSTEM RESPONSE

```

FORTRAN IVV02 1-1
SUBROUTINE SYS1
VERSION 1.0 29-NOV-79

PAGE 001

THIS SUBROUTINE WILL READ IN THE SYSTEM RESPONSE FILES
AND PLACE THEM IN A COMMON BLOCK TO BE PASSED TO OTHER
ROUTINES

COMMON /SYSTA/TRANA, TRAMP, CLUTA, CLUTP, FSTART, FEND, NPOINT

INTEGER TRANA(512), TRAMP(512), CLUTA(512), CLUTP(512), NPOINT

TYPE 900

TYPE *, 'OLD OR NEW DATA (1=>NEW, 0=>OLD)'

ACCEPT *, FLAG

IF (FLAG) 50, 50, 10

TYPE *, 'ENTER THE STARTING FREQ IN GHZ: '

ACCEPT *, FSTART

TYPE *, 'ENTER THE ENDING FREQ IN GHZ: '

ACCEPT *, FEND

TYPE *, 'ENTER THE NUMBER OF FREQ POINTS: '

ACCEPT *, NPOINT

TYPE *, 'ENTER THE NUMBER OF SAMPLES AT EACH FREQ: '

ACCEPT *, NSAMP2

TYPE *, 'SET UP REFLECTING PLANE FOR TRANSFER FUNCTION MEASUREMENT'

PAUSE '***** HIT RETURN TO PROCEED *****'

CALL SMDAT(TRANA, TRAMP, FSTART, FEND, NPOINT, NSAMP2)

TYPE *, 'SET UP FOR CLUTTER MEASUREMENT'

PAUSE '***** HIT RETURN TO PROCEED *****'

CALL SMDAT(CLUTA, CLUTP, FSTART, FEND, NPOINT, NSAMP2)

TYPE *, 'STORE DATA ON DISC? (Y OR N)'

ACCEPT 900, C

IF (C EQ 'N') GOTO 300

TYPE 901

CALL ASSIGN(12, -1, 'NEW', 'NC', 1)

WRITE(12, *) FSTART

WRITE(12, *) FEND

WRITE(12, *) NPOINT

DO 30 K=1, NPOINT

WRITE(12, *) TRANA(K)

WRITE(12, *) TRAMP(K)

CONTINUE

CALL CLOSE(12)

TYPE 902

CALL ASSIGN(12, -1, 'NEW', 'NC', 1)

WRITE(12, *) FSTART

WRITE(12, *) FEND

WRITE(12, *) NPOINT

DO 40 K=1, NPOINT

WRITE(12, *) CLUTA(K)

WRITE(12, *) CLUTP(K)

CONTINUE

CALL CLOSE(12)

GO TO 300

TYPE 901

0049 CALL ASSIGN(12, -1, 'OLD', 'NC', 1)
0050 READ(12, *) FSTART
0051 READ(12, *) FEND
0052 READ(12, *) NPOINT
0053 DO 100 K=1, NPOINT
0054 READ(12, *) TRANA(K)
0055 READ(12, *) TRAMP(K)
0056 CONTINUE
0057 CALL CLOSE(12)
0058 TYPE 902
0059 CALL ASSIGN(12, -1, 'OLD', 'NC', 1)
0060 READ(12, *) FSTART
0061 READ(12, *) FEND
0062 READ(12, *) NPOINT
0063 DO 200 K=1, NPOINT
0064 READ(12, *) CLUTA(K)
0065 READ(12, *) CLUTP(K)
0066 CONTINUE
0067 CALL CLOSE(12)
0068 RETURN
0069 800
0070 900
0071 901
0072 902
0073 END

LOCAL VARIABLES. PSECT \$DATA, SIZE = 000044 (18 WORDS)

NAME	TYPE	OFFSET	NAME	TYPE	OFFSET	NAME	TYPE	OFFSET
C	L*1	000022	FLAG	R*4	000024	K	I*2	000032
NSAMP2	I*2	000030						

COMMON BLOCK /SYSTA /, SIZE = 010012 (2053 WORDS)

NAME	TYPE	OFFSET	NAME	TYPE	OFFSET	NAME	TYPE	OFFSET
TRANA	I*2	000000	TRAMP	I*2	002000	CLUTA	I*2	004000
CLUTP	I*2	006000	FSTART	R*4	010000	FEND	R*4	010004
NPOINT	I*2	010010						

LOCAL AND COMMON ARRAYS:

NAME	TYPE	SECTION	OFFSET	-----SIZE-----	DIMENSIONS
CLUTA	I*2	SYSTA	004000	002000 (512)	(512)
CLUTP	I*2	SYSTA	006000	002000 (512)	(512)
TRANA	I*2	SYSTA	000000	002000 (512)	(512)
TRAMP	I*2	SYSTA	002000	002000 (512)	(512)

SUBROUTINES, FUNCTIONS, STATEMENT AND PROCESSOR-DEFINED FUNCTIONS.

NAME	TYPE	NAME	TYPE	NAME	TYPE	NAME	TYPE
ASSIGN	R*4	CLOSE	R*4	.SMDAT	R*4		

0045
0046
0047
0048
0049

VERSION 1.0 30-NOV-79

THIS PROGRAM WILL TAKE EXPERIMENTAL DATA FOR THE SPHERE AND CORRECT IT FOR THE SYSTEM RESPONSE. IT WILL PRINT BOTH THE CORRECTED AND UNCORRECTED DATA AND FINALLY DISPLAY IT ON THE HIGH RESOLUTION CRT.

ALSO IT DESIRED IT WILL GENERATE IF DESIRED ANALYTICAL DATA FOR THE SPHERE AND STORE IT IN A FILE. IT WILL ALSO PRINT THIS DATA IF DESIRED TO A FILE AND ALSO DISPLAY IT ON THE HIGH RESOLUTION CRT MONITOR.

COMMON/RANGE1/DIST,IRFLAG,IUNIT
COMMON/OBJ/OBJA,OBJP,NSAMP2
COMMON/SYSTA/TRANA,TRAMP,CLUTA,CLUTP,FSTART,FEND,NPOINT

INTEGER OBJA(512),OBJP(512),TRANA(512)
INTEGER TRAMP(512),CLUTA(512),CLUTP(512),NPOINT,NSAMP2
BYTE A

TYPE 900
TYPE 912
ACCEPT *, IUNIT

THIS SECTION WILL GENERATE CORRECTED SPHERE DATA FROM EXPERIMENTAL DATA

TYPE 902
CALL SYS2
STEP=(FEND-FSTART)/FLOAT(NPOINT)
TYPE *, PRINT THE SYSTEM RESPONSE DATA (Y OR N)
ACCEPT 1000,A
IF (A EQ 'N') GO TO 100
WRITE(IUNIT,917)
WRITE(IUNIT,905)FSTART,FEND,STEP,NPOINT
WRITE(IUNIT,906)
DO 20 K=1,NPOINT
AMPLIT=FLOAT(TRANA(K))*05
PHASE=FLOAT(TRAMP(K))*25
FREQ=START+FLOAT(K-1)*STEP
WRITE(IUNIT,907)K,FREQ,AMPLIT,PHASE
CONTINUE

CALL SPHRAT
CALL SWEEP(10,....)
TYPE 903
ACCEPT 1000,A
IF (A EQ 'N') GO TO 220
WRITE(IUNIT,904)
WRITE(IUNIT,905)FSTART,FEND,STEP,NPOINT
WRITE(IUNIT,906)

DO 210 K=1,NPOINT
AMPLIT=FLOAT(OBJA(K))*05
PHASE=FLOAT(OBJP(K))*25
FREQ=START+FLOAT(K-1)*STEP
WRITE(IUNIT,907)K,FREQ,AMPLIT,PHASE
CONTINUE
CALL CORRDAT

HERE LIST THE CORRECTED SPHERE DATA

TYPE 915
ACCEPT 1000,A
IF (A EQ 'N') GO TO 280
WRITE(IUNIT,909)
WRITE(IUNIT,905)FSTART,FEND,STEP,NPOINT
WRITE(IUNIT,906)
DO 277 K=1,NPOINT
INDI=K
AMPLIT=FLOAT(OBJA(K))*05
PHASE=FLOAT(OBJP(K))*25
FREQ=START+FLOAT((INDI-1)*STEP
WRITE(IUNIT,907)K,FREQ,AMPLIT,PHASE
CONTINUE
CONTINUE

THIS SECTION WILL STORE THE CORRECTED DATA FOR SYSTEM RESPONSE

TYPE 902
ACCEPT 1000,A
IF (A EQ 'N') GO TO 400
TYPE 901
CALL ASSIGN(20,,-1,'NEW','NC',)
WRITE(20,*)FSTART
WRITE(20,*)FEND
WRITE(20,*)NPOINT
DO 310 K=1,NPOINT
WRITE(20,*)OBJA(K)
WRITE(20,*)OBJP(K)
CONTINUE
CALL CLOSE(20)

THIS SECTION WILL CORRECT FOR RANGE

TYPE 914
ACCEPT *,IRFLAG
CALL RANGE
TYPE 913,DIST
CALL RANCR
TYPE 916
ACCEPT 1000,A
IF (A EQ 'N') GO TO 470
WRITE(IUNIT,913)DIST

WRITE(IUNIT,911)
WRITE(IUNIT,905)FSTART,FEND,STEP,NPOINT
WRITE(IUNIT,906)
DO 410 K=1,NPOINT
INDI=K
AMPLIT=FLOAT(OBJA(K))*05
PHASE=FLOAT(OBJP(K))*25
FREQ=START+FLOAT((INDI-1)*STEP

0036
0037
0038
0039
0040
0041
0042

210
220
C
C

0043

0044

0045

0046

0047

0048

0049

0050

0051

0052

0053

0054

0055

0056

0057

277

280

C

C

C

400

0072

0073

0074

C

0075

0076

0077

0078

0079

0081

0082

0083

0084

0085

0086

0087

0088

0089

```

0090 0128 STOP ***** END OF PROGRAM *****
0091 0129 END
LOCAL VARIABLES, PSECT $DATA, SIZE = 000074 ( 30 WORDS)
NAME TYPE OFFSET NAME TYPE OFFSET NAME TYPE OFFSET
A L*1 000032 AMPLIT R*4 000042 FREQ R*4 000052
IND1 I*2 000056 K I*2 000040 PHASE R*4 000046
STEP R*4 000034

COMMON BLOCK /RANGE1/, SIZE = 000010 ( 4 WORDS)
NAME TYPE OFFSET NAME TYPE OFFSET NAME TYPE OFFSET
DIST R*4 000000 IFLAG I*2 000004 IUNIT I*2 000006

COMMON BLOCK /OBJ /, SIZE = 004002 ( 1025 WORDS)
NAME TYPE OFFSET NAME TYPE OFFSET NAME TYPE OFFSET
OBJA I*2 000000 OBJP I*2 002000 NSAMP2 I*2 004000

COMMON BLOCK /SYSTA /, SIZE = 010012 ( 2053 WORDS)
NAME TYPE OFFSET NAME TYPE OFFSET NAME TYPE OFFSET
TRANA I*2 000000 TRAMP I*2 002000 CLUTA I*2 004000
CLUTP I*2 006000 FSTART R*4 010000 FEED R*4 010004
NPOINT I*2 010010

LOCAL AND COMMON ARRAYS:
NAME TYPE SECTION OFFSET SIZE DIMENSIONS
CLUTA I*2 SYSTA 004000 002000 ( 512 ) (512)
CLUTP I*2 SYSTA 006000 002000 ( 512 ) (512)
OBJA I*2 OBJ 000000 002000 ( 512 ) (512)
OBJP I*2 OBJ 002000 002000 ( 512 ) (512)
TRANA I*2 SYSTA 000000 002000 ( 512 ) (512)
TRAMP I*2 SYSTA 002000 002000 ( 512 ) (512)

SUBROUTINES, FUNCTIONS, STATEMENT AND PROCESSOR-DEFINED FUNCTIONS
NAME TYPE NAME TYPE NAME TYPE NAME TYPE NAME TYPE
ASSIGN R*4 CLOSE R*4 CORDAT R*4 FLOAT R*4 RANCOR R*4
RANGE R*4 SPHDAT R*4 SWEEP R*4 SYS2 R*4

```

```

WRITE(IUNIT,907)K,FREQ,AMPLIT,PHASE
CONTINUE
THIS SECTION WILL STORE THE RANGE CORRECTED DATA
TYPE 901
ACCEPT 1000,A
IF (A EQ 'N') GO TO 500
TYPE 800
CALL ASSIGN(20,-1,'NEW','NC',)
WRITE(20,*FSTART)
WRITE(20,*FEND)
WRITE(20,*NPOINT)
WRITE(20,*OBJA(K))
WRITE(20,*OBJP(K))
CONTINUE
CALL CLOSE(20)
THIS SECTION WILL DISPLAY THE DATA
CONTINUE
FORMAT STATEMENTS
FORMAT(////,ENTER THE FILE NAME FOR THE RANGE
1CORRECTED DATA ')
FORMAT(////,ENTER THE FILE NAME FOR THE CORRECTED DATA,')
FORMAT(////,DO YOU WANT TO STORE THE CORRECTED DATA (Y OR N)
1)
FORMAT(////,***** PROGRAM SPHERE *****')
FORMAT(////,DO YOU WANT TO STORE THE RANGE CORRECTED
1DATA (Y OR N) ? ')
FORMAT(////, THIS SECTION WILL GENERATE CORRECTED SPHERE DATA
1FROM // EXPERIMENTAL DATA')
FORMAT(////,PRINT THE UNCORRECTED DATA (Y OR N) ? ')
FORMAT(////,***** UNCORRECTED SPHERE DATA *****')
FORMAT(15X,'STARTING FREQUENCY OHZ ',IP615 7/15X,
1ENDING FREQUENCY IN OHZ ',IP615 7/15X,'FREQUENCY STEP OHZ:
2,IP615 7/15X,'NUMBER OF STEPS: ',I7)
FORMAT(11X,75('*/12X,'POINT #',5X,'FREQUENCY',7X,
1AMPLITUDE DB ',5X,'PHASE DEGREES/1X,75('*/1)')
FORMAT(10X,17,5X,IP615 7,3X,IP615 7)
FORMAT(////,////, ***** CORRECTED EXPERIMENTAL SPHERE
1DATA *****')
FORMAT(////,////, ***** EXPERIMENTAL SPHERE DATA CORRECTED
1RANGE *****')
FORMAT(////,ENTER LOGICAL UNIT NUMBER FOR OUTPUT (7->
1TERMINAL) ?)
FORMAT(////, CALCULATED RANGE TO THE TARGET= ',IP615 7,
1METERS')
FORMAT(////, ENTER THE RANGE CALCULATION FLAG(// 1->DIRECT
1MEASUREMENT// 2->FOURIER ANALYSIS //3->INPUT FLAG)
FORMAT(////,PRINT SPHERE DATA CORRECTED FOR SYSTEM RESPONSE
1(Y OR N) ?)
FORMAT(////,PRINT SPHERE DATA CORRECTED FOR RANGE (Y OR N) ?)
FORMAT(////,***** TRANSFER CHARACTERISTIC OF SYSTEM **
1*****')
FORMAT(////,////, ***** SYSTEM CLUTTER *****')
FORMAT(A1)

```

0048 901 FORMAT(//,'\$', 'ENTER THE TRANSFER FUNCTION FILE NAME. ')
 0049 END

LOCAL VARIABLES. PSECT \$DATA, SIZE = 000030 (12 WORDS)

NAME	TYPE	OFFSET	NAME	TYPE	OFFSET	NAME	TYPE	OFFSET
C	L*1	000012	FLAG	R*4	000014	K	I*2	000022
NSAMP2	I*2	000020						

COMMON BLOCK /SYSTA /, SIZE = 010012 (2053 WORDS)

NAME	TYPE	OFFSET	NAME	TYPE	OFFSET	NAME	TYPE	OFFSET
TRANA	I*2	000000	TRAMP	I*2	002000	CLUTA	I*2	004000
CLUTP	I*2	006000	FSTART	R*4	010000	FEND	R*4	010004
NPOINT	I*2	010010						

LOCAL AND COMMON ARRAYS:

NAME	TYPE	SECTION	OFFSET	-----SIZE-----	DIMENSIONS
CLUTA	I*2	SYSTA	002000	(512)	(512)
CLUTP	I*2	SYSTA	004000	(512)	(512)
TRANA	I*2	SYSTA	006000	(512)	(512)
TRAMP	I*2	SYSTA	002000	(512)	(512)

SUBROUTINES, FUNCTIONS, STATEMENT AND PROCESSOR-DEFINED FUNCTIONS.

NAME	TYPE	NAME	TYPE	NAME	TYPE	NAME	TYPE
ASSION	R*4	CLOSE	R*4	SN DAT	R*4		

FORTPAN IUV02 1-1 FRI 30-NOV-79 00:20:50 PAGE 001
 SUBROUTINE SYS2
 VERSION 1 0 29-NOV-79

THIS SUBROUTINE WILL READ IN THE SYSTEM RESPONSE FILES
 AND PLACE THEM IN A COMMON BLOCK TO BE PASSED TO OTHER
 ROUTINES

COMMON /SYSTA/ TRANA, TRAMP, CLUTA, CLUTP, FSTART, FEND, NPOINT
 BYTE A
 INTEGER TRANA(S12), TRAMP(S12), CLUTA(S12), CLUTP(S12), NPOINT

```

0002 C      TYPE %00
0003 C      IF (FLAG) GO TO 50, 50, 10
0004 C      ACCEPT *, FLAG
0005 C      TYPE *, 'ENTER THE STARTING FREQ IN GHZ: '
0006 C      ACCEPT *, FSTART
0007 C      TYPE *, 'ENTER THE ENDING FREQ IN GHZ: '
0008 C      ACCEPT *, FEND
0009 C      TYPE *, 'ENTER THE NUMBER OF FREQ. POINTS: '
0010 C      ACCEPT *, NPOINT
0011 C      TYPE *, 'ENTER THE NUMBER OF SAMPLES AT EACH FREQ. '
0012 C      ACCEPT *, NSAMP2
0013 C      TYPE *, 'SET UP REFLECTING PLANE FOR TRANSFER FUNCTION MEASUREMENT'
0014 C      CALL SHDRT( TRANA, TRAMP, FSTART, FEND, NPOINT, NSAMP2 )
0015 C      TYPE *, '***** HIT RETURN TO PROCEED *****'
0016 C      TYPE *, 'STORE DATA ON DISC (Y OR N)'
0017 C      ACCEPT $00, C
0018 C      IF (C.EQ.'N') GOTO 300
0019 C      TYPE %01
0020 C      CALL ASSIGN( I2, -1, 'NEW', 'NC', 1 )
0021 C      WRITE( I2, *) FSTART
0022 C      WRITE( I2, *) FEND
0023 C      WRITE( I2, *) NPOINT
0024 C      DO 30 K=1, NPOINT
0025 C      WRITE( I2, *) TRANA(K)
0026 C      WRITE( I2, *) TRAMP(K)
0027 C      CONTINUE
0028 C      CALL CLOSE( I2 )
0029 C      GO TO 300
0030 C      TYPE %01
0031 C      CALL ASSIGN( I2, -1, 'OLD', 'NC', 1 )
0032 C      READ( I2, *) FSTART
0033 C      READ( I2, *) FEND
0034 C      READ( I2, *) NPOINT
0035 C      DO 100 K=1, NPOINT
0036 C      READ( I2, *) TRANA(K)
0037 C      READ( I2, *) TRAMP(K)
0038 C      CONTINUE
0039 C      CALL CLOSE( I2 )
0040 C      RETURN
0041 C      FORMAT (A1)
0042 C      FORMAT(//11, '**** SUBROUTINE SYS2 OBTAINS THE SYSTEM RESPONSE
0043 C      1 FILES ****')
  
```

THIS SUBROUTINE WILL READ IN THE SYSTEM RESPONSE FILES
 AND PLACE THEM IN A COMMON BLOCK TO BE PASSED TO OTHER
 ROUTINES

0044 900
 0045 900
 0046 900
 0047 900
 0048 900
 0049 900

0001 SUBROUTINE CORDAT
 THIS SUBROUTINE WILL TAKE THE DATA THAT WAS TAKEN FROM
 SPDAT AND CORRECT IT WITH THE DATA FROM SUBROUTINE
 SYSIMP, WHICH IS THE SYSTEM RESPONSE.

0002 VERSION 1.0 30-NOV-79
 0003 COMMON/OBJA/OBJA,OBJP,NSAMP2
 COMMON/SYSTA/TRANA,TRAMP,CLUTA,CLUTP,FSTART,FEND,NPOINT

0004 INTEGER OBJA(512),OBJP(512),TRANA(512),TRAMP(512)
 0005 INTEGER CLUTA(512),CLUTP(512),NPOINT,NSAMP2

 SUBTRACT ANTENNA CLUTTER FROM OBJECT DATA. THIS CLUTTER DATA
 MUST NOT!!! BE CORRECTED FOR THE SYSTEM TRANSFER FUNCTION
 THE NEXT STEP IS TO DIVIDE BY THE TRANSFER CHARACTERISTIC
 OF THE SYSTEM IN ARRAYS TRANA(AMPLITUDE) AND TRAMP(PHASE).

0006 *****
 0007 PI=3.1415926
 0008 DEG=PI/180
 0009 DO 100 K=1,NPOINT
 0010 TDBAMP=FLOAT(TRANA(K))*05
 0011 TDBAMP=FLOAT(TRAMP(K))*25*DEG
 0012 OBJPH=FLOAT(OBJA(K))*25*DEG

 0013 TDBAMP=>TRANSFER CHARACTERISTIC IN DBR.
 0014 TRPH=>PHASE OF TRANSFER CHARACTERISTIC IN RADIAN

 0015 ***** DIVIDE BY TRANSFER CHARACTERISTIC *****
 0016
 0017 ADDRES=OBJAMP-TDBAMP
 PRES=(OBJPH-TRPH)
 IF(PRES GT PI)PRES=PI-2*PI
 IF(PRES LT -PI)PRES=PI-2*PI

0018 ***** REPLACE DATA INTO INTEGER ARRAY *****
 0019
 0020 OBJA(K)=IFIX(20*ADDRES)
 0021 OBJP(K)=IFIX(10*PRES/DEG)*4.
 0022 CONTINUE
 0023 RETURN
 END

LOCAL VARIABLES: PSECT \$DATA, SIZE = 000066 (27 WORDS)

NAME	TYPE	OFFSET	NAME	TYPE	OFFSET
ADDRES	R=4	000044	DEG	R=4	000016
OBJPH	R=4	000040	OBJBAMP	R=4	000034
PRES	R=4	000050	TDBAMP	R=4	000024
			TRPH	R=4	000030

0001 SUBROUTINE SHDAT(OBJA,OBJP,FSTART,FEND,NPOINT,NSAMP2)
 THIS SUBROUTINE WILL OBTAIN DATA FOR AN OBJECT OVER THE FREQ
 RANGE SET WITH THE NUMBER OF POINTS SPECIFIED.

0002 INTEGER OBJA(512),OBJP(512),NPOINT,NSAMP2
 0003 INTEGER TRANA(512),TRAMP(512),CLUTA(512),CLUTP(512)

0004 STEP=(FEND-FSTART)/FLOAT(NPOINT)
 0005 CALL SHEEP(1,FSTART,1,4)
 0006 DO 100 K=1,NPOINT
 0007 FREQ=FSTART+FLOAT(K-1)*STEP
 0008 CALL SHEEP(1,FREQ,1,4)
 0009 CALL PHAMP2(1A,IP,NSAMP2)
 0010 OBJA(K)=IA-2048
 0011 OBJP(K)=IP-2048
 0012 CONTINUE
 0013 CALL SHEEP(1,FSTART,1,4)
 0014 RETURN
 0015 END

LOCAL VARIABLES: PSECT \$DATA, SIZE = 010040 (2064 WORDS)

NAME	TYPE	OFFSET	NAME	TYPE	OFFSET	NAME	TYPE	OFFSET
FEND	R=4	000006	FREQ	R=4	010026	FSTART	R=4	000004
1A	I=2	010032	IP	I=2	010034	K	I=2	010024
NPOINT	I=2	000010	NSAMP2	I=2	000012	STEP	R=4	010020

LOCAL AND COMMON ARRAYS:

NAME	TYPE	SECTION	OFFSET	SIZE	DIMENSIONS
CLUTA	I=2	\$DATA	004014	002000	(512) (512)
CLUTP	I=2	\$DATA	006014	002000	(512) (512)
OBJA	I=2	\$DATA	000000	002000	(512) (512)
OBJP	I=2	\$DATA	000002	002000	(512) (512)
TRANA	I=2	\$DATA	000014	002000	(512) (512)
TRAMP	I=2	\$DATA	002014	002000	(512) (512)

SUBROUTINES, FUNCTIONS, STATEMENT AND PROCESSOR-DEFINED FUNCTIONS.

NAME	TYPE	NAME	TYPE	NAME	TYPE	NAME	TYPE
FLOAT	R=4	PHAMP2	R=4	SHEEP	R=4		

FORTRAN IV V02.1-1 FRI 24-AUG-79 00:19:19

```

SUBROUTINE PHAMP2(IAMP,IPHASE,NUM)
  THIS ROUTINE WILL TAKE NUM READINGS FROM A/D CHANNELS
  0 AND 1 0=>PHASE 1=>AMPLITUDE
  AMP=0
  PHAS=0
  DO 5 J=1,200
    CONTINUE
  DO 10 Y=1,NUM
    IAMP=IADINP(0,1)
    IPHASE=IADINP(0,0)
    AMP=AMP+FLOAT(IAMP)
    PHAS=PHAS+FLOAT(IPHASE)
  DO 20 J=1,20
    CONTINUE
  CONTINUE
  IAMP=IFIX(IAMP/FLOAT(NUM))
  IPHASE=IFIX(IPHASE/FLOAT(NUM))
  RETURN
  END
  
```

FORTRAN IV STORAGE MAP FOR PROGRAM UNIT PHAMP2
 LOCAL VARIABLES. PSECT @DATA. SIZE = 000050 (20. WORDS)

NAME	TYPE	OFFSET	NAME	TYPE	OFFSET
AMP	R=4	000006	IAMP	I=2	000000
IPHASE	I=2	000002	IPHASE	I=2	000024
NUM	I=2	000020	NUM	I=2	000016

SUBROUTINES, FUNCTIONS, STATEMENT AND PROCESSOR-DEFINED FUNCTIONS.

NAME	TYPE	NAME	TYPE	NAME	TYPE
FLOAT	R=4	IADINP	I=2	IFIX	I=2

FORTRAN IV V02.1-1 FRI 24-AUG-79 00:18:52 PAGE 002

```

SUBROUTINE SHEEP(MODE,FREQ,IBAND,IEEENO)
  MODE IS THE SHEEPER MODE 1-9. MODE 1 IS DISCRETE MODE FOR SETTING
  THE CW FREQUENCY. OTHER MODES ARE OUTLINED IN THE SHEEPER IEEE
  MANUAL.
  IF MODE=10 THEN THE PROGRAM WILL RESET THE INTERFACE
  IF IBAND=4 THEN FULL SHEEP 2-18 OHZ OTHERWISE THE
  PROGRAM WILL COMPUTE THE NECESSARY BAND
  INITIALIZE IBAND2 AND MODE1 TO ZERO IN THE MAIN LINE
  
```

```

0002 BYTE CMD(17),MD(3),BND(3)
0003 DATA CMD(17)/'15',MD(3)/'15',BND(3)/'15/
0004 DATA CMD(11)/'V',/CMD(6)/'E',/MD(11)/'M',/BND(11)/'B'/
0005 IF (MODE=10) 3,2,3
0006 CALL IBIFC
0007 GO TO 2000
0008 IF (MODE=MODE1) 5,10,5
0009 ENCODE(1,1000,MD(2)) MODE
0010 CALL IBIFC
0011 CALL ISEEN
0012 CALL ISEND(MD,IEEENO)
0013 DO 8 ITER=1,500
0014 CONTINUE
0015 MODE1=MODE
0016 IF (IBAND=4) 25,20,25
0017 IF (IBAND=4) 25,20,25
0018 IF (IBAND=4) 25,20,25
0019 IF (FREQ GE 2.00) AND (FREQ LT 6.05)) IBAND1=1
0020 IF (FREQ GE 6.05) AND (FREQ LT 12.4)) IBAND1=2
0021 IF (FREQ GE 12.4) AND (FREQ LT 18.01), IBAND1=3
0022 IF (IBAND2=IBAND1) 36,38,36
0023 ENCODE(1,1000,BND(2)) IBAND1
0024 CALL ISEND(BND,IEEENO)
0025 IBAND2=IBAND1
0026 GO TO (40,50,60,70),IBAND1
0027 B0=2,00022
0028 B1=4,18734E-04
0029 B2=1,27261E-10
0030 GO TO 80
0031 B0=5,99786
0032 B1=6,38009E-04
0033 B2=2,03858E-10
0034 GO TO 80
0035 B0=12,0018
0036 B1=5,96325E-04
0037 B2=9,44848E-11
0038 GO TO 80
0039 B0=1,99636
0040 B1=1,59929E-03
0041 B2=6,01267E-11
0042
0043
0044
  
```

FORTRAN IV V02.1-1 FRI 24-AUG-79 00:18:52 PAGE 002
 THESE CONSTANTS WERE DERIVED USING PROGRAM CALAB BAS ON
 AUG-24-1979


```

0045 C
0046 IV1=IFIX((-B1+SQRT(B1**2-4*B2*(B0-FREQ)))/(2*B2))
0047 ETCODE(4,1001,CND(2)) IV1
0048 CALL IBSEND(CND,IEEENO)
0049 DO 90 ITER=1,200
0050 CONTINUE
0051 FORMAT(I1)
0052 RETURN
0053 END

```

DELAY OF 5.32 NS TO STEP

```

FORTRAN IV STORAGE MAP FOR PROGRAM UNIT SHEEP
LOCAL VARIABLES: PSECT SDATA, SIZE = 000070 ( 28 WORDS)
NAME TYPE OFFSET NAME TYPE OFFSET
B0 R*4 000036 B1 R*4 000042 B2 R*4 000046
FREQ R*4 000002 IBAND I*2 000004 IBAND1 I*2 000032
IBAND2 I*2 000034 IEEENO I*2 000006 ITER I*2 000030
IV1 I*2 000052 MODE I*2 000000 MODE1 I*2 000026

```

LOCAL AND COMMON ARRAYS:

```

NAME TYPE SECTION OFFSET SIZE DIMENSIONS
CND L*1 SDATA 000022 000003 ( 2 ) (3)
CND L*1 SDATA 000010 000007 ( 4 ) (7)
PID L*1 SDATA 000017 000003 ( 2 ) (3)

```

SUBROUTINES, FUNCTIONS, STATEMENT AND PROCESSOR-DEFINED FUNCTIONS.

```

NAME TYPE NAME TYPE NAME TYPE NAME TYPE
IBIFC I*2 IBREN I*2 IBSEND I*2 IFIX I*2 SORT R*4

```

```

10 DIM A(500), B(500), F(500)
20 DIM B$(20)
30 PRINT 'INPUT DATA FILE NAME',
40 INPUT A$
50 PRINT 'DATE: ', DATE$
60 OPEN A$ FOR INPUT AS FILE #1
70 INPUT #1, B$
90 B$=SEG$(B$, 5, 20)
90 F1=VAL(B$)
100 INPUT #1, F2 \ INPUT #1, N
110 PRINT 'START FREQ. GHZ. ', F1, ' STOP FREQ. GHZ. ', F2, ' DATA POINTS ', N
120 FOR I=0 TO N-1
130 D=(F2-F1)/N
140 INPUT #1, A
150 A(I)=A$.OS
160 INPUT #1, B
170 B(I)=B$.25
180 F(I)=F1+I*D
190 NEXT I
200 F(N-1)=F2
210 REGION('UPPER', 1)
220 REGION('LOWER', 2)
230 GRAPH('LINES', N, F(1), A(1), 1)
240 LABEL('UNDERLINE', 'AMPLITUDE IN DB', 1)
250 GRAPH('LINES', N, F(1), B(1), 2)
260 LABEL('UNDERLINE', 'PHASE IN DEGREES', 2)
270 LINPUT I$
280 DISPLAY+CLEAR
290 CLOSE #1
300 GO TO 30
310 END

```

APPENDIX II

```

0059 ACCEPT 700,ANS
0060 IF (ANS.EQ.'N') GO TO 1000
0061 TYPE *,'ENTER THE NAME FOR DATA FILE:'
0062 CALL ASSIGN(20,*,',NEH',NC',1,1)
0063 WRITE (20,*)NUMPTS
0064 WRITE (20,*)FSTART
0065 WRITE (20,*)FEND
0066 WRITE (20,*)KAS
0067 WRITE (20,*)KAE
0068 WRITE (20,*)KPI
0069 WRITE (20,*)KAX
0070 WRITE (20,*)KAY
0071 DO 200 I=1,NUMPTS
0072   N=I
0073   WRITE (20,*)MAG(N)
0074   WRITE (20,*)ANGLE(N)
0075 CONTINUE
0076 200
0077 800
0078 810
0079 811
0080 801
0081 700
0082 1000
0083 END

```

```

LOCAL VARIABLES. PSECT $DATA, SIZE = 010134 ( 2094, WORDS)
NAME TYPE OFFSET NAME TYPE OFFSET NAME TYPE OFFSET
A R#4 010026 AMP R#4 010074 ANG R#4 010110
ANS L#1 010024 C R#4 010000 CPI R#4 010104
F C#8 010004 FEND R#4 010036 FREQ R#4 010060
FSTART R#4 010032 I I#2 010070 IPOL I#2 010046
IUNIT I#2 010052 KAE R#4 010020 KAS R#4 010014
N I#2 010072 NUMPTS I#2 010050 REA R#4 010100
STEPF R#4 010064 STEPK R#4 010054 WAV R#4 010042
COMMON BLOCK /, SIZE = 000050 ( 20, WORDS)
NAME TYPE OFFSET NAME TYPE OFFSET NAME TYPE OFFSET
S01 C#8 000000 S02 C#8 000010 S03 C#8 000020
S04 C#8 000030 S05 C#8 000040 S06 C#8 000050
COMMON BLOCK /SCT, SIZE = 000024 ( 10, WORDS)
NAME TYPE OFFSET NAME TYPE OFFSET NAME TYPE OFFSET
FTHETA C#8 000000 FPSI C#8 000010 PSI R#4 000020
LOCAL AND COMMON ARRAYS:

```

```

FORTRAN IHW02 1-1 SUN 21-OCT-79 02:12:32 PAGE 001
0001 PROGRAM BISCAT
0002 COMMON /SCT/THETA, FPSI, PSI
0003 COMMON S01, S02, S03, S04, S05, S06, S07, S08, S09, S10, S11, S12, S13, S14, S15, S16, S17, S18, S19, S20, S21, S22, S23, S24, S25, S26, S27, S28, S29, S30, S31, S32, S33, S34, S35, S36, S37, S38, S39, S40, S41, S42, S43, S44, S45, S46, S47, S48, S49, S50, S51, S52, S53, S54, S55, S56, S57, S58, S59, S60, S61, S62, S63, S64, S65, S66, S67, S68, S69, S70, S71, S72, S73, S74, S75, S76, S77, S78, S79, S80, S81, S82, S83, S84, S85, S86, S87, S88, S89, S90, S91, S92, S93, S94, S95, S96, S97, S98, S99, S100
0004 COMPLEX S01, S02, S03, S04, S05, S06, S07, S08, S09, S10, S11, S12, S13, S14, S15, S16, S17, S18, S19, S20, S21, S22, S23, S24, S25, S26, S27, S28, S29, S30, S31, S32, S33, S34, S35, S36, S37, S38, S39, S40, S41, S42, S43, S44, S45, S46, S47, S48, S49, S50, S51, S52, S53, S54, S55, S56, S57, S58, S59, S60, S61, S62, S63, S64, S65, S66, S67, S68, S69, S70, S71, S72, S73, S74, S75, S76, S77, S78, S79, S80, S81, S82, S83, S84, S85, S86, S87, S88, S89, S90, S91, S92, S93, S94, S95, S96, S97, S98, S99, S100
0005 REAL*4 VA, MAG(512), ANGLE(512), KAS, KAE, PSI, THETA
0006 BYTE ANS
0007 DATA C/Z, 997925E+10/
0008
0009 TYPE *, 'ENTER SPHERE RADIUS (A) (CM):'
0010 ACCEPT *, A
0011 TYPE *, 'ENTER STARTING FREQ (GHZ):'
0012 ACCEPT *, FSTART
0013 TYPE *, 'ENTER ENDING FREQ (GHZ):'
0014 ACCEPT *, FEND
0015 WAV=2*3.1415926*(1.0E+9/C)
0016 KAS=FSTART*WAV*A
0017 KAE=FEND*WAV*A
0018 TYPE *, 'ENTER SCATTERING ANGLE THETA (DEGREES):'
0019 ACCEPT *, THETA
0020 THETA=THETA*3.1415926/180.0
0021 TYPE *, 'ENTER POLARIZATION SCATTERING ANGLE PSI (DEGREES):'
0022 ACCEPT *, PSI
0023 PSI=PSI*3.1415926/180.0
0024 TYPE *, 'IN WHICH POLARIZATION CALCULATE FIELD (0=>THETA, 1=>PSI):'
0025 ACCEPT *, IPOL
0026 TYPE *, 'ENTER NUMBER OF POINTS'
0027 ACCEPT *, NUMPTS
0028 TYPE *, 'ENTER LOGICAL UNIT NUMBER FOR OUTPUT'
0029 ACCEPT *, IUNIT
0030 WRITE (IUNIT, 800)A, FSTART, KAS, FEND, KAE, NUMPTS, THETA*(180./3.1415926)
0031 IF (IPOL.EQ.0) WRITE (IUNIT, 810)
0032 IF (IPOL.EQ.1) WRITE (IUNIT, 811)
0033 WRITE (IUNIT, 801)
0034
0035 STEPK=(VAE-YAS)/NUMPTS
0036 FREQ=FSTART
0037 STEPF=(FEND-FSTART)/NUMPTS
0038 KA=KAS
0039 DO 100 I=1, NUMPTS
0040   N=I
0041   CALL BSCAT
0042   IF (IPOL.EQ.0) F=FTHETA
0043   IF (IPOL.EQ.1) F=FPSI
0044   AMP=COS(F)
0045   REA=REAL(F)
0046   CPI=ATN(REAL(F)/
0047     MAG(N)*AMP)
0048   ANG=ATN2(CPI, REA)*(180./3.1415926)
0049   MAG(N)=AMP
0050   ANGLE(N)=ANG
0051   IF (AMP.EQ.0) AMP=1.0E-35
0052
0053 WRITE (IUNIT, *)N, FREQ, KA, 10*ALOG10(AMP), ANG
0054 FREQ=FREQ+STEPF
0055 KA=KA+STEPK
0056 CONTINUE
0057 100
0058 TYPE *, 'STORE DATA FOR DISPLAY (Y OR N) : '

```

```

0059 ACCEPT 700,ANS
0060 IF (ANS.EQ.'N') GO TO 1000
0061 TYPE *,'ENTER THE NAME FOR DATA FILE:'
0062 CALL ASSIGN(20,*,',NEH',NC',1,1)
0063 WRITE (20,*)NUMPTS
0064 WRITE (20,*)FSTART
0065 WRITE (20,*)FEND
0066 WRITE (20,*)KAS
0067 WRITE (20,*)KAE
0068 WRITE (20,*)KPI
0069 WRITE (20,*)KAX
0070 WRITE (20,*)KAY
0071 DO 200 I=1,NUMPTS
0072   N=I
0073   WRITE (20,*)MAG(N)
0074   WRITE (20,*)ANGLE(N)
0075 CONTINUE
0076 200
0077 800
0078 810
0079 811
0080 801
0081 700
0082 1000
0083 END

```

THIS SUBROUTINE WILL CALL SUBROUTINES BSCAT1-BSCAT4 FOR THE CALCULATION OF THE BISTATIC SCATTERING OF A PERFECTLY CONDUCTING SPHERE IT WILL RETURN THE SCATTERING COEFFICIENT F AS A FUNCTION OF SCATTERING ANGLE THETA AND ANGLE PSI.
 THE SCATTERED FIELD AMPLITUDE IN THE THETA AND PSI POLARIZATIONS ARE FTHETA AND FPSI

COMMON/SCT/FTHETA, FPSI, PSI
 COMMON S01, S02, SC1, SC2, KA, THETA
 COMPLEX B1, B2, B3, B4
 REAL *4 YA, THETA, PSI

IF (YA GT (4)) GO TO 100
 CALL BSCAT1
 FTHETA=COS(PSI)*SC1
 FPSI=-SIN(PSI)*SC2
 GO TO 1000
 IF (YA GT (1. 0)) GO TO 200
 CALL BSCAT2
 FTHETA=COS(PSI)*SC1
 FPSI=-SIN(PSI)*SC2
 GO TO 1000
 IF (YA GT (20. 0)) GO TO 300
 CALL BSCAT3
 B1=S01*SC1
 B2=S02*SC2
 FTHETA=COS(PSI)*B1
 FPSI=-SIN(PSI)*B2
 GO TO 1000
 CONTINUE

PSI>20. 0
 CALL BSCAT4
 FTHETA=COS(PSI)*SC1
 FPSI=-SIN(PSI)*SC2
 RETURN
 END

LOCAL VARIABLES: PSECT \$DATA, SIZE = 000040 (16. WORDS)

NAME	TYPE	OFFSET	NAME	TYPE	OFFSET
B1	C*8	000000	B2	C*8	000010
B4	C*8	000030	B3	C*8	000020

COMMON BLOCK / , SIZE = 000050 (20. WORDS)

NAME	TYPE	OFFSET	NAME	TYPE	OFFSET
------	------	--------	------	------	--------

THIS SUBROUTINE CALCULATES S1 AND S2 FOR A PERFECTLY CONDUCTING SPHERE IN THE RANGE KA < 4 AS A FUNCTION OF THETA THE BISTATIC SCATTERING ANGLE

COMMON S01, S02, SC1, SC2, KA, THETA
 COMPLEX S01, S02, SC1, SC2
 REAL *4 KA, THETA

SC1=KA**3*(1. 5+COS(THETA))
 SC2=KA**3*(1. 5-COS(THETA)+1.)
 RETURN
 END

COMMON BLOCK / , SIZE = 000050 (20. WORDS)

NAME	TYPE	OFFSET	NAME	TYPE	OFFSET
S01	C*8	000000	S02	C*8	000010
SC2	C*8	000030	KA	R*4	000040

SUBROUTINES, FUNCTIONS, STATEMENT AND PROCESSOR-DEFINED FUNCTIONS.

NAME	TYPE	NAME	TYPE	NAME	TYPE
COS	R*4				

FORTMAN IW02 1-1 SIN 21-OCT-79 38:24:50 PAGE 001
SUBROUTINE BSCAT2

THIS PROGRAM WILL CALCULATE THE SCATTERING CONSTANTS
OF A PERFECTLY CONDUCTING SPHERE IN THE RANGE
4/3 < KA < 1 AS A FUNCTION OF BISTATIC ANGLE THETA
SEE RADAR CROSS-SECTION HANDBOOK GEORGE T RUCK ED.
PLENUM PRESS 1970.

COMMON S01, S02, SC1, SC2, KA, THETA
COMPLEX S01, S02, SC1, SC2
REAL KA, THETA

T1= 5+COS(THETA)

T2=(3-(11.0/45.0)*COS(THETA)+(1.0/12.0)*COS(2*THETA))*KA**2

T3=(1.0/120.0)*((1907.0/70.0)-(2531.0/105.0)*COS(THETA)+
1157.0/42.0)*COS(2*THETA)+(1.0/3.0)*COS(3*THETA))*KA**4

T4=KA**6*((1.0/6.0)*((4*COS(THETA)-1)+(1.0/3.0)*((1+2*COS(THETA))
1*KA**2))

SC1R=KA**3*(T1-T2+T3)
SC1I=T4
SC1=CMPLX(SC1R, SC1I)

C1= 5+COS(THETA)+1

C2=(3-(29.0/60.0)*COS(THETA)-(1.0/18.0)*COS(2*THETA))*KA**2

C3=(1.0/60.0)*((1343.0/105.0)+(3769.0/280.0)*COS(THETA)+
1157.0/63.0)*COS(2*THETA)+(1.0/8.0)*COS(3*THETA))*KA**4

C4=KA**6*((1.0/6.0)*((4-COS(THETA))* 2*(COS(THETA)+2)*KA**2)

SC2R=KA**3*(C1+C2+C3)

SC2I=C4

SC2=CMPLX(SC2R, SC2I)

RETURN
END

LOCAL VARIABLES: PSECT 9DATA, SIZE = 000110 (36. WORDS)

NAME	TYPE	OFFSET	NAME	TYPE	OFFSET
C1	R=4	000030	C2	R=4	000034
C4	R=4	000044	SC1I	R=4	000024
			SC1R	R=4	000020

FORTMAN IW02 1-1 SUBROUTINE BSCAT3 PAGE 001

THIS SUBROUTINE FINDS THE SCATTERING COEFFICIENTS SC1, SC2, SC1, SC2
USING A POLYNOMIAL APPROXIMATION IN THE RESONANCE REGION
FOR A PERFECTLY CONDUCTING SPHERE. RANGE 10<KA<20. KA=RAE VECTOR
A=RADIUS OF SPHERE THETA=BISTATIC SCATTERING ANGLE

COMMON S01, S02, SC1, SC2, KA, THETA
COMPLEX S01, S02, SC1, SC2
COMPLEX T1, T2, T3, T4, T5, T6, B1, B2, B3, CON
COMPLEX CON1, CON2, CON3, CON4, C1, C2, C3, C4, C5, C6, C7, C9
COMPLEX C11, C12, C13, C14, C15, XT, XTH
COMPLEX CON5, CON6, CON7, CON8, CON9
REAL *4 KA, THETA
CON=(0.0, 1.0)

X=KA

X3=X**3

XM3=X**(-2.0/3.0)

COST2=COS(THETA/2.0)

SINT2=SIN(THETA/2.0)

COS1=COS(THETA)

XT=CON*THETA*X

XTM=X*XT

PI=3.1415926

PT=(PI-THETA)

PTM=(PI-THETA)

P1=-2*KA+COST2

T1=(KA/2)*CEXP(CON*P1)

P2=-1/(2*KA*(COST2**3))

T2=1.0*CON*P2

T3=(7.0/(4*(KA**2)))*((SINT2**2)/(COST2**6))

S01=T1*(T2-T3)

P4=-COST/(2*KA*(COST2**3))

T4=(1.0*CON*P4)

T5=(1.0/(4*(KA**2)))*((6.0+COST)*(SINT2**2)/
1(COST2**6))

S02=T1*(T4+T5)

***** CALCULATE CREEPING WAVE TERMS *****

X=KA

P1=PI*(X+(1.0/12.0))

B1=CEXP(CON*P1)

B2=-CON*X3*SQRT(X/(2*PI*SINT))

C1=B2*B1

```

0038 CON1=( 932506./1.616911)
0039 C2=2 715175*(X23*CON1)
0040 P1=( 8750/(X*THETA)))
0041 C3=(1 9-CON*P1)
0042 CON2=( 700283.-.404308)
0043 CON3=( 141774..081853)
0044 B2=PTM(X3)*CON2
0045 B3=PTM(XM3)*CON3
0046 C4=CERP(XTM-B2*B3)
0047 C5=CON*(1 0+CON*P1)
0048 B2=PTM(X3*CON2
0049 B3=PTM(XM3*CON3
0050 C4=CERP(XTM-B2*B3)
0051 T1=C2*(C3+C4)-(C5*C6))
0052 CON4=(1 032306./1.788026)
0053 CON5=(2 232697.-1.289048)
0054 CON6=(.141482..081684)
0055 C7=1 991727*(XM23)*CON4
0056 B2=PTM(X3*CON5
0057 B3=PTM(XM3*CON6
0058 C9=CERP(XTM-B2*B3)
0059 B2=PTM(X3*CON5
0060 B3=PTM(XM3*CON6
0061 C11=CERP(XTM-B2*B3)
0062 T2=C7*(C3+C9)-(C5*C6))
0063 CON7=(1 607133.-.927879)
0064 CON8=(.069415..057397)
0065 C12= 201776/(X*SINT)
0066 B2=PTM(X3*CON7
0067 B3=PTM(XM3*CON8
0068 C13=CERP(XTM-B2*B3)
0069 B2=PTM(X3*CON7
0070 B3=PTM(XM3*CON8
0071 C14=CERP(XTM-B2*B3)
0072 T3=C12*(C13-CON*C14)
0073 SC1=C1*(T1+T2+T3)
0074 ***** CALCULATE SECOND CREEPING WAVE TERM *****
0075 C1=C1
0076 P2= 339397/(X*SINT)

```

```

0076 C TA=P2*(C4-CON*C6)
0077 P2= 175966/(X*SINT)
0078 T5=P2*(C9-CON*C11)
0079 CON9=(. 848747./1.470073)
0080 C15=1.614208*(XM23*CON9
0081 T6=C15*(C3*C13)-(C5*C14))
0082 SC2=C1*(T4+T5+T6)
0083 RETURN
0084 END

```

LOCAL VARIABLES: PSECT \$DATA, SIZE = 000730 (236. WORDS)

NAME	TYPE	OFFSET	NAME	TYPE	OFFSET	NAME	TYPE	OFFSET
B1	C#8	000060	B2	C#8	000070	B3	C#8	000100
CON	C#8	000110	CON1	C#8	000120	CON2	C#8	000150
CON3	C#8	000140	CON4	C#8	000150	CON5	C#8	000200
CON6	C#8	000360	CON7	C#8	000370	CON8	C#8	000400
CON9	C#8	000410	COST	R#4	000454	COST2	R#4	000480
C1	C#8	000160	C11	C#8	000260	C12	C#8	000270
C13	C#8	000300	C14	C#8	000310	C15	C#8	000320
C2	C#8	000170	C3	C#8	000200	C4	C#8	000210
C5	C#8	000220	C6	C#8	000230	C7	C#8	000240
C9	C#8	000250	PI	R#4	000460	PT	R#4	000464
PTM	R#4	000470	P1	R#4	000474	P2	R#4	000478
P4	R#4	000504	SINT	R#4	000450	SINT2	R#4	000484
T1	C#8	000000	T2	C#8	000010	T3	C#8	000020
T4	C#8	000030	T5	C#8	000040	T6	C#8	000050
X	R#4	000420	XM23	R#4	000434	XM3	R#4	000450
XT	C#8	000330	XTM	C#8	000340	X3	R#4	000424
COMMON BLOCK / /, SIZE = 000050 (20. WORDS)								
NAME	TYPE	OFFSET	NAME	TYPE	OFFSET	NAME	TYPE	OFFSET
S01	C#8	000000	S02	C#8	000010	SC1	C#8	000020
SC2	C#8	000030	KA	R#4	000040	THETA	R#4	000044

SUBROUTINES, FUNCTIONS, STATEMENT AND PROCESSOR-DEFINED FUNCTIONS

NAME TYPE NAME TYPE NAME TYPE NAME TYPE NAME TYPE
 CEMP C=8 C=8 R=4 SIN R=4 SQRT R=4 TAN R=4

FORTTRAN IJW02 1-1 SIN 21-OCT-79 38:26:12 PAGE 001
 SUBROUTINE BSCAT4

C THIS SUBPROGRAM WILL CALCULATE BISTATIC SCATTERING
 C COEFFICIENTS FOR THE PERFECTLY CONDUCTING SPHERE. IN THE
 C RANGE KA<20

C COMMON S01, S02, SC1, SC2, KA, THETA
 C COMPLEX S01, S02, SC1, SC2, C1
 C REAL KA, THETA

C P1=2*KA*COS(THETA/2)
 C C1=CMPLX(0.0, -PI)
 C SC1=-56*KA*CEXP(C1)
 C SC2=SC1
 C RETURN
 C END

C LOCAL VARIABLES: PSECT SDATA, SIZE = 000024 (10. WORDS)

NAME TYPE OFFSET NAME TYPE OFFSET NAME TYPE OFFSET

C1 C=8 000000 P1 R=4 000010

COMMON BLOCK / /, SIZE = 000050 (20. WORDS)

NAME TYPE OFFSET NAME TYPE OFFSET NAME TYPE OFFSET

S01 C=8 000000 S02 C=8 000010 SC1 C=8 000020

SC2 C=8 000030 KA R=4 000040 THETA R=4 000044

SUBROUTINES, FUNCTIONS, STATEMENT AND PROCESSOR-DEFINED FUNCTIONS.

NAME TYPE NAME TYPE NAME TYPE NAME TYPE NAME TYPE

CEMP C=8 CMPLX C=8 C=8 R=4

FORTTRAN IJW02 1-1 THU 18-OCT-79 00:04:05 PAGE 001
 PROGRAM SPSCAT

C COMMON KA, F
 C COMPLEX F
 C REAL KA, MAG(S12), ANGLE(S12), KAS, KAE
 C BYTE ANS
 C DATA C/2, 9*7925E+10/

C TYPE *, ENTER SPHERE RADIUS (A) (CM.):

0007 ACCEPT *, A

0008 TYPE *, ENTER STARTING FREQ (GHZ):

0009 ACCEPT *, FSTART

0010 TYPE *, ENTER ENDING FREQ (GHZ):

0011 ACCEPT *, FEND

0012 MAV=2*3.1415926*(1.0E+9/C)

0013 KAS=FSTART*MAV*KA

0014 KAE=FEND*MAV*KA

0015 TYPE *, ENTER NUMBER OF POINTS

0016 ACCEPT *, NUMPTS

0017 TYPE *, ENTER LOGICAL UNIT NUMBER FOR OUTPUT

0018 ACCEPT *, IUNIT

0019 WRITE (IUNIT, 800) A, FSTART, KAS, FEND, KAE, NUMPTS

0020 WRITE (IUNIT, 801)

0021

C STEPK=(KAE-KAS)/NUMPTS

0022 FREQ=FSTART

0023 STEPF=(FEND-FSTART)/NUMPTS

0024 KA=KAS

0025 DO 100 I=1, NUMPTS

0026 N=1

0027 CALL SCAT

0028 AMP=CABS(F)

0029 REA=REAL(F)

0030 CPI=AIMAG(F)

0031 ANG=ATAN2(CPI, REA)*(180./3.1415926)

0032 MAG(N)=AMP

0033 ANGLE(N)=ANG

0034 WRITE (IUNIT, *) N, FREQ, KA, 10*ALOG10(AMP), ANG

0035 FREQ=FREQ+STEPF

0036 KA=KA+STEPK

0037 CONTINUE

0038 TYPE *, STORE DATA FOR DISPLAY (Y OR N):

0039 ACCEPT 700, ANS

0040 IF (ANS.EQ.'N') GO TO 1000

0041 TYPE *, ENTER THE NAME FOR DATA FILE:

0042 CALL ASSIGN(20, 1, 'NEW', 'NC', 1, 1)

0043 WRITE (20, *) NUMPTS

0044 WRITE (20, *) FSTART

0045 WRITE (20, *) FEND

0046 WRITE (20, *) A

0047 DO 200 I=1, NUMPTS

0048 N=I

0049 WRITE (20, *) MAG(N)

0050 WRITE (20, *) ANGLE(N)

```

0054 200 CONTINUE
0055 800 FORMAT(//)
1' START KAA='F15.7/' FSTART='F15.7/' END KAA='F15.7/'
2' NUMPTS='I7//)' FEND='F15.7/'
0056 901 FORMAT(//73(' '))// POINT #,' FREQUENCY ',' K#A
1' AMP DB '//'73(' '))//
0057 700 FORMAT (A1)
0058 1000 STOP '+++++ END OF PROGRAM +++++'
0059 END

```

LOCAL VARIABLES, PSECT 9DATA, SIZE = 010112 (2085. WORDS)

NAME	TYPE	OFFSET	NAME	TYPE	OFFSET	NAME	TYPE	OFFSET
A	R#4	010016	AMP	R#4	010062	ANG	R#4	010076
ANS	L#1	010014	C	R#4	010000	CPX	R#4	010072
FEND	R#4	010026	FREQ	R#4	010046	FSTART	R#4	010022
I	I#2	010056	IUNIT	I#2	010040	KAE	R#4	010010
KAE	R#4	010004	N	I#2	010060	NUMPTS	I#2	010055
PEA	R#4	010066	STEPF	R#4	010052	STEPK	R#4	010042
WAV	R#4	010032						

Common BLOCK / /, SIZE = 000014 (6 WORDS)

NAME	TYPE	OFFSET	NAME	TYPE	OFFSET	NAME	TYPE	OFFSET
V#	R#4	000000	F	C#8	000004			

LOCAL AND COMMON ARRAYS:

NAME	TYPE	SECTION	OFFSET	SIZE	DIMENSIONS
TABLE	R#4	9DATA	004000	(1024)	(512)
W#	R#4	9DATA	000000	(1024)	(512)

SUBROUTINES, FUNCTIONS, STATEMENT AND PROCESSOR-DEFINED FUNCTIONS

NAME	TYPE	NAME	TYPE	NAME	TYPE	NAME	TYPE
AIMAG	R#4	ALOG10	R#4	ASSION	R#4	ATAN2	R#4
REAL	R#4	SCAT	R#4			CABS	R#4

THIS PROGRAM WILL CALCULATE THE SCATTERED FIELD FROM A PERFECTLY CONDUCTING SPHERE THIS IS A FAR FIELD APPROXIMATION AFTER RADAR CROSS SECTION HANDBOOK GEORGE T. RUCK EDITOR PLENUM PRESS 1970. PAGES 146-150
VERSION 1 3 OCT-17-79

```

COMMON KA,F
COMPLEX F,T1,T2,T3,C1,C2,C3,C4,C5,C6,C7
COMPLEX CON,CON1,CON2,CON3,CON4,B1,B2,F01,FC1
COMPLEX CON5,CON6,CON7,CON8,CON9
REAL KA
CON=(0,0,1,00)
IF (KA GT .4) GO TO 100
P1=(3,0/2,0)*(KA)**3
F=CHPLX(P1,0,0)
GO TO 1000
0007 C
0008 IF (KA GT (.8)) GO TO 200
P1=(3,0/2,0)*(KA**2,0)*(1-(5,0/54,0)*(KA**2))*(17,0/750,0)
1(KA**4)-(6,651923E+06/11,907E+06)*(KA**6)
P2=(1,0/2,0)*(KA**6)*(1+(6,0/5,0)*(KA**2))
F=CHPLX(P1,P2)
GO TO 1000
0013 100
0015 IF (KA GT (.8)) GO TO 200
P1=(3,0/2,0)*(KA**2,0)*(1-(5,0/54,0)*(KA**2))*(17,0/750,0)
1(KA**4)-(6,651923E+06/11,907E+06)*(KA**6)
P2=(1,0/2,0)*(KA**6)*(1+(6,0/5,0)*(KA**2))
F=CHPLX(P1,P2)
GO TO 1000
0016 C
0017 IF (KA GT 20) GO TO 300
***** OPTICAL TERM C1 *****
0019 C
0021 Y=KA
0022 B1=CON*(1/2*Y)
0023 B2=CON*(-2*Y)
0024 F01=(Y/2)*CEXP(B2)*(1,0-B1)
***** (KEEPING WAVE TERM FC1) *****
0025 C
0026 Y3=KA**3/1,0/2,0)
0027 YM2=KA**2/1,0/2,0)
0028 YM3=KA**1/2,0/3,0)
0029 C0A1=741196,1,283788)
0030 CON2=(2,000002,-1,170172)
0031 CON3=(44586,1,257150)
0032 CON4=-93454,1,170000)
0033 CON5=(7,014224,-4,049663)
0034 CON6=(434877,256419)
0035 CON7=(759921,1,383588)
0036 CON8=(5,048974,-9,915014)
0037 CON9=(312321,180319)
0038 P1=P1*(Y-(1,0/6,0))
0039 P1=CON*(P1)
0040 C1=CON*(Y**4,0/2,0)*CEXP(B1)
0041 C2=1,357588*(CON1*KM23)

```

U.S. PATENT OFFICE PATENT APPLICATION NO. 3,500,000

FORTRAN IWA02.1-1 WED 02-APR-80 00:02:41 PAGE 001
PROGRAM ANTPAT

AUTHOR C. WERNER 6-MAR-80

THIS PROGRAM WILL MEASURE THE PATTERN OF AN ANTENNA USING
A STEPPER MOTOR CONTROLLED TURNTABLE AND THE HEMLETT-PACKARD
8620C MICROHAVE SNEEPER AND 8410B NETWORK ANALYZER IN THE
RANGE OF 2-18 GHZ.

INTEGER AMP(512), PHA(512)
BYTE STRING

TYPE *, '***** ANTENNA PATTERN MEASUREMENT SYSTEM *****'
TYPE *, 'OLD OR NEW DATA? (0=>OLD 1=>NEW)'
ACCEPT *, IFLAG

IF IFLAG EQ 0 GO TO 500
TYPE *, 'ENTER THE FREQUENCY OF OPERATION IN GHZ.'
ACCEPT *, FORT
TYPE *, 'ENTER THE NUMBER OF DATA POINTS.'
ACCEPT *, N
TYPE *, 'ENTER THE NUMBER OF SAMPLES/DATA POINT.'
ACCEPT *, NSAMP
TYPE *, 'ENTER THE ANTENNA SHEEP IN DEGREES.'
ACCEPT *, ANGLE
TYPE *, 'ENTER THE FILENAME FOR THE DATA.'
CALL ASSIGN(15, '-1, NEW, INC', 1, 1)
TYPE *, '***** IS THE ANTENNA POSITIONED ? *****'
PAUSE '***** HIT RETURN TO CONTINUE *****'
THETA=ANGLE*3.1415926/180.
DTHETA=THETA/(N-1)
A=0
CALL SHEEP(1, FORT, 1, 4)
CALL STEP2(THETA/2, 0, 1)
DO 100 I=1, N
INDEX=I
CALL PHAMP2(1A, IP, NSAMP)
AMP(INDEX)=1A-2048
PHA(INDEX)=IP-2048
CALL STEP2(DTHETA, 0)
CONTINUE
CALL STEP2(THETA/2, 0, 1)
WRITE(15, *) FORT
WRITE(15, *) ANGLE
WRITE(15, *) NSAMP
DO 200 J=1, N
WRITE(15, *) AMP(J)
WRITE(15, *) PHA(J)
CONTINUE
CALL SHEEP(10, FORT, 1, 4)

GO TO 700
TYPE *, 'ENTER FILENAME FOR DATA.'

0001 C
0002 C
0003 C
0004 C
0005 C
0006 C
0007 C
0008 C
0009 C
0010 C
0011 C
0012 C
0013 C
0014 C
0015 C
0016 C
0017 C
0018 C
0019 C
0020 C
0021 C
0022 C
0023 C
0024 C
0025 C
0026 C
0027 C
0028 C
0029 C
0030 C
0031 C
0032 C
0033 C
0034 C
0035 C
0036 C
0037 C
0038 C
0039 C
0040 C
0041 C
0042 C
0043 C
0044 C
0045 C
0046 C
0047 C
0048 C
0049 C
0050 C
0051 C
0052 C
0053 C
0054 C
0055 C
0056 C
0057 C
0058 C
0059 C
0060 C
0061 C
0062 C
0063 C
0064 C
0065 C
0066 C
0067 C
0068 C
0069 C
0070 C
0071 C
0072 C
0073 C
0074 C
0075 C
0076 C
0077 C
0078 C
0079 C
0080 C
0081 C
0082 C
0083 C
0084 C
0085 C
0086 C
0087 C
0088 C
0089 C
0090 C
0091 C
0092 C
0093 C
0094 C
0095 C
0096 C
0097 C
0098 C
0099 C
0100 C

0042 C
0043 C
0044 C
0045 C
0046 C
0047 C
0048 C
0049 C
0050 C
0051 C
0052 C
0053 C
0054 C
0055 C
0056 C
0057 C
0058 C
0059 C
0060 C
0061 C
0062 C
0063 C
0064 C
0065 C
0066 C
0067 C
0068 C
0069 C
0070 C
0071 C
0072 C
0073 C
0074 C
0075 C
0076 C
0077 C
0078 C
0079 C
0080 C
0081 C
0082 C
0083 C
0084 C
0085 C
0086 C
0087 C
0088 C
0089 C
0090 C
0091 C
0092 C
0093 C
0094 C
0095 C
0096 C
0097 C
0098 C
0099 C
0100 C

LOCAL VARIABLES: PSECT DATA, SIZE = 000424 (139 WORDS)

NAME	TYPE	OFFSET	NAME	TYPE	OFFSET	NAME	TYPE	OFFSET	NAME	TYPE	OFFSET
B1	C#8	000170	B2	C#8	000200	CON	C#8	000120			
CON1	C#8	000130	CON2	C#8	000140	CON3	C#8	000150			
CON4	C#8	000160	CON5	C#8	000230	CON6	C#8	000240			
CON7	C#8	000250	CON8	C#8	000260	CON9	C#8	000270			
C1	C#8	000030	C2	C#8	000040	C3	C#8	000050			
C4	C#8	000060	C5	C#8	000070	C6	C#8	000100			
C7	C#8	000110	F01	C#8	000220	F01	C#8	000210			
P1	R#4	000030	P1	R#4	000200	P2	R#4	000004			
T1	C#8	000000	T2	C#8	000010	T3	C#8	000020			
V	R#4	0000310	VM23	R#4	000324	X#3	R#4	000020			
V2	R#4	0000314									

COMMON BLOCK / SIZE = 000014 (6 WORDS)

NAME	TYPE	OFFSET	NAME	TYPE	OFFSET	NAME	TYPE	OFFSET
F	C#8	000004						

FUNCTIONS, FUNCTIONS, STATEMENT AND PROCESSOR-DEFINED FUNCTIONS

NAME	TYPE	NAME	TYPE	NAME	TYPE	NAME	TYPE
CEXP	C#8	CMPLY	C#8				

FORTRAN IVV02 1-1 THU 21-FEB-80 05:03:15 PAGE 001
PROGRAM CVEXP

AUTHOR C WERNER 21-AUG-80

THIS PROGRAM WILL FIND THE FREQUENCY SWEPT HOLOGRAM OF A TARGET WITH VERTICAL SYMMETRY. THE FREQUENCY RANGE WILL BE BETWEEN FBEGIN AND FSTOP WITH NPTS FREQUENCY PTS. THE ANGLE RANGE WILL BE THETA WITH NLINES IN THAT ANGULAR SHEEP. THE REAL PART OF THE SCATTERED FIELD WILL BE SCALED FOR DISPLAY BY PROGRAM CDISP. THE TARGET WILL BE CORRECTED FOR SYSTEM RESPONSE AND RANGE BY USE OF A REFERENCE TARGET.

INTEGER REFA(128), REFP(128), TARA(128), TARP(128)
BYTE NAME(720)

TYPE *, '***** 2D FREQUENCY SWEPT HOLOGRAM *****'
ACCEPT *, FBEGIN
TYPE *, 'ENTER STARTING FREQUENCY GHZ.'
ACCEPT *, FSTOP
TYPE *, 'ENTER ENDING FREQUENCY GHZ.'
ACCEPT *, NPTS
TYPE *, 'ENTER THE NUMBER OF FREQUENCY POINTS (<128).'
ACCEPT *, THETA
TYPE *, 'ENTER ANGULAR SHEEP IN DEGREES.'
ACCEPT *, NLINES
TYPE *, 'ENTER THE NUMBER OF LINES.'
ACCEPT *, NAME
TYPE *, 'ENTER THE NUMBER OF SAMPLES/FREQUENCY POINT.'
ACCEPT *, NSAMP
TYPE *, 'ENTER THE NAME OF THE FILE FOR DATA STORAGE.'
TYPE *, ' '
CALL GTLIN(NAME, '?')
OPEN(UNIT=15, NAME=NAME, TYPE='NEW', ACCESS='SEQUENTIAL',
IFORM='UNFORMATTED')
WRITE(15) FBEGIN, FSTOP, NLINES, THETA, NPTS
DTHETA=(THETA/NLINES)*(3.141526/180.)

GET SYSTEM RESPONSE

TYPE *, '**** PLACE REFERENCE TARGET IN THE FIELD ****'
PAUSE '**** HIT RETURN TO CONTINUE ****'
CALL SHDAT(REFA, REFP, FBEGIN, FSTOP, NPTS, NSAMP)

GET SCALE FACTOR FOR DISPLAY

TYPE *, '**** PLACE IMAGE TARGET IN THE FIELD ****'
PAUSE '**** HIT RETURN TO CONTINUE ****'
CALL SHDAT(TARA, TARP, FBEGIN, FSTOP, NPTS, NSAMP)
RADC = 25*3.141526/180.05
AMP=0
DO 10 K=1, NPTS
TARA(K)=TARA(K)-REFA(K)

00033 TARP(K)=TARP(K)-REFP(K)
00034 IF (TARP(K) GT 720) TARP(K)=TARP(K)-1440
00036 IF (TARP(K) LT -720) TARP(K)=TARP(K)+1440
00038 AMP=AMP*(TARA(K)*.05)
00039 CONTINUE
10
00040 AMP=AMP/NPTS
00041 TYPE *, 'AVERAGE AMPLITUDE IN DB: ', AMP
00042 TYPE *, 'ENTER DYNAMIC RANGE FOR DISPLAY IN DB: '
ACCEPT *, DBNORM
00043 AMAX=(DBNORM/2)
00044 AMIN=-AMAX
00045 AMAX=10 0**((AMAX/10.0)
00046 AMIN=10 0**((AMIN/10.0)
00047 AMIN=10 0**((AMIN/10.0)
00049 TYPE *, 'AMAX=', AMAX, ' AMIN=', AMIN
00049 SCALE=(200.0*(2.0**5))/(AMAX-AMIN)
00050 TYPE *, 'SCALE FACTOR FOR DATA=', SCALE
C
C COLLECT HOLOGRAM DATA
DO 500 J=1, NLINES
CALL SHDAT(TARA, TARP, FBEGIN, FSTOP, NPTS, NSAMP)
DO 100 K=1, NPTS
TARA(K)=TARA(K)-REFA(K)
TARP(K)=TARP(K)-REFP(K)
IF (TARP(K) GT 720) TARP(K)=TARP(K)-1440
IF (TARP(K) LT -720) TARP(K)=TARP(K)+1440
RNDNM=10 0**((TARA(K)*.05)-AMP)/10.0)*COS(TARP(K)*RADC)
I2=IFIX(RNDNM*SCALE)
TYPE *, K, I2
WRITE(15) I2
CONTINUE
100
00064 CALL STEP2(DTHETA, 0)
00065 CONTINUE
00066 CONTINUE
00067 CLOSE(UNIT=15)
00068 STOP '**** END OF PROGRAM ****'
00069 END

LOCAL VARIABLES, PSECT \$DATA, SIZE = 002154 (566 WORDS)

NAME	TYPE	OFFSET	NAME	TYPE	OFFSET	NAME	TYPE	OFFSET
AMAX	R*4	002110	AMIN	R*4	002114	AMMAX	R*4	002100
AMMIN	R*4	002104	AMP	R*4	002066	DBNORM	R*4	002074
DTHETA	R*4	002056	FBEGIN	R*4	002034	FSTOP	R*4	002040
I2	I*2	002132	J	I*2	002124	K	I*2	002072
NLINES	I*2	002052	NPTS	I*2	002044	NSAMP	I*2	002054
RADC	R*4	002062	RNDNM	R*4	002126	SCALE	R*4	002120
THETA	R*4	002046						

LOCAL AND COMMON ARRAYS:

NAME	TYPE	SECTION	OFFSET	SIZE	DIMENSIONS
REFA	L*1	\$DATA	002000	000024 (10)	(20)
REFP	I*2	\$DATA	000000	000400 (128)	(128)
TARA	I*2	\$DATA	000400	000400 (128)	(128)
TARP	I*2	\$DATA	001000	000400 (128)	(128)

UNIVERSITY MICROFILMS
SERIALS ACQUISITION
300 N ZEEB RD
ANN ARBOR MI 48106

0001 FORTRAN IUV02 1-1 SAT 23-FEB-80 01:31:06 PAGE 001
 PROGRAM CDISP
 C AUTHOR C. WERNER 19-FEB-80
 C
 C COMMON/DISPL/IZ, IZINIT, NPTS, IXBEG, IYBEG, ILEN, THETA
 0002 INTEGER IZ(512), IZ(18192)
 0003 BYTE A, NAME(20)
 0004 DATA PI/3.1415926/
 0005
 C
 C TYPE *, '***** 2D HOLOGRAM DISPLAY *****'
 0006 TYPE *, 'ENTER THE DATA FILENAME.'
 0007 TYPE *
 0008 CALL GTL(INAME, '?')
 0009 OPEN UNIT=15, NAME=NAME, TYPE='OLD', ACCESS='SEQUENTIAL',
 0010 IFORM='UNFORMATTED')
 0011 READ(15) FSTART, FEND, NLINES, ANGLE, NPTS
 0012 TYPE *, 'FREQUENCY GHZ (START):', FSTART
 0013 TYPE *, 'FREQUENCY GHZ (END):', FEND
 0014 TYPE *, 'NUMBER OF LINES:', NLINES, 'POINTS/LINE:', NPTS
 0015 TYPE *, 'SHEEP ANGLE DEG:', ANGLE
 0016 NPOINT=NLINES*NPTS
 0017 DO I=1, NPOINT
 0018 READ(15) Z(J)
 0019 CONTINUE
 0020
 0021 TYPE *, 'LOG COMPRESSION (Y OR N):'
 0022 ACCEPT 1000, A
 0023 IF (A.EQ.'Y') GO TO 25
 0024 TYPE *, 'ENTER CONTRAST SCALE FACTOR:'
 0025 ACCEPT *, SCALF
 0026 SCALF=SCALF*5
 0027 DO 20 J=1, NPOINT
 0028 Z(J)=IFIX(SCALF*Z(J))
 0029 IF (Z(J).GT.100) Z(J)=100
 0030 IF (Z(J).LT.-100) Z(J)=-100
 0031 CONTINUE
 0032 GO TO 30
 0033 TYPE *, 'ENTER LOG COMPRESSION SCALE FACTOR:'
 0034 ACCEPT *, SCALL
 0035 DO 28 J=1, NPOINT
 0036 IF (Z(J).LT.0) Z(J)=IFIX(-100*ALOG10(1.0-SCALL*Z(J)/10.0))
 0037 IF (Z(J).GE.0) Z(J)=IFIX(100*ALOG10(1.0+SCALL*Z(J)/10.0))
 0038 CONTINUE
 0039 TYPE *, 'ENTER THE INITIAL Z VALUE (500-1000):'
 0040 ACCEPT *, IZINIT
 0041 TYPE *, 'ENTER THE STARTING X POSITION (0.0-1.0):'
 0042 ACCEPT *, XSTART
 0043 IYS=IFIX(XSTART*4096)
 0044 TYPE *, 'ENTER THE START Y POSITION (0.0-1.0):'
 0045 ACCEPT *, YSTART
 0046 IYS=IFIX(YSTART*4096)
 0047 CALL IDISP(IXS, IYS, IZINIT)
 0048
 0049 TYPE *, 'POSITION AND INTENSITY CORRECT (Y OR N):'
 0050 ACCEPT 1000, A
 0051

0054 IF (A.EQ.'N') GO TO 30
 0055 TYPE *, 'ENTER THE LENGTH OF THE LINE (0-1000):'
 0056 ACCEPT *, ILEN
 0057 PAUSE 'HIT RETURN TO CONTINUE.'
 0058 DTHETA=ANGLE*PI/(FLOAT(NLINES)*180)
 0059 DFREQ=FEND-FSTART
 0060 ILENS=IFIX(ILEN*(FSTART/DFREQ))
 0061 DO 400 J=1, NLINES
 0062 THETA=(J-1)*DTHETA
 0063 IYBEG=IYS+IFIX(ILENS*COS(THETA))
 0064 IYBEG=IYS+IFIX(ILENS*SIN(THETA))
 0065 DO 300 INDEX=1, NPTS
 0066 IZ(INDEX)=Z((J-1)*NPTS+INDEX)
 0067 CONTINUE
 0068 CALL LINDSP
 0069 CONTINUE
 0070 CALL IDISP(IXS, IYS, IZINIT)
 0071 TYPE *, 'DISPLAY SAME DATA AGAIN (Y OR N):'
 0072 ACCEPT 1000, A
 0073 IF (A.EQ.'Y') GO TO 30
 0074 TYPE *, 'RESCALE DATA (Y OR N):'
 0075 ACCEPT 1000, A
 0076 IF (A.EQ.'Y') GO TO 15
 0077 CALL CLOSE(15)
 0078 TYPE *, 'DISPLAY A NEW FILE (Y OR N):'
 0079 ACCEPT 1000, A
 0080 IF (A.EQ.'Y') GO TO 5
 0081 FORMAT (A1)
 0082 STOP '***** END OF DISPLAY PROGRAM *****'
 0083 END
 0084
 0085 LOCAL VARIABLES, PSECT \$DATA, SIZE = 040206 (8259 WORDS)
 0086
 0087 NAME TYPE OFFSET NAME TYPE OFFSET NAME TYPE OFFSET
 A L*1 040040 ANGLE R*4 040054 DFREQ R*4 040114
 DTHETA R*4 040110 FEND R*4 040046 FSTART R*4 040042
 ILENS I*2 040120 INDEX I*2 040122 IXS I*2 040100
 IYS I*2 040106 J I*2 040062 NLINES I*2 040072
 NPOINT I*2 040060 PI R*4 040024 SCALF R*4 040064
 SCALL R*4 040070 XSTART R*4 040074 YSTART R*4 040102
 COMMON BLOCK /DISPL /, SIZE = 002016 (519 WORDS)
 NAME TYPE OFFSET NAME TYPE OFFSET NAME TYPE OFFSET
 IZ I*2 000000 IZINIT I*2 002000 NPTS I*2 002002
 IYBEG I*2 002004 IYBEG I*2 002006 ILEN I*2 002010
 THETA R*4 002012
 LOCAL AND COMMON ARRAYS:
 NAME TYPE SECTION OFFSET SIZE DIMENSIONS
 IZ I*2 DISPL 000000 002000 (512) (512)

0001 FORTRAN IUV02 1-1 SAT 23-FEB-80 01:31:06 PAGE 001
 PROGRAM CDISP
 C AUTHOR C. WERNER 19-FEB-80
 C
 C COMMON/DISPL/IZ, IZINIT, NPTS, IXBEG, IYBEG, ILEN, THETA
 0002 INTEGER IZ(512), IZ(18192)
 0003 BYTE A, NAME(20)
 0004 DATA PI/3.1415926/
 0005
 C
 C TYPE *, '***** 2D HOLOGRAM DISPLAY *****'
 0006 TYPE *, 'ENTER THE DATA FILENAME.'
 0007 TYPE *
 0008 CALL GTL(INAME, '?')
 0009 OPEN UNIT=15, NAME=NAME, TYPE='OLD', ACCESS='SEQUENTIAL',
 0010 IFORM='UNFORMATTED')
 0011 READ(15) FSTART, FEND, NLINES, ANGLE, NPTS
 0012 TYPE *, 'FREQUENCY GHZ (START):', FSTART
 0013 TYPE *, 'FREQUENCY GHZ (END):', FEND
 0014 TYPE *, 'NUMBER OF LINES:', NLINES, 'POINTS/LINE:', NPTS
 0015 TYPE *, 'SHEEP ANGLE DEG:', ANGLE
 0016 NPOINT=NLINES*NPTS
 0017 DO I=1, NPOINT
 0018 READ(15) Z(J)
 0019 CONTINUE
 0020
 0021 TYPE *, 'LOG COMPRESSION (Y OR N):'
 0022 ACCEPT 1000, A
 0023 IF (A.EQ.'Y') GO TO 25
 0024 TYPE *, 'ENTER CONTRAST SCALE FACTOR:'
 0025 ACCEPT *, SCALF
 0026 SCALF=SCALF*5
 0027 DO 20 J=1, NPOINT
 0028 Z(J)=IFIX(SCALF*Z(J))
 0029 IF (Z(J).GT.100) Z(J)=100
 0030 IF (Z(J).LT.-100) Z(J)=-100
 0031 CONTINUE
 0032 GO TO 30
 0033 TYPE *, 'ENTER LOG COMPRESSION SCALE FACTOR:'
 0034 ACCEPT *, SCALL
 0035 DO 28 J=1, NPOINT
 0036 IF (Z(J).LT.0) Z(J)=IFIX(-100*ALOG10(1.0-SCALL*Z(J)/10.0))
 0037 IF (Z(J).GE.0) Z(J)=IFIX(100*ALOG10(1.0+SCALL*Z(J)/10.0))
 0038 CONTINUE
 0039 TYPE *, 'ENTER THE INITIAL Z VALUE (500-1000):'
 0040 ACCEPT *, IZINIT
 0041 TYPE *, 'ENTER THE STARTING X POSITION (0.0-1.0):'
 0042 ACCEPT *, XSTART
 0043 IYS=IFIX(XSTART*4096)
 0044 TYPE *, 'ENTER THE START Y POSITION (0.0-1.0):'
 0045 ACCEPT *, YSTART
 0046 IYS=IFIX(YSTART*4096)
 0047 CALL IDISP(IXS, IYS, IZINIT)
 0048
 0049 TYPE *, 'POSITION AND INTENSITY CORRECT (Y OR N):'
 0050 ACCEPT 1000, A
 0051

0001 SUBROUTINE LINDSP
 C THIS SUBROUTINE WILL DISPLAY A LINE OF DATA
 C UP TO 512 POINTS LONG.
 C
 0002 COMMON/DISPL/IZ, IZINIT, NPTS, IXBEG, IYBEG, ILEN, THETA
 0003 INTEGER IZ(512)

0004 COSV=COS(THETA)
 0005 SINV=SIN(THETA)
 0006 DY=ILEN*COSV/NPTS
 0007 DX=ILEN*SINV/NPTS
 0008 Y=FLOAT(IXBEG)
 0009 V=FLOAT(IYBEG)
 0010 DO 100 K=1, NPTS
 0011 Y=Y+DY
 0012 V=V+DX
 0013 IX=IFIX(X)
 0014 IY=IFIX(Y)
 0015 IZVAL=IZ(K)+IZINIT
 0016 CALL IDISP(IX, IY, IZVAL)
 0017 CONTINUE
 0018 CALL IDISP(IXBEG, IYBEG, 0)
 0019 RETURN
 0020 END

FORTRAN IV STORAGE MAP FOR PROGRAM UNIT LINDSP
 LOCAL VARIABLES, PSECT \$DATA, SIZE = 000056 (23. WORDS)

NAME	TYPE	OFFSET	NAME	TYPE	OFFSET	NAME	TYPE	OFFSET
COSV	R*4	000004	DX	R*4	000014	DY	R*4	000020
IX	I*2	000036	IY	I*2	000040	IZVAL	I*2	000042
K	I*2	000034	SINV	R*4	000010	X	R*4	000024
Y	R*4	000030						

COMMON BLOCK /DISPL /, SIZE = 002016 (519. WORDS)

NAME	TYPE	OFFSET	NAME	TYPE	OFFSET	NAME	TYPE	OFFSET
IZ	I*2	000000	IZINIT	I*2	002000	NPTS	I*2	002002
IXBEG	I*2	002004	IYBEG	I*2	002006	ILEN	I*2	002010
THETA	R*4	002012						

LOCAL AND COMMON ARRAYS:

NAME	TYPE	SECTION	OFFSET	-----SIZE-----	DIMENSIONS
IZ	I*2	DISPL	000000	002000 (512)	(512)

SUBROUTINES, FUNCTIONS, STATEMENT AND PROCESSOR-DEFINED FUNCTIONS.

FORTRAN IV V02 1-1 SUBROUTINE STEP2(RADROT, NDIR)
 0001

0002 C AUTHOR C. WERNER 21-FEB-80
 0003 C
 0004 C RADROT= ROTATION IN RADIANS
 0005 C NDIR= DIRECTION FLAG, 0=>CLOCK 1=>CCW
 C
 0002 MCM=1024
 0003 MCCM=1536
 0004 IMCM=1280
 0005 IMCCM=1792
 C
 0006 STEPS/RAD=10000/PI
 0007 STRD=10000.0/3.14159
 0008 ISTEP=IFIX(STRD*RADROT)
 0009 IF (NDIR) 10, 10, 20
 0010 ION=MCM
 0011 IOFF=IMCM
 0012 GO TO 22
 0013 ION=MCCM
 0014 IOFF=IMCCM
 0015 CALL DOUT(., IERR, IOFF)
 0016 DO 25 J=1, 200
 0017 CONTINUE
 0018 DO 500 I=1, ISTEP
 0019 DO 50 J=1, 200
 0020 CONTINUE
 0021 CALL DOUT(., IERR, IOFF)
 0022 DO 70 J=1, 200
 0023 CONTINUE
 0024 DO 500 CONTINUE
 0025 RETURN
 0026 END

LOCAL VARIABLES: PSECT \$DATA, SIZE = 000050 (20. WORDS)

NAME	TYPE	OFFSET	NAME	TYPE	OFFSET	NAME	TYPE	OFFSET
IERR	I*2	000026	IOFF	I*2	000024	ION	I*2	000022
ISTEP	I*2	000020	IMCCM	I*2	000012	IMCM	I*2	000010
J	I*2	000030	K	I*2	000032	MCM	I*2	000006
MCM	I*2	000004	NDIR	I*2	000002	RADROT	R*4	000000
STRD	R*4	000014						

SUBROUTINES, FUNCTIONS, STATEMENT AND PROCESSOR-DEFINED FUNCTIONS.

NAME TYPE NAME TYPE NAME TYPE NAME TYPE NAME TYPE

DATE
ILME